

*Kinetics of Reactions*  
*in*  
*Aqueous Solutions*

by

Andrew William Hakin

A Thesis submitted  
for the degree of  
Doctor of Philosophy  
in the  
Faculty of Science  
at the  
University of Leicester

Department of Chemistry,  
The University,  
LEICESTER. LE1 7RH

April 1987

UMI Number: U545714

All rights reserved

INFORMATION TO ALL USERS

The quality of this reproduction is dependent upon the quality of the copy submitted.

In the unlikely event that the author did not send a complete manuscript and there are missing pages, these will be noted. Also, if material had to be removed, a note will indicate the deletion.



UMI U545714

Published by ProQuest LLC 2015. Copyright in the Dissertation held by the Author.  
Microform Edition © ProQuest LLC.

All rights reserved. This work is protected against  
unauthorized copying under Title 17, United States Code.



ProQuest LLC  
789 East Eisenhower Parkway  
P.O. Box 1346  
Ann Arbor, MI 48106-1346



To  
Mum, Dad & Linda

Statement

This thesis is based upon work conducted by the author, in the Department of Chemistry of the University of Leicester, during the period between October 1984 and November 1986.

All the work recorded in this thesis is original unless otherwise acknowledged in the text or by references. This work is not being presented for any other degree.

April 1987

Andrew William Hakin  
University of Leicester

## Acknowledgements

I am indebted to my supervisor, Dr. Michael Blandamer, for his guidance, assistance, encouragement and not least his enthusiasm throughout the period of this research.

I am grateful to Dr. John Burgess for many helpful discussions and to Mr. P. Acton for the maintenance of the spectrophotometers.

Many thanks to Mrs. C. A. Crane for drawing the diagrams and to both Mrs. Crane and Miss V. Orson-Wright for help with the production of this typescript.

The award of a travel grant to Holland and a maintenance grant, by the Science Engineering Research Council, is acknowledged.

---

List of Publications - A. W. Hakin

- [1] M.J.Blandamer, J.Burgess, B.Clark, A.W.Hakin, M.W.Hyett, S.Spencer, N.Taylor - J.Chem.Soc., Faraday Trans. I, 81, 2357, (1985)
  
- [2] J.B.F.N.Engberts, M.J.Blandamer, J.Burgess, B.Clark, A.W.Hakin - J.Chem.Soc., Chem.Commun. 414, (1985)
  
- [3] J.B.F.N.Engberts, M.J.Blandamer, J.Burgess, B.Clark, A.W.Hakin - J.Chem.Soc., Faraday Trans. I, 83, 865, (1987)
  
- [4] M.J.Blandamer, J.Burgess, A.W.Hakin, J.M.W.Scott - Water and Aqueous Solutions 137-142 (1986) (ed. G.W.Neilson and J.E.Enderby: Bristol, Adam Hilgar)
  
- [5] M.J.Blandamer, J.Burgess, A.W.Hakin - J.Chem.Soc., Faraday Trans. I, 82, 2989, (1986)
  
- [6] M.J.Blandamer, J.Burgess, B.Clark, A.W.Hakin, N.Gossal, S.Radulovic, P.P.Duce, P.Guardado, F.Sanchez, C.D.Hubbard, E.A.Abu-Gharib - J.Chem.Soc., Faraday Trans I, 82, 1471, (1985)
  
- [7] M.J.Blandamer, J.Burgess, P.Guardado, A.W.Hakin, S.Nuttall, S.Radulovic - J.Chem.Soc., Faraday Trans I, 83, 559, (1987)
  
- [8] M.J.Blandamer, J.Burgess, A.W.Hakin - J.Chem.Soc., Faraday Trans I, 82, 3681, (1986)
  
- [9] M.J.Blandamer, J.Burgess, A.W.Hakin - J.Chem.Soc., Faraday Trans I (1986) *in press*
  
- [10] M.J.Blandamer, J.Burgess, M.Cottrell, A.W.Hakin - J.Chem.Soc., Faraday Trans I (1987) *in press*

## LIST OF CONTENTS

	<u>Page No.</u>
CHAPTER 1 - Introduction	1
CHAPTER 2 - Experimental details of collection and data analysis	6
CHAPTER 3 - Criticism of the Wells approach to the calculation of single ion transfer parameters	22
CHAPTER 4 - Alkaline hydrolysis of low-spin iron(II) complexes in 'urea + water' mixtures	34
CHAPTER 5 - Alkaline hydrolysis of low-spin iron(II) complexes in 'methyl alcohol + water' mixtures	69
CHAPTER 6 - Salt effects on the neutral hydrolysis of phenyldichloroacetate and its para-methoxy derivative	92
CHAPTER 7 - Pitzer's equations for the activity coefficients of salts and the relationship between osmotic coefficients, activity coefficients, and the excess Gibbs function	124
CHAPTER 8 - Pairwise Gibbs function cosphere - cosphere group interaction parameters	137
CHAPTER 9 - Salt effects on the alkaline hydrolysis of bromophenol blue	162
CHAPTER 10 - Internal pressures of water and deuterium oxide	181
CHAPTER 11 - Excess pressures for aqueous solutions	209
CHAPTER 12 - Partial molar volumes and isobaric heat capacities of solutes in aqueous solution	246
APPENDIX 1	272
APPENDIX 2	284
APPENDIX 3	292
APPENDIX 4	302
APPENDIX 5	323
APPENDIX 6	343
APPENDIX 7	366
APPENDIX 8	368



# CHAPTER 1

Introduction

Kinetics is defined by the Collins English Dictionary as "the branch of chemistry concerned with the rates of chemical reactions". This simple definition does not do justice to a subject from which so much information on systems, and in particular aqueous systems, has been obtained. The work presented in this Thesis identifies pathways for the interpretation of kinetic results and in this respect can be divided into two parts. Chapters 3 to 6 deal with the interpretation of patterns of rate constants for reactions in binary aqueous mixtures and in aqueous salt solutions. By way of contrast, Chapters 7 to 12 use properties of aqueous solutions as a basis for predicting trends in kinetic parameters.

For reactions involving ions important quantities are transfer parameters for ions between solutions in water and in binary aqueous mixtures. These thermodynamic properties have been calculated by different authors (see for example references 1-5). Chapter 3 develops a criticism of the Wells<sup>3,6,7</sup> approach towards these calculations. Chapters 4 and 5 describe how solubility data are combined with kinetic data in an initial state/transition state analysis. The role of added cosolvent on reaction rates is therefore pinpointed in terms of the stabilisation/destabilisation of reacting solutes. In particular cosolvent effects on the alkaline hydrolysis of low-spin iron(II) diimine complexes are investigated<sup>8</sup>. In Chapter 6 the effects of added salts on rate constants for hydrolysis of the neutral substrate, phenyl dichloroacetate<sup>9</sup> and the para-methoxy derivative are explained in terms of cosphere-cosphere overlap effects involving added ions<sup>10,11</sup>.

The theme of aqueous salt solutions is continued in Chapters 7 to 9. Chapter 7 introduces Pitzer's<sup>12-14</sup> equations for activity coefficients of salts in solution and discusses how mean ionic activity coefficients,  $\gamma_{\pm}$ , osmotic coefficients,  $\phi$ , and the excess Gibbs function,  $G^E$ , are related. In Chapter 8 Pitzer's<sup>12-14</sup> equations are combined with the ideas of Savage and Wood<sup>15</sup> to yield pairwise cosphere-cosphere group interaction parameters for ions. In Chapter 9, Pitzer's<sup>13</sup> equation for the activity coefficients of single ions is used to explain trends in rate constants for the alkaline hydrolysis of bromophenol blue<sup>16</sup> in aqueous salt solutions. In Chapter 10 attention turns to a thermodynamic property called the internal pressure<sup>17</sup>,  $\Pi$ . The analysis concentrates on obtaining equations which describe the dependences of internal pressures on temperature and pressure for water and deuterium oxide. Equations which describe related dependences of the temperature of maximum densities (TMD's) are also reported for both systems. The merits of using  $\Pi = 0$  isotherms for obtaining kinetic data are commented on. Chapter 11 deals with excess pressures<sup>18,19</sup> in aqueous salt solutions and aqueous solutions of neutral solutes. Various methods for calculating excess pressures are investigated leading to the conclusion that an excess pressure depends on the definition of the volumetric properties for a given system<sup>20</sup>. The final Chapter, Chapter 12, concentrates on the unimolecular solvolysis of alkyl halides and seeks to clarify the controversy concerning the isobaric heat capacities of activation of such reactions. Partial molar isobaric heat capacities are calculated using an

extrathermodynamic assumption proposed by Grunwald<sup>21</sup> in which activity coefficients of two substances X and Y, in this case two different water structures<sup>22</sup>, are related to the molality of added solute Z (e.g. an alkyl halide) in aqueous solution. Attempts are reported to derive an absolute scale for partial molar isobaric heat capacities of ions in aqueous solution.

A description of the equipment used for collecting spectrophotometric data together with a description of the methods used to calculate rate constants is given in Chapter 2.

## References Chapter 1

- (1) M.H.Abraham, T.Hill, R.A.Schulz, R.A.C.Watt, J.Chem.Soc., Faraday Trans. I, 80, 489, (1984)
- (2) D.Feakins, A.S.Willmott, A.R.Willmott, J.Chem. Soc., Faraday Trans. I, 69, 122, (1973)
- (3) C.F.Wells, Aust.J.Chem., 36, 1739, (1983)
- (4) C.L.De Ligny, D.Bax, M.Alfenaar, Rec.Trav.Chim., 88, 1183, (1969)
- (5) M.J.Blandamer, J.Burgess, B.Clark, A.W.Hakin, N. Gossal, S.Radulovic, P.P.Duce, P.Guardado, F. Sanchez, C.D.Hubbard, E-E.A.Abu-Gharib, J.Chem. Soc., Faraday Trans. I, 82, 1471, (1985)
- (6) C.F.Wells, J.Chem.Soc., Faraday Trans. I, 69, 984, (1973)
- (7) C.F.Wells, J.Chem.Soc., Faraday Trans. I, 82, 2577, (1986)
- (8) M.J.Blandamer, J.Burgess, P.Guardado, A.W.Hakin, S.Nuttall, S.Radulovic, J.Chem.Soc., Faraday Trans. I, 83, 559, (1987)
- (9) J.F.J.Engbersen, PhD Thesis, Groningen Univ., Holland, (1976)
- (10) J.B.F.N.Engberts, M.J.Blandamer, J.Burgess, B. Clark, A.W.Hakin, J.Chem.Soc., Faraday Trans. I, 83, 865, (1987)
- (11) J.B.F.N.Engberts, M.J.Blandamer, J.Burgess, B. Clark, A.W.Hakin, J.Chem.Soc., Chem.Comm., 414, (1985)
- (12) K.S.Pitzer, J.Phys.Chem., 77, 268, (1973)
- (13) K.S.Pitzer, "Activity Coefficients in Electrolyte Solutions" ed.R.M.Pytkowicz, CRC Press, Boca Raton, Florida, Vol.1, Chapt.7, (1979)
- (14) R.C.Phutela, K.S.Pitzer, J.Phys.Chem., 82, 1, (1986)
- (15) J.J.Savage, R.H.Wood, J.Soln.Chem., 5, 753, (1976)
- (16) J.R.Velasco, F.S.Burgos, M.C.Carmona, J.H.Toledo, An.Quim., 80, 173, (1984)

- (17) J.H.Hildebrand, R.L.Scott, "Solubility of Non Electrolytes", Reinhold, New York (1930)
- (18) R.E.Gibson, J.Am.Chem.Soc., 56, 4, (1934)
- (19) J.V.Leyendekker, J.Chem.Soc., Faraday Trans. I, 77, 1529, (1981)
- (20) M.J.Blandamer, J.Burgess, A.W.Hakin, J.Chem.Soc., Faraday Trans. I, 82, 2989, (1986)
- (21) E.Grunwald, J.Am.Chem.Soc., 106, 5414, (1984)
- (22) R.Lumry, E.Battistel, C.Jolicoeur, Faraday Soc., Disc, 17, 93, (1982)



# CHAPTER 2

Experimental details of  
collection and data analysis

## 2.1 Introduction

This Chapter describes the methods by which kinetic data were collected and gives details of the computer controlled spectrophotometers used to collect absorbance data. A method of analysis for a first order reaction is summarised. Details of the computer programs which drive and then perform the analysis are given in Appendix 1.

## 2.2 Kinetic Analysis

All rate constants reported in this Thesis are either first or second order. However all reactions were monitored under first order conditions. In a typical first order process chemical substance A reacts to give product P; e.g.  $A \longrightarrow P$ . The integrated rate equation for such a reaction takes the following form;

$$\ln([A]_0/[A]_t) = kt \quad [2.1]$$

$[A]_0$  = the concentration of substance A at time  $t=0$

$[A]_t$  = the concentration of substance A at time  $t$

Equation [2.1] can be written as shown in equation [2.2];

$$[A]_t = [A]_0 \exp(-kt) \quad [2.2]$$

The concentration of substance A decreases exponentially with time at a rate determined by the constant  $k$ .

The half life of the reaction,  $t_{1/2}$ , is defined as the time taken for the concentration of substance A to fall to half of its original value i.e. when  $t = t_{1/2}$ ,  $[A]_t = (1/2)[A]_0$ .

Hence;

$$t_{1/2} = \ln 2/k \quad [2.3]$$

All of the reactions described in this Thesis were monitored for at least 2.5 half lives.

In the case of second order reactions, the ISOLATION METHOD was used to follow the reaction under pseudo first order conditions. In a given chemical reaction two substances A and B form product P;  $A + B \longrightarrow P$ . If k is a second order rate constant;

$$-d[A]/dt = k [A][B] \quad [2.4]$$

If substance B is present in large excess over substance A, the concentration of B can be assumed constant throughout the reaction and the term [B] incorporated into the rate constant;

$$k_{\text{obs}} = k [B] \quad [2.5]$$

where  $k_{\text{obs}}$  is a first order rate constant. The rate law can now be written in a simplified first order form and as such be treated in the manner shown earlier.

$$-d[A]/dt = k_{\text{obs}} [A] \quad [2.6]$$

An example of this type of behaviour (Chapter 9), concerns the alkaline hydrolysis of the sodium salt of bromophenol blue. A more usual pattern for the rate law concerns cases where  $k_{\text{obs}}$  is a linear function of [B]; the law takes the

following form.

$$k_{\text{obs}} = k_1 + k_2 [B] \quad [2.7]$$

Here  $k_1$  describes a dissociative reaction and  $k_2$  describes an associative reaction. Examples of this behaviour are dealt with in Chapters 4 and 5.

All reactions were characterised by following the change in concentration of either reactant or product with time. A convenient method of accomplishing this is spectrophotometrically, in which the changes in absorbance with time are followed. The link between absorbance and concentration is established through the Beer-Lambert law. The absorbance,  $P$ , of a single substance A, in dilute solution, in monochromatic light of wavelength,  $\lambda$ , is given by equation [2.8].

$$P = \log_{10}(I_0/I_t) = \epsilon_\lambda l[A] \quad [2.8]$$

where  $I_0$  and  $I_t$  are the intensities at wavelength  $\lambda$  of the incident and transmitted light.

$\epsilon_\lambda$  = molar extinction coefficient of A at wavelength  $\lambda$ .

$l$  = pathlength /m

$[A]$  = concentration of species A /mol m<sup>-3</sup>

The total absorbance of a solution at wavelength  $\lambda$  is obtained as the sum over all substances;

$$P = \epsilon_a[A]l + \epsilon_b[B]l + \dots$$

Where  $\epsilon_a$  and  $\epsilon_b$  are the molar absorption coefficients of species A and B in the solution at wavelength  $\lambda$ .

For the simple first order reaction described earlier the combination of equations [2.1] and [2.8] leads to an expression from which the rate constant can be obtained directly from absorbance data.

$$\begin{aligned}
 \text{At time } t=0 & \quad P_0 = \epsilon_a [A]_0 l + \epsilon_b [B]_0 l \\
 \text{At time } t & \quad P_t = \epsilon_a [A]_t l + \epsilon_b [B]_t l \\
 \text{At time } t=\infty & \quad P_\infty = \epsilon_b [B]_\infty l = \epsilon_b l ([A]_0 + [B]_0) \\
 & \quad (\text{completion}) \quad = \epsilon_b l ([A]_t + [B]_t)
 \end{aligned}$$

$$\Rightarrow [A]_0 = (P_0 + P_\infty) / (\epsilon_a l + \epsilon_b l)$$

$$\Rightarrow [A]_t = (P_t + P_\infty) / (\epsilon_a l + \epsilon_b l)$$

$$\text{Therefore :} \quad \ln\{(P_0 - P_\infty) / (P_t - P_\infty)\} = kt \quad [2.9]$$

The UV/visible window has proved very useful, because in this region the changes in absorption are dramatic for solutions in which transition metal complex reactions are undergoing reaction. The spectrophotometers are described in the following section. The non-linear least squares procedure used to solve equation [2.9] is dealt with in Section 2.5.

### 2.3 The Hewlett Packard 8451A Diode Array Spectrophotometer

The Hewlett Packard 8451A diode array spectrophotometer, a single beam, microprocessor controlled instrument, operated in the UV/visible window over the wavelength range 190 to 820 nm. This spectrophotometer was capable of measuring absorbances either every 0.1 of a second, at up to 25 separate wavelengths, or every 0.7 of a second for a full

spectrum. It could reproduce a specific wavelength to within  $\pm 0.05$  nm and had a spectral bandwidth of 2 nm.

Central to the operation of the spectrophotometer were two 8-bit microcomputers, the Z-80 and the HP 85A. The Z-80 microcomputer controlled the internal hardware (lamp, shutter, etc.) and performed measurements. The HP 85A handled the data, controlled peripherals, and acted as an interface between the user and the basic instrument. A block diagram of the spectrophotometer is shown in Figure 2.1.

Light from a deuterium lamp was focussed at the sample cell (3 cm<sup>3</sup> quartz, pathlength 1 cm) by an ellipsoidal mirror, then reflected onto a monozone holographic grating by a second ellipsoidal mirror. The grating dispersed light onto a linear photodiode array. The photodiode array was a series of 328 individual light sensitive cells and control circuits etched onto a semiconductor chip. A shutter positioned between the lamp and the optical mirrors, cut off radiation from the lamp for measurement of dark current before and after each sample measurement.

A series of BASIC programs guided the user through procedures to set up the spectrophotometer, to collect and then store on disk absorbance/time data. Details of such programs are given in Appendix 1. The spectrum obtained from each scan was displayed on a cathode ray tube and at the end of each run a hard copy of the collected spectra, together with the printed absorbances and time data, was obtained from the in-built thermal printer/plotter. Figure 2.2 gives an example of the initial output from a typical kinetic run. Once the data had been stored on disk to

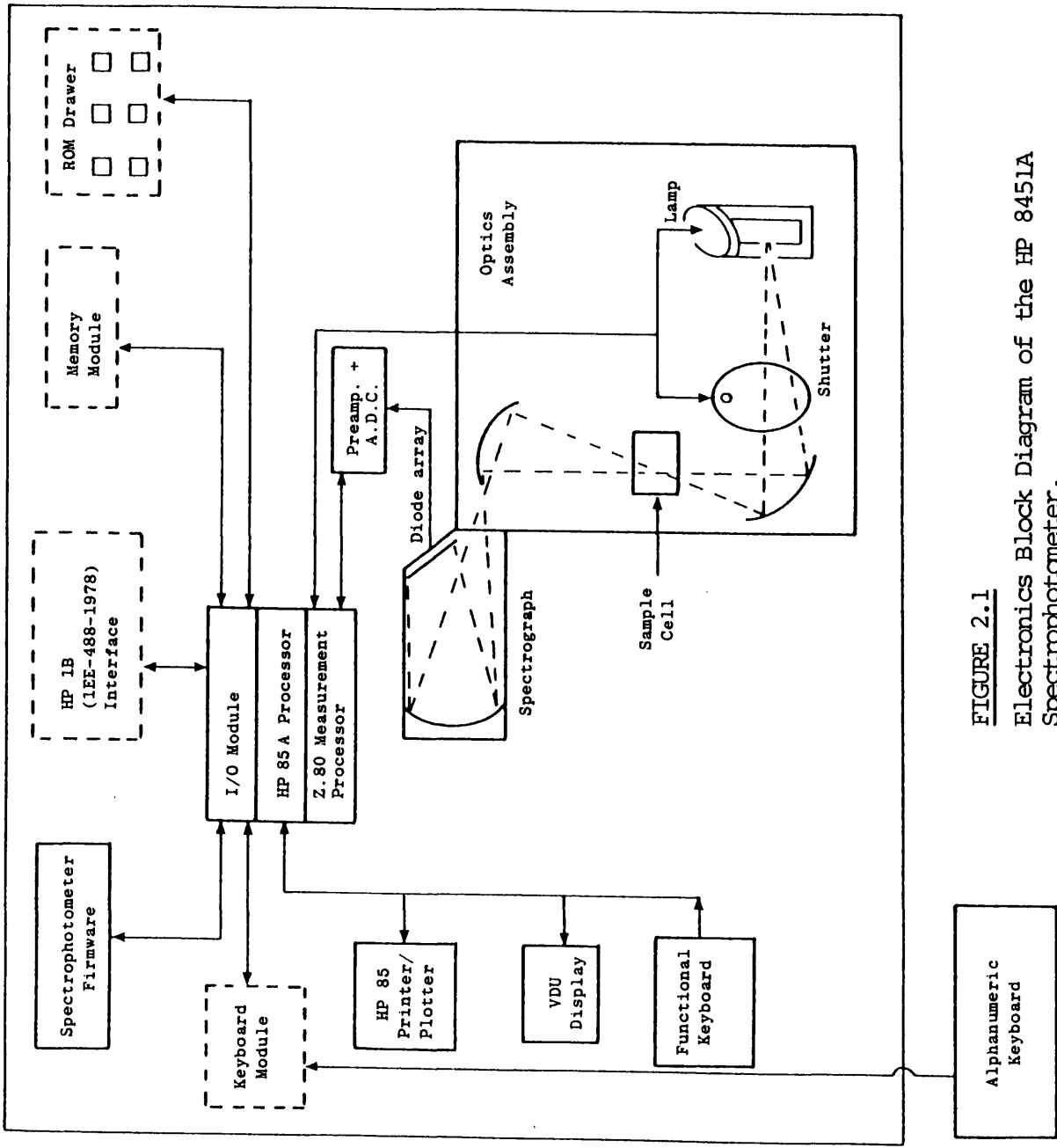
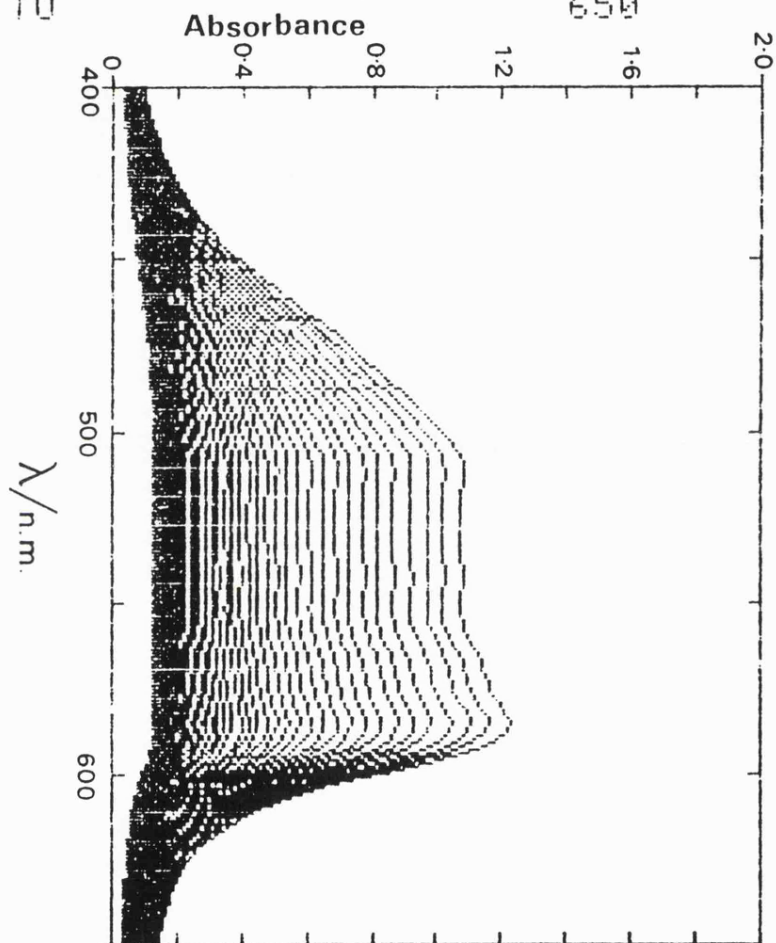


**FIGURE 2.1**  
**Electronics Block Diagram of the HP 8451A Spectrophotometer.**

```
HELLO
FIRST ORDER LOG
SYSTEM=                               3
WAVELENGTH =                          592
TIME STEP =                            20
RUN TIME =                             800
NUMBER OF READINGS =                   41
RANGE =                                 400
TO                                       650
```



```
DATA ON DISC
THAT IS ALL, FOLKS
```

FIGURE 2.2

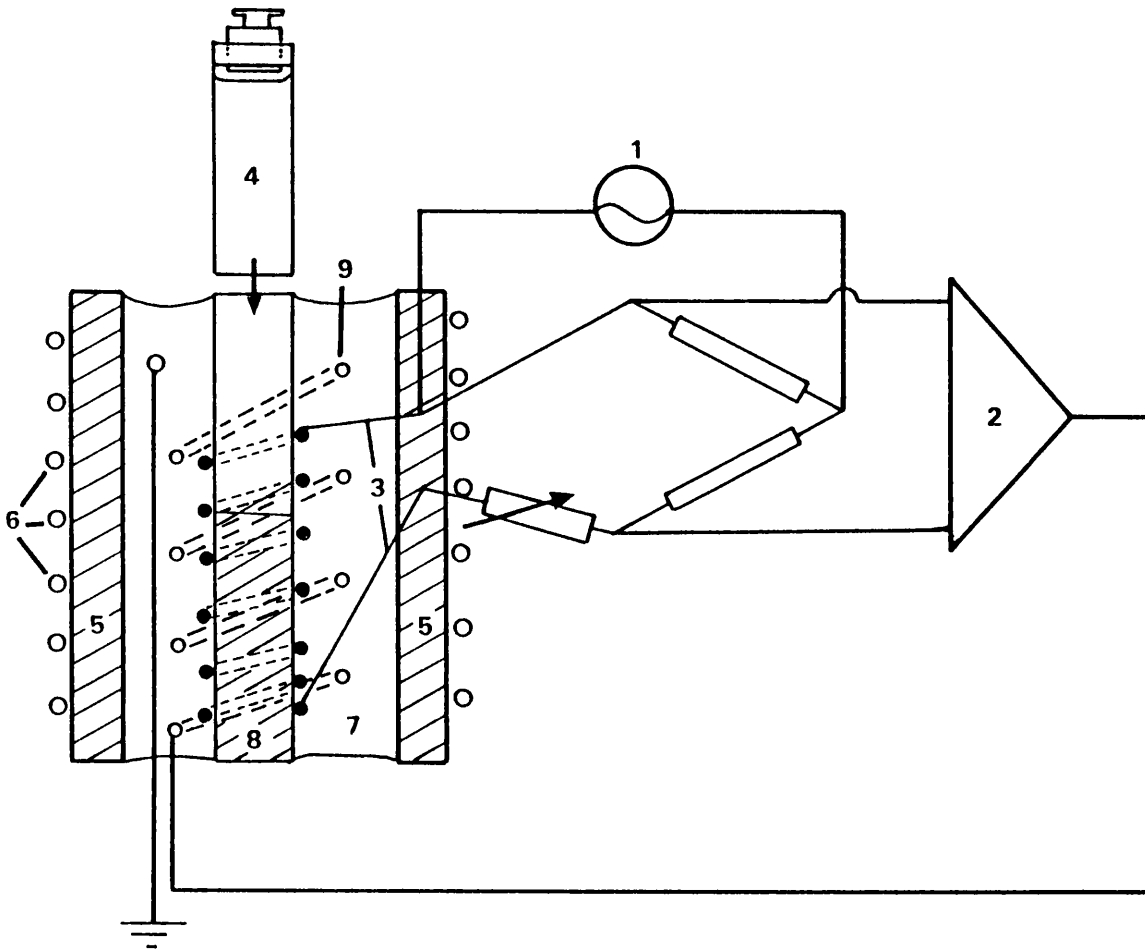
Example of the output from the data-logging program used on the HP 8451A Spectrophotometer. Alkaline hydrolysis of Complex C (see Chapter 5);  $[\text{NaOH}] \text{ mol dm}^{-3} = 0.27$ ; 0% MeOH at 298.15 K.

create a semipermanent record it could be recalled into the computer built into the spectrophotometer by a separate program which dealt with the kinetic analysis. Appendix 1 Section 2 describes such a program and Section 2.5 sets out the mathematical methods used in such an analysis.

Within the spectrophotometer the sample cell was housed in an insulated copper cell holder. The cell block (Figure 2.3) was water cooled via a coiled small bore copper pipe around its exterior and thermostatted by a platinum resistance thermometer, connected to a Wheatstone bridge, coiled around an inner copper block. If the bridge was in balance then the system was at the correct temperature and the heater coil, wrapped around the inner copper block was switched off. If, however, the temperature fell, the unbalanced bridge switched on the heater, via the amplifier. Heating continued until the system was once again at equilibrium. A temperature probe inserted in the insulation between the two copper blocks and connected to a microprocessor thermometer displayed the temperature within the block. Once a sample cell was placed in the system and allowed to reach thermal equilibrium over a period of approximately five minutes then a constant temperature of  $25.00 \pm 0.01$  celsius was readily maintained.

#### 2.4 The Unicam SP 1800 Ultraviolet Spectrophotometer

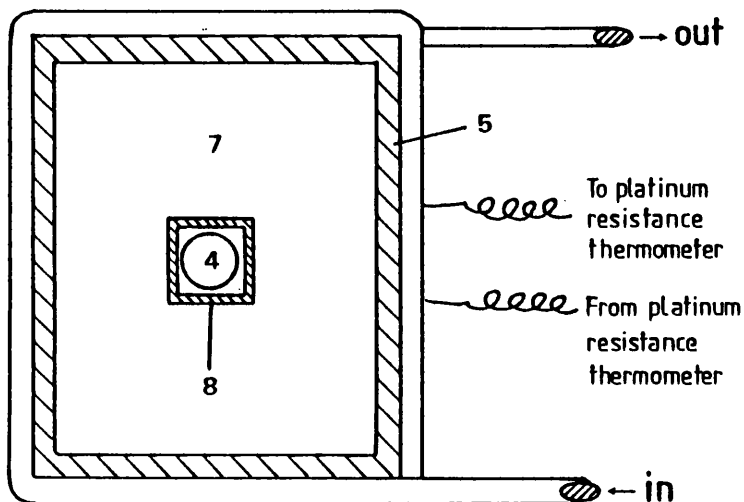
The Unicam SP 1800 was a UV/visible spectrophotometer with a working range of 190 to 820 nm and a capability of handling up to 3 sample cells and three reference cells (Figure 2.4). Absorbance readings were obtained as a function of time at a single wavelength. The



**FIGURE 2.3**

Diagram of the Thermostatted Cell Block positioned in the HP 8451A Spectrophotometer.

1. Oscillator
2. Amplifier
3. Platinum Resistance Thermometer acting as an arm of Wheatstone Bridge
4. Sample Cell
5. Outer Copper Block
6. Water Pipes
7. Insulating Material
8. Inner Copper Block
9. Heater Coil



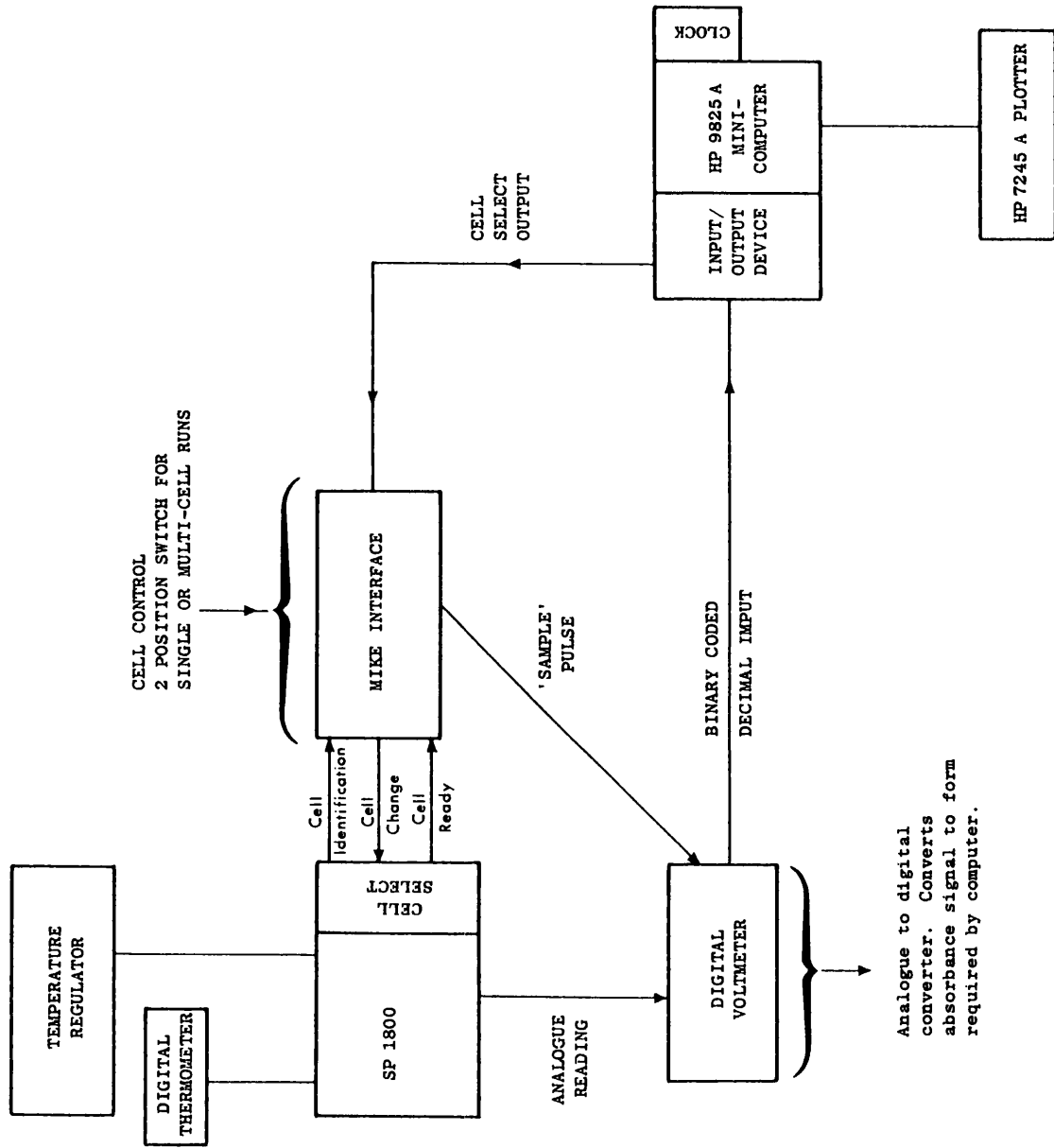


**FIGURE 2.4**  
**SP-1800 Spectrophotometer and HP 9825A Apparatus.**

spectrophotometer was directly connected to a Microprocessor Instrumentation of Kinetic Experiments (MIKE) interface which in turn was connected through a digital voltmeter to a Hewlett Packard 9825A (24K) minicomputer equipped with a real time clock, various utility ROM cartridges and input/output ports. The complete system was controlled by a HEWLETT PACKARD BASIC program, written by Dr.M.J.Blandamer.

After loading the program from a data cartridge the user was prompted to supply information necessary to initiate a run i.e. the number of cells to be analysed, estimates of the initial and final absorbance readings, an estimated rate constant, the number of readings before calculation of a rate constant and finally the number of readings between consecutive calculations. Once this information had been entered, the correct wavelength set, and the reaction in each cell initiated the kinetic run was started by a simple keystroke. At time intervals calculated from the input information, the computer supplied a 'cell select' binary signal, unique to each cell, to the MIKE interface. This signal was compared to the cell in the light beam of the spectrophotometer using the 'cell identification' signal. If the signals were not the same, the cell block within the spectrophotometer was moved using the 'cell select' signal until the correct cell was in position. At this point a 'sample pulse' was sent to the digital voltmeter to accept an analogue absorbance reading from the Unicam SP 1800 (a signal delay of 1.5 seconds was incorporated into the system between the 'cell ready' and 'sample pulse' signals to allow the analogue meter on the

Unicam SP 1800 to settle). The absorbance reading was encoded into binary by the digital voltmeter and fed back into the minicomputer. Finally a signal was sent from the minicomputer to the MIKE interface in order to clear all lines in readiness for the next reading. Absorbance and time data were stored in the computer's memory for each cell and printed out by a thermal printer together with the iterative rate constants calculated at user specified intervals. At any point during a run a cell could be 'aborted', by typing the cell number into the minicomputer; this procedure had no effect on the remaining cells. When all of the cells had been monitored for at least 2.5 half lives the minicomputer calculated the final values of rate constant,  $P_0$ ,  $P_\infty$  and standard deviation of the fit for each cell using the method of non-linear least squares described in the next section. At the end of each analysis first order plots were obtained from the Hewlett Packard 7245A plotter connected to the minicomputer.

The cell block within the Unicam SP 1800 was thermostatted using the same method as described for the HP 8451A spectrophotometer (see Figure 2.3).

### 2.5 Method of Absorbance/Time Data Analysis

The analysis is based on the non-linear least squares method described by P. Moore<sup>1</sup>.

In a rearranged version of equation [2.9] the absorbance at time  $t$ ,  $P_t$  is expressed in the following form;

$$P_t = (P_0 - P_\infty) \exp(-kt) + P_\infty \quad [2.10]$$

Hence at a given time  $t$  the dependent variable absorbance,  $P_t$ , is defined by the three independent variables  $P_0$ ,  $P_\infty$ , and  $k$ .

$$P_t = P_t [P_0, P_\infty, k] \quad [2.11]$$

The general differential of equation [2.11] is given by equation [2.12];

$$dP = (\partial P_t / \partial P_0)_{P_\infty, k} dP_0 + (\partial P_t / \partial P_\infty)_{P_0, k} dP_\infty + (\partial P_t / \partial k)_{P_0, P_\infty} dk \quad [2.12]$$

The differentials of equation [2.10] with respect to each of the independent variables take the following form;

$$(\partial P_t / \partial P_0)_{P_\infty, k} = \exp(-kt) = \alpha_1 \quad [2.13]$$

$$(\partial P_t / \partial P_\infty)_{P_0, k} = 1 - \exp(-kt) = \alpha_2 \quad [2.14]$$

$$(\partial P_t / \partial k)_{P_0, P_\infty} = -t(P_0 - P_\infty) \exp(-kt) = \alpha_3 \quad [2.15]$$

The analysis is initiated using estimates of  $P_0$ ,  $P_\infty$ , and  $k$  entered into the minicomputer at the beginning of the run. From these estimates, absorbances  $P_t(\text{calc})$ , at each time  $t$  are calculated and the differences between observed and calculated  $P_t$  at each data point are obtained.

$$\text{i.e. } dP_t = P_t(\text{obs}) - P_t(\text{calc})$$

In order to improve the fit,  $\alpha_1$ ,  $\alpha_2$ , and  $\alpha_3$  are calculated from equations [2.13], [2.14] and [2.15] at each time step  $t$  and the quantity  $Q$ , defined by equation [2.16], is minimized.

$$Q = \Sigma (dP_t - \alpha_1 dP_o - \alpha_2 dP_\infty - \alpha_3 dk)^2 \quad [2.16]$$

When Q is at a minimum  $dQ/dX = 0$ .

$$dQ/dP_o = \Sigma \alpha_1^2 dP_o + \Sigma \alpha_1 \alpha_2 dP_\infty + \Sigma \alpha_1 \alpha_3 dk - \Sigma \alpha_1 dP_t = 0 \quad [2.17]$$

$$dQ/dP_\infty = \Sigma \alpha_2 \alpha_1 dP_o + \Sigma \alpha_2^2 dP_\infty + \Sigma \alpha_2 \alpha_3 dk - \Sigma \alpha_2 dP_t = 0 \quad [2.18]$$

$$dQ/dk = \Sigma \alpha_3 \alpha_1 dP_o + \Sigma \alpha_3 \alpha_2 dP_\infty + \Sigma \alpha_3^2 dk - \Sigma \alpha_3 dP_t = 0 \quad [2.19]$$

This information can be arranged in matrix form;

$$\begin{array}{ccc|ccc} \Sigma \alpha_1^2 & \Sigma \alpha_2 \alpha_1 & \Sigma \alpha_3 \alpha_1 & dP_o & \Sigma \alpha_1 dP_t \\ \Sigma \alpha_2 \alpha_1 & \Sigma \alpha_2^2 & \Sigma \alpha_2 \alpha_3 & dP_\infty & \Sigma \alpha_2 dP_t \\ \Sigma \alpha_3 \alpha_1 & \Sigma \alpha_2 \alpha_3 & \Sigma \alpha_3^2 & dk & \Sigma \alpha_3 dP_t \end{array}$$

X
β
Y

Thus;  $Y = \beta X \quad [2.20]$

Calculated parameters  $\alpha_1$ ,  $\alpha_2$  and  $\alpha_3$  are placed in array X and equation [2.20] solved for  $\beta$  (i.e. for  $dP_o$ ,  $dP_\infty$ , and  $dk$ ) using a linear least squares method<sup>2</sup>. The computed correctors improved estimates of  $P_o$ ,  $P_\infty$  and  $k$ ; i.e.  $P_o(\text{improved}) = P_o(\text{previous}) + dP_o$ . Improved  $P_t(\text{calc})$  at time  $t$  is obtained from equation [2.10] and compared to the observed absorbance  $P_t(\text{obs})$ . If the agreement between  $P_t(\text{calc})$  and  $P_t(\text{obs})$  is poor, the cycle is repeated until either  $\Sigma [P_t(\text{obs}) - P_t(\text{calc})]^2$  is at a minimum or is comparable to the magnitude of the estimated experimental

precision. The analysis is complete and estimates of  $P_0$ ,  $P_\infty$  and  $k$  together with their standard errors are obtained.

## References Chapter 2

- (1) P.Moore, J.Chem.Soc., Faraday Trans. I, 68, 1890  
, (1972)
- (2) D.Z.Arbritton, A.L.Schmeltekoft, "Modern Spectroscopy, Modern Research II", Ed.K.N.Rao, Academic Press, New York, (1976)



# CHAPTER 3

Criticism of the Wells approach  
to the calculation of single ion  
transfer parameters

### 3.1 Introduction

Several criticisms were made by Blandamer et al<sup>1,2</sup> of the methods used by Wells<sup>3-5</sup> to calculate transfer parameters for ions. The major points of disagreement are summarised below.

[1] The first and possibly one of the most important points concerns the identification of the ion which is transferred. Wells states<sup>3,4</sup> that the target quantity is  $\Delta(\text{aq} \rightarrow \text{x}_2) \mu^\ddagger(\text{H}^+; \text{sln}; \text{c-scale})$ . However throughout the analysis the solvated proton  $\text{H}^+(\text{H}_2\text{O})_4$  is identified<sup>3</sup>. In fact Wells<sup>3</sup> describes the solvated ion  $\text{H}^+(\text{H}_2\text{O})_5$ , in which an  $\text{H}_2\text{O}$  molecule is weakly bonded to the trigonal pyramidal  $\text{H}^+(\text{H}_2\text{O})_4$  structure at the apical position to form a tetrahedral structure. This has the advantage that the solvated protons can be treated as spheres of radius  $3r(\text{H}_2\text{O})$  ( $r$  is the radius of a water molecule) which can be used in the Born<sup>6</sup> equation. This structure is described as a sphere of water molecules surrounding  $\text{H}_3\text{O}^+$ . Hence it is not clear which ion transfer quantity is being characterised. This point is important because;

$$\begin{aligned} \Delta(\text{aq} \rightarrow \text{x}_2) \mu^\ddagger(\text{H}^+; \text{sln}; \text{c-scale}) \\ \neq \Delta(\text{aq} \rightarrow \text{x}_2) \mu^\ddagger(\text{H}_3\text{O}^+; \text{sln}; \text{c-scale}) \\ \neq \Delta(\text{aq} \rightarrow \text{x}_2) \mu^\ddagger(\text{H}^+(\text{H}_2\text{O})_4; \text{sln}; \text{c-scale}) \end{aligned}$$

The three ions  $\text{H}^+$ ,  $\text{H}_3\text{O}^+$  and  $\text{H}^+(\text{H}_2\text{O})_4$  are different. If the Born equation is used to calculate the three quantities above then three different ionic radii are required.

[2] At a key stage in the analysis an extrathermodynamic assumption is made by Wells which effectively sets the chemical potentials of pure alcohol, ROH, and water equal. i.e.  $\mu^\circ(\text{ROH};1;\text{T}) = \mu^\circ(\text{H}_2\text{O};1;\text{T})$ . This has the effect of simplifying the non-Born contribution<sup>3</sup> to the transfer chemical potential of  $\text{H}^+$  (c.f. Appendix 2 Section 1).

$$\begin{aligned} \Delta(\text{aq} \rightarrow x_2) \mu^\#(\text{H}^+; \text{c-scale}; \text{non-Born}; \text{sln}; \text{T}) \\ = \alpha[\mu^\#(\text{ROH}_2^+; \text{c-scale}; \text{sln}; x_2; \text{T}) - \mu^\#(\text{H}_3\text{O}^+; \text{c-scale}; \text{sln}; x_2; \text{T})] \\ = -\alpha[\text{RTln}K^\#(\text{c-scale}; \text{sln}; \text{T})] \end{aligned}$$

[3] At a stage in the analysis used to calculate  $K^\#(\text{c-scale}; \text{sln}; x_2; \text{T})$  Wells<sup>3</sup> appears to switch from a description of the system in which 'alcohol + water' forms the solvent to a description of the system as an aqueous solution. In effect it is assumed that the properties of the aqueous mixture over the whole range of added  $x_{\text{ROH}}$  are ideal. This assumption is invalid (c.f. Appendix 2 Section 2).

[4] Finally the standard states defined by Wells are ill-defined and, on thermodynamic grounds, are of doubtful significance. Wells<sup>5</sup> has written the equilibrium equation [3.1.5] of Appendix 2 Section 1 as;



Wells states that "the standard states of all species in [equation above] are defined on the molar scale as solutes

in the mixture for  $i = 1 \text{ mol dm}^{-3}$  and  $y_i = 1.0$  with  $y \rightarrow 1.0$  and  $[i] \rightarrow 0$ ". This statement requires that all substances are solutes. This cannot be correct. At least one substance (or a mixture of substances) must be the solvent.

Wells has responded<sup>4</sup> to the points raised by restating his method. Nevertheless Wells offers some new definitions which are helpful in understanding his approach.

In an attempt to clarify the problems it is advantageous to consider the following descriptions of two systems. System A is an aqueous solution of  $\text{H}^+$ . The chemical potential of  $\text{H}^+$  in system A is written;

$$\mu(\text{H}^+; \text{aq}) = \mu^\#(\text{H}^+; \text{aq}) + RT \ln[(c(\text{H}^+)^{\text{aq}} y(\text{H}^+)^{\text{aq}}) / c_r] \quad [3.1]$$

where  $\lim(c(\text{H}^+)^{\text{aq}} \rightarrow 0) y(\text{H}^+)^{\text{aq}} = 1.0$ ;  $c_r = 1.0 \text{ mol dm}^{-3}$  and  $\mu^\#(\text{H}^+; \text{aq})$  defines the chemical potential of  $\text{H}^+$  in a solution where  $c(\text{H}^+)^{\text{aq}} = 1.0$  and  $y(\text{H}^+)^{\text{aq}} = 1.0$ . System B is a solution in which the solute is  $\text{H}^+$  and the solvent is a mixture of alcohol + water. The chemical potential of  $\text{H}^+$  in this system is written;

$$\mu(\text{H}^+; x_1) = \mu^\#(\text{H}^+; x_1) + RT \ln[(c(\text{H}^+)^{x_1} y(\text{H}^+)^{x_1}) / c_r] \quad [3.2]$$

where  $x_1$  denotes the amount of water in the alcohol + water system and  $\lim(c(\text{H}^+)^{x_1} \rightarrow 0) y(\text{H}^+)^{x_1} = 1.0$ ;  $c_r = 1.0 \text{ mol dm}^{-3}$ .  $\mu^\#(\text{H}^+; x_1)$  defines the chemical potential of  $\text{H}^+$  in solution in the mixture, mole fraction  $x_1$ , where  $c(\text{H}^+)^{x_1} = 1.0$  and  $y(\text{H}^+)^{x_1} = 1.0$ .

The transfer chemical potential of  $\text{H}^+$ , imagined as a

transfer of  $H^+$  from system A into system B, is thus defined by equation [3.3].

$$\Delta(aq \rightarrow x_2)\mu(H^+) = \mu^\#(H^+; x_1) - \mu^\#(H^+; aq) \quad [3.3]$$

### 3.2 Descriptions of a Solute, j, in a Solvent Mixture

#### "Water + ROH"

A given system contains  $n_j$  moles of solute-j in a solvent mixture which contains  $n_1$  moles of solvent 1 and  $n_2$  moles of solvent 2. The mole fraction of solvent 1,  $x_1$ , in the mixture is given by  $n_1/(n_1+n_2+n_j)$  and similarly the mole fraction of solvent 2,  $x_2$ , in the mixture is given by  $n_2/(n_1+n_2+n_j)$ . If the volume of the system is  $V$ , then the concentration of solute-j in solution,  $c_j$ , is given by  $(n_j/V)$ . In such a system the chemical potential of substance 1 can be related to the mole fraction  $x_1$  using equation [3.4].

$$\mu_1(\text{sln}; T; p) = \mu_1^*(1; T; P) + RT \ln(x_1 f_1) \quad [3.4]$$

where  $\lim(x_1 \rightarrow 1) f_1 = 1.0$ . The reference chemical potential for substance 1 is the pure liquid. If  $x_1 = 1$  and  $f_1 = 1$  then  $\mu_1(\text{sln}; T; p) = \mu_1^*(1; T; p)$ . In a similar fashion the chemical potential for substance 2 is given by equation [3.5].

$$\mu_2(\text{sln}; T; p) = \mu_2^*(1; T; p) + RT \ln(x_2 f_2) \quad [3.5]$$

where  $\lim(x_2 \rightarrow 1.0) f_2 = 1.0$ . The reference chemical potential of substance 2 is once again defined as the pure

liquid i.e if  $x_2 = 1.0$  and  $f_2 = 1.0$  then  $\mu_2(\text{sln};T;p) = \mu_2^*(l;T;p)$ . The chemical potential of the solute-j in solution is given by equation [3.6].

$$\mu_j(\text{sln};T;p) = \mu_j^\#(\text{sln};c\text{-scale};T;p) + RT \ln[c_j y_j / c_r] \quad [3.6]$$

At constant  $x_1$  and  $x_2$  limit( $c_j \rightarrow 0$ )  $y_j = 1.0$ ;  $c_r = 1 \text{ mol dm}^{-3}$ . The reference chemical potential,  $\mu_j^\#(\text{sln};c\text{-scale};T;p)$  is defined as chemical potential of solute-j in solution where  $c_j = 1.0 \text{ mol dm}^{-3}$ ,  $y_j = 1.0$  and the solvent is a mixture at constant  $x_1$  and  $x_2$ .

The Wells description of the same system is very different. Here it is advantageous to define the mole fraction of substance 1 in the mixture in the absence of solute as  $x_1^\circ$  and similarly that of substance 2 as  $x_2^\circ$ . In defining the chemical potential of the solute there is no disagreement with the previous description.

$$\mu_j(\text{sln};T;p) = \mu_j^\#(\text{sln};c\text{-scale};T;p) + RT \ln[c_j y_j / c_r] \quad [3.7]$$

However the definitions of the chemical potentials of the solvents using the Wells<sup>4</sup> procedures disagree with the previous descriptions. For solvent 1, it is recognised that the solute may bind a number of solvent molecules to form a new solute. Then the mole fraction of the solvent changes when the solute is added.

$$\begin{aligned} \mu_1(\text{sln};T;p;x_1;x_2;c_j) &= \mu_1^w(\text{sln};T;p;x_1^\circ;x_2^\circ;c_j=0) \\ &+ RT \ln(f_1^w) \end{aligned} \quad [3.8]$$

Similarly for solvent 2, the composition may change as a result of incorporation of solvent 2 into the solute.

$$\mu_2(\text{sln}; T; p; x_1; x_2; c_j) = \mu_2^w(\text{sln}; T; p; x_1^\circ; x_2^\circ; c_j=0) + RT \ln(f_2^w) \quad [3.9]$$

Superscript w identifies definitions used by Wells. The standard states of substances 1 and 2 are defined in the particular mixture, mole fractions  $x_1^\circ$  and  $x_2^\circ$ , where the concentration of solute-j is zero<sup>4</sup>.  $f_1^w$  and  $f_2^w$  are activity coefficients for substances 1 and 2 in the solution containing solute-j. By definition  $\lim(c_j \rightarrow 0) f_1^w = 1.0$  and  $f_2^w = 1.0$ . The form of the dependence of  $f_1^w$  and  $f_2^w$  on  $c_j$  is unknown. But the assumption is made that the mixture (1+2) is 'ideal' in the absence of solute-j; it is perhaps better to write 'W-ideal'. Accepting the difference between the two descriptions, it should be noted that despite the difference between the standard states used in the descriptions the same quantities in each case are being defined. Therefore equations [3.4] and [3.8] yield equation [3.10].

$$\mu_1^*(l; T; p) + RT \ln(x_1 f_1) = \mu_1^w(\text{aq}; T; p; x_1^\circ; x_2^\circ; c_j=0) + RT \ln(f_1^w) \quad [3.10]$$

If  $\mu_1^w(\text{aq}; T; p; x_1^\circ; x_2^\circ; c_j=0)$  is rewritten as  $\{\mu_1^*(l; T; p) + RT \ln(x_1^\circ f_1^\circ)\}$ , the latter still representing the chemical potential of substance 1 in the pure solvent mixture, then equation [3.10] can be written in the form;

$$\mu_1^*(l;T;p) + RT\ln(x_1 f_1) = \mu_1^*(l;T;p) + RT\ln(x_1^\circ f_1^\circ) + RT\ln(f_1^W) \quad [3.11]$$

$$\Rightarrow f_1 = (x_1^\circ/x_1) f_1^\circ f_1^W \quad [3.12]$$

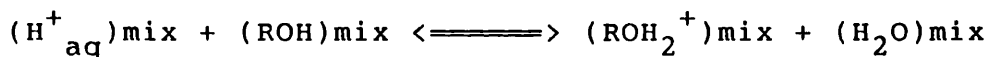
As  $c_j \rightarrow 0$ ,  $(x_1^\circ/x_1) \rightarrow 1.0$ ,  $f_1^W \rightarrow 1.0$  and  $f_1 \rightarrow f_1^\circ$ .

In a similar fashion equations [3.5] and [3.9] yields equation [3.13].

$$f_2 = (x_2^\circ/x_2) f_2^\circ f_2^W \quad [3.13]$$

As  $c_j \rightarrow 0$ ,  $(x_2^\circ/x_2) \rightarrow 1.0$ ,  $f_2^W \rightarrow 1.0$  and  $f_2 \rightarrow f_2^\circ$ . Equations [3.12] and [3.13] can be compared to equations 10 and 11 of reference 4. For both equations it can only be assumed that the dependence of  $f_1^W$  on  $c_j$  is sensible.

Returning back to the paper by Wells<sup>4</sup>, he defines a chemical equilibrium;



This equilibrium, as written, raises two points.  $H_{aq}^+$  is defined by Wells as  $H^+(H_2O)_b$  where  $b \geq 5$ . However in this instance if the above equilibrium is to have the correct stoichiometry then  $H_{aq}^+$  must be written as  $H_3O^+$ . As mentioned in the introduction there is a lack of clarity in defining the transferred ion;  $H^+$ ,  $H_3O^+$ ,  $H^+(H_2O)_4$  or  $H^+(H_2O)_5$ . The latter equilibrium can be rewritten as;



One would normally analyse this equilibrium in the

following way. At equilibrium,

$$\mu(\text{ROH}; x_1; T; p) + \mu(\text{H}_3\text{O}^+; x_1; T; p) = \mu(\text{ROH}_2^+; x_1; T; p) + \mu(\text{H}_2\text{O}; x_1; T; p) \quad [3.14]$$

In other words the sum of the chemical potentials of the reactants in the mixture at constant  $x_1$  temperature,  $T$ , and pressure,  $p$ , equals the sum of the chemical potentials of the products in the mixture at the same  $x_1$ , temperature and pressure. In the normal way, using the equations shown earlier in this Chapter, this equation can be expanded to give;

$$\begin{aligned} & \mu^*(\text{ROH}; l; T; p) + RT \ln(x(\text{ROH})f(\text{ROH})) \\ & + \mu^\#(\text{H}_3\text{O}^+; x_1; \text{sln}; T; p) + RT \ln[c(\text{H}_3\text{O}^+)y(\text{H}_3\text{O}^+)/c_r] \\ = & \mu^*(\text{H}_2\text{O}; l; T; p) + RT \ln(x(\text{H}_2\text{O})f(\text{H}_2\text{O})) \\ & + \mu^\#(\text{ROH}_2^+; x_1; \text{sln}; T; p) + RT \ln[c(\text{ROH}_2^+)y(\text{ROH}_2^+)/c_r] \quad [3.15] \end{aligned}$$

By definition the Gibbs function for reaction,  $\Delta_r G^\#$ , for this equilibrium is written as;

$$\Delta_r G^\#(T; c\text{-scale}; x_1) = \mu^*(\text{H}_2\text{O}; l; T; p) + \mu^\#(\text{ROH}_2^+; x_1; \text{sln}; T; p) - \mu^*(\text{ROH}; l; T; p) - \mu^\#(\text{H}_3\text{O}^+; x_1; \text{sln}; T; p) \quad [3.16]$$

$$= -RT \ln K^\#(\text{sln}; x_1; T; p) \quad [3.17]$$

Therefore;

$$K^\#(x_1; T) = [c(\text{ROH}_2^+)y(\text{ROH}_2^+)x_1 f_1] / [c(\text{H}_3\text{O}^+)y(\text{H}_3\text{O}^+)x_2 f_2] \quad [3.18]$$

This same analysis is repeated using the terminology

applied by Wells. Hence equation [3.14] is written;

$$\begin{aligned} \mu(\text{ROH}; x_1; x_2; T; p) + \mu(\text{H}_3\text{O}^+; x_1; x_2; T; p) \\ = \mu(\text{ROH}_2^+; x_1; x_2; T; p) + \mu(\text{H}_2\text{O}; x_1; x_2; T; p) \end{aligned} \quad [3.19]$$

Then;

$$\begin{aligned} \mu^W(\text{ROH}; x_1^\circ; x_2^\circ; T; p) + RT \ln(f_2^W) \\ + \mu^\#(\text{H}_3\text{O}^+; x_1^\circ; x_2^\circ; T; p) + RT \ln[c(\text{H}_3\text{O}^+)y(\text{H}_3\text{O}^+)/c_r] \\ = \mu^W(\text{H}_2\text{O}; x_1^\circ; x_2^\circ; T; p) + RT \ln(f_1^W) \\ + \mu^\#(\text{ROH}_2^+; x_1^\circ; x_2^\circ; T; p) + RT \ln[c(\text{ROH}_2^+)y(\text{ROH}_2^+)/c_r] \end{aligned} \quad [3.20]$$

Hence by definition using the Wells standard states;

$$\begin{aligned} \Delta_r G^\#(T; c\text{-scale}; x_1^\circ; x_2^\circ) = \\ \mu^W(\text{H}_2\text{O}; x_1^\circ; x_2^\circ; T; p) + \mu^\#(\text{ROH}_2^+; x_1^\circ; x_2^\circ; T; p) \\ - \mu^W(\text{ROH}; x_1^\circ; x_2^\circ; T; p) - \mu^\#(\text{H}_3\text{O}^+; x_1^\circ; x_2^\circ; T; p) \end{aligned} \quad [3.21]$$

$$= -RT \ln K^W(x_1^\circ; x_2^\circ; T) \quad [3.22]$$

Therefore;

$$K^W(x_1^\circ; x_2^\circ; T) = [f_1^W y(\text{ROH}_2^+) c(\text{ROH}_2^+) / [f_2^W y(\text{H}_3\text{O}^+) c(\text{H}_3\text{O}^+)]] \quad [3.23]$$

Substituting the values of  $f_1$  and  $f_2$ , defined in equations [3.12] and [3.13], into equation [3.18] gives equation [3.24].

$$\begin{aligned} K^\#(T; x_1) = \{ (c(\text{ROH}_2^+) y(\text{ROH}_2^+) / (c(\text{H}_3\text{O}^+) y(\text{H}_3\text{O}^+))) \} [x_1^\circ / x_2^\circ] \\ [f_1^\circ / f_2^\circ] [f_1^W / f_2^W] \end{aligned} \quad [3.24]$$

According to Wells he requires  $\Delta_r G^W(T; c\text{-scale}; x_1)$  which is calculated from equation [3.23]. Two approximations are made. The first sets the ratio of the activity coefficients of  $\text{ROH}_2^+$  and  $\text{H}_3\text{O}^+$  equal to one i.e.  $[y(\text{ROH}_2^+)/y(\text{H}_3\text{O}^+)] = 1.0$ . Whilst the second sets the ratio  $[f_1^W/f_2^W] = 1.0$ . Thus from equation [3.24];

$$[f_1^W/f_2^W] = [f_1 x_1 f_2 x_2 / f_1^\circ x_1^\circ f_2^\circ x_2^\circ] = 1.0$$

Hence;

$$K^W(x_1^\circ; x_2^\circ; T) = [c(\text{ROH}_2^+)/c(\text{H}_3\text{O}^+)] \quad [3.25]$$

The outcome is in effect the characterisation of the ratio  $c(\text{ROH}_2^+)$  to  $c(\text{H}_3\text{O}^+)$  by the quantity  $K^W(x_1^\circ; x_2^\circ; T)$ . Although it may be helpful to define this quantity it is important to probe, using the analysis outlined above, the precise significance of the property. Wells does not do this. Rather he assumes that  $K_w(x_1^\circ; x_2^\circ; T)$  is directly related to the difference between the standard chemical potentials of  $\text{ROH}_2^+$  and  $\text{H}_3\text{O}^+$  in the mixture. This is clearly incorrect as can be seen from equation [3.21]. Thus  $K^W(x_1^\circ; x_2^\circ; T)$  is also related to the difference in chemical potentials of water and ROH in the solvent. This difference depends on (a) the difference in the chemical potentials of pure ROH and  $\text{H}_2\text{O}$  (b) the composition of the mixture and (c) the non-ideal properties of the mixture. Therefore considerable doubt remains over the transfer parameters reported by Wells.

### 3.3 Conclusions

The Wells method for the calculation of the transfer chemical potential of  $H^+$  is rejected in favour of a more direct and less ambiguous technique. In the following two Chapters which deal with transfer quantities, the TATB assumption has been used as the basis of the calculations used to obtain transfer chemical potentials of ions (see Chapter 4). Hence reported trends in initial and transition state parameters will differ in their conclusions from those reported by Wells<sup>2,7</sup>.

### References Chapter 3

- (1) M.J.Blandamer, J.Burgess, B.Clark, A.W.Hakin, N. Gossal, S.Radulovic, P.P.Duce, P.Guardado, F. Sanchez, C.D.Hubbard, E-E.A.Abu-Gharib, J.Chem. Soc., Faraday Trans. I, 82, 1471, (1985)
- (2) B.Briggs, PhD Thesis, Leicester Univ., (1985)
- (3) C.F.Wells, J.Chem.Soc., Faraday Trans. I, 69, 984, (1973)
- (4) C.F.Wells, J.Chem.Soc., Faraday Trans. I, 82, 2577, (1986)
- (5) C.F.Wells, Aust.J.Chem., 36, 1739, (1983)
- (6) R.A.Robinson, R.H.Stokes, "Electrolyte Solutions", 2nd Edition, London, Butterworths (1959)
- (7) G.S.Groves, C.F.Wells, J.Chem.Soc., Faraday Trans. I, 81, 3091, (1985)



# CHAPTER

# 4

Alkaline hydrolysis of low-spin  
iron(II) complexes in 'Urea + water'  
mixtures

#### 4.1 Introduction

This Chapter reports the effects of added urea on first order rate constants for the alkaline hydrolysis of two low-spin iron(II) complex ions,  $[\text{Fe}(\text{gmi})_3]^{2+}$  and  $[\text{Fe}(\text{phen})_3]^{2+}$  (see Figure 4.1).



FIGURE 4.1

The extrathermodynamic assumption based on transfer parameters for tetraphenylarsonium tetraphenylboronate, (TATB), is used in conjunction with solubility data<sup>1-6</sup> to construct a Table of single ion transfer parameters applicable to the urea + water system. Transfer chemical potentials of the iron(II) complex ions, calculated from solubility data<sup>1</sup> and relevant single ion parameters, were used to probe the effects of added urea on the transfer chemical potentials of the initial and transition states for the reactions of hydroxide ions and iron(II) complexes. In Chapter 5 where kinetic data are analysed for reactions in a binary mixture of methyl alcohol and water the importance of well defined reference states is stressed<sup>8</sup>. In such systems the pure liquids, water and cosolvent are most convenient. In this Chapter however the situation is slightly different. Kinetic data are analysed for reactions carried out in a Typically Non-aqueous solvent system<sup>9</sup> which is an aqueous solution of urea. The composition of

the solvent is varied by changing the molality,  $m_u$ , or mass per cent,  $w_u\%$ , of urea. In a given solution of urea in water which contains  $n_u$  moles of urea and  $n_1$  moles of water, the molality of urea,  $m_u$ , in solution is given by  $m_u = n_u/(n_1M_1)$  where  $M_1$  is the molar mass of water. Similarly the mass per cent of urea in solution,  $w_u\%$ , is given by  $w_u\% = [(n_uM_u)/(n_1M_1+n_uM_u)]*100$ , where  $M_u$  is the molar mass of urea.

## 4.2 Experimental

### 4.2.1 Materials

All solutions of urea were prepared by weight using Gold Label ACS urea and fresh deionised water. A concentrated solution of the sulphate salt of  $[\text{Fe}(\text{phen})_3]^{2+}$  was obtained from Koch-Light Laboratories Ltd. and used without further purification.

$[\text{Fe}(\text{gmi})_3]^{2+}$  was prepared by S.Radulovic using iron(II) chloride, glyoxal and methylamine. The perchlorate salt of this cation was prepared by precipitation following addition of sodium perchlorate to the iron(II) complex solution. A concentrated solution of the salt was prepared in water.  $[\text{Fe}(\text{phen})_3]^{2+}$  produced a bright red solution in water and was characterised by an intense absorption band<sup>10</sup> in the visible region of the spectrum centered at  $\lambda_{\text{max}} = 510 \text{ nm}$ .  $[\text{Fe}(\text{gmi})_3]^{2+}$  produced a violet solution in water and was characterised by an intense absorption band<sup>11</sup> centered at  $\lambda_{\text{max}} = 554 \text{ nm}$  (see Figure 4.2 and 4.3).

### 4.2.2 Reaction Mechanism

The complexes studied in this Chapter and Chapter 5 contain

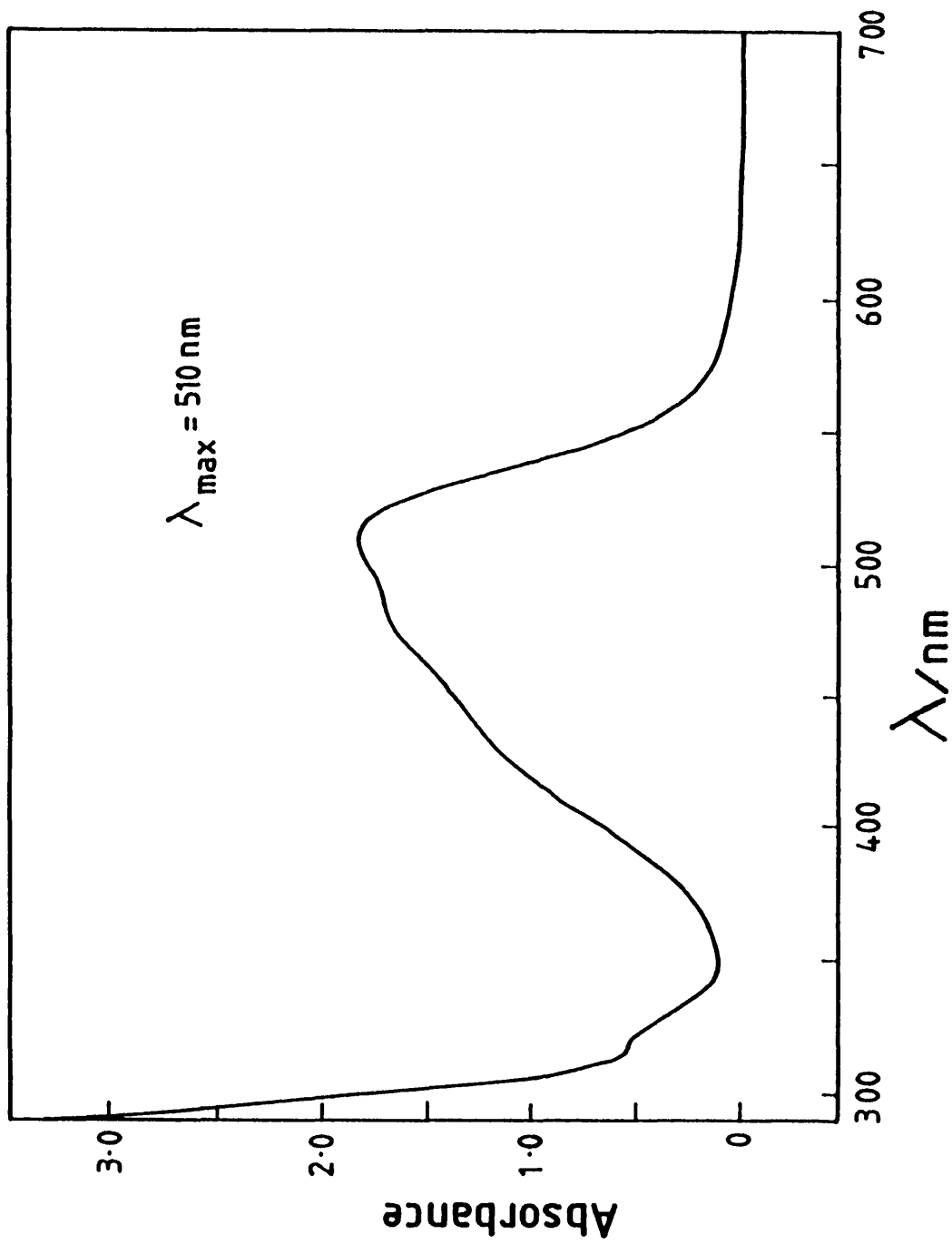


**FIGURE 4.2**  
Dependence of absorbance on wavelength of the iron(II), 1,10-phenanthroline complex ion  $[\text{Fe}(\text{phen})_3]^{2+}$ .

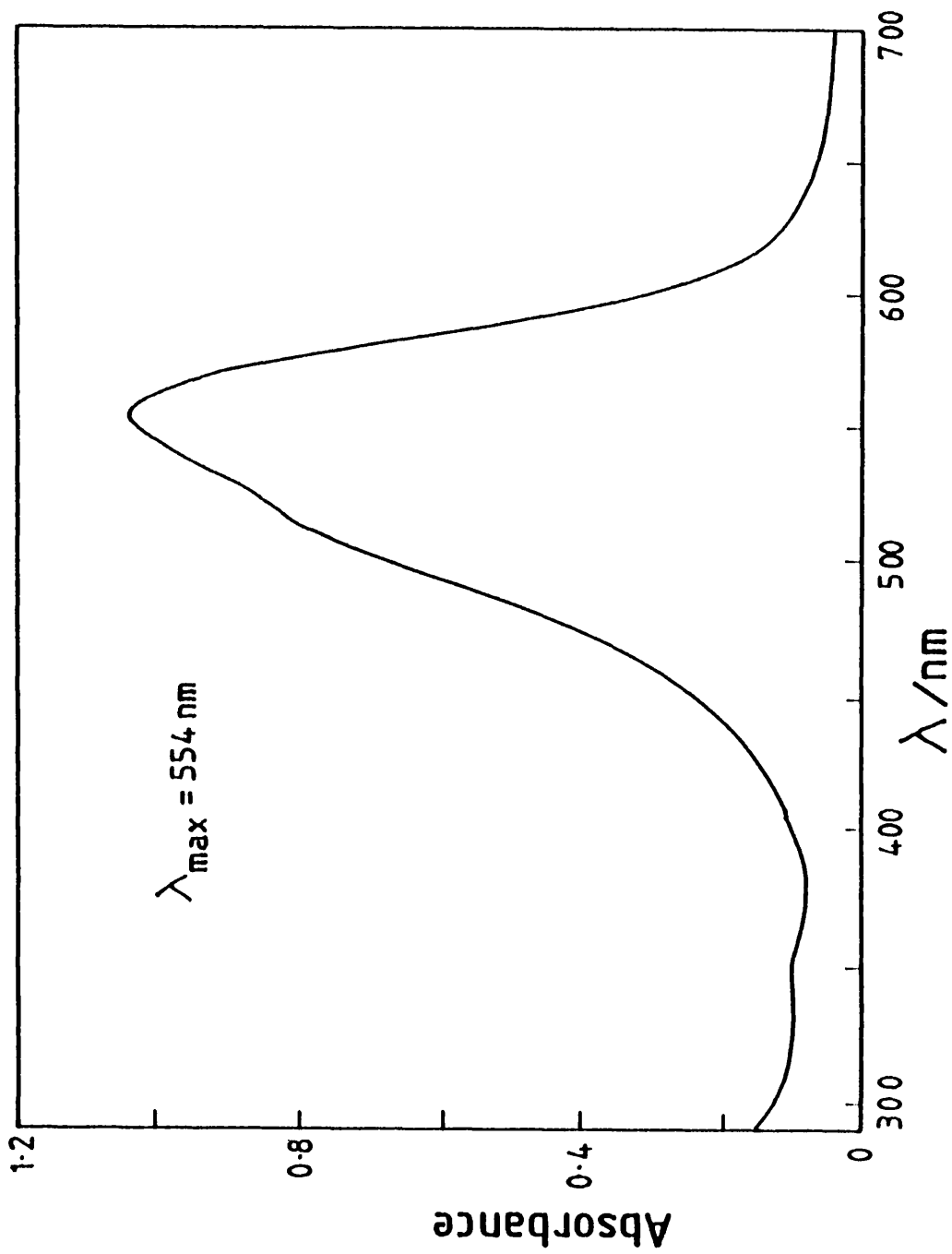


**FIGURE 4.3**  
Dependence of absorbance on wavelength of the iron(II) glyoxal bis-N-methylamine complex ion  $[\text{Fe}(\text{gmi})_3]^{2+}$ .

the iron atom in the +2 oxidation state, and as a result the arrangement of six  $d$  electrons needs to be taken into consideration. All of the complexes studied can be regarded as having octahedral,  $O_h$ , symmetry and unlike the majority of iron(II) complexes they are low-spin. This is demonstrated by the electron occupation diagram (Figure 4.4) which represents the splitting of a set of  $d$  orbitals by an octahedral electrostatic crystal field. The iron  $d_{x^2-y^2}$  and  $d_z^2$  orbitals are raised in energy whilst the  $d_{xy}$ ,  $d_{yz}$  and  $d_{zx}$  orbitals are lowered in energy.

All of the iron(II) complexes investigated contain the chelating unit shown below.



The intense colours of these complexes in aqueous solutions are believed to be due to transitions of  $d$  electrons from the iron atom to ligand orbitals to form a metal to ligand charge transfer band. More precisely the filled iron  $d$  orbitals,  $d_{xy}$ ,  $d_{yz}$  and  $d_{zx}$ , push electron density onto the lower lying vacant  $\pi$  antibonding orbitals of the ligands - such transitions invariably occur in the visible region and lead to the stabilisation of the complex.

For the alkaline hydrolysis reactions studied in this and the following Chapter, two possible positions of attack of hydroxide ions on the complex have been discussed<sup>12</sup>. The

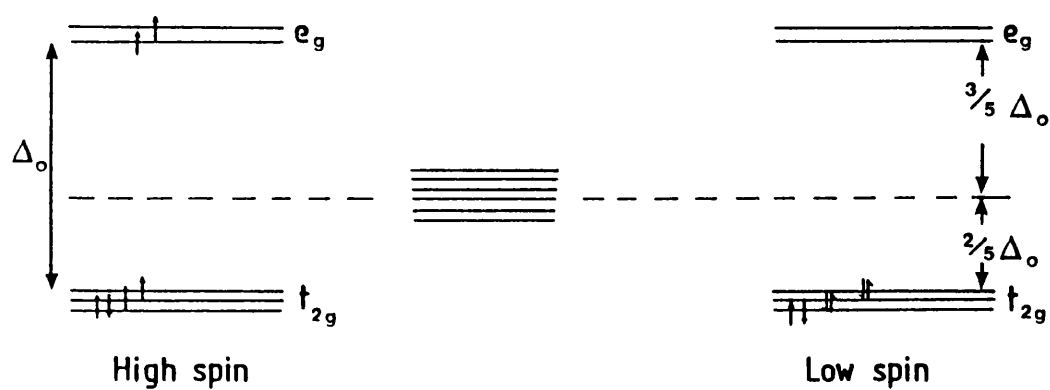
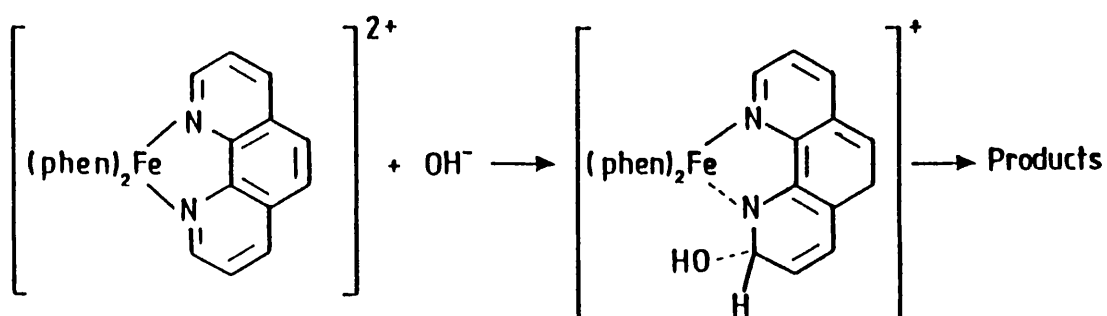


**FIGURE 4.4**

Energy level diagrams showing the splitting of a set of d-orbitals by an octahedral electrostatic crystal field.

first involves direct attack at the central iron atom and the second involves attack at the ligand (see scheme 1). The second possibility is thought to be the more plausible<sup>12,13</sup>.

Attack by hydroxide anions at the 2-position of the complexed pyridine ring causes part of the aromatic character of that ring to be lost, thus weakening the iron-nitrogen bond. The proximity of the OH-group to the central iron atom should aid the <sup>S<sub>N</sub>1</sup> transfer of OH from the carbon atom to the iron and hence break the iron-nitrogen bond. The ligand is then free to fall away.



Such a mechanism points towards the formation of some transient intermediate. Evidence for such intermediates has been obtained from the investigation of the alkaline hydrolysis of iron(II) hexadentate Schiff base in two neutral water in oil microemulsions<sup>14,15</sup>.

#### 4.2.3 Kinetics

Kinetics of reaction were measured under conditions in which  $[NaOH] \gg [complex]$  corresponding to typical first order conditions (see Chapter 2). The reactions were

monitored using an HP 8451A diode array spectrophotometer, by the decrease in absorbance at  $\lambda_{\max}$  with time. The data were analysed using the non-linear least squares method outlined in Chapter 2 to obtain estimates of the first order rate constants. The rates of the alkaline hydrolysis reactions of both  $[\text{Fe}(\text{phen})_3]^{2+}$  and  $[\text{Fe}(\text{gmi})_3]^{2+}$  ions are known to follow the rate equation<sup>16</sup>;

$$-d[\text{complex}]/dt = k_1[\text{complex}] + k_2[\text{complex}][\text{NaOH}] \quad [4.1]$$

where  $k_1$  is the first order rate constant for the aquation of the complex and  $k_2$  is a second order rate constant. Under conditions in which  $[\text{NaOH}] \gg [\text{complex}]$  then an observed rate constant is defined by equation [4.2].

$$k_{\text{obs}} = k_1 + k_2[\text{NaOH}] \quad [4.2]$$

Both  $k_1$  and  $k_2$  are calculated using a linear least squares procedure<sup>17</sup>. The rate of aquation characterised by  $k_1$  was found to be negligible compared to the rate of the second order reaction under the conditions described above.

#### 4.2.4 Solubilities

Solubilities were measured<sup>6,7</sup> using either the absorbances of saturated solutions in the UV/visible region or flame photometry.

### 4.3 The TATB Assumption and Calculation of Single Ion Transfer Quantities

A given solution contains  $n_1$  moles of water,  $n_u$  moles of urea and  $n_j$  moles of added solute-j where  $n_j < n_1$  and  $n_u$ . At equilibrium the total Gibbs function of the system at temperature T and pressure p is given by equation [4.3].

$$G^{\text{eq}}(\text{sys};T;p) = n_1\mu_1^{\text{eq}}(\text{sys};T;p) + n_u\mu_u^{\text{eq}}(\text{sys};T;p) + n_j\mu_j^{\text{eq}}(\text{sys};T;p) \quad [4.3]$$

Any description of such a system must be consistent with the same  $G^{\text{eq}}(\text{sys};T;p)$  and the same equilibrium chemical potentials for each substance. In the following account the system is described as a solution of substance-j in a solvent composed of a mixture of 'urea + water'<sup>8</sup>. Hence the molality of solute-j is given by equation [4.4].

$$m_j = n_j / (n_1 M_1 + n_u M_u) \quad [4.4]$$

where  $M_1$  and  $M_u$  are the molar masses of water and urea respectively. If the system has a volume V then the concentration of added solute-j in solution is given by;

$$c_j = n_j / V \quad [4.5]$$

The concentration of solute-j,  $c_j$ , is related to its chemical potential in a solvent of composition  $w_u\%$  by equation [4.6].

$$\mu_j(\text{aq}; w_u\%; T; p) = \mu_j^\#(\text{aq}; w_u\%; \text{c-scale}; T; p) + RT \ln[(c_j y_j(\text{aq}; w_u\%))/c_r] \quad [4.6]$$

By definition  $\lim(c_j \rightarrow 0) y_j(\text{aq}; w_u\%) = 1$ ;  $c_r = 1 \text{ mol dm}^{-3}$ . The reference state of the solute is a solution in which  $c_j = 1.0 \text{ mol dm}^{-3}$  and  $y_j(\text{aq}; w_u\%) = 1.0$  and the chemical potential of substance-j is described by  $\mu_j^\#(\text{aq}; w_u\%; \text{c-scale}; T; p)$ . If solute-j is a salt which on complete dissociation forms  $v$  ions (i.e.  $v = v_+ + v_-$ ) then the chemical potential of the salt-j in a system of composition  $w_u\%$  is given by;

$$\mu_j(\text{aq}; w_u\%; T; p) = \mu_j^\#(\text{aq}; w_u\%; \text{c-scale}; T; p) + vRT \ln[(Q c_j y_\pm(\text{aq}; w_u\%))/c_r] \quad [4.7]$$

where  $Q$  is a function of the stoichiometry of the salt ( $= (v_+^{v_+} v_-^{v_-})^{1/v}$ );  $y_\pm$  is a mean ionic activity coefficient and where by definition  $\lim(c_j \rightarrow 0) y_\pm = 1$  at all temperatures and pressures. The reference chemical potential of the salt  $\mu_j^\#(\text{aq}; w_u\%; \text{c-scale}; T; p)$  thus depends on the composition of the aqueous urea solution and on the corresponding reference chemical potentials of the ions. A transfer chemical potential for solute-j is defined as the difference between the chemical potentials of the solute in reference states in the solvent, urea + water, and in water.

$$\Delta(\text{aq} \rightarrow w_u\%) \mu_j^\#(\text{c-scale}; \text{sln}; T; p) = \mu_j^\#(\text{aq}; w_u\%; \text{c-scale}; T; p) - \mu_j^\#(\text{c-scale}; \text{aq}; T; p) \quad [4.8]$$

Hence for a 1:1 salt;

$$\begin{aligned} \Delta(\text{aq} \rightarrow w_u\%) \mu_j^\#(\text{c-scale}; \text{sln}; T; p) = \\ \Delta(\text{aq} \rightarrow w_u\%) \mu_+^\#(\text{c-scale}; \text{sln}; T; p) \\ + \Delta(\text{aq} \rightarrow w_u\%) \mu_-^\#(\text{c-scale}; \text{sln}; T; p) \quad [4.9] \end{aligned}$$

The single ion transfer parameters reported in this Chapter are based on the extrathermodynamic assumption set out in equation [4.10].

$$\begin{aligned} \Delta(\text{aq} \rightarrow w_u\%) \mu^\#(\text{Ph}_4\text{As}^+; \text{c-scale}; T; p) \\ = \Delta(\text{aq} \rightarrow w_u\%) \mu^\#(\text{Ph}_4\text{B}^-; \text{c-scale}; T; p) \quad [4.10] \end{aligned}$$

i.e. the transfer chemical potential of the  $\text{Ph}_4\text{B}^-$  anion, or  $\text{Ph}_4\text{As}^+$  cation, is defined as one half the transfer chemical potential of the corresponding salt. The transfer chemical potentials for  $\text{Ph}_4\text{AsBPh}_4$  in various aqueous urea solutions were taken from the work of Kundu and Das<sup>2</sup>. These authors reported transfer parameters on the mole fraction scale, x-scale, and for consistency with previous work<sup>8</sup> these estimates were converted to the concentration scale, c-scale, using equation [4.11]<sup>8</sup>.

$$\begin{aligned} \Delta(\text{aq} \rightarrow w_u\%) \mu_j^\#(\text{c-scale}) = \Delta(\text{aq} \rightarrow w_u\%) \mu_j^\#(\text{x-scale}) \\ + RT \ln \left[ \frac{(10^2/M_1)}{\{((10^2 - w_u\%)/M_1) + (w_u\%/M_u)\}} \left\{ \frac{\rho(\text{aq})}{\rho(w_u\%)} \right\} \right] \quad [4.11] \end{aligned}$$

Here  $\rho(\text{aq})$  is the density of water at ambient temperature and pressure and  $\rho(w_u\%)$  is the density of a solution of urea containing  $w_u\%$  urea at ambient temperature and pressure. The densities of urea solutions in the region 5.67  $w_u\%$  to 43.84  $w_u\%$  were calculated using equation

[4.12], taken from the work of Desnoyers et al<sup>18</sup>.

$$\phi_v = 44.20 + 0.126m_u - 0.004m_u^2 \quad [4.12]$$

where  $m_u$  is the molality of added urea. Hence the volume of the solution was calculated from equation [4.13].

$$V/\text{cm}^3 = 10^3 V_1^* + m_u \phi_v \quad [4.13]$$

where  $M_1 = 0.018015 \text{ kg mol}^{-1}$  and  $V_1^*/\text{cm}^3 \text{ g}^{-1} = 1.002961$  (ref. 19). The mass of the solution was calculated from equation [4.14].

$$M = 1.0 + m_u M_u \quad [4.14]$$

Hence the density of solution was calculated in the usual way by the combination of equations [4.13] and [4.14]. Figure 4.5 shows a plot of the density of aqueous urea solutions against the weight per cent of added urea over the range  $6 \leq w_u \% \leq 43$ .

Once this basis for single ion transfer parameters (i.e. TATB) has been established, single ion transfer parameters for other anions and cations readily follow from solubility data of salts in aqueous urea solutions. The solubility of a salt-j in an aqueous urea solution and pure water are denoted by the symbols  $S_j^{\text{eq}}(\text{aq}; w_u \%)$  and  $S_j^{\text{eq}}(\text{aq})$  respectively. These solubilities are related to the reference chemical potential of the salt by equation [4.15].

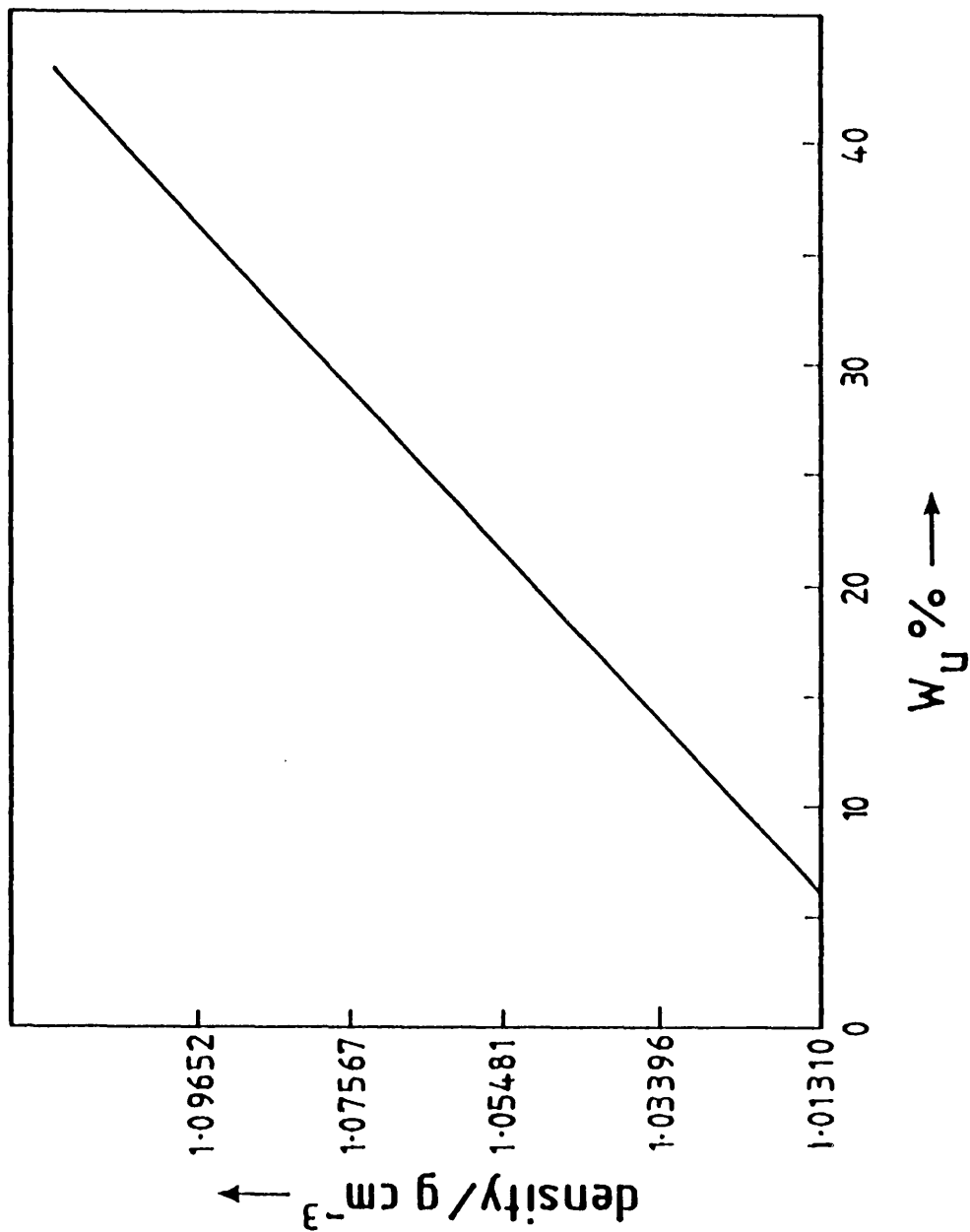


**FIGURE 4.5**

Density of aqueous urea solutions against weight per cent urea in solution in the region  $5.67 \ll W_U \ll 43.84$ .

$$\Delta(\text{aq} \rightarrow w_u\%) \mu_j^\#(\text{c-scale; sln; T; p}) = -\nu RT \ln[(S_j^{\text{eq}}(\text{aq}; w_u\%) y_{\pm}^{\text{eq}}(\text{aq}; w_u\%)) / (S_j^{\text{eq}}(\text{aq}) y_{\pm}^{\text{eq}}(\text{aq}))] \quad [4.15]$$

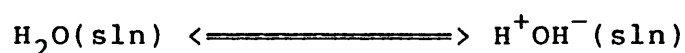
The assumption is made that,  $y_{\pm}^{\text{eq}}(\text{aq}; w_u\%) / y_{\pm}^{\text{eq}}(\text{aq}) = 1.0$ .

#### 4.4 The Self Dissociation of Water and Transfer Parameters for H<sup>+</sup> and OH<sup>-</sup>

The chemical potential of water in the solvent urea + water is given by equation [4.16].

$$\mu_1(\text{aq}; T; p) = \mu_1^*(l; T; p) + RT \ln(x_1 f_1) \quad [4.16]$$

where  $x_1$  is the mole fraction of water in the system and  $f_1$  is a rational activity coefficient;  $\lim(x_1 \rightarrow 1) f_1 = 1.0$  at all temperatures and pressures. At equilibrium, a small amount of water undergoes dissociation.



The water in solution is in equilibrium with effectively a 1:1 electrolyte. The chemical potential of H<sup>+</sup>OH<sup>-</sup> in water is given by equation [4.17].

$$\mu(\text{H}^+\text{OH}^-; \text{aq}) = \mu^\#(\text{H}^+\text{OH}^-; \text{aq}) + 2RT \ln[(c(\text{H}^+\text{OH}^-) y_{\pm}(\text{H}^+\text{OH}^-)) / c_r] \quad [4.17]$$

At equilibrium the latter two equations can be equated;

$$\mu_1^*(l; T; p) + RT \ln(x_1 f_1) = \mu^\#(\text{H}^+\text{OH}^-; \text{aq}) + 2RT \ln[(c(\text{H}^+\text{OH}^-) y_{\pm}(\text{H}^+\text{OH}^-)) / c_r] \quad [4.18]$$

A standard equilibrium constant for the self dissociation of water is thus defined by equation [4.19].

$$\begin{aligned}\Delta_r G^\circ(\text{aq}; T) &= \mu^\#(\text{H}^+\text{OH}^-; \text{aq}) - \mu_1^*(1; T; p) \\ &= -RT \ln \left[ \frac{\{c(\text{H}^+\text{OH}^-) y_{\pm}(\text{H}^+\text{OH}^-)\}^2}{(c_r^2 x_1 f_1)} \right]_{\text{aq}} \quad [4.19]\end{aligned}$$

where;

$$K_w^\#(\text{c-scale}; T; \text{aq}) = -RT \ln \left[ \frac{\{c(\text{H}^+\text{OH}^-) y_{\pm}(\text{H}^+\text{OH}^-)\}^2}{(c_r^2 x_1 f_1)} \right]_{\text{aq}} \quad [4.20]$$

For dilute solutions  $(x_1 f_1)$  is approximately unity. By definition;

$$\begin{aligned}pK_w^\#(\text{c-scale}; T; \text{aq}) &= -\log_{10} K_w^\#(\text{c-scale}; T; \text{aq}) \\ &\approx -\log_{10} \left[ \frac{\{c(\text{H}^+\text{OH}^-) y_{\pm}(\text{H}^+\text{OH}^-)\}^2}{c_r^2} \right] \quad [4.21]\end{aligned}$$

Turning to the effects of added urea on the self dissociation of water, the reference state for pure water is retained however the reference state for  $\text{H}^+\text{OH}^-$  is now altered to depend on the composition of the system  $w_u\%$ . Equation [4.21] can be rewritten;

$$\begin{aligned}\Delta_r G(\text{aq}; w_u\%; T) &= \mu^\#(\text{H}^+\text{OH}^-; \text{aq}; w_u\%; T) - \mu_1^*(1; T; p) \\ &= -RT \ln K_w^\#(\text{aq}; w_u\%; T) \quad [4.22]\end{aligned}$$

where;

$$\begin{aligned}K_w^\#(\text{c-scale}; \text{aq}; w_u\%; T) &= \\ &= -RT \ln \left[ \frac{\{c(\text{H}^+\text{OH}^-) y_{\pm}(\text{H}^+\text{OH}^-)\}^2}{(c_r^2 x_1 f_1)} \right]_{\text{aq}; w_u\%} \quad [4.23]\end{aligned}$$

In dilute aqueous urea solutions the assumption which sets  $(x_1 f_1) = 1.0$  is invalid. However an apparent quantity can be defined using equation [4.24].

$$\begin{aligned} pK_w^\#(c\text{-scale}; \text{appar}; \text{aq}; w_u\%; T) &= \\ &= -\log_{10} K_w^\#(c\text{-scale}; \text{appar}; \text{aq}; w_u\%; T) \\ &\approx -RT \ln \left[ \frac{\{c(\text{H}^+\text{OH}^-) y_{\pm}(\text{H}^+\text{OH}^-)\}^2}{c_r^2} \right]_{\text{aq}; w_u\%} \quad [4.24] \end{aligned}$$

The target quantity in this analysis is the transfer parameter for the  $\text{H}^+\text{OH}^-$  electrolyte,  $\Delta(\text{aq} \rightarrow w_u\%) \mu^\#(\text{H}^+\text{OH}^-; \text{sln}; T)$ . This can be obtained through equation [4.25]; (cf. equation [4.8]).

$$\begin{aligned} \Delta(\text{aq} \rightarrow w_u\%) \mu^\#(c\text{-scale}; \text{sln}; T) &= \mu^\#(\text{H}^+\text{OH}^-; c\text{-scale}; \text{aq}; w_u\%; T) \\ &\quad - \mu^\#(\text{H}^+\text{OH}^-; c\text{-scale}; \text{aq}; T) \quad [4.25] \end{aligned}$$

$$\begin{aligned} &= [\mu^\#(\text{H}^+\text{OH}^-; \text{aq}; w_u\%; T) - \mu_1^*(1; T; p)] \\ &\quad - [\mu^\#(\text{H}^+\text{OH}^-; \text{aq}; T) - \mu_1^\#(1; T; p)] \quad [4.26] \end{aligned}$$

$$\begin{aligned} &= [-RT \ln K^\#(c\text{-scale}; T; \text{aq}; w_u\%)] - [-RT \ln K^\#(c\text{-scale}; T; \text{aq})] \\ &\quad [4.27] \end{aligned}$$

Then;

$$\begin{aligned} \Delta(\text{aq} \rightarrow w_u\%) \mu^\#(c\text{-scale}; \text{sln}; T) &= RT \ln \{x_1 f_1\}_{\text{aq}; w_u\%} \\ &\quad + RT \{ \ln(10) \{ pK_w(\text{appar}; c\text{-scale}; \text{aq}; w_u\%; T) \\ &\quad - pK_w(c\text{-scale}; T; \text{aq}) \} \} \quad [4.28] \end{aligned}$$

Hence the transfer parameters for  $\text{H}^+\text{OH}^-$  are defined by the difference between  $pK_w$  parameters plus a correction factor<sup>4</sup> for the non-ideal properties of aqueous urea solutions.

#### 4.5 Initial and Transition State Analysis

Under conditions in which complex concentration in solution is small compared to hydroxide concentration within the reaction mixture (cf. equations [4.1] and [4.2] ) the second order rate constant,  $k_2$ , is related to the molar Gibbs function of activation,  $\Delta^\ddagger G^\#(c\text{-scale})$ , through Transition State Theory<sup>20</sup>.

$$[(k_2 c_r s h)/(k_B T)] = \exp[-\Delta^\ddagger G^\#(c\text{-scale})/RT] \quad [4.29]$$

where  $c_r = 1 \text{ mol dm}^{-3}$  and  $s = 1 \text{ second}$ . These quantities are included to preserve dimensional consistency.  $h$  is Plancks constant and  $k_B$  the Boltzmann constant. It is further assumed that the transmission is unity and/or is independent of solvent composition. A transfer Gibbs function of activation is obtained by considering second order rate constants in water,  $k_2(aq;T)$ , and in aqueous urea solution,  $k_2(aq;w_u\%;T)$ .

$$\Delta(aq \rightarrow w_u\%) \Delta^\ddagger G^\#(c\text{-scale};T) = -RT \ln[k_2(aq;T)/k_2(aq;w_u\%;T)] \quad [4.30]$$

$$\begin{aligned} &= \Delta(aq \rightarrow w_u\%) \mu_{\ddagger}^\#(c\text{-scale};sln;T) \\ &- \Delta(aq \rightarrow w_u\%) \mu^\#(\text{complex};c\text{-scale};sln;T) \\ &- \Delta(aq \rightarrow w_u\%) \mu^\#(\text{OH}^-;c\text{-scale};sln;T) \quad [4.31] \end{aligned}$$

Hence the effects of added solvent on the transition state,  $\Delta(aq \rightarrow w_u\%) \mu_{\ddagger}^\#(c\text{-scale};sln;T)$ , can be calculated from the appropriate solubility and kinetic data.

$$\begin{aligned} \Delta(\text{aq} \rightarrow \text{w}_u\%) \mu_{\ddagger}^{\#}(\text{c-scale}; \text{sln}; T) = & \\ & \Delta(\text{aq} \rightarrow \text{w}_u\%) \Delta^{\ddagger G \#}(\text{c-scale}; T) \\ & + \Delta(\text{aq} \rightarrow \text{w}_u\%) \mu^{\#}(\text{complex}; \text{c-scale}; \text{sln}; T) \\ & + \Delta(\text{aq} \rightarrow \text{w}_u\%) \mu^{\#}(\text{OH}^{-}; \text{c-scale}; \text{sln}; T) \quad [4.32] \end{aligned}$$

The overall effect of solvent on the initial state is obtained by combining the transfer parameters for the two reactants, complex and hydroxide ions.

$$\begin{aligned} \Delta(\text{aq} \rightarrow \text{w}_u\%) \mu_{is}^{\#}(\text{c-scale}; \text{sln}; T) = & \\ & \Delta(\text{aq} \rightarrow \text{w}_u\%) \mu^{\#}(\text{complex}; \text{c-scale}; \text{sln}; T) \\ & + \Delta(\text{aq} \rightarrow \text{w}_u\%) \mu^{\#}(\text{OH}^{-}; \text{c-scale}; \text{sln}; T) \quad [4.33] \end{aligned}$$

#### 4.6 Results

Tables 4.1 and 4.2 report observed first order rate constants for the alkaline hydrolysis of  $[\text{Fe}(\text{phen})_3]^{2+}$  and  $[\text{Fe}(\text{gmi})_3]^{2+}$  ions in aqueous urea solutions. The dependences on hydroxide concentrations were fitted to equation [4.2] using a linear least squares technique to produce estimates of  $k_1$  and  $k_2$  for each urea solution. Estimates of  $k_2$  together with their standard errors are reported for both iron complexes in Tables 4.3 and 4.4. In all cases rate constants  $k_1$ , describing the aquation rate, were found to be negligibly small in comparison to the second order rate constants.

Single ion transfer parameters, all expressed using the concentration scale, are reported in Table 4.5 together with the relevant literature reference. This information is represented in plots of single ion transfer parameters against  $w_u\%$  urea in aqueous solution; Figure 4.6. Single

Table 4.1

First order rate constants for reaction between  $[\text{Fe}(\text{phen})_3]^{2+}$  and hydroxide ions in water and urea + water mixtures at constant ionic strength  $I=0.33 \text{ mol dm}^{-3}$  at 298K

[NaOH] /mol dm <sup>-3</sup>	wt% Urea			
	0	10	20	30
	$10^4 \text{ k/s}^{-1}$			
0.0050	1.066	1.207	1.450	2.183
0.0075	1.307	1.545	1.888	2.360
0.0100	1.450	1.753	2.171	2.557
0.0150	1.853	2.224	2.449	2.891
0.0200	2.362	2.669	2.961	3.412

Table 4.2

First order rate constants for reaction between  $[\text{Fe}(\text{gmi})_3]^{2+}$  and hydroxide ions in water and urea + water mixtures at constant ionic strength  $I=0.33 \text{ mol dm}^{-3}$  at 298K.

[NaOH] /mol dm <sup>-3</sup>	wt% Urea			
	0	10	20	30
	$10^5 \text{ k/s}^{-1}$			
0.0050	2.63	3.48	3.98	4.98
0.0075	4.65	5.52	7.10	8.24
0.0100	5.51	7.02	9.69	11.66
0.0150	8.66	10.37	16.67	21.78
0.0200	11.40	14.77	22.95	30.67

Table 4.3

Second order rate constants for reaction between  $[\text{Fe}(\text{phen})_3]^{2+}$  and hydroxide ions in water and urea + water mixtures at constant ionic strength  $I=0.33 \text{ mol dm}^{-3}$  and 298K

wt% Urea	$10^3 \text{ k/dm}^3 \text{ mol}^{-1} \text{ s}^{-1}$
0	8.430 (+ 0.378)
10	9.528 (+ 0.366)
20	9.310 (+ 0.986)
30	8.038 (+ 0.428)

Table 4.4

Second order rate constants for reaction between  $[\text{Fe}(\text{gmi})_3]^{2+}$  and hydroxide ions in water and urea + water mixtures at constant ionic strength  $I=0.33 \text{ mol dm}^{-3}$  and 298K

wt% Urea	$10^3 \text{ k/dm}^3 \text{ mol}^{-1} \text{ s}^{-1}$
0	5.696 (+ 0.297)
10	7.356 (+ 0.278)
20	12.727 (+ 0.258)
30	17.526 (+ 0.742)

Table 4.5

Single ion transfer parameters (c-scale) from water to urea + water mixtures at 298K using the  $\text{Ph}_4\text{As}^+/\text{Ph}_4\text{B}^-$  assumption. Units of transfer parameters are  $\text{kJmol}^{-1}$ .

ref		wt% Urea			
		11.52	20.31	29.64	36.83
17	$\text{H}^+$	-1.19	-2.15	-4.06	-4.76
5	$\text{Li}^+$	2.44	3.16	2.77	3.07
5	$\text{Na}^+$	2.85	3.82	3.68	4.02
2	$\text{K}^+$	2.64	3.66	3.47	3.77
5	$\text{Rb}^+$	2.54	3.46	3.27	3.57
5	$\text{Cs}^+$	2.44	3.26	2.97	3.07
2	$\text{Ph}_4\text{As}^+/\text{BPh}_4^-$	-1.26	-2.99	-3.64	-4.23
†	$\text{OH}^{-*}$	-1.78	-2.12	-0.96	-
6	$\text{ClO}_4^{-*}$	-2.96	-4.64	-4.43	-
5	$\text{Cl}^-$	-2.58	-3.37	-3.01	-3.18
5	$\text{Br}^-$	-2.78	-3.65	-3.41	-3.68
5	$\text{I}^-$	-2.88	-3.87	-3.71	-4.18
2	$\text{Pi}^-$	-3.27	-5.33	-6.44	-7.33
3	$\text{BrO}_3^{-**}$	-3.52	-4.61	-5.74	-6.86
3	$\text{IO}_3^{-**}$	-5.53	-7.16	-8.24	-9.27
3	$\text{SO}_4^{2-**}$	-2.53	-5.77	-7.78	-9.90
3	$\text{CrO}_4^{2-**}$	-10.41	-14.42	-17.61	-20.86
3	$\text{Cr}_2\text{O}_7^{2-**}$	-6.33	-9.80	-13.23	-15.38

\* - values at 10, 20 and 30 wt% Urea

\*\* - Single ion transfer parameters calculated from the standard potentials of the silver-silver bromate, silver-silver iodate, silver-silver sulphate, silver-silver chromate and silver-silver dichromate electrodes.

† - Calculated from  $\text{H}^+\text{OH}^-$  data from references 1,4 and 5.

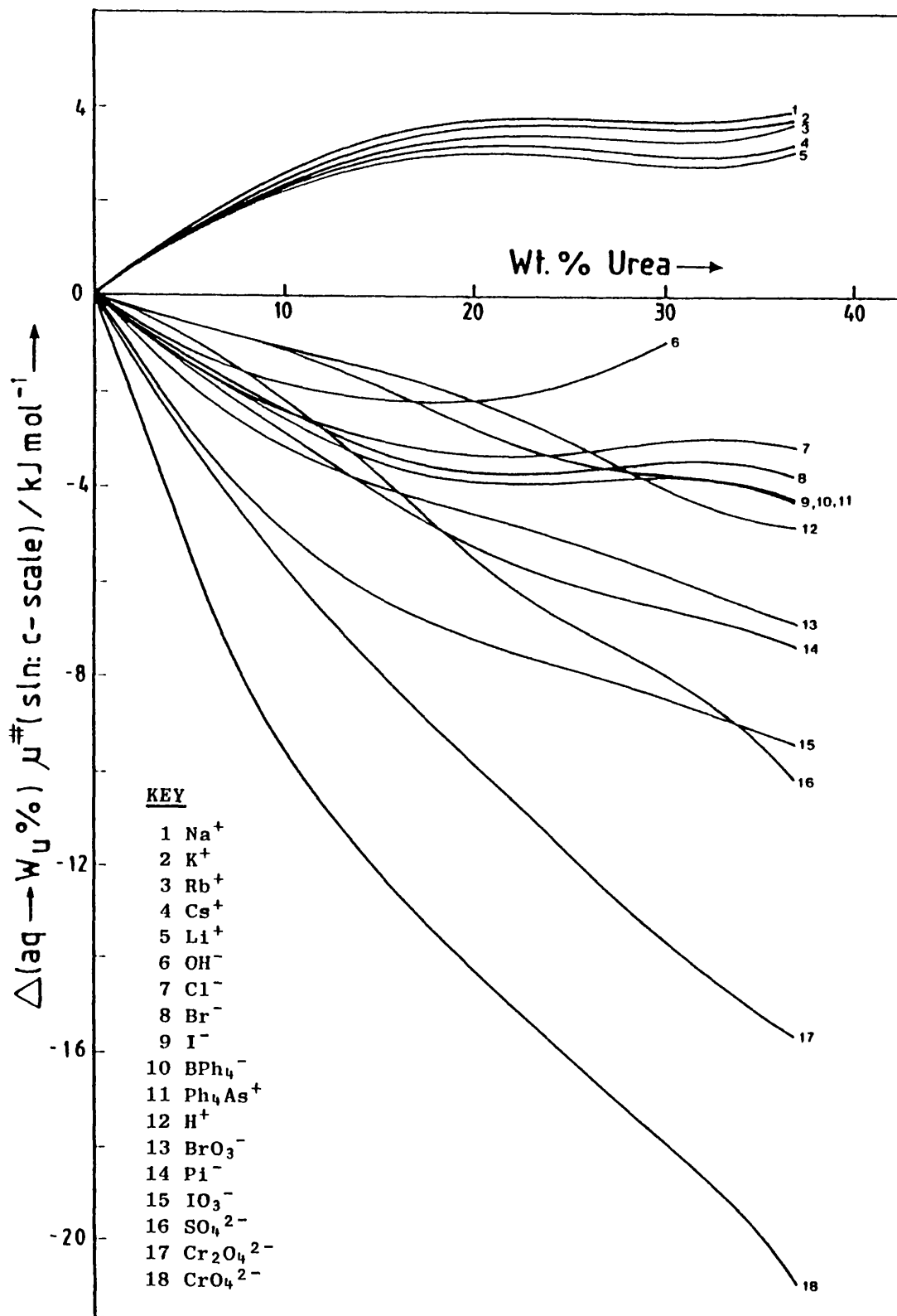


FIGURE 4.6

Single ion transfer parameters (c-scale) from water to 'urea + water' mixtures at 298 K using the Ph<sub>4</sub>As<sup>+</sup>/Ph<sub>4</sub>B<sup>-</sup> assumption.

ion transfer parameters for  $H^+$  ions were recalculated from the data of Kundu and Mazumdar<sup>21</sup> using estimates of parameters for  $K^+$  and  $Cl^-$  ions calculated by Das and Kundu<sup>2</sup> using the TATB assumption. The transfer parameters for  $H^+OH^-$  from various authors<sup>1,4,5</sup> show good agreement, see Figure 4.7. However the estimates diverge at high  $w_u\%$ . A single line was drawn through these points and values interpolated from this curve were used in conjunction with transfer values for  $H^+$  ions<sup>21</sup> to calculate single ion transfer quantities for  $OH^-$  ions.

Solubility data for the  $[Fe(phen)_3]^{2+}$  and  $[Fe(gmi)_3]^{2+}$  complexes were obtained by S.Radulovic<sup>7</sup> for the perchlorate salts. These data were used in conjunction with transfer parameters for  $OH^-$  and  $ClO_4^-$  ions to investigate the effects of solvent on the initial and transition states for both complexes. Tables 4.6 and 4.7 report calculated initial and transition state transfer chemical potentials as a function of  $w_u\%$ . The same information is represented graphically for the  $[Fe(phen)_3]^{2+}$  and  $[Fe(gmi)_3]^{2+}$  complexes in Figures 4.8 and 4.9 respectively.

#### 4.7 Discussion

The Gibbs function for activation,  $\Delta^\ddagger G^\#$ , for the alkaline hydrolysis of  $[Fe(gmi)_3]^{2+}$  cations decreased with increase in  $w_u\%$  urea in solution and as a consequence the rate of reaction increased at 298.15 K and ambient pressure with increase in  $w_u\%$  urea. At 10  $w_u\%$  urea both the initial and transition states are destabilised. In the case of the initial state this is due to the large destabilisation of

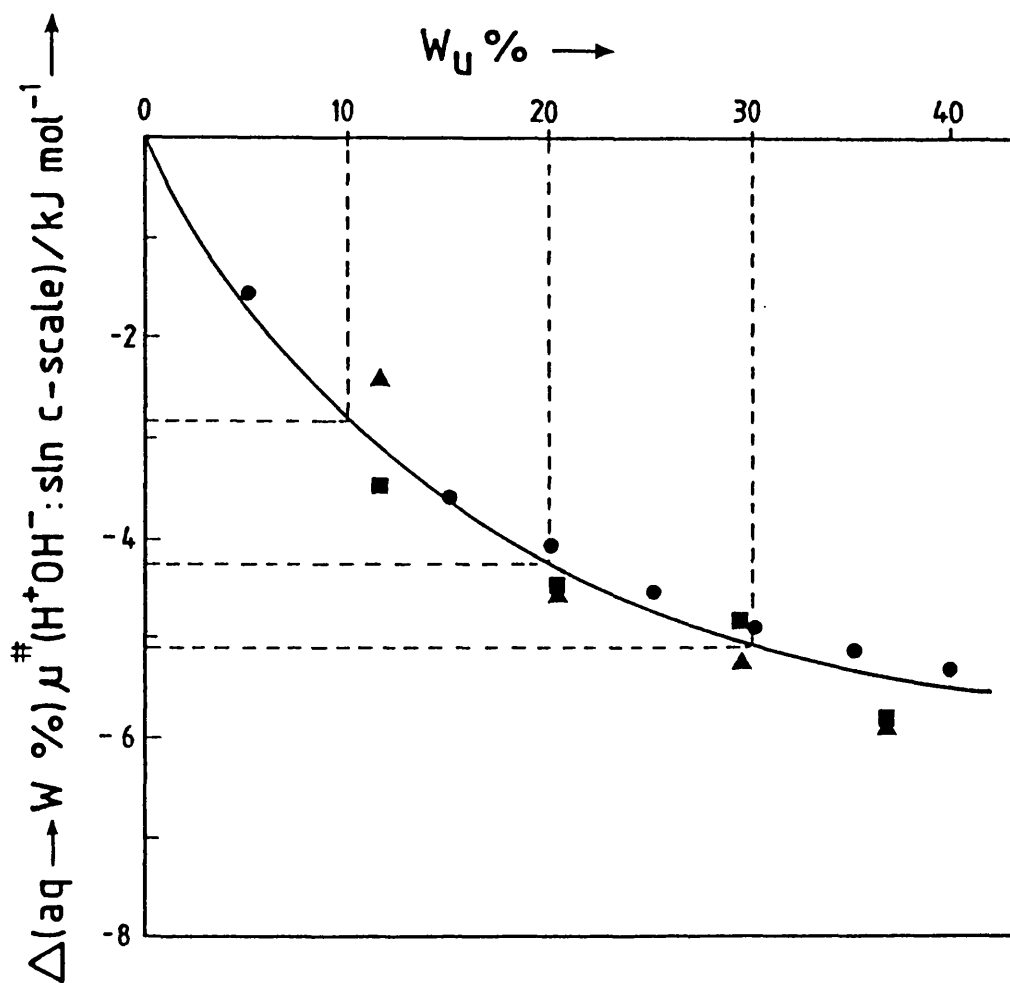


FIGURE 4.7

Dependence on  $W_u\%$  of  $\Delta(aq + W_u\%) \mu^\#(H^+OH^-; c\text{-scale}; 298.15 \text{ K}; \text{ambient pressure})$ ; data from reference 4 (●), 5 (▲), and 1 (■).

Table 4.6

Transfer parameters, for reaction of  $[\text{Fe}(\text{phen})_3]^{2+}$  with hydroxide ions, from water to urea + water mixtures at 298K on the c-scale. Units of transfer are  $\text{kJmol}^{-1}$ .

Wt.% Urea	0	10	20	30
$\Delta(\text{aq} \rightarrow \text{w}_u\%) \Delta^\ddagger G(\text{c})^*$	0	-0.30	-0.25	0.12
$\Delta(\text{aq} \rightarrow \text{w}_u\%) \mu^\#(\text{c}) \text{ salt}^{**}$	0	-3.97	-8.47	-12.01
$\Delta(\text{aq} \rightarrow \text{w}_u\%) \mu^\#(\text{c}) (2\text{ClO}_4^-)$	0	-5.92	-9.28	-8.85
$\Delta(\text{aq} \rightarrow \text{w}_u\%) \mu^\#(\text{c}) [\text{Fe}(\text{phen})_3]^{2+}$	0	1.95	0.81	3.16
$\Delta(\text{aq} \rightarrow \text{w}_u\%) \mu^\#(\text{c}) \text{OH}^-$	0	-1.78	-2.12	-0.96
$\Delta(\text{aq} \rightarrow \text{w}_u\%) \mu_{is}^\#(\text{c})$	0	0.17	-1.30	-4.12
$\Delta(\text{aq} \rightarrow \text{w}_u\%) \mu_{\ddagger}^\#(\text{c})$	0	-0.13	-1.55	-4.00

\* - (c) represents (c-scale;sln;T)

\*\* - salt is  $[\text{Fe}(\text{phen})_3(\text{ClO}_4)_2]$ . Solubility data ref.7.

Table 4.7

Transfer parameters, for reaction of  $[\text{Fe}(\text{gmi})_3]^{2+}$  with hydroxide ions, from water to urea + water mixtures at 298K on the c-scale. Units of transfer are  $\text{kJmol}^{-1}$ .

Wt.% Urea	0	10	20	30
$\Delta(\text{aq} \rightarrow \text{w}_u\%) \Delta^\ddagger G(\text{c})^*$	0	-0.63	-1.99	-2.79
$\Delta(\text{aq} \rightarrow \text{w}_u\%) \mu^\#(\text{c}) \text{ salt}^{**}$	0	-2.88	-7.54	-10.21
$\Delta(\text{aq} \rightarrow \text{w}_u\%) \mu^\#(\text{c}) (2\text{ClO}_4^-)$	0	-5.92	-9.28	-8.85
$\Delta(\text{aq} \rightarrow \text{w}_u\%) \mu^\#(\text{c}) [\text{Fe}(\text{gmi})_3]^{2+}$	0	3.05	1.74	-1.36
$\Delta(\text{aq} \rightarrow \text{w}_u\%) \mu^\#(\text{c}) \text{OH}^-$	0	-1.78	-2.12	-0.96
$\Delta(\text{aq} \rightarrow \text{w}_u\%) \mu_{\text{is}}^\#(\text{c})$	0	1.27	-0.38	-2.32
$\Delta(\text{aq} \rightarrow \text{w}_u\%) \mu_{\ddagger}^\#(\text{c})$	0	0.63	-2.37	-5.10

\* - (c) represents (c-scale;sln;T)

\*\* - salt is  $[\text{Fe}(\text{gmi})_3(\text{ClO}_4)_2]$ . Solubility data ref. 7.

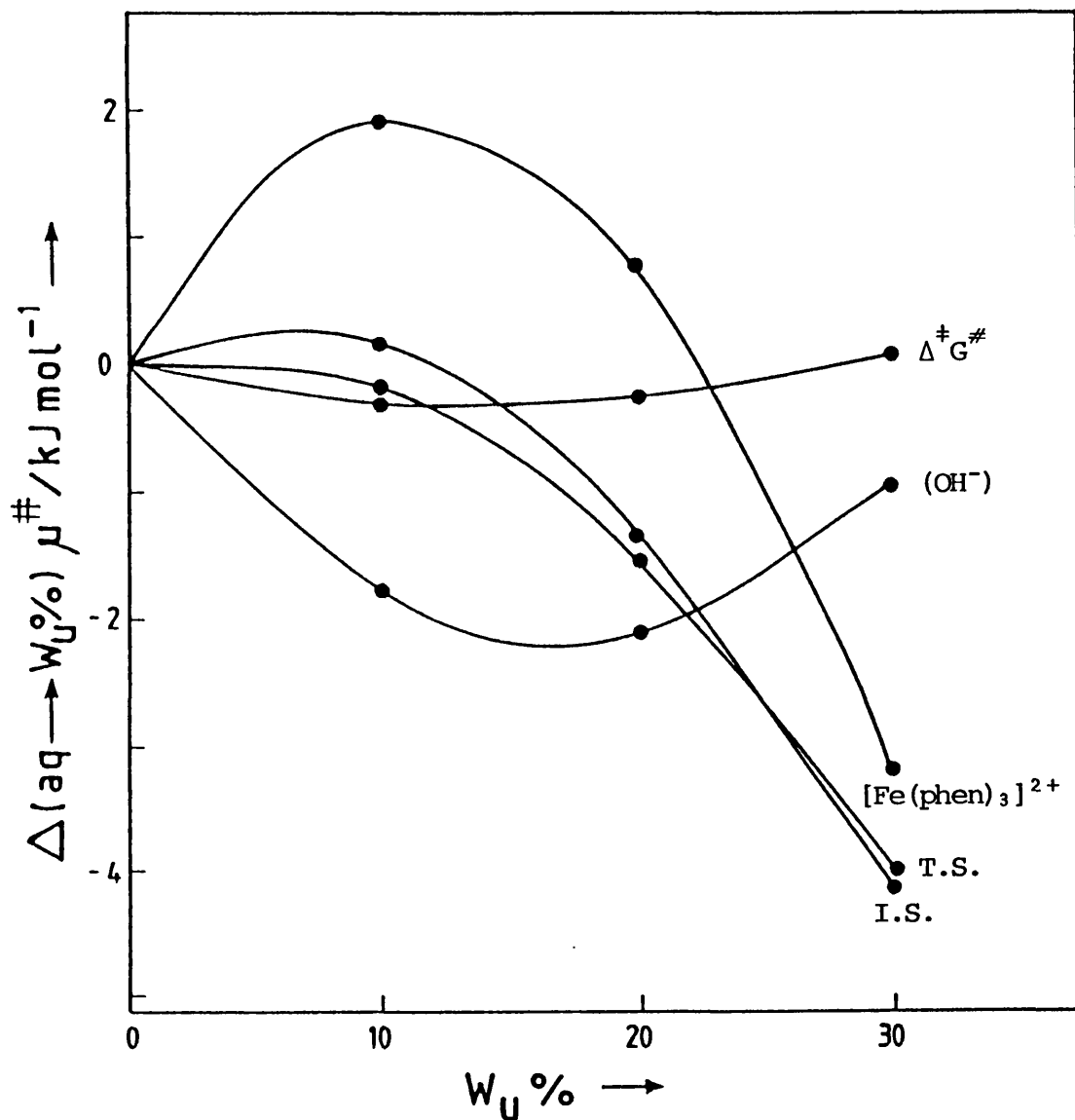
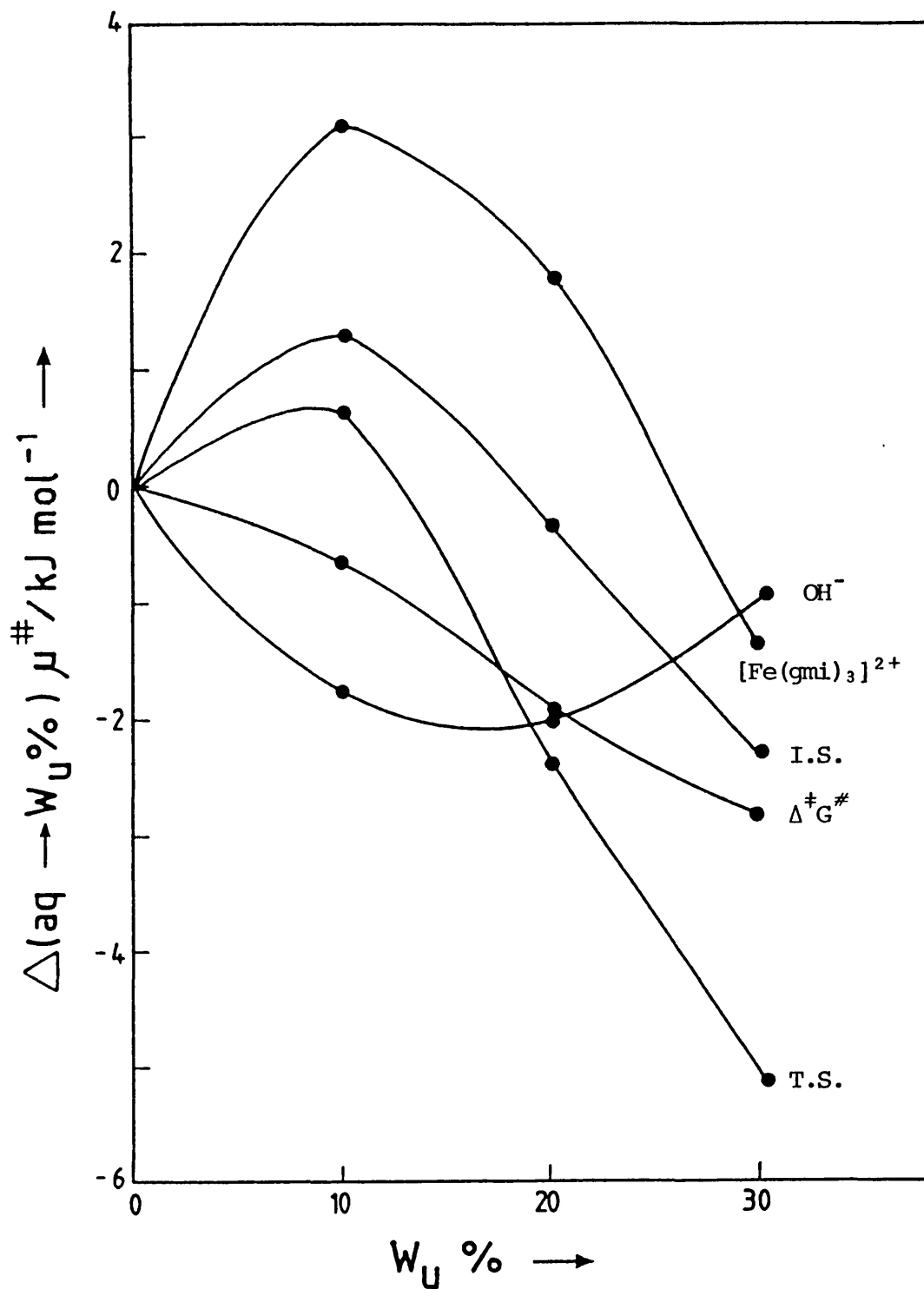


FIGURE 4.8

Dependence for the reference Gibbs function for activation,  $\Delta^\ddagger G^\ddagger$  (c-scale) and related reference state chemical potentials (c-scale) on weight per cent urea,  $W_U\%$ , for reactions of  $[\text{Fe}(\text{phen})_3]^{2+}$  with hydroxide ions at 298 K.



**FIGURE 4.9**

Dependence for the reference Gibbs function for activation,  $\Delta^\ddagger G^\#$  (c-scale) and related reference state chemical potentials (c-scale) on weight per cent urea,  $W_U\%$ , for reaction of  $[\text{Fe}(\text{gmi})_3]^{2+}$  with hydroxide ions at 298 K.

$[\text{Fe}(\text{gmi})_3]^{2+}$  ions and only moderate stabilisation of the hydrophilic hydroxide ions. However with increased  $w_u\%$  urea both initial and transition states are stabilised, the transition state to an increasingly large degree producing a decrease in  $\Delta^\ddagger G^\#$ . The stabilisation of the initial state at 20  $w_u\%$  urea can be attributed to an increased stabilisation of  $\text{OH}^-$  ions and the decreased stabilisation of the  $[\text{Fe}(\text{gmi})_3]^{2+}$  ions whilst at 30  $w_u\%$  urea both the complex and hydroxide ions are stabilised. This information is summarised in Figure 4.11.

Turning to the alkaline hydrolysis of  $[\text{Fe}(\text{phen})_3]^{2+}$  cations it is clear, Figure 4.8, that rate constants for this reaction mask considerable changes in the transfer chemical potentials of the initial and transition states when urea is added to the system. At 10  $w_u\%$  urea the effects on both the initial and transition state chemical potentials are small. The transition state is marginally stabilised and conversely the initial state is destabilised due to the greater destabilisation of the  $[\text{Fe}(\text{phen})_3]^{2+}$  ions compared to the stabilisation of the hydroxide anions. As a result an overall decrease in the Gibbs function for activation is observed. At 20  $w_u\%$  urea the transition state is stabilised to a greater extent. The destabilising effect of urea on  $[\text{Fe}(\text{phen})_3]^{2+}$  ions decreases and the stabilisation of  $\text{OH}^-$  ions increases. Hence an overall stabilisation of the transfer chemical potential of the initial state was observed. A solvent containing 30  $w_u\%$  urea marks a crossover point at which  $[\text{Fe}(\text{phen})_3]^{2+}$  ions are found to be stabilised to a greater extent in solution than hydroxide ions. Hence the initial state can be seen to

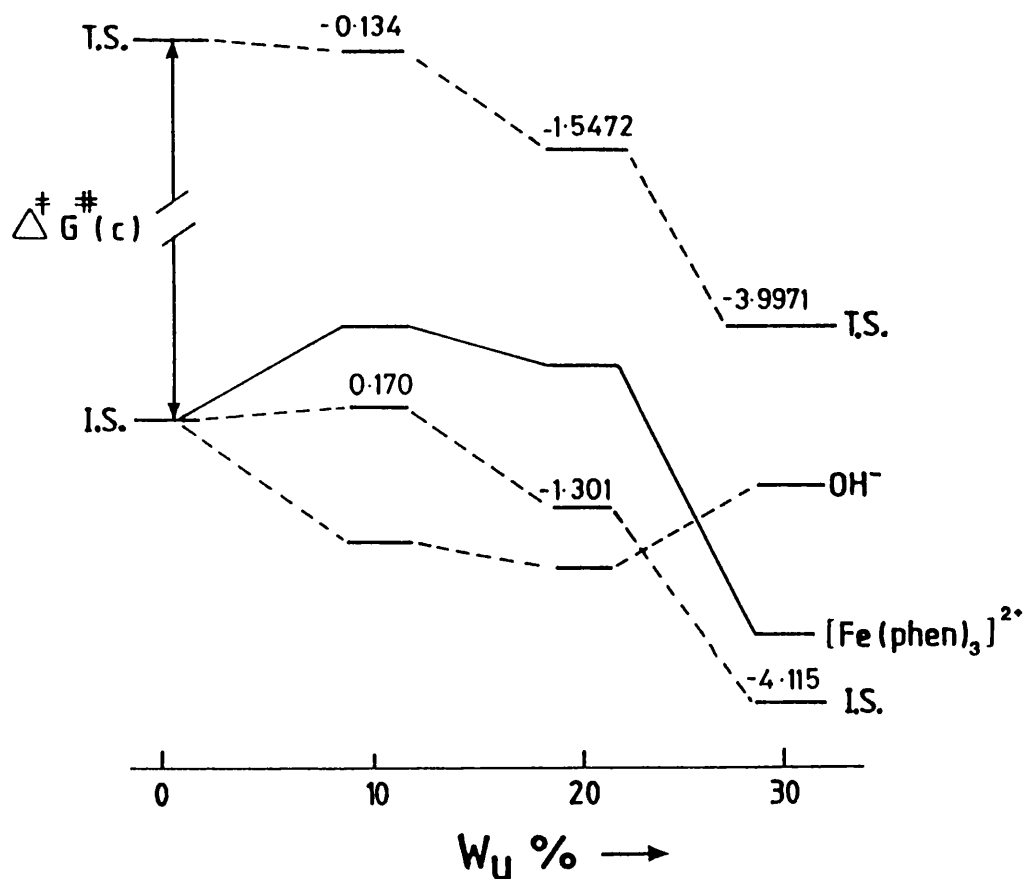


FIGURE 4.10

Dependence for the reference Gibbs function for activation,  $\Delta^{\ddagger}G^{\ddagger}$  (c-scale) and related reference state chemical potentials (c-scale) on weight per cent urea,  $W_U\%$ , for reactions of  $[\text{Fe}(\text{phen})_3]^{2+}$  with hydroxide ions at 298 K.

be greatly stabilised. The transition state is also stabilised to a larger extent and as throughout the range of urea solutions the effect on the Gibbs function for activation was found to be marginal. This information is summarised in Figure 4.11.

The trends summarised in Figures 4.10 and 4.11 are complicated. It is not clear why hydroxide anions showed such a degree of stabilisation in urea + water systems whilst in methyl alcohol + water systems<sup>8</sup> OH<sup>-</sup> anions are clearly destabilised. The merits of the initial state, transition state analysis are however immediately apparent. Modest dependences of rate constant, in both systems, mask striking dependencies on  $w_u$  of both the transfer chemical potentials of the initial and transition states.

An extension of the above approach to the analysis of kinetic data would be to consider the effects of pairwise group interaction parameters using the model developed by Savage<sup>22</sup>, Wood<sup>23</sup> and Lilley<sup>24</sup>. Although no more than a broad indication of the trends of a parameter describing pairwise interactions between urea and the iron(II) complexes can be obtained it is interesting to note that pairwise interaction parameters,  $g(X\rightleftharpoons Y)$  where X and Y denote functional groups, of  $g(\text{CH}_2\rightleftharpoons\text{CONH})$  and  $g(\text{CONH}\rightleftharpoons\text{OH})$  are 55 and  $-31 \text{ kJ mol}^{-1}$  respectively. In other words added urea destabilises the hydrophobic ligands around the iron(II) atom i.e. a positive  $g(\text{CH}_2\rightleftharpoons\text{CONH})$  and incorporating an OH<sup>-</sup> group into the same hydrophobic ligand produces a stabilising influence e.g.  $g(\text{CONH}\rightleftharpoons\text{OH}) < 0$ . This line of argument points a possible way forward in the analysis of kinetic data describing reactions in aqueous

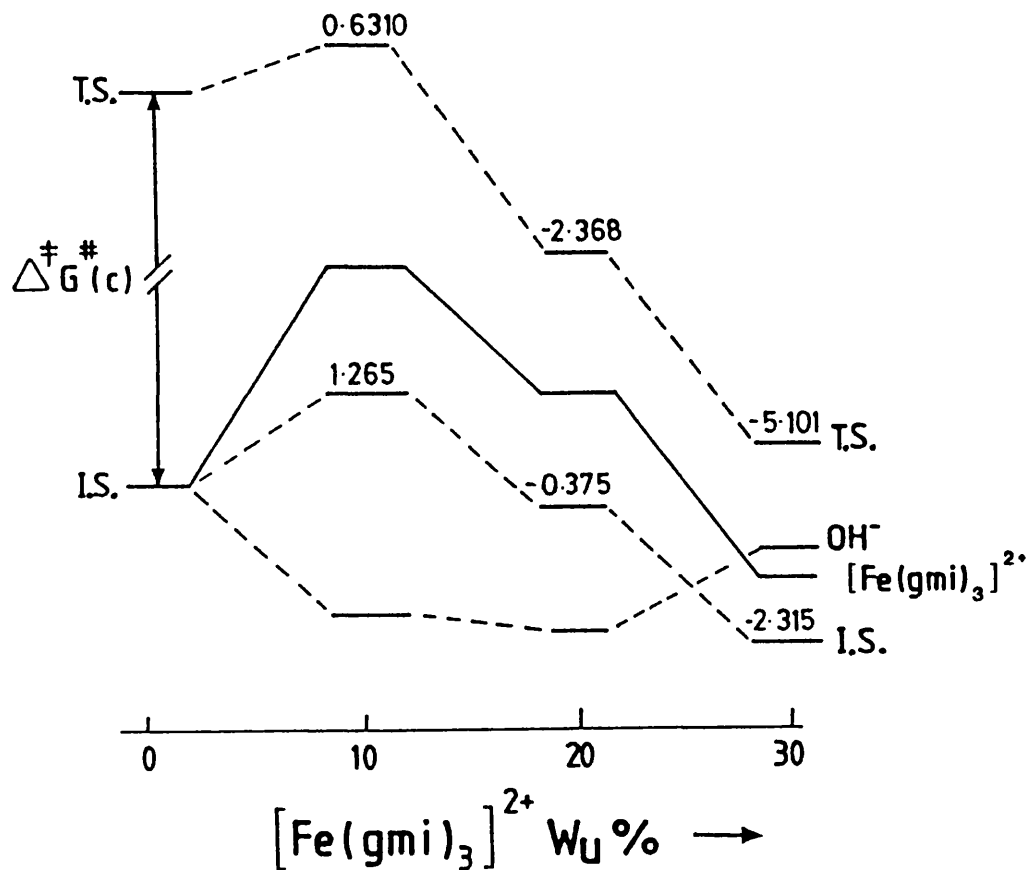


FIGURE 4.11

Dependence for the reference Gibbs function for activation,  $\Delta^{\ddagger}G^{\ddagger}$  (c-scale) and related reference state chemical potentials (c-scale) on weight per cent urea,  $W_U\%$ , for reaction of  $[\text{Fe}(\text{gmi})_3]^{2+}$  with hydroxide ions at 298 K.

solutions, by introducing thermodynamic parameters describing group interactions. These pairwise interaction parameters are investigated further in Chapter 7, which describes the background to the subject, and Chapter 8 which develops a technique for calculating pairwise Gibbs function cosphere-cosphere group interaction parameters and shows how they may be used to calculate the cosphere-cosphere overlap contribution to Setschenow coefficients for gaseous hydrocarbons dissolved in aqueous salt solutions.

## References Chapter 4

- (1) A.K.Das, K.K.Kundu, J.Chem.Phys., 79, 2604, (1975)
- (2) K.K.Kundu, A.K.Das, J.Soln.Chem., 8, 259, (1979)
- (3) U.N.Dash, B.B.Das, U.K.Biswal, T.Panda, Thermochem.Acta, 91, 329, (1985)
- (4) H.Gillet, L.Avedikion, J.P.Morel, Can.J.Chem., 53, 455, (1975)
- (5) A.K.Das, K.K.Kundu, J.Soln.Chem., 5, 431, (1976)
- (6) P.Guardado *private communication*
- (7) S.Radulovic *private communication*
- (8) M.J.Blandamer, J.Burgess, B.Clark, A.W.Hakin, N. Gossal, S.Radulovic, P.P.Duce, P.Guardado, F. Sanchez, C.D.Hubbard, E-E.A.Abu-Gharib, J.Chem. Soc., Faraday Trans. I, 82, 1471, (1985)
- (9) M.J.Blandamer, "Advances in Physical Organic Chemistry", Vol 14, Edited V.Gold, Academic Press, London, (1977)
- (10) M.L.Moss, M.G.Mellon, G.F.Smith, Analyt.Chem., 14, 931, (1942)
- (11) P.Krumholz, J.Am.Chem.Soc., 75, 2163, (1953)
- (12) R.D.Gillard, Co-ordination Chem.Rev., 16, 67, (1965)
- (13) M.J.Blandamer, J.Burgess, D.L.Roberts, J.Chem. Soc., Dalton, 1086, (1978)
- (14) B.Briggs, PhD Thesis, Leicester Univ., (1985)
- (15) M.J.Blandamer, J.Burgess, B.Clark, P.P.Duce, J.M.W.Scott, J.Chem.Soc., Faraday Trans. I, 80, 739, (1984)
- (16) J.Burgess, R.H.Prince, J.Chem.Soc., 4697, (1965)
- (17) D.Z.Arbritton, A.L.Schmeltekoft, "Modern Spectroscopy, Modern Research II", Ed.K.N.Rao, Academic Press, New York, (1976)
- (18) N.Desrosiers, G.Perron, J.G.Mathieson, B.E.Conway, J.E.Desnoyers, J.Soln.Chem., 3, 789, (1974)
- (19) G.S.Kell, J.Chem.Eng.Dat., 12, 66, (1967)

- (20) S.Glasstone, K.J.Laidler, H.Eyring, "The Theory of Rate Processes", McGraw-Hill, New York, (1941)
- (21) K.K.Kundu, K.Mazumdar, J.Chem.Soc., Faraday Trans. I, 71, 1422, (1975)
- (22) J.J.Savage, R.H.Wood, J.Soln.Chem., 5, 733, (1976)
- (23) J.J.Spitzer, S.K.Suri, R.H.Wood, J.Soln.Chem., 14, 561, (1985)
- (24) G.M.Blackburn, T.H.Lilley, P.J.Blackburn, J.Chem .Soc., Faraday Trans. I, 81, 2191, (1985)



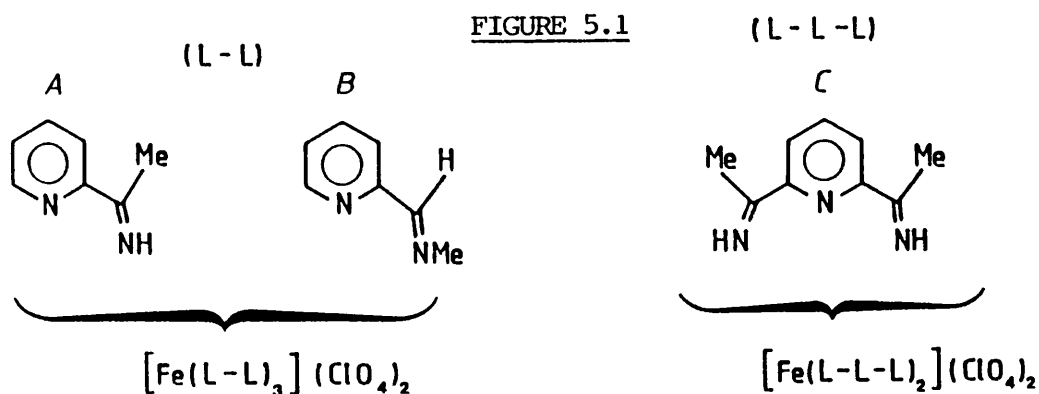
# CHAPTER

# 5

Alkaline hydrolysis of low-spin  
iron(II) complexes in 'Methyl  
alcohol + water' mixtures

## 5.1 Introduction

This Chapter reports observed first order, and linear least squares estimates of second order rate constants at 298.15 K for the alkaline hydrolysis of one tridentate and two bidentate low-spin iron(II) complexes in binary mixtures of methyl alcohol and water. These mixtures contained 0, 20, 40, 60 and 80 ideal volume per cent,  $v\%(id)$ , of the alcohol (see Section 5.2.2 for a definition of  $v\%(id)$ ). The structures of the iron(II) complexes are shown in Figure 5.1.



Single ion transfer chemical potentials calculated using the TATB assumption<sup>1</sup> were used in an investigation of the effects of added methyl alcohol on the transfer chemical potentials of the initial and transition states involved in chemical reaction (see chapter 4).

## 5.2 Experimental

### 5.2.1 Materials

The complexes were prepared from the appropriate amine, carbonyl compound and iron(II) chloride<sup>2</sup>, by S.Radulovic, and were precipitated as perchlorates by saturating the iron(II) chloride solution with sodium perchlorate. The methyl alcohol was 99.9% spectrophotometric grade.

### 5.2.2 Kinetics

Concentrated aqueous solutions of the iron(II) complexes (present as perchlorates) were used. Kinetics of reaction between the iron(II) complexes and hydroxide ions were monitored in 0, 20, 40, 60 and 80 v%(id) methyl alcohol + water mixtures at constant ionic strength,  $I = 0.33 \text{ mol dm}^{-3}$  at 298.15 K. The composition of the solvent mixtures was described in terms of ideal volume per cent, v%(id). This term is defined for example in the case of 60 v%(id) methyl alcohol as follows. If the volume before mixing of the reaction mixture has a total volume  $V/\text{cm}^3$  then the mixture contains  $(60/100) \cdot V/\text{cm}^3$  of methyl alcohol. Constant ionic strength was maintained by addition of sodium chloride solution to the reaction mixture. In all systems  $[\text{complex}] \leq 10^{-4} \text{ mol dm}^{-3}$  and hydroxide ions were present in vast excess compared to the concentration of the iron complex. Reactions were monitored at five separate hydroxide concentrations in the region,  $0.05 \leq [\text{NaOH}]/\text{mol dm}^{-3} \leq 0.18$  for the tridentate complex, C, and  $0.001 \leq [\text{NaOH}]/\text{mol dm}^{-3} \leq 0.020$  for the two bidentate complexes, A and B. Reactions were followed by monitoring the decrease in absorbance at  $\lambda_{\text{max}}$  with time using an HP 8451A diode array spectrophotometer (see Chapter 2). For each complex  $\lambda_{\text{max}}$  was obtained from a full wavelength scan  $190 \leq \lambda/\text{nm} \leq 800$  using a dilute aqueous solution of the complex; Figures 5.2 to 5.4 (the program is included as Appendix 1; program AWH 1). No change in the position of  $\lambda_{\text{max}}$  was noted when methyl alcohol was added to the system. For complex A,  $\lambda_{\text{max}} = 572 \text{ nm}$ , complex B,  $\lambda_{\text{max}} = 550 \text{ nm}$  and, complex C,  $\lambda_{\text{max}} = 592 \text{ nm}$ .

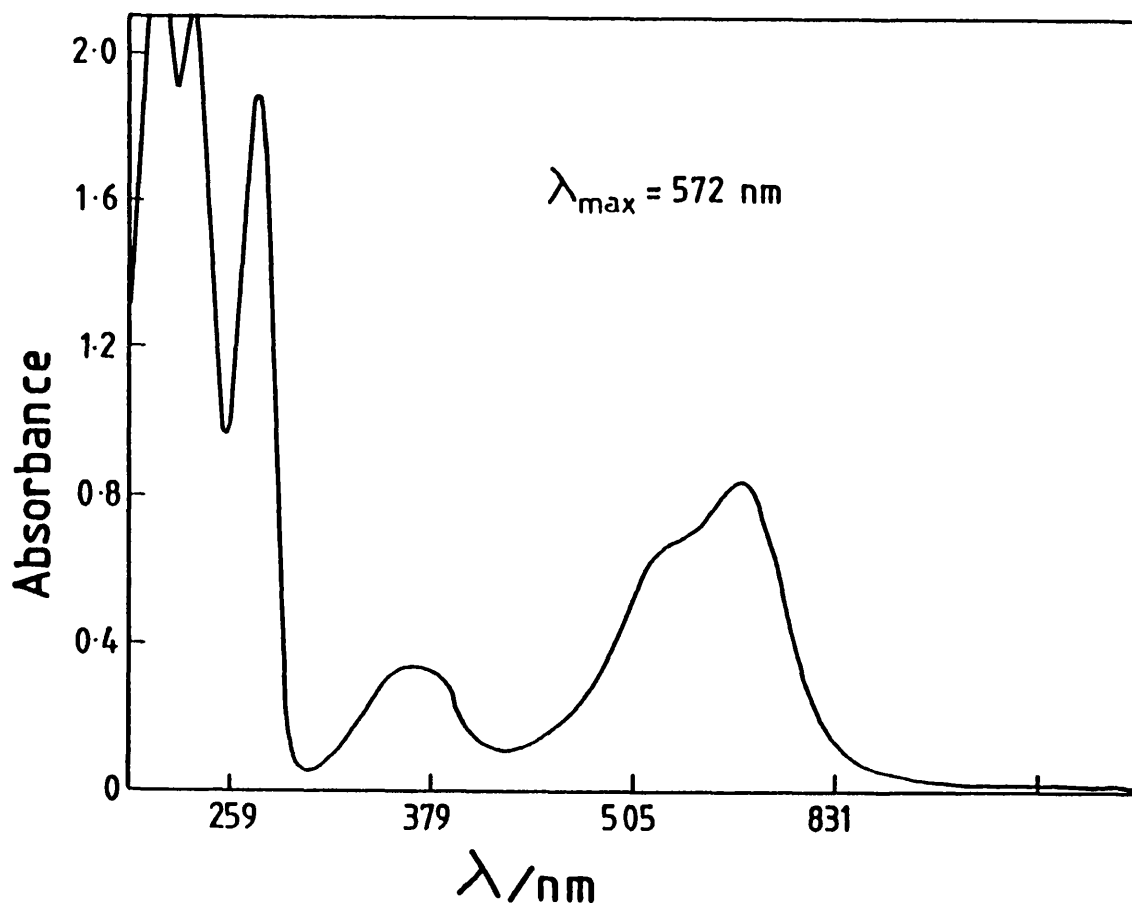


FIGURE 5.2

Dependence of absorbance on wavelength of iron(II) complex, Complex A.

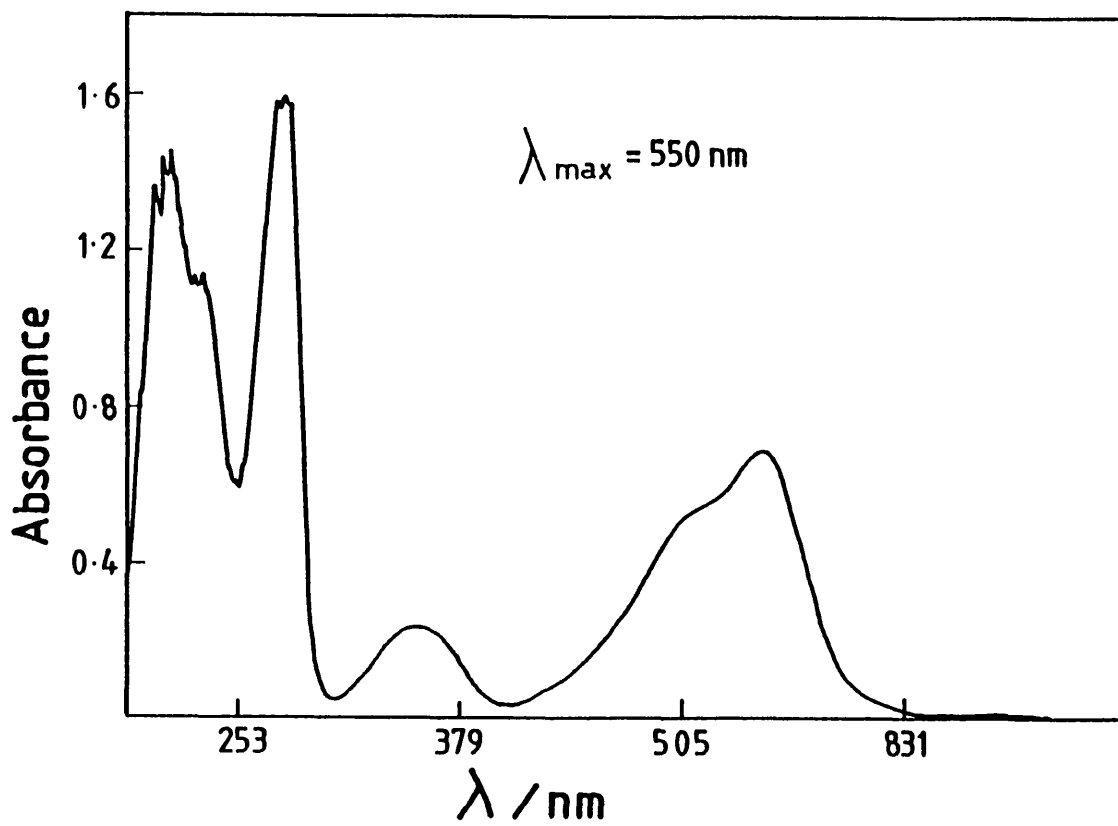


FIGURE 5.3

Dependence of absorbance on wavelength of iron(II) complex, Complex B.

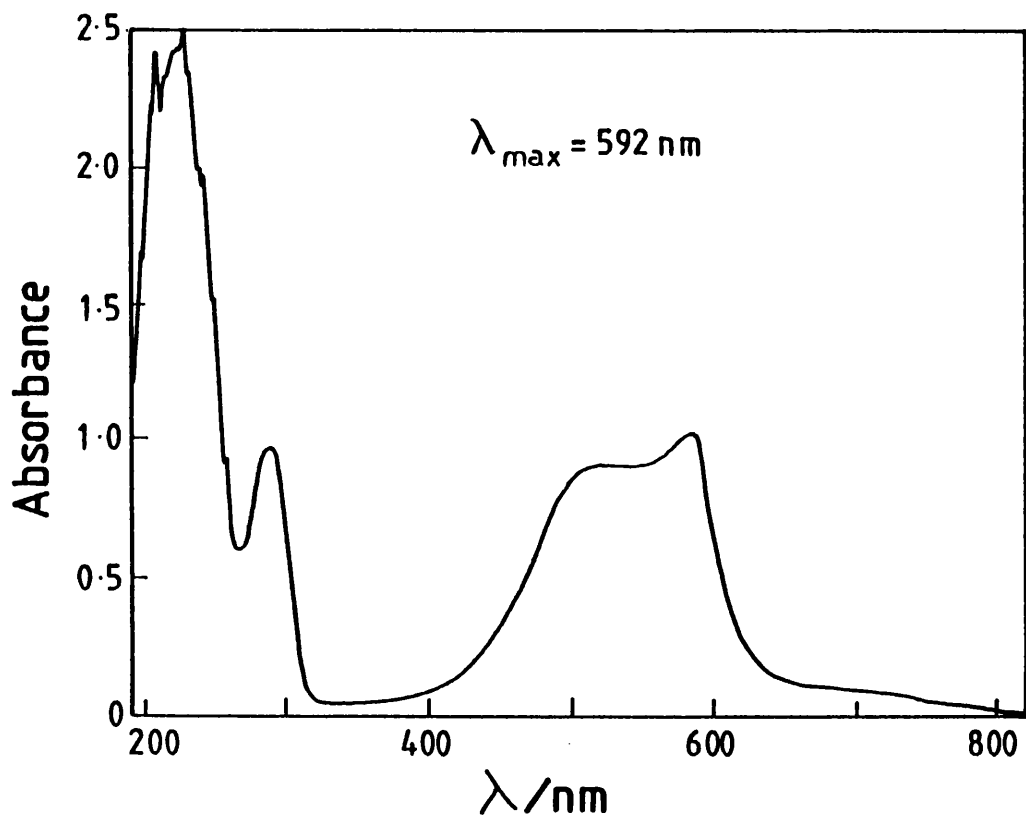


FIGURE 5.4

Dependence of absorbance on wavelength of iron(II) complex, Complex C.

The solubilities<sup>4</sup> of iron(II) complexes in methyl alcohol + water mixtures were determined from the absorbances at  $\lambda_{\text{max}}$  of saturated solutions at 298.15 K. Transfer chemical potentials of the hydroxide ion were taken from a compilation<sup>1</sup> based on the TATB assumption.

### 5.3 Results

The reactions are known to follow the rate law<sup>3</sup> given by equation [4.1] of Chapter 4. Reactions were allowed to proceed for at least 2.5 half lives and in all cases the absorbance  $P_{\infty}$  (see Chapter 2) was close to zero, indicating that the reaction had gone to completion. Addition of methyl alcohol to the reaction mixture containing complex C produced a notable decrease in rate constant dependent on the proportion of alcohol in the mixture. The effect of added methyl alcohol on complexes A and B was not as straight forward. Up to 40 v%(id) methyl alcohol the rate constants for reactions involving complex A decreased compared to the rate constant for reaction in aqueous solution. However at higher alcohol concentrations, 60 and 80 v%(id), the rate constant increased slightly relative to the lower alcohol concentration but at no time did it exceed the rate constant for reaction in aqueous solution. For complex B little effect on rate constant was produced by 20 v%(id) methyl alcohol. However rate constants in 40, 60 and 80 v%(id) methyl alcohol increased relative to rate constants in aqueous solution. Observed first order rate constants for reactions involving complexes A, B and C are reported in Tables 5.1, 5.2 and 5.3 respectively.

Second order rate constants were estimated using the

Table 5.1

First order rate constants for reaction between complex A and hydroxide ions in water and methyl alcohol + water mixtures at constant ionic strength  $I=0.33 \text{ moldm}^{-3}$  at 298K.

[NaOH] / $\text{moldm}^{-3}$	0	20	V(id) % MeOH 40	60	80
			$10^5 \text{ k/s}^{-1}$		
0.001	3.59	1.82	1.82	2.74	2.90
0.005	14.43	11.24	9.66	10.75	12.65
0.010	26.01	22.92	19.16	21.99	25.56
0.015	40.16	33.14	27.88	32.17	36.92
0.020	56.13	42.62	38.35	40.90	47.98

Table 5.2

First order rate constants for reaction between complex B and hydroxide ions in water and methyl alcohol + water mixtures at constant ionic strength  $I=0.33 \text{ moldm}^{-3}$  at 298K.

[NaOH] / $\text{moldm}^{-3}$	0	20	V(id) % MeOH 40	60	80
			$10^5 \text{ k/s}^{-1}$		
0.001	0.50	0.41	0.50	0.94	2.60
0.005	1.02	0.95	1.65	2.26	5.04
0.010	2.00	1.77	2.38	3.91	7.83
0.015	2.48	2.50	3.37	5.67	9.92
0.020	2.93	3.08	4.01	6.80	12.80

Table 5.3

First order rate constants for reaction between complex C and hydroxide ions in water and methyl alcohol + water mixtures at constant ionic strength  $I=0.33 \text{ mol dm}^{-3}$  at 298K.

[NaOH] / $\text{mol dm}^{-3}$	0	20	V(id) % MeOH 40	60	80
			$10^4 \text{ k/s}^{-1}$		
0.050	1.59	1.10	0.94	0.82	0.67
0.100	4.77	2.89	2.23	1.85	1.55
0.120	6.61	3.86	3.00	2.63	1.66
0.150	8.40	5.56	3.99	3.24	2.33
0.180	12.64	7.20	5.41	4.41	2.81

method of linear least squares in which observed first order rate constants,  $k_{\text{obs}}$ , for each alcohol mixture were fitted to equation [4.2] of Chapter 4. In all cases estimates of  $k_1$  were negligible compared to the estimates of the second order rate constant  $k_2$ . Plots of  $k_{\text{obs}}$  against sodium hydroxide concentration for complex A at 0, 20, 40, 60 and 80 v%(id) methyl alcohol are included as Figure 5.5. Estimated second order rate constants,  $k_2$ , and their standard errors for each complex are reported in Tables 5.4, 5.5 and 5.6.

#### 5.4 Initial State, Transition State Analysis

Kinetic and solubility<sup>4</sup> data were combined using the procedures set down in Section 4.5 of Chapter 4 to obtain the effect of added methyl alcohol on the initial and transition states of each complex. In summary form the effect of added cosolvent on the initial state is calculated using equation [5.1].

$$\begin{aligned} \Delta(\text{aq} \rightarrow \text{v}\%(\text{id}))\mu_{\text{is}}^{\ddagger}(\text{c-scale}; \text{sln}; \text{T}) = \\ \Delta(\text{aq} \rightarrow \text{v}\%(\text{id}))\mu^{\ddagger}(\text{iron complex}; \text{c-scale}; \text{sln}; \text{T}) \\ + \Delta(\text{aq} \rightarrow \text{v}\%(\text{id}))\mu^{\ddagger}(\text{OH}^{-}; \text{c-scale}; \text{sln}; \text{T}) \quad [5.1] \end{aligned}$$

The effects of cosolvent on the transition state can be obtained using equation [5.2].

$$\begin{aligned} \Delta(\text{aq} \rightarrow \text{v}\%(\text{id}))\mu_{\ddagger}^{\ddagger}(\text{c-scale}; \text{sln}; \text{T}) = \\ \Delta(\text{aq} \rightarrow \text{v}\%(\text{id}))\Delta^{\ddagger}G^{\ddagger}(\text{c-scale}; \text{T}) \\ + \Delta(\text{aq} \rightarrow \text{v}\%(\text{id}))\mu^{\ddagger}(\text{iron complex}; \text{c-scale}; \text{sln}; \text{T}) \\ + \Delta(\text{aq} \rightarrow \text{v}\%(\text{id}))\mu^{\ddagger}(\text{OH}^{-}; \text{c-scale}; \text{sln}; \text{T}) \quad [5.2] \end{aligned}$$

FIGURE 5.5

Dependence of first order rate constants,  $k_{\text{obs}}/\text{s}^{-1}$ , on sodium hydroxide concentration for reactions of iron(III) complex, Complex A, with hydroxide ions at 298 K in various 'water + methyl alcohol' mixtures.

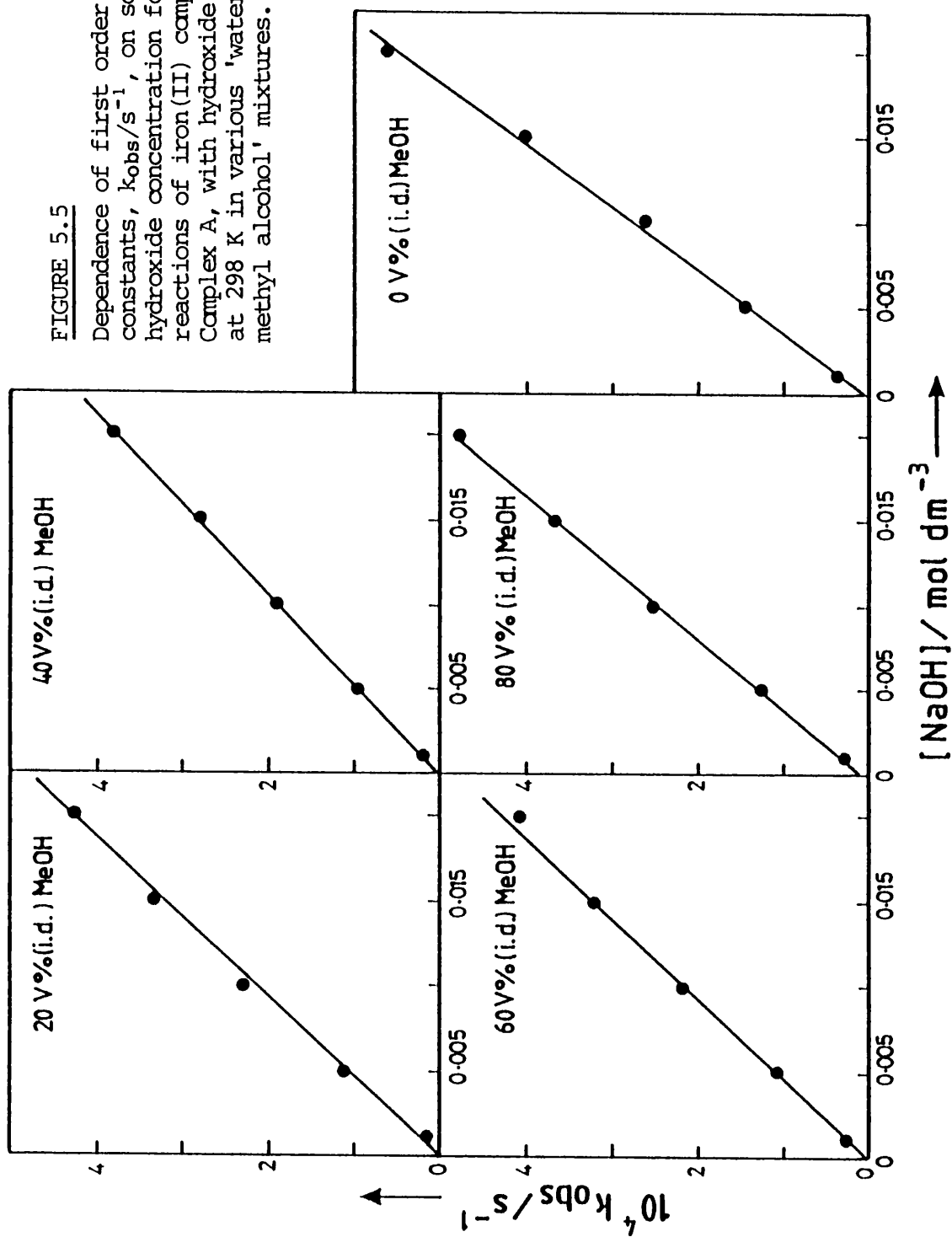


Table 5.4

Second order rate constants for reaction between complex A and hydroxide ions in water and MeOH + water mixtures at constant ionic strength  $I=0.33 \text{ mol dm}^{-3}$  and 298K

V%(id) MeOH	$10^2 \text{ k/dm}^3 \text{ mol}^{-1} \text{ s}^{-1}$
0	2.278 (+ 0.091)
20	2.153 (+ 0.059)
40	1.901 (+ 0.028)
60	2.035 (+ 0.050)
80	2.383 (+ 0.043)

Table 5.5

Second order rate constants for reaction between complex B and hydroxide ions in water and MeOH + water mixtures at constant ionic strength  $I=0.33 \text{ mol dm}^{-3}$  and 298K

V%(id) MeOH	$10^3 \text{ k/dm}^3 \text{ mol}^{-1} \text{ s}^{-1}$
0	1.312 (+ 0.118)
20	1.434 (+ 0.047)
40	1.810 (+ 0.137)
60	3.151 (+ 0.125)
80	5.257 (+ 0.171)

where  $k_2$  is obtained from the estimated values of the second order rate constants,  $k_2$ .

Table 5.6

Second order rate constants for reaction between complex C and hydroxide ions in water and MeOH + water mixtures at constant ionic strength  $I=0.33 \text{ mol dm}^{-3}$  and 298K

v%(id) MeOH	$10^3 k/\text{dm}^3 \text{mol}^{-1} \text{s}^{-1}$
0	8.204 (+ 0.837)
20	4.737 (+ 0.313)
40	3.408 (+ 0.250)
60	2.722 (+ 0.202)
80	1.637 (+ 0.096)

These results can be explained in the following way; hydroxide ions are sufficiently hydrophilic to retain their hydration shell essentially intact up to even as high as 60 v%(id) methyl alcohol. At 80 v%(id) methyl alcohol the hydroxide ions are then greatly destabilized because there is insufficient water to maintain their hydration shells. This effect is almost the reverse of the trends shown in Chapter 4, where the hydroxide ions are stabilized with increased proportion of water.

Concomitant effects on the initial state transfer chemical potentials (equation (5.2)) of complex A and C are

where  $\Delta(\text{aq} \rightarrow \text{v}\%(\text{id}))\Delta^\ddagger G^\#(\text{c-scale}; T)$  is obtained from the estimated values of the second order rate constants,  $k_2$ .

$$\Delta(\text{aq} \rightarrow \text{v}\%(\text{id}))\Delta^\ddagger G^\#(\text{c-scale}; T) = RT \ln[k_2(\text{aq}; T) / k_2(\text{aq}; \text{v}\%(\text{id}); T)] \quad [5.3]$$

Tables 5.7, 5.8 and 5.9 report calculated initial and transition state transfer chemical potentials and Figures 5.6, 5.7 and 5.8 plot these data against  $\text{v}\%(\text{id})$  methyl alcohol for complexes A, B and C respectively.

### 5.5 Discussion

The effect of added methyl alcohol on the transfer chemical potential of the hydroxide ion is almost negligible up to 40  $\text{v}\%(\text{id})$  methyl alcohol, with only a very slight stabilisation effect at 20  $\text{v}\%(\text{id})$  alcohol. However at 60 and 80  $\text{v}\%(\text{id})$  methyl alcohol the hydroxide ion is increasingly destabilised. These results can be explained in the following way; hydroxide ions are sufficiently hydrophilic to retain their hydration shell essentially intact up to even as high as 60  $\text{v}\%(\text{id})$  methyl alcohol. At 80  $\text{v}\%(\text{id})$  methyl alcohol the hydroxide ions are then greatly destabilised because there is insufficient water to maintain their hydration shells. This effect is almost the reverse of the trends shown in Chapter 4, where the hydroxide ions are stabilised with increased proportion of urea.

Cosolvent effects on the initial state transfer chemical potentials (equation [5.2]) of complex A and C are

Table 5.7

Transfer parameters, for reaction of complex A with hydroxide ions, from water to methyl alcohol + water mixtures at 298K on the c-scale. Units of transfer are  $\text{kJmol}^{-1}$ .

v(id)% MeOH	0	20	40	60	80
$\Delta(\text{aq} \rightarrow \text{v}\%(\text{id})) \Delta^\ddagger G(\text{c})^*$	0	0.59	0.89	0.73	0.34
$\Delta(\text{aq} \rightarrow \text{v}\%(\text{id})) \mu^\#(\text{c}) \text{salt}^{**}$	0	-2.63	-6.67	-9.67	-9.87
$\Delta(\text{aq} \rightarrow \text{v}\%(\text{id})) \mu^\#(\text{c}) (2\text{ClO}_4^-)^\dagger$	0	0.06	-0.16	0.34	3.16
$\Delta(\text{aq} \rightarrow \text{v}\%(\text{id})) \mu^\#(\text{c}) \text{A}$	0	-2.69	-6.51	-10.01	-12.93
$\Delta(\text{aq} \rightarrow \text{v}\%(\text{id})) \mu^\#(\text{c}) \text{OH}^-$	0	-0.12	-0.02	1.44	5.78
$\Delta(\text{aq} \rightarrow \text{v}\%(\text{id})) \mu_{\text{is}}^\#(\text{c})$	0	-2.81	-6.53	-8.57	-7.25
$\Delta(\text{aq} \rightarrow \text{v}\%(\text{id})) \mu_{\ddagger}^\#(\text{c})$	0	-2.22	-5.63	-7.84	-6.92

\* - (c) represents (c-scale;sln;T)

\*\* - salt is the perchlorate salt of complex A.  
Solubility data from ref.4.

† - Solubility data from Ref.6.

Table 5.8

Transfer parameters, for reaction of complex B with hydroxide ions, from water to methyl alcohol + water mixtures at 298K on the c-scale. Units of transfer are  $\text{kJmol}^{-1}$ .

V(id)% MeOH	0	20	40	60	80
$\Delta(\text{aq}\rightarrow\text{v}\%(\text{id}))\Delta^\ddagger G(\text{c})^*$	0	-0.22	-0.80	-2.17	-3.44
$\Delta(\text{aq}\rightarrow\text{v}\%(\text{id}))\mu^\ddagger(\text{c}) \text{ salt}^{**}$	0	-2.39	-4.39	-6.02	-3.35
$\Delta(\text{aq}\rightarrow\text{v}\%(\text{id}))\mu^\ddagger(\text{c})(2\text{ClO}_4^-)^\dagger$	0	0.06	-0.16	0.34	3.16
$\Delta(\text{aq}\rightarrow\text{v}\%(\text{id}))\mu^\ddagger(\text{c}) \text{ B}$	0	-2.45	-4.23	-6.36	-6.51
$\Delta(\text{aq}\rightarrow\text{v}\%(\text{id}))\mu^\ddagger(\text{c}) \text{ OH}^-$	0	-0.12	-0.02	1.44	5.78
$\Delta(\text{aq}\rightarrow\text{v}\%(\text{id}))\mu_{\text{is}}^\ddagger(\text{c})$	0	-2.57	-4.25	-4.91	-0.73
$\Delta(\text{aq}\rightarrow\text{v}\%(\text{id}))\mu_{\ddagger}^\ddagger(\text{c})$	0	-2.79	-5.04	-7.09	-4.17

\* - (c) represents (c-scale;sln;T)

\*\* - salt is the perchlorate salt of complex B.  
Solubility data from ref.4.

† - Solubility data from Ref.6.

Table 5.9

Transfer parameters, for reaction of complex C with hydroxide ions, from water to methyl alcohol + water mixtures at 298K on the c-scale. Units of transfer are  $\text{kJmol}^{-1}$ .

V(id)% MeOH	0	20	40	60	80
$\Delta(\text{aq} \rightarrow \text{v}(\text{id}))\Delta_{\ddagger}^{\#}G(\text{c})^*$	0	1.36	2.18	2.73	4.00
$\Delta(\text{aq} \rightarrow \text{v}(\text{id}))\mu_{\ddagger}^{\#}(\text{c}) \text{ salt}^{**}$	0	-4.24	-7.77	-12.03	-12.51
$\Delta(\text{aq} \rightarrow \text{v}(\text{id}))\mu_{\ddagger}^{\#}(\text{c})(2\text{ClO}_4^-)^{\dagger}$	0	0.06	-0.16	0.34	3.16
$\Delta(\text{aq} \rightarrow \text{v}(\text{id}))\mu_{\ddagger}^{\#}(\text{c}) \text{ C}$	0	-4.30	-7.61	-12.37	-15.67
$\Delta(\text{aq} \rightarrow \text{v}(\text{id}))\mu_{\ddagger}^{\#}(\text{c}) \text{ OH}^-$	0	-0.12	-0.02	1.44	5.78
$\Delta(\text{aq} \rightarrow \text{v}(\text{id}))\mu_{\text{is}}^{\#}(\text{c})$	0	-4.42	-7.63	-10.93	-9.89
$\Delta(\text{aq} \rightarrow \text{v}(\text{id}))\mu_{\ddagger}^{\#}(\text{c})$	0	-3.06	-5.45	-8.20	-5.89

\* - (c) represents (c-scale;sln;T)

\*\* - salt is the perchlorate salt of complex C.  
Solubility data from ref.4.

† - Solubility data from Ref.6.

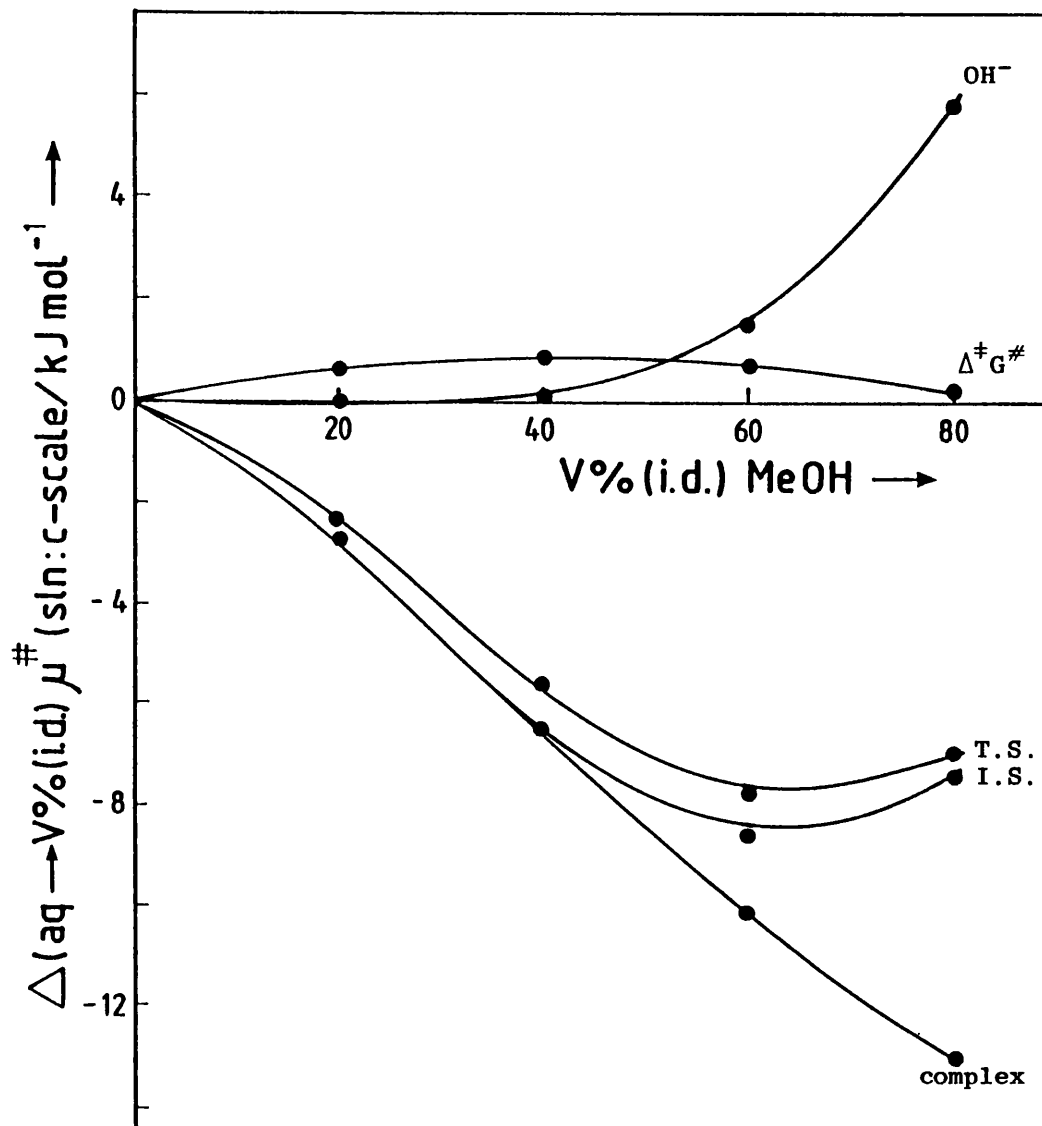


**FIGURE 5.6**

Dependence of the reference Gibbs function for activation,  $\Delta^{\ddagger}G^{\ddagger}$  (c-scale), and related reference state chemical potentials (c-scale) on ideal volume per cent methyl alcohol,  $V\%(\text{i.d.})$ , for reaction of Complex A with hydroxide ions at 298 K.

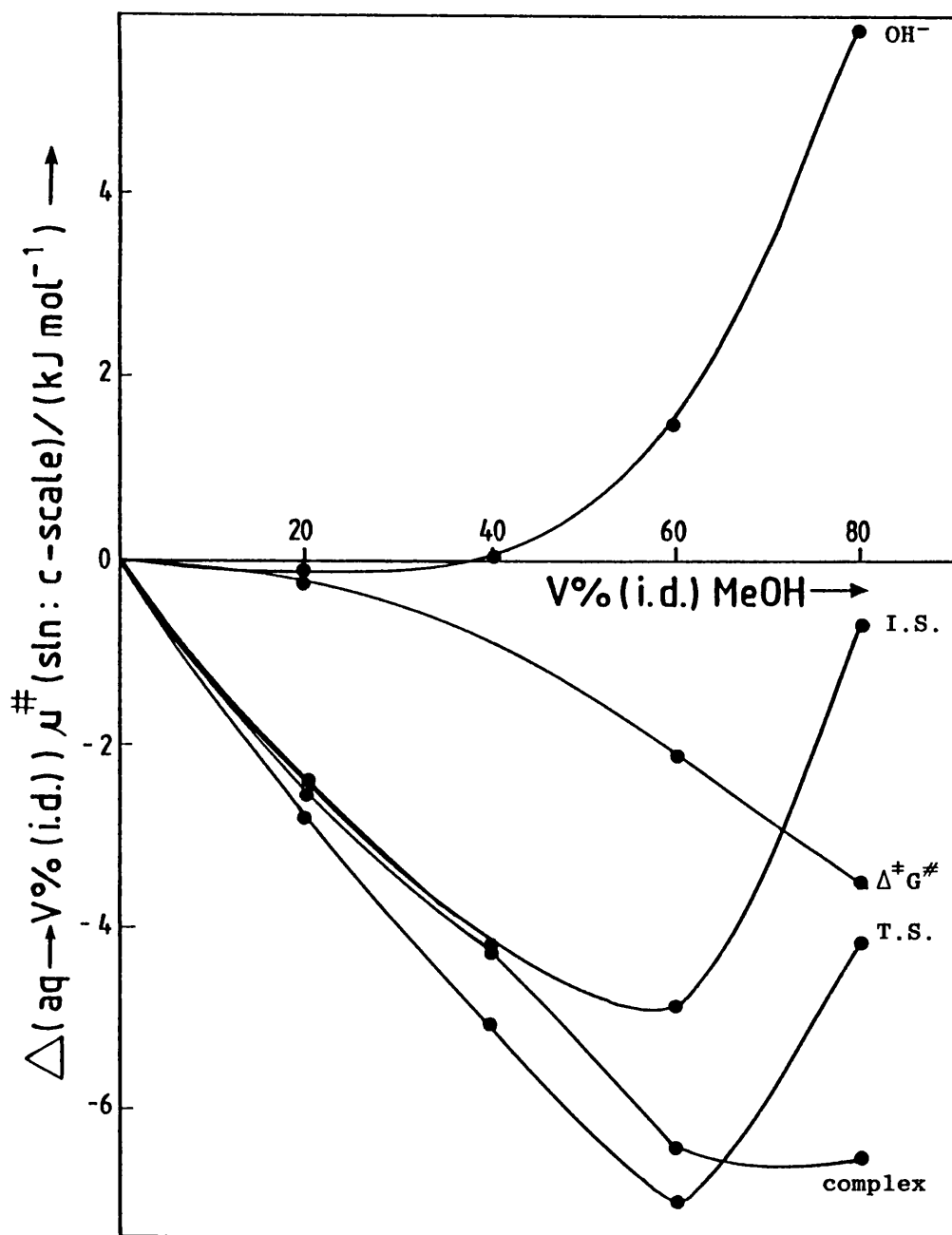


FIGURE 5.7

Dependence of the reference Gibbs function for activation,  $\Delta^\ddagger G^\ddagger$  (c-scale), and related reference state chemical potentials (c-scale) on ideal volume per cent methyl alcohol, V% (id), for reaction of Complex B with hydroxide ions at 298 K.

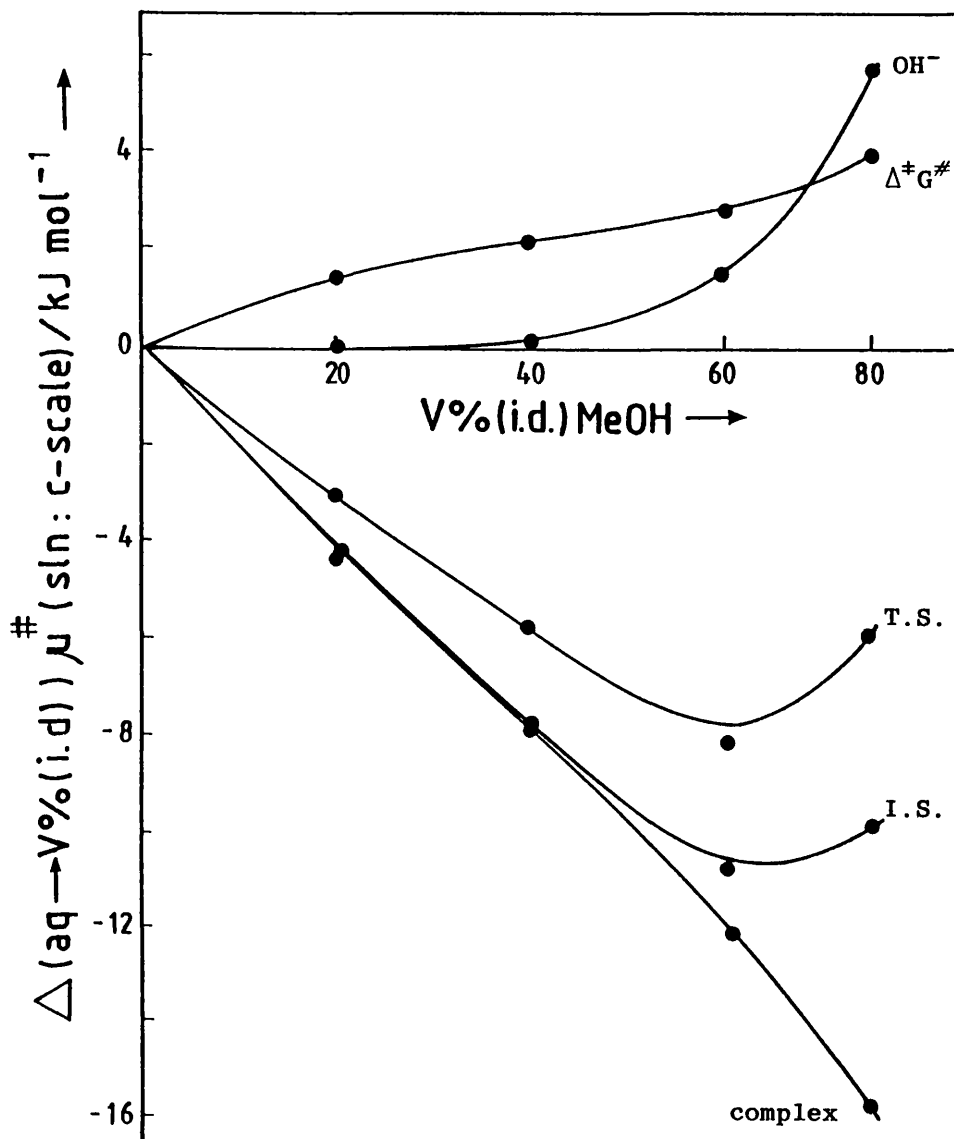


FIGURE 5.8

Dependence of the reference Gibbs function for activation,  $\Delta^\ddagger G^\ddagger$  (c-scale), and related reference state chemical potentials (c-scale) on ideal volume per cent methyl alcohol,  $V\% (i.d.)$ , for reaction of Complex C with hydroxide ions.

dominated by the increasingly large stabilisation of the iron(II) complex in alcohol rich mixtures. However at 80 v%(id) methyl alcohol the destabilising effect of the solvent mixture on the hydroxide ion is sufficiently intense to produce a notable destabilisation of the overall initial state relative to 60 v%(id) methyl alcohol. The Gibbs function for activation,  $\Delta^\ddagger G^\ddagger$ , for complex A increases with increased methyl alcohol proportion up to 40 v%(id). At 60 and 80 v%(id) methyl alcohol there are small decreases in  $\Delta^\ddagger G^\ddagger$ ; however they are not large enough to demand a change in sign. A similar situation can be seen with complex C. However in this case there is no decrease in  $\Delta^\ddagger G^\ddagger$  at 40 v%(id) methyl alcohol. Indeed  $\Delta^\ddagger G^\ddagger$  increases almost linearly over the range 0 to 80 v%(id) methyl alcohol. The effect of a positive change in the Gibbs function for activation can thus be seen to be an artefact of the increased stabilisation of the overall initial state in alcohol + water mixtures relative to the stabilisation of the overall transition state (defined in equation [5.2]).

The solvent effects on the initial and transition states of complex B are different from those on complex A and C. The first point to notice is the reduced stabilisation of the iron complex up to 80 v%(id) methyl alcohol relative to the stabilisation of complexes A and C in the same mixtures. Indeed at 80 v%(id) methyl alcohol destabilisation of hydroxide ions is now the major contribution to the destabilisation of the initial state relative to 20, 40 and 60 v%(id) alcohol. The transition state is stabilised to a greater degree than the initial

state. However it too shows a marked destabilisation at 80 v%(id) methyl alcohol due to the relatively large destabilisation of the hydroxide anion. As a result the decrease in the Gibbs function for activation,  $\Delta^\ddagger G^\ddagger$ , with increased alcohol proportion in the mixture can be seen to be dominated by the effects of added methyl alcohol on the transition state.

Comparison of Figures 5.6 and 5.7 reveals the striking effect the introduction of a methyl group onto a ligand can have on the kinetics of reaction. Indeed it is not only the kinetics of reaction of the complex which are affected but also the stability of the complex in the alcohol + water mixtures. Hence the effects of stabilisation/destabilisation by added cosolvent on the initial and transition states are modified.

Just as the second order rate constants for the nucleophilic attack of hydroxide ions at 5-methyl ferriin are lower than those for the unsubstituted complex<sup>3</sup>, the second order rate constants for complex B are lower than those for complex A due to the electron release of the methyl group<sup>5</sup>. The methyl group attached to the nitrogen atom in complex B pushes electron density onto the nitrogen atom thus increasing the strength of the nitrogen-iron bond. The electron density around the iron atom will also be increased. These two factors demand that nucleophilic attack by hydroxide anions will be discouraged and hence the second order rate constant,  $k_2$ , decreases. The methyl group in complex A is too far removed from the nitrogen centre to produce such an effect.

Overall the transition state stabilisation follows

the same general pattern for the three iron complexes. Stabilisation of the transition state up to 60 v%(id) methyl alcohol is consistent with the dispersal of charges on going from the initial to the transition state, and hence transfer of the transition state to a less polar, alcohol rich, solvent will result in a stabilisation of the transition state. At 80 v%(id) methyl alcohol the transition state becomes much less stabilised than at lower methyl alcohol concentrations because the highly alcohol rich solvent is not sufficiently polar to accomodate the dispersed charges as adequately as at 60 v%(id) methyl alcohol.

## References Chapter 5

- (1) B. Briggs, PhD Thesis Leicester Univ., (1985)
- (2) P. Krumholz, J. Am. Chem. Soc., 75, 2163, (1953)
- (3) J. Burgess, R. H. Prince, J. Chem. Soc., 4697, (1965)
- (4) S. Radulovic *private communication*
- (5) J. March, "Advanced Organic Chemistry: Reactions, Mechanisms, and Structure", 2nd Edition, McGraw-Hill, (1977)
- (6) M. H. Abraham, T. Hill, H. C. Ling, R. A. Schulz, R. A. C. Watt, J. Chem. Soc., Faraday Trans. I, 80, 489, (1984)



# CHAPTER

# 6

Salt effects on the neutral  
hydrolysis of Phenylchloroacetate  
and its para-methoxy derivative

## 6.1 Introduction

Reaction rates in aqueous solution of both charged and neutral solutes are sensitive to the addition of added salts<sup>1,2,3</sup>. In this Chapter, rate constants for the neutral hydrolysis of phenyldichloroacetate (PDCA) and the para-methoxy derivative (p-OMePDCA) are reported for reaction at 298.15 K in aqueous solutions containing MX and R<sub>4</sub>NX salts where M = Li<sup>+</sup>, Na<sup>+</sup>, K<sup>+</sup>, Rb<sup>+</sup>, Cs<sup>+</sup>, R = Me, Et, Bu and X = F<sup>-</sup>, Cl<sup>-</sup> and Br<sup>-</sup>. In addition the dependence on temperature was determined for the neutral hydrolysis of p-OMePDCA in salt solutions containing 0.2 mol dm<sup>-3</sup> and 0.9 mol dm<sup>-3</sup> tetrabutylammonium bromide, 0.2 mol dm<sup>-3</sup> and 0.9 mol dm<sup>-3</sup> tetrabutylammonium fluoride, 0.9 mol dm<sup>-3</sup> tetrabutylammonium chloride and 0.9 mol dm<sup>-3</sup> potassium bromide. The dependence on temperature is reported for the p-OMePDCA ester and the unsubstituted derivative over the temperature range 293.15 ≤ T/K ≤ 318.15. Solvent isotope effects are reported for the neutral hydrolysis of PDCA in aqueous solutions containing 0.9 mol dm<sup>-3</sup> Bu<sub>4</sub>NBr, Bu<sub>4</sub>NF, Me<sub>4</sub>NF and CsF at 298.15 K.

Trends in rate constants are discussed in terms of the properties of the salt solutions. In particular the effect of cosphere-cosphere overlap is identified as a major contribution to the observed patterns of kinetic salt effects.

## 6.2 Salt Solutions

### 6.2.1 Ionic Hydration

Consider the situation in which a salt-j is added to water such that in the resulting solution each ion is unaware of

the presence of any other ion i.e. the solution is infinitely dilute. For such a situation the hydration model proposed by Frank and Wen<sup>4</sup> for alkali metal and halide ions is applicable (see Figure 6.1).

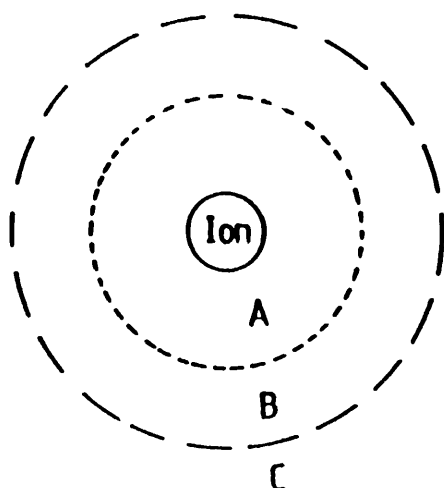


FIGURE 6.1

Model for ionic hydration in aqueous solution.

Three zones of solvent structure are identified within the model. Zone A contains electrostricted water. Water molecules within this zone represent the primary hydration shell of the solute. Zone C contains water molecules unperturbed by the presence of the anion and can be thought of as the bulk solvent. Zone B contains water molecules in a mismatch region between zones A and C where the organisation of the water molecules differs from that of the bulk. The organisation within zone B is often called 'structure broken' and the extent of the zone depends on ion size. Large ions such as  $I^-$  and  $Br^-$  have large zone B regions and are called electrostrictive structure breakers. However for smaller ions such as  $F^-$  and  $Li^+$  zone B does not

exist, these ions are called electrostrictive structure formers. The hydration of tetraalkylammonium ions is controlled by the apolar alkyl groups. These ions are classed as hydrophobic water structure formers, the degree of structure enhancement increasing with the size of the alkyl group. The  $\text{Me}_4\text{N}^+$  ion is often regarded as a structure breaker whereas the  $\text{Et}_4\text{N}^+$  ion appears to have no marked structural effects on bulk water<sup>5</sup>. Hence only  $\text{Pr}_4\text{N}^+$  and the higher alkylammonium ions are regarded as structure formers.

### 6.2.2 Real Salt Solutions

To a first approximation a major contribution to the non-ideal properties of aqueous salt solutions stems from charge-charge interactions. The chemical potential of a 1:1 salt-j in aqueous solution is related to composition using equation [6.1].

$$\mu_j(\text{aq}; T; p) = \mu_j(\text{aq}; T; p; m_j=1; \gamma_{\pm}=1) + 2RT \ln(m_j \gamma_{\pm} / m^\circ) \quad [6.1]$$

where  $\gamma_{\pm}$  is the mean ionic activity coefficient and  $m^\circ = 1 \text{ mol kg}^{-1}$ . Equation [6.1] can be written in the form;

$$\begin{aligned} \mu_j(\text{aq}; T; p) = & \underbrace{\mu_j(\text{aq}; T; p; m_j=1; \gamma_{\pm}=1)}_{\text{ideal part}} + 2RT \ln(m_j / m^\circ) \\ & + 2RT \ln(\gamma_{\pm}) \quad [6.2] \\ & \leftarrow \text{non ideal} \rightarrow \end{aligned}$$

In very dilute solutions the hydration shells of ions remain undisturbed such that there are no cosphere-

cosphere interactions. The non-ideal part of the chemical potential can be modelled for very dilute aqueous solution by the Debye-Huckel Limiting Law (DHLL).

$$\ln \gamma_{\pm} = -S_{\gamma} |z_+ z_-| (I/m^{\circ})^{1/2} \quad [6.3]$$

where  $I$  is the ionic strength ( $= 0.5 \sum m_j z_j^2$ );  $|z_+ z_-|$  the modulus of the product of the charge numbers and  $S_{\gamma}$  depends on the temperature and the dielectric properties of the solvent.

In slightly more concentrated solutions the non-ideal part of the chemical potential is modelled by the Debye-Huckel equation.

$$\ln \gamma_{\pm} = (-S_{\gamma} |z_+ z_-| (I/m^{\circ})^{1/2}) / (1 + B(I/m^{\circ})^{1/2}) \quad [6.4]$$

However, this equation is only a first approximation for in dilute aqueous solution trends in  $\ln \gamma_{\pm}$  cannot be predicted by the Debye-Huckel treatment alone. The presence of some underlying pattern to  $\ln \gamma_{\pm}$  led Desnoyers<sup>6</sup> and workers to draw attention to the effects of cosphere-cosphere overlap as an important factor in determining the properties of aqueous salt solutions. In effect in dilute solution equation [6.4] can be extended to the form;

$$\ln \gamma_{\pm} = \text{Debye-Huckel} + f(\text{cosphere}) \quad [6.5]$$

Where  $f(\text{cosphere})$  represents the effect of cosphere overlap on  $\ln \gamma_{\pm}$ . If  $f(\text{cosphere}) < 0$  then there is a lowering of the chemical potential of the salt,  $\mu_j$ , and hence a

stabilisation of the salt solution. Conversely if  $f(\text{cosphere}) > 0$  then  $\mu_j$  is increased giving a destabilising effect.

Extension of the Debye-Huckel treatment to more concentrated salt systems by the addition of new terms to the equation has received interest from many workers. The work of Pitzer<sup>7</sup> in this area is particularly noteworthy and is discussed in Chapter 7. The treatments discussed by Pitzer are applied to group interaction parameters in Chapter 8 and to the analysis of kinetic data for the alkaline hydrolysis of the sodium salt of bromophenol blue<sup>8,9</sup> in Chapter 9.

Cosphere overlap effects are not limited to interactions in salt solutions. The properties of solutions containing salts and neutral solutes can also be understood in terms of cosphere interactions. In this Chapter patterns in kinetic parameters are discussed in terms of cosphere-cosphere overlap effects.

## 6.3 Experimental

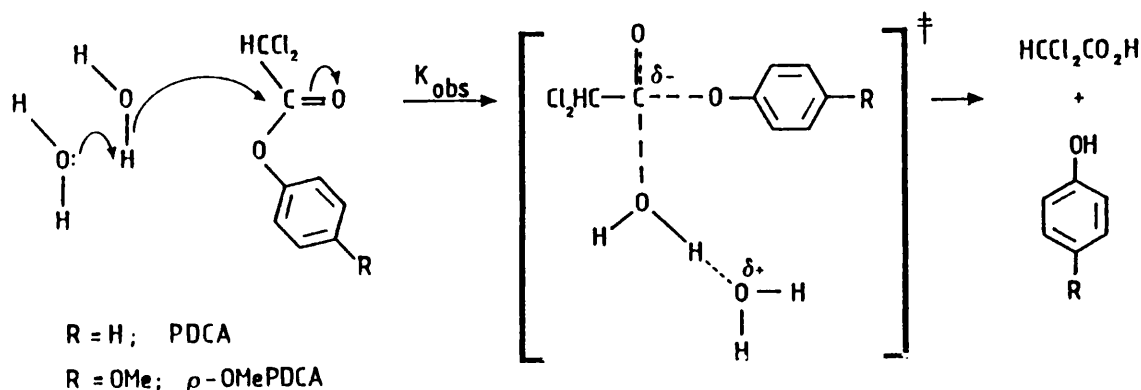
### 6.3.1 Preparation of Phenyl dichloroacetate and the para-Methoxy Derivative

Dichloroacetyl chloride (0.1 mol), dissolved in 15 cm<sup>3</sup> of absolute ether, were added dropwise to equivalent amounts of the desired phenol and pyridine in 50 cm<sup>3</sup> of absolute ether. This mixture was stirred for three hours under nitrogen, in a flask fitted with a double surface water condenser, at room temperature. The resulting mixture was filtered to remove pyridine.HCl; crude ester was obtained after evaporation of the ether. The ester was

recrystallised from a 50/50 mixture of dried ether and 60-80 dried petroleum ether. The product was characterised by its melting point<sup>10</sup> (PDCA 320.55 - 320.57 K, p-OMePDCA 335.35 - 335.95 K).

### 6.3.2 Investigation of the Kinetics of the Neutral Hydrolysis of PDCA and its para-Methoxy Derivative in Aqueous Salt Solutions.

The neutral hydrolysis in aqueous solution of PDCA and p-OMePDCA has the mechanism<sup>11-15</sup> shown in Scheme 1. Rate determining water-catalysed attack by water at the carbonyl group forms two products, dichloroacetic acid and a characteristic phenol.



Scheme 1

Reactions were monitored by observing the formation of phenol using the HP 8451A diode array spectrophotometer at a predetermined  $\lambda_{\text{max}}$  ( $\lambda_{\text{max}}$  PDCA = 272 nm,  $\lambda_{\text{max}}$  pOMePDCA = 288 nm). Solutions of alkali metal and tetraalkylammonium halide salts were prepared using  $10^{-2}$  mol dm<sup>-3</sup> hydrochloric acid to a concentration of 0.9 mol dm<sup>-3</sup>. The acid inhibited possible base catalysis of the reaction<sup>10</sup>. As a further

precaution pH measurements of the solutions containing tetraalkylammonium fluorides confirmed the solutions were acid. Several preliminary studies were made of the effects of added tetrabutylammonium bromide and potassium bromide on the reaction rate (Figure 6.3 and Table 6.1). As a result it was decided to study the effect of various added salts at a common concentration of  $0.9 \text{ mol dm}^{-3}$ . This molarity gave a significant change in rate constant for all added salts compared to the reaction rate in the absence of added salt.

In a typical kinetic run  $2 \text{ cm}^3$  of a salt solution were pipetted into a  $3 \text{ cm}^3$  quartz cell which was placed in the HP 8451A diode array spectrophotometer and allowed to come to thermal equilibrium. After approximately five minutes the reaction was initiated by adding to the cell one drop of a very dilute solution of reactant in acetonitrile. The reaction was monitored for at least 2.5 half lives and the absorbance/time data analysed using the method of non-linear least squares to obtain the rate constant (see Chapter 2). All reactions followed first order kinetics and each run was repeated at least three times to produce an averaged first order rate constant for reaction in each salt solution. At worst the rate constant was reproducible to within approximately three per cent.

Occasionally a rapid jump in absorbance was recorded in the middle of a run - Figure 6.4. At first this was believed to be due to phenol oxidation<sup>16</sup>. However this problem was resolved by ensuring the reactant and the salt solution were thoroughly mixed.

No rate constants were obtained for the reactions in

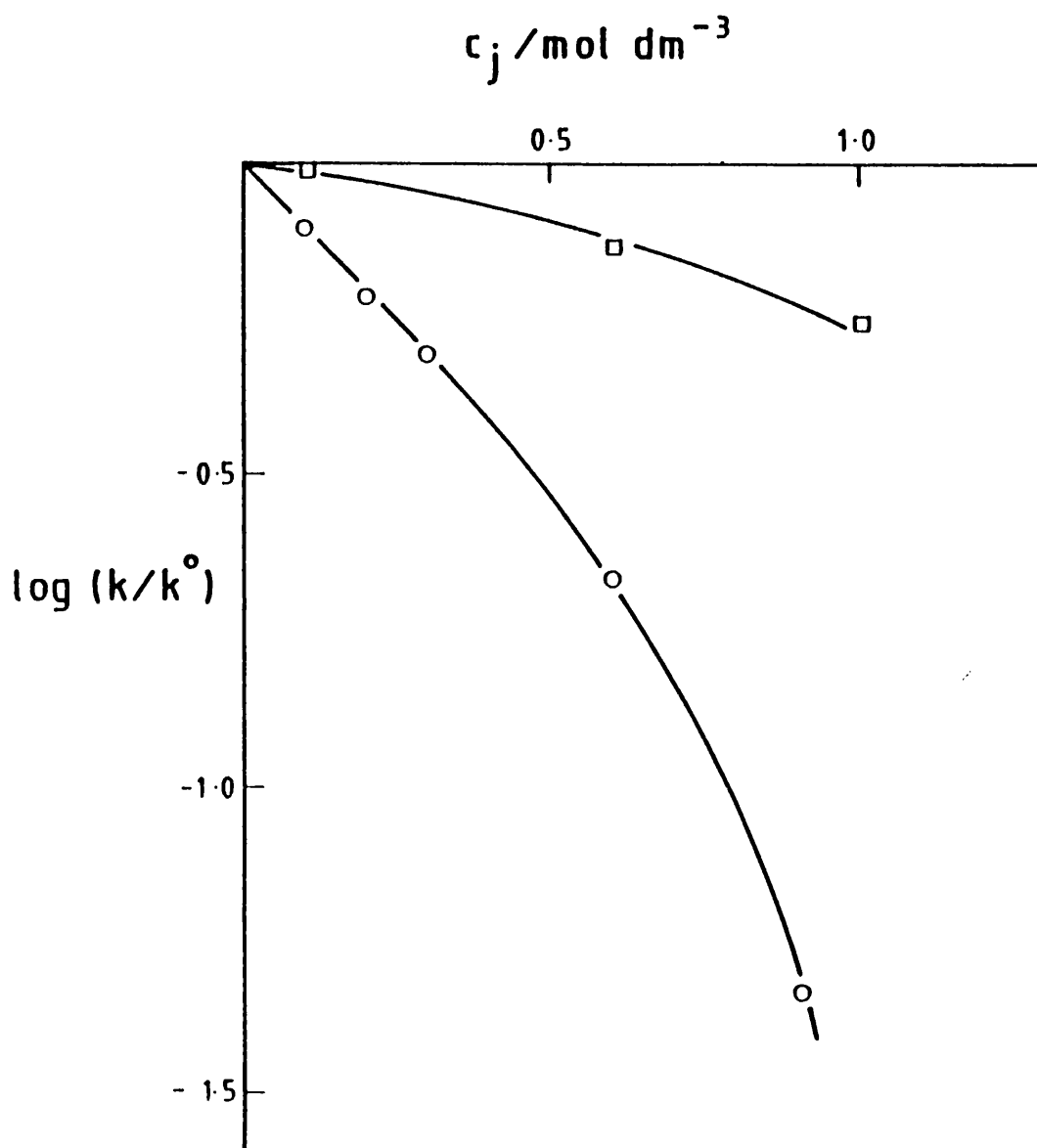


**FIGURE 6.3**

Dependence of  $\log(k/k_0)$  on concentration of added salt ( $\text{mol dm}^{-3}$ ).  $\square$  = potassium bromide,  $\circ$  = tetrabutylammonium bromide.

Table 6.1

First order rate constants for the neutral hydrolysis of PDCA in aqueous solutions containing known concentrations of potassium bromide and tetrabutylammonium bromide at 298K.

KBr /mol dm <sup>-3</sup>	10 <sup>3</sup> k /s <sup>-1</sup>	log(k/k <sub>0</sub> )
0.00	3.263	-
0.10	3.175	-0.012
0.30	3.160	-0.014
0.50	3.102	-0.022
0.07	2.942	-0.045
1.00	2.489	-0.118
1.50	2.117	-0.188

Bu <sub>4</sub> NBr /mol dm <sup>-3</sup>	10 <sup>3</sup> k /s <sup>-1</sup>	log(k/k <sub>0</sub> )
0.00	3.263	-
0.10	2.895	-0.052
0.20	2.273	-0.157
0.30	1.869	-0.242
0.60	0.903	-0.558
0.90	0.240	-0.133

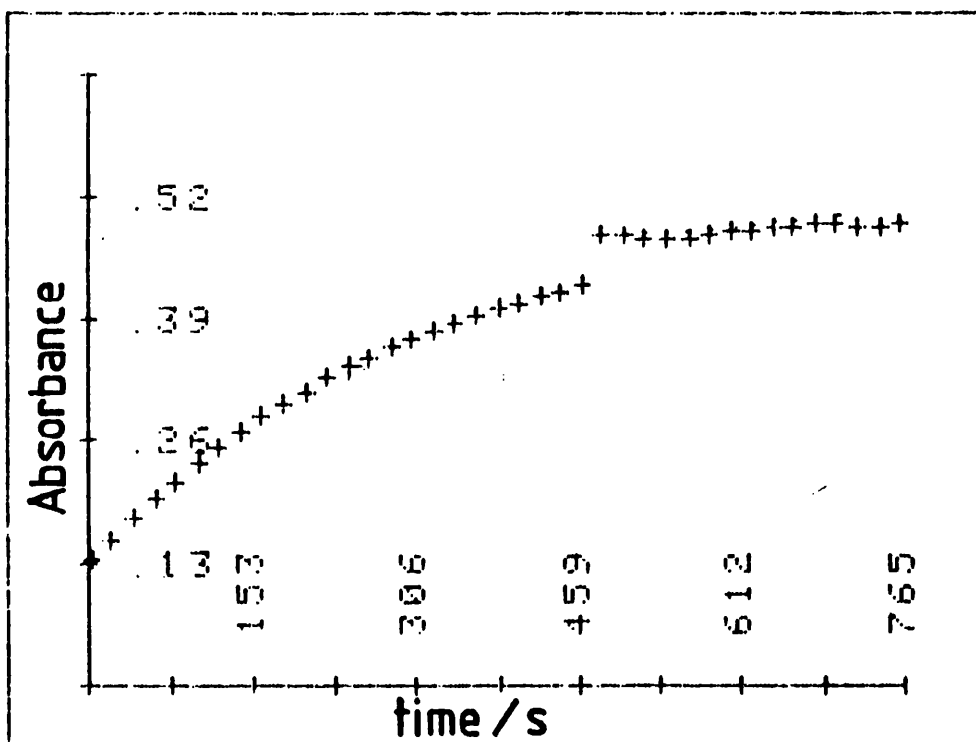


FIGURE 6.4

Dependence of absorbance on time at  $\lambda_{\max} = 274$  for the neutral hydrolysis of phenyldichloroacetate at 298 K. [Discontinuity in curve due to insufficient mixing of reactant and aqueous salt solution.]

the presence of iodide salts because (i) iodide ions absorb strongly in a charge-transfer-to-solvent transition in the region of phenol absorbance and (ii) on irradiation iodide anions produce the  $I_3^-$  species which has a large charge transfer band in the same region of the electromagnetic spectrum. These bands effectively mask any phenol band produced during the course of the reaction<sup>17</sup>.

Dependences of rate constant on temperature were studied in a similar fashion by adjusting the temperature of the thermostatically controlled cell block within the spectrophotometer. The enthalpy of activation,  $\Delta^\ddagger H^\infty$  was calculated using a plot of  $\ln(k/T)$  against  $(1/T)$ . The slope of the graph yields the enthalpy of activation.  $\Delta^\ddagger H^\infty$  was obtained to a higher degree of accuracy by a linear least squares fit of the data to equation [6.6].

$$\ln(k/T) = A + B/T \quad [6.6]$$

Here parameter B corresponds to the gradient of the graph. A BASIC program for an HP 85 computer which describes a linear least squares procedure is included for reference in Appendix 1. The entropy of activation,  $\Delta^\ddagger S^\#$ , was calculated using the Eyring equation [6.7].

$$k = (k_B T/h) \exp(-\Delta^\ddagger H^\infty/RT) \exp(\Delta^\ddagger S^\#/R) \quad [6.7]$$

where  $k_B$  is the Boltzmann constant,  $h$  is Plank's constant and  $R$  is the gas constant.

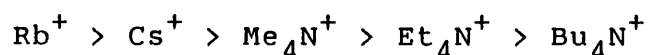
In the solvent isotope studies it was necessary to replace the salt solutions containing HCl ( $10^{-2}$  mol dm<sup>-3</sup>)

with salt solutions containing deuterium chloride ( $10^{-2}$  mol  $\text{dm}^{-3}$ ).  $\text{DCl}(\text{aq})$  was made by adding appropriate quantities of 37 weight per cent  $\text{DCl}$  in deuterium oxide to deuterium oxide. The ratio of the observed rate constants in both solvents is defined as the solvent deuterium isotope effect (SDIP); equation [6.8].

$$\text{SDIP} = k(\text{H}_2\text{O})/k(\text{D}_2\text{O}) \quad [6.8]$$

#### 6.4 Results

First order rate constants for reaction in the presence of added salts for the unsubstituted and p-OMe substituted reactant are given in Tables 6.2 and 6.3 respectively. This information has been represented graphically in the form of plots of  $\ln(k/k_0)$  (where  $k_0$  is the first order rate constant in the absence of added salt) against the anion of the salt (Figures 6.5 and 6.6). Data for PDCA have been taken from reference 16 over the same salt range as p-OMePDCA to give an overall picture for both reactants. From these figures it is possible to see the rate retarding effect of the chloride and bromide salts compared to the rate accelerating effect of the fluoride salts. For the bromide salts a pattern is established in which the rate constants decrease in the order;



Intuitively one might expect the trend in rate constants for the fluoride salts, to be the reverse of that described for the bromide salts i.e. the largest rate constant would be for the reactions conducted in the presence of tetrabutylammonium fluoride. However there appears to be no

Table 6.2

First order rate constants for the neutral hydrolysis of PDCA in the presence of fluoride salts at a concentration of  $0.9 \text{ mol dm}^{-3}$  at 298K.

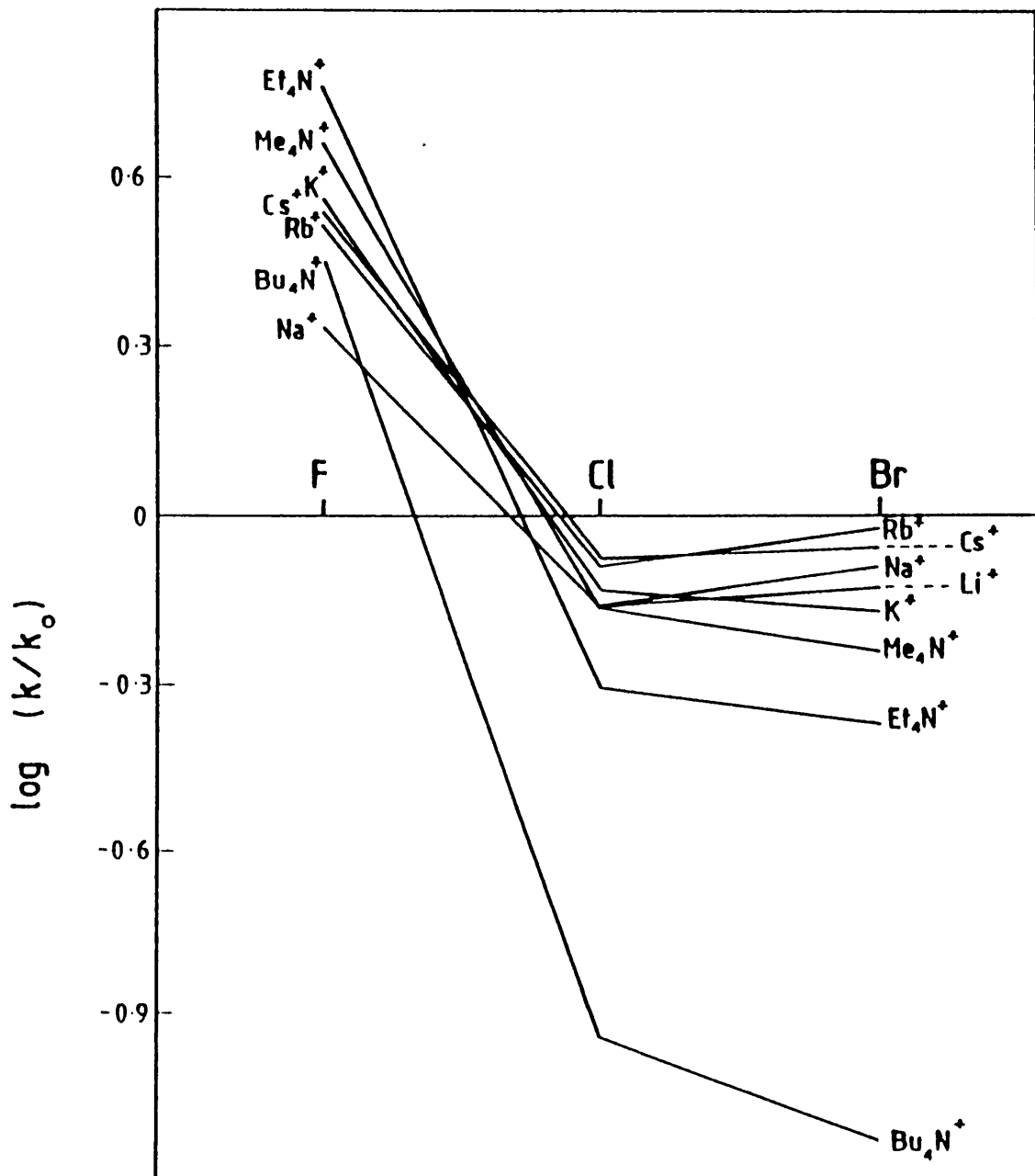
Added salt	Rate Constant $10^2 k_{\text{obs}}/\text{s}^{-1}$
RbF	0.106
Me <sub>4</sub> NF	1.491
Et <sub>4</sub> NF	1.880
Bu <sub>4</sub> NF	9.750

Table 6.3

First order rate constants for the neutral hydrolysis of p-OMe PDCA in the presence of fluoride, chloride and bromide salts at a concentration of 0.9 moldm<sup>-3</sup> at 298K. Rate constant with no added salt  $k_0/s^{-1} = 2.730 \times 10^{-3}$ .

Added Salt	Rate Constant $10^3 k_{\text{obs}}/s^{-1}$
NaF	6.782
KF	8.062
RbF	7.827
CsF	11.640
Me <sub>4</sub> NF	10.040
Et <sub>4</sub> NF	7.958
Bu <sub>4</sub> NF	6.518

Added Salt	Rate Constant $10^3 k_{\text{obs}}/s^{-1}$	Added Salt	Rate Constant $10^3 k_{\text{obs}}/s^{-1}$
LiCl	2.199	LiBr	2.108
NaCl	1.881	NaBr	1.897
KCl	2.063	KBr	1.965
RbCl	2.517	RbBr	2.209
CsCl	2.068	CsBr	1.953
Me <sub>4</sub> NCl	1.935	Me <sub>4</sub> NBr	1.613
Et <sub>4</sub> NCl	1.362	Et <sub>4</sub> NBr	1.110
Bu <sub>4</sub> NCl	0.262	Bu <sub>4</sub> NBr	0.173



**FIGURE 6.5**

Log ( $k/k_0$ ) against anion  $X^-$  (where  $X^- = F^-, Cl^-, Br^-$ ) for  $M^+$  and  $R_4N^+$  for the neutral hydrolysis of phenyl-dichloroacetate in aqueous solution at 298 K where  $[salt] = 0.9 \text{ mol dm}^{-3}$ .

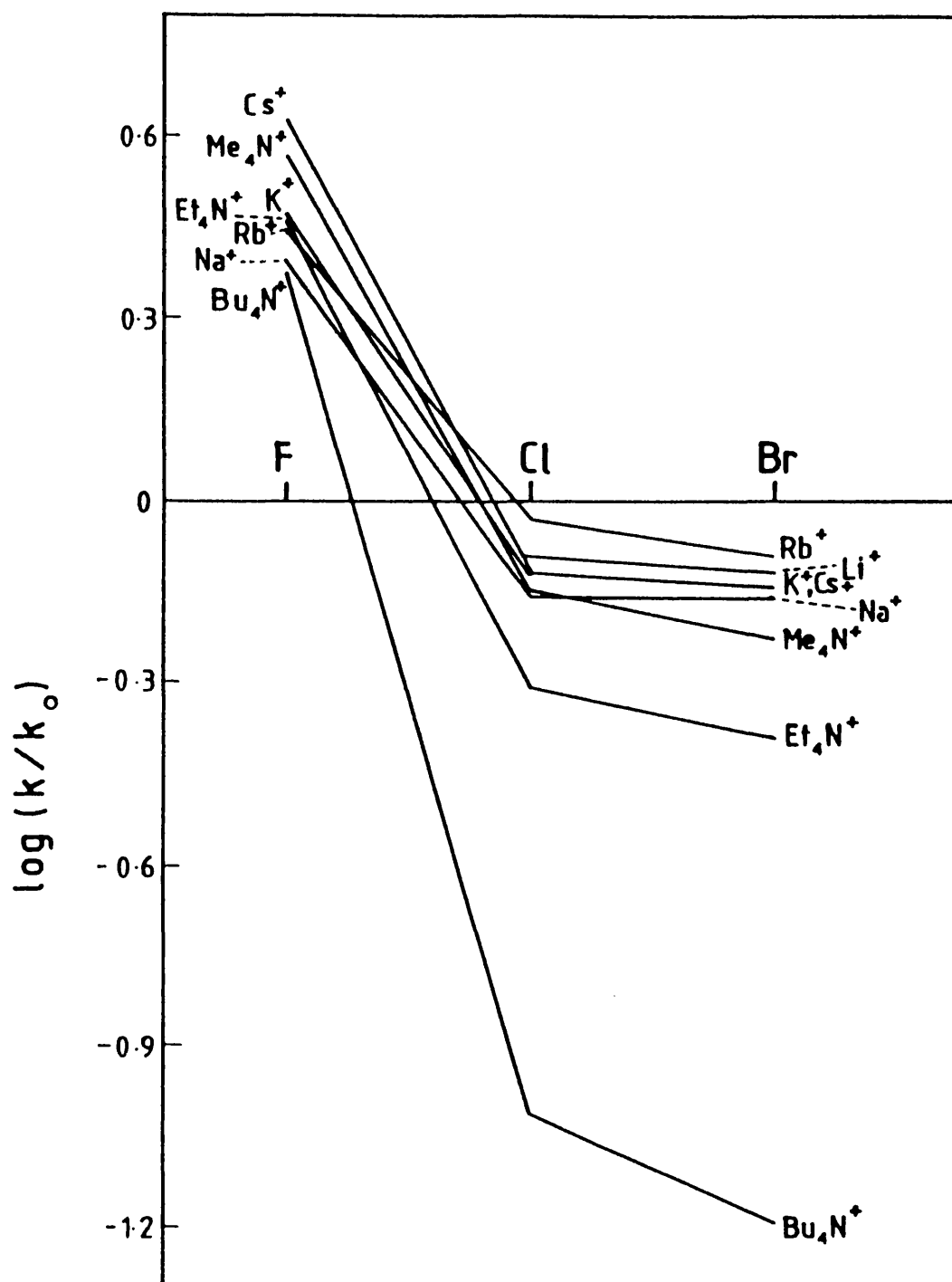


FIGURE 6.6

Log ( $k/k_0$ ) against the anion  $X^-$  (where  $X^- = F^-, Cl^-$  and  $Br^-$ ) for  $M^+$  and  $R_4N^+$  salts for the neutral hydrolysis of para-methoxy phenyldichloroacetate in aqueous solution at 298 K where  $[salt] = 0.9 \text{ mol dm}^{-3}$ .

such trend. Despite this it should be noted that the change in rate constant on going from  $\text{Bu}_4\text{NBr}$  to  $\text{Bu}_4\text{NF}$  is still the largest observed for both esters.

Table 6.4 reports activation parameters for the reaction of p-OMePDCA solutions containing 0.9 and 0.2 mol  $\text{dm}^{-3}$  tetrabutylammonium bromide, 0.9 mol  $\text{dm}^{-3}$  tetrabutylammonium chloride, 0.9 and 0.2 mol  $\text{dm}^{-3}$  tetrabutylammonium fluoride, 0.9 mol  $\text{dm}^{-3}$  potassium bromide and in the absence of added salt. The activation parameters for the neutral hydrolysis of PDCA in the absence of added salt are also reported in this Table. A plot of  $\ln(k/T)$  against  $(1/T)$  for the neutral hydrolysis of p-OMePDCA in the absence of added salt is included as Figure 6.7. Inspection of these results identifies large changes in the activation enthalpies and entropies of reaction which are masked in the changes in rate constant. For example, in the case of 0.9 mol  $\text{dm}^{-3}$  potassium bromide, an overall decrease in the rate constant is observed. This could normally be explained in terms of an increase in the enthalpy of activation. However results point towards a decrease in the enthalpy of activation which is over compensated by a decrease in the entropy of activation. Similarly, in the case of tetrabutylammonium bromide 0.9 mol  $\text{dm}^{-3}$  for which an overall reaction rate increase is observed. This would normally be explained in terms of a decrease in the enthalpy of activation. However the results point towards an increase in  $\Delta^\ddagger H^\circ$  with a more than compensating increase in the entropy of activation. These patterns indicate the dominant role of the entropy term in this type of reaction and points towards an explanation in

Table 6.4

Activation parameters for the neutral hydrolysis of p-OMe PDCA in aqueous salt solutions of known concentration.

(a) no added salt

Temperature /K	$10^3 k_{obs}$ /s <sup>-1</sup>	$\Delta^\ddagger G^\#$ kJmol <sup>-1</sup>	$-\Delta^\ddagger S^\#$ JK <sup>-1</sup> mol <sup>-1</sup>
298	2.723	87.52	201.9
303	3.334	88.62	202.2
308	4.088	89.60	202.1
313	4.874	90.64	202.2
318	5.823	91.66	202.2

$\Delta^\ddagger H^\infty / \text{kJmol}^{-1} = 27.34 \pm 0.33$

(b) 0.9 moldm<sup>-3</sup> KBr

Temperature /K	$10^3 k_{obs}$ /s <sup>-1</sup>	$\Delta^\ddagger G^\#$ kJmol <sup>-1</sup>	$-\Delta^\ddagger S^\#$ JK <sup>-1</sup> mol <sup>-1</sup>
293	1.603	87.40	223.6
298	1.965	88.42	223.3
303	2.259	89.60	223.5
308	2.689	90.67	223.4
313	3.046	91.86	223.6

$\Delta^\ddagger H^\infty / \text{kJmol}^{-1} = 21.88 \pm 0.91$

(c) 0.2 moldm<sup>-3</sup> Bu<sub>4</sub>NF

Temperature /K	$10^3 k_{obs}$ /s <sup>-1</sup>	$\Delta^\ddagger G^\#$ kJmol <sup>-1</sup>	$-\Delta^\ddagger S^\#$ JK <sup>-1</sup> mol <sup>-1</sup>
293	3.036	85.84	163.3
298	4.147	86.59	162.1
303	5.499	87.36	162.9
308	6.838	88.28	163.3
313	8.918	89.06	163.2

$\Delta^\ddagger H^\infty / \text{kJmol}^{-1} = 38.00 \pm 1.06$

(d) 0.9 mol dm<sup>-3</sup> Bu<sub>4</sub>NF

Temperature /K	10 <sup>3</sup> k <sub>obs</sub> /s <sup>-1</sup>	Δ <sup>‡</sup> G <sup>#</sup> kJ mol <sup>-1</sup>	-Δ <sup>‡</sup> S <sup>#</sup> JK <sup>-1</sup> mol <sup>-1</sup>
298	6.518	85.45	86.89
303	9.980	85.85	86.78
308	15.213	86.23	86.86
313	21.505	86.77	86.95

Δ<sup>‡</sup>H<sup>∞</sup>/kJ mol<sup>-1</sup> = 59.55 ± 1.55

(e) 0.9 mol dm<sup>-3</sup> Bu<sub>4</sub>NCl

Temperature /K	10 <sup>4</sup> k <sub>obs</sub> /s <sup>-1</sup>	Δ <sup>‡</sup> G <sup>#</sup> kJ mol <sup>-1</sup>	-Δ <sup>‡</sup> S <sup>#</sup> JK <sup>-1</sup> mol <sup>-1</sup>
298	2.615	93.47	189.8
303	3.288	94.50	190.1
308	4.340	95.37	189.9
313	5.497	96.34	189.9
318	7.058	97.28	189.9

Δ<sup>‡</sup>H<sup>∞</sup>/kJ mol<sup>-1</sup> = 36.86 ± 0.80

(f) 0.2 mol dm<sup>-3</sup> Bu<sub>4</sub>NBr

Temperature /K	10 <sup>3</sup> k <sub>obs</sub> /s <sup>-1</sup>	Δ <sup>‡</sup> G <sup>#</sup> kJ mol <sup>-1</sup>	-Δ <sup>‡</sup> S <sup>#</sup> JK <sup>-1</sup> mol <sup>-1</sup>
298	1.694	88.81	196.6
303	2.085	89.80	196.6
308	2.562	90.79	196.7
313	3.207	91.73	196.5
318	3.861	92.74	196.6

Δ<sup>‡</sup>H<sup>∞</sup>/kJ mol<sup>-1</sup> = 30.22 ± 0.47

(g) 0.9 moldm<sup>-3</sup> Bu<sub>4</sub>NBr

Temperature /K	10 <sup>4</sup> kobs /s <sup>-1</sup>	Δ <sup>‡</sup> G <sup>#</sup> kJmol <sup>-1</sup>	-Δ <sup>‡</sup> S <sup>#</sup> JK <sup>-1</sup> mol <sup>-1</sup>
298	1.733	94.44	183.8
303	2.265	95.39	183.9
308	2.936	96.34	184.0
313	3.922	97.20	183.8
318	5.027	98.13	183.8

Δ<sup>‡</sup>H<sup>∞</sup>/kJmol<sup>-1</sup> = 39.68 ± 0.62

(h) no added salt for the neutral hydrolysis of the unsubstituted ester PDCA.

Temperature /K	10 <sup>3</sup> kobs /s <sup>-1</sup>	Δ <sup>‡</sup> G <sup>#</sup> kJmol <sup>-1</sup>	-Δ <sup>‡</sup> S <sup>#</sup> JK <sup>-1</sup> mol <sup>-1</sup>
298.15	3.263	87.21	196.1
300.65	3.663	87.67	196.0
303.15	3.991	88.25	196.2
308.15	4.905	89.18	196.1
313.15	5.996	90.14	196.1

Δ<sup>‡</sup>H<sup>∞</sup>/kJmol<sup>-1</sup> = 28.73 ± 0.50

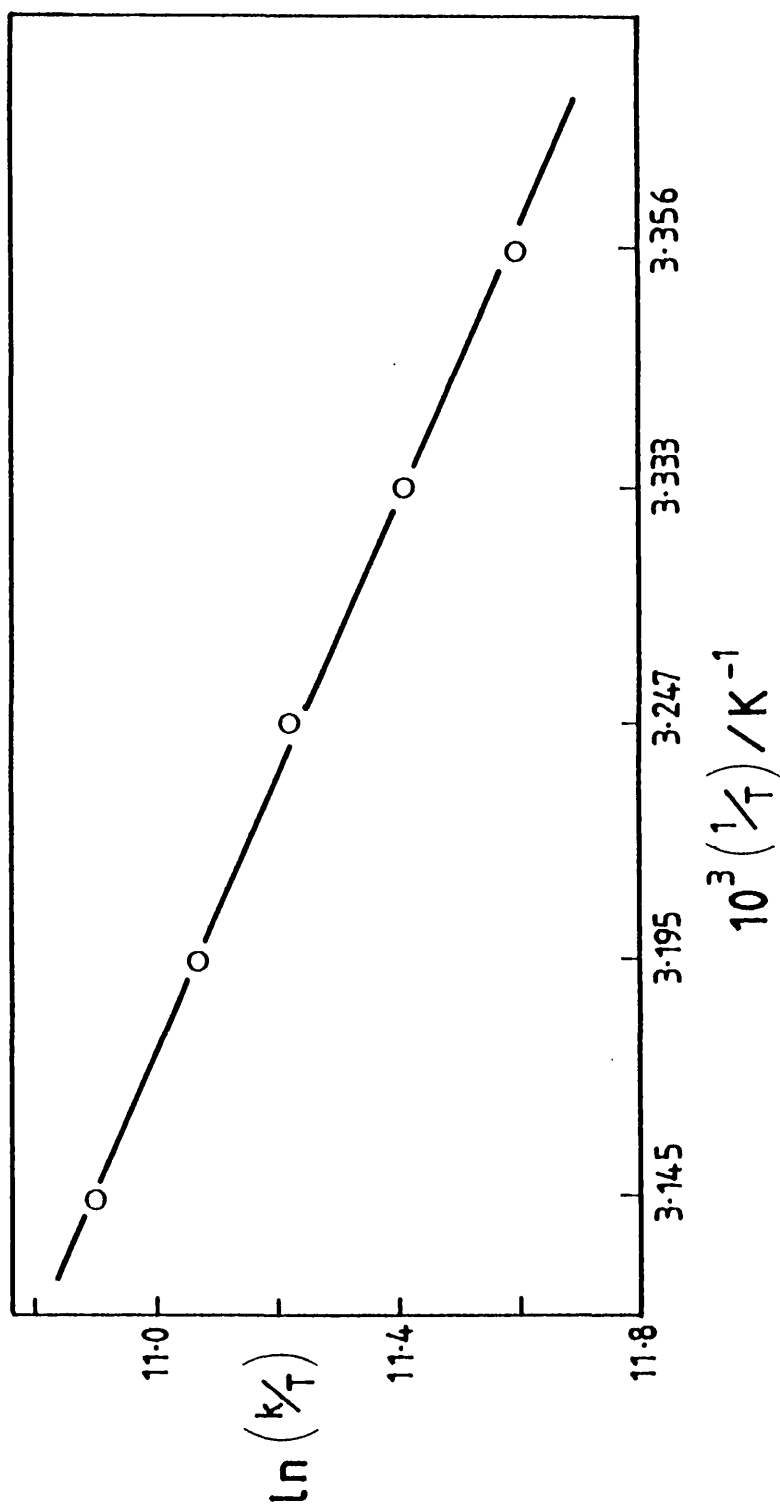


FIGURE 6.7

$\ln(k/T)$  against the  $10^3 (1/T) / K^{-1}$  for the neutral hydrolysis of p-methoxy phenyldichloroacetate in 0.01 mol dm<sup>-3</sup> hydrochloric acid.

which the structure of the solution is critical.

Solvent deuterium isotope effects (Table 6.5) are consistent with work conducted by previous authors<sup>10</sup> in which it was concluded that the parameters vary with added salt type and concentration i.e. the solvent isotope effect is sensitive to change in solvent arrangement around the reacting solute during the activation process. The tabulated values are also in line with a mechanism which involves water-catalysed attack by water at a carbonyl group<sup>15</sup>.

### 6.5 Discussion

In explaining the patterns observed in Figures 6.5 and 6.6 one must first comment on the striking similarity they hold with the pattern identified by Desnoyers<sup>6</sup> in connection with  $\ln\gamma_{\pm}$ . Figure 6.8 reproduces a Desnoyers type plot for the salts investigated during the course of this Chapter.

Table 6.6 summarises<sup>18-21</sup>  $\ln\gamma_{\pm}$  used for the salts investigated. The patterns observed in Figures 6.8, 6.5 and 6.6 can be explained in terms of cosphere-cosphere overlap effects.

A starting point is the model for salt solutions proposed by Gurney<sup>22</sup>, in which each solute molecule is surrounded by a cosphere of solvent molecules. By definition organisation of solvent structure within such a cosphere differs from the organisation of the bulk solvent, the organisation within the cosphere being characteristic of each solute. The properties of these solutions can be explained, at least in part, in terms of the impact of cosphere-cosphere overlap in the solutions<sup>6</sup>.

Table 6.5

Solvent deuterium isotope effects for the neutral hydrolysis of PDCA in the presence of known concentrations ( $\text{mol dm}^{-3}$ ) of added salts at 298K.

salt	$10^3 k(\text{H}_2\text{O})$ / $\text{s}^{-1}$	$10^3 k(\text{D}_2\text{O})$ / $\text{s}^{-1}$	$k(\text{H}_2\text{O})/k(\text{D}_2\text{O})$
0.9M $\text{Bu}_4\text{NBr}$	0.303	0.082	3.690
0.9M $\text{Bu}_4\text{NF}$	9.750	4.745	2.055
0.9M $\text{Me}_4\text{NF}$	1.490	0.543	2.744
0.9M $\text{CsF}$	1.510	0.499	3.026

All rate constants are the average of at least 3 separate runs.

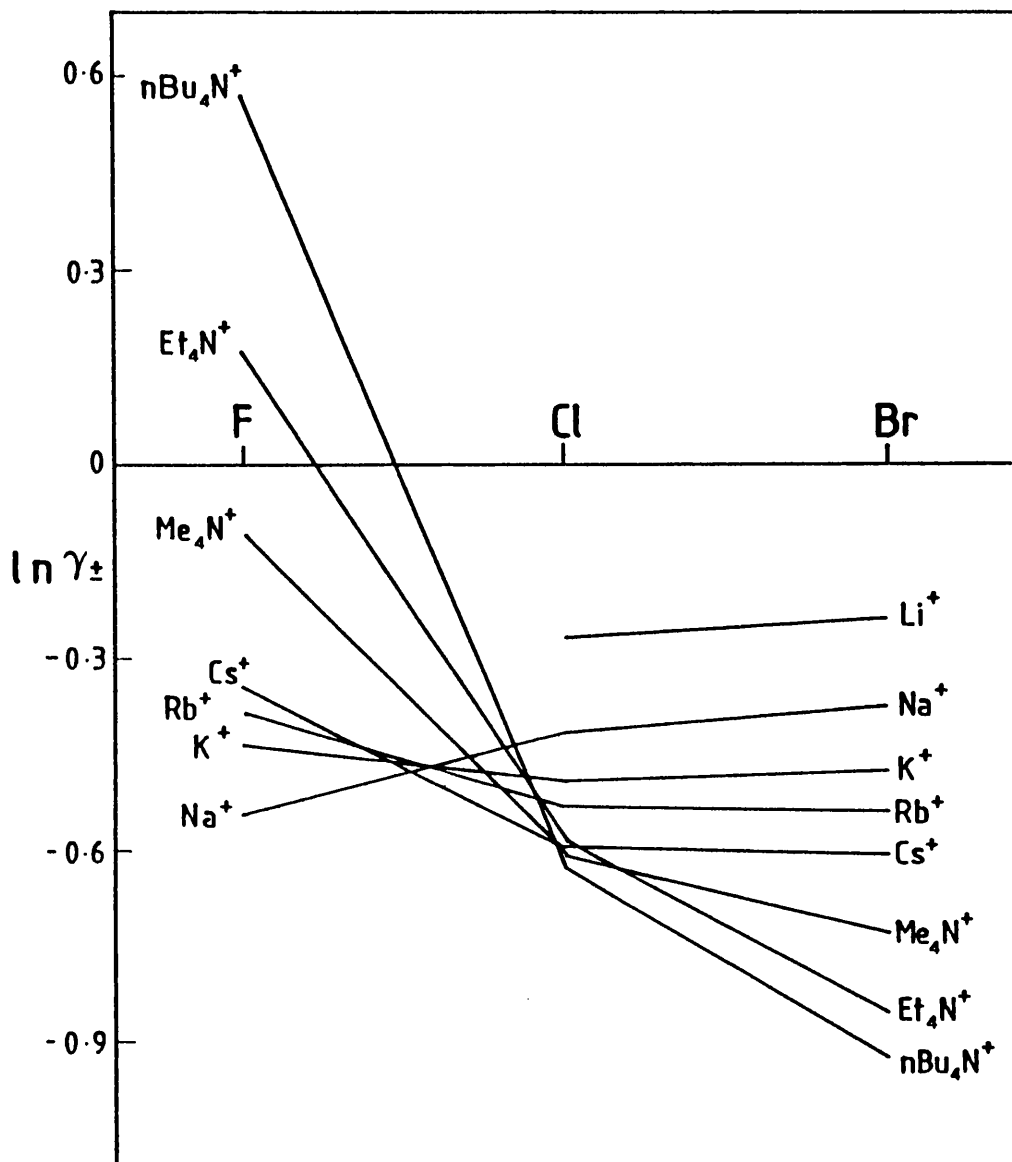


FIGURE 6.8

$\ln \gamma_{\pm}$  against the anions  $X^{-}$  (where  $X^{-} = F^{-}$ ,  $Cl^{-}$  and  $Br^{-}$ ) for  $M^{+}$  and  $R_4N^{+}$  salts in aqueous solution at 298 K where  $[salt] = 0.9 \text{ mol dm}^{-3}$ .

Table 6.6

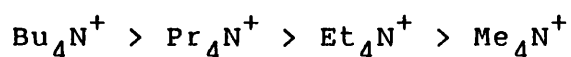
Activity coefficients,  $\gamma_{\pm}$ , of MX and  $R_4NX$  electrolytes at  $[\text{salt}] = 0.9\text{mol dm}^{-3}$  in aqueous solvent at 298K. (where X=  $F^{-}$ ,  $Cl^{-}$ ,  $Br^{-}$ ; M=  $Li^{+}$ ,  $Na^{+}$ ,  $K^{+}$ ,  $Rb^{+}$ ,  $Cs^{+}$ ; R= Me, Et, Bu)

Salt	Reference	$\gamma_{\pm}$	$\ln\gamma_{\pm}$
LiCl	21	0.764	-0.269
NaCl	21	0.659	-0.417
KCl	21	0.610	-0.494
RbCl	21	0.590	-0.528
CsCl	21	0.553	-0.592
LiBr	21	0.789	-0.237
NaBr	21	0.687	-0.375
KBr	21	0.622	-0.475
RbBr	21	0.586	-0.534
CsBr	21	0.547	-0.603
NaF	21	0.582	-0.541
KF	21	0.646	-0.437
RbF	18	0.682	-0.383
CsF	18	0.710	-0.343
Me <sub>4</sub> NCl	19	0.546	-0.605
Et <sub>4</sub> NCl	19	0.557	-0.585
Bu <sub>4</sub> NCl	19	0.625	-0.470
Me <sub>4</sub> NBr	19	0.483	-0.728
Et <sub>4</sub> NBr	19	0.427	-0.851
Bu <sub>4</sub> NBr	19	0.397	-0.924
Me <sub>4</sub> NF	20	0.902	-0.103
Et <sub>4</sub> NF	20	1.192	0.176
Bu <sub>4</sub> NF	20	1.785	0.579

The overall influence of the solute on the structure of water in solution can be split into two types; electrostrictive structure breakers and hydrophobic structure formers. The effect of overlap between these solutes was summarised by Desnoyers<sup>6</sup> together with the influence of overlap on the excess thermodynamic properties, Figure 6.9.

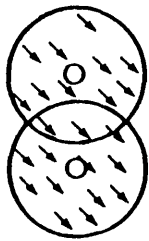
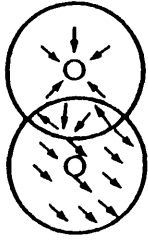
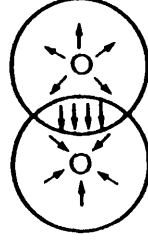
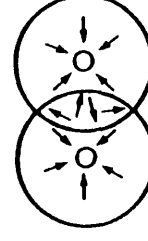
Turning to the patterns observed in Figures 6.8, 6.5 and 6.6, in tetrabutylammonium bromide solutions, cation-cation cosphere interactions dominate the properties of the solution.  $\text{Bu}_4\text{N}^+$  cations are strongly hydrophobic whereas bromide anions are less hydrophilic than chloride or fluoride anions. Attraction between the hydrophobic  $\text{Bu}_4\text{N}^+$  cospheres results in water being incorporated into the overlap region between the cospheres. The total Gibbs function of the system decreases to less than that for the corresponding ideal solution (which is imagined as a solution in which there are no cosphere-cosphere interactions). The reaction rate is therefore retarded (c.f a negative deviation from the DHLL for the  $\ln\gamma_{\pm}$  plot).

The hydrophobic nature of R in  $\text{R}_4\text{N}^+$  decreases in the order;



Therefore a steady rate increase is observed on going down the series as the hydrophobic effect becomes less dominant. A corresponding increase in the total Gibbs function is expected, although it will never exceed that of the ideal solution.

The alkalimetal bromide salts have a very small and similar retardation effect on the reaction rate. The total

		EFFECT OF OVERLAP AND RESULTING FORCE	CONTRIBUTION TO EXCESS FUNCTIONS			
			$\bar{G}^{EX}$	$\bar{V}^{EX}$	$\bar{H}^{EX}$	$\bar{S}^{EX}$
	Hb-Hb	less str. form. attraction	-	-	+	+
	Hb-HI	more str. br. repulsion	+	-	+	+
	HI-HI opp. sign	less str. br. attraction	-	+	-	-
	HI-HI same sign	more str. br. repulsion	+	-	+	+

**FIGURE 6.9**

Structural hydration interaction model. Hb, hydrophobic ion; HI, hydrophilic ion; str. form., structure forming; str. br., structure breaking. [Taken from Ref. 6]

Gibbs function of these systems is only slightly less than that for the corresponding ideal solution and a balance is struck between hydrophilic-hydrophilic (same-sign) and hydrophilic-hydrophobic (opposite-sign) cosphere-cosphere interactions. The attraction between oppositely charged ions slightly dominates the cosphere interactions, hence a slight rate retardation is observed. The trend in  $\log(k/k_0)$  for chloride salts is similar but less significant than for bromide salts. Chloride anions are more hydrophilic than bromide anions.

For the fluoride salts MF and  $R_4NF$  the total Gibbs function of the system is greater than the Gibbs function of the ideal solution, as demonstrated by an acceleration in reaction rate and a positive deviation from the DHLL for the  $\ln\gamma_{\pm}$  plot. The hydration characteristics of the fluoride salts are dominated by the repulsion between solute cospheres i.e hydrophobic-hydrophilic ( $R_4N^+-F^-$ ) cosphere interactions for the tetraalkylammonium fluoride salt solutions and hydrophilic-hydrophilic (same-sign), ( $M^+-M^+$ ) and ( $F^- - F^-$ ) cosphere interactions for the alkali metal fluoride salts.

The activation parameters for these reactions point towards a more complicated situation than the above explanation offers. However at this stage it is not possible to identify any clear patterns.

As a consequence of the reaction being the attack of water, one might expect a simple relationship between the practical osmotic coefficient and rate constants. In particular a relationship between  $\beta^0$  coefficients (see Chapters 7 and 8) and rate constants might be expected,

where  $\beta^\circ$  represents the pairwise interactions of the solutes, both cosphere and hard-sphere, after the charging process has been subtracted. In Chapter 8 it is shown how  $\beta^\circ$  and salt concentration are related for apolar solutes in salt solutions. Therefore it could be expected that a correlation exists between  $\beta^\circ$  and the salt concentration for the ester and for the transition state. This implies a correlation exists between rate constants and  $\beta^\circ$ . Figure 6.10 shows a plot of  $\ln(k/k_0)$  against  $\beta^\circ$  in which there appears to be a broad correlation. However scatter is observed. This is understandable because in principle  $\beta^\circ$  could be used to calculate independent Setschenow coefficients of both the initial and transition states. However a plot of  $\ln(k/k_0)$  against  $\beta^\circ$  effectively compares  $\beta^\circ$  to the difference between the properties of the initial and transition states. This procedure obviously magnifies any error incorporated into the initial and transition state parameters and so the plot provides an exacting test for a possible correlation between  $\beta^\circ$  and kinetic parameters.

This Chapter has pinpointed cosphere-cosphere overlap as an important factor in determining the properties of aqueous salt solutions by using the neutral hydrolysis water-catalysed reaction as a probe to investigate water structure when various electrolytes are added. It has also identified complicated underlying patterns which exist for the enthalpies and entropies of activation in this class of reaction. The theme of salt effects is continued in Chapters 7, 8 and 9.

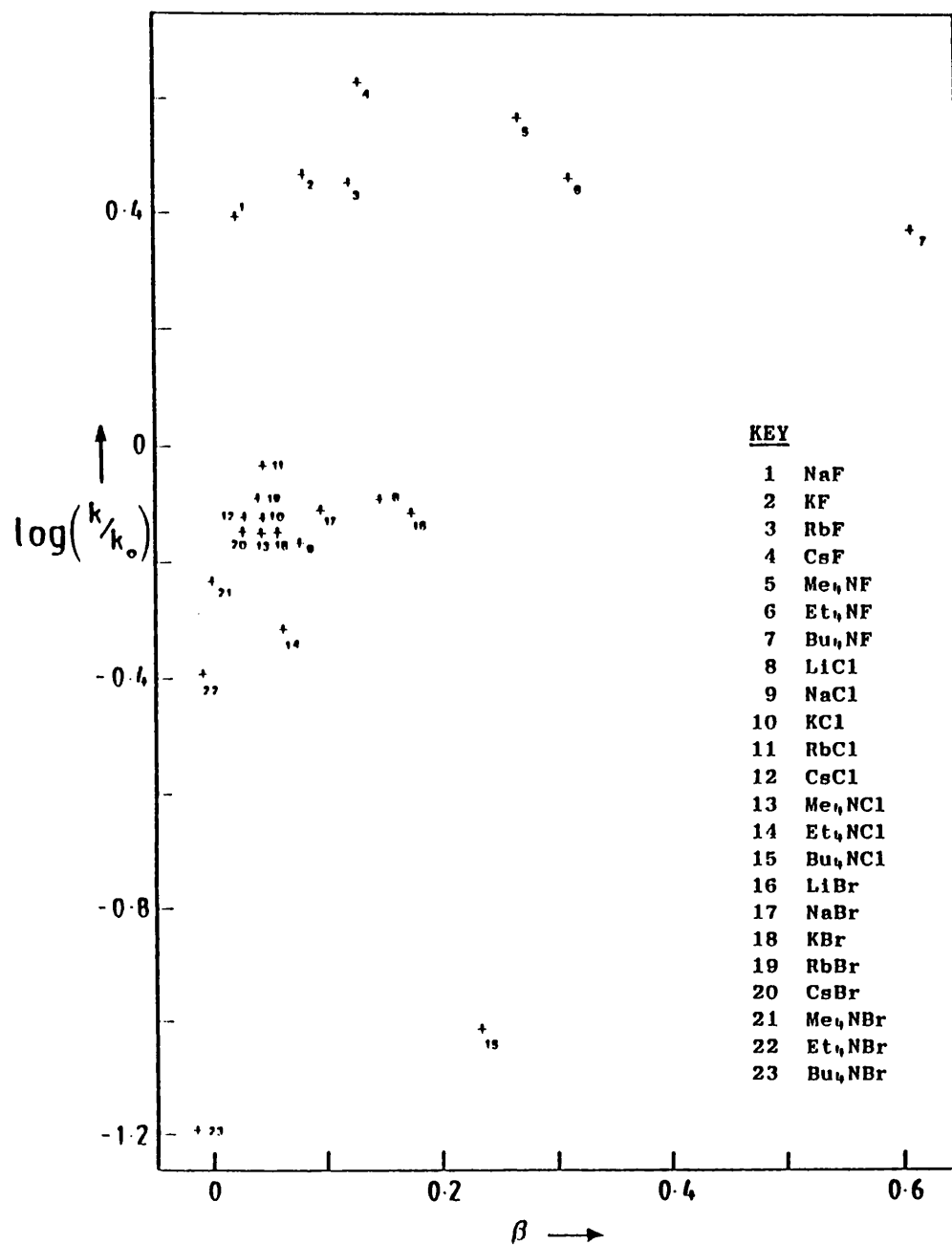


FIGURE 6.10

$\log(k/k_0)$  calculated from the first order rate constants for the neutral hydrolysis of para-methoxy phenyldichloroacetate against  $\beta^\circ$  parameters, tabulated by Pitzer [Ref. 7].

## References Chapter 6

- (1) L.Menninga, J.B.F.N.Engberts, J.Am.Chem.Soc., 98, 7652, (1976)
- (2) N.F.Ashford, M.J.Blandamer, J.Burgess, D.Laycock, M.Waters, P.Wellings, R.Woodhead, F.M.Mckhail, J.Chem.Soc.,Dalton.Trans., 869, (1979)
- (3) M.J.Blandamer, J.Burgess, P.P.Duce, S.J.Hamshere, J.J.Walker, J.Chem.Soc.,Dalton Trans., 1809, (1980)
- (4) H.S.Frank, W.-Y.Wen, Diss. Faraday Soc., 24, 133, (1957)
- (5) R.L.Kay, "Advances in Chemistry Series", 73 1, (1963)
- (6) J.E.Desnoyers, M.Arel, G.Perron, C.Jolicoeur, J.Phys.Chem., 73, 2346, (1969)
- (7) K.S.Pitzer, "Activitty Coefficients in Electrolyte Solution" ,Vol.1, CRC Press Inc., (1979)
- (8) C.S.Amis, V.K.LaMer, J.Am.Chem.Soc., 61, 905, (1939)
- (9) J.R.Velasco, F.S.Burgos, M.C.Carmona, J.H.Toledo, An.Quim., 80, 173, (1984)
- (10) J.F.J.Engbersen, PhD Thesis, Groeningen University, Holland, (1976)
- (11) W.P.Jenks, J.Carriuolo, J.Am.Chem.Soc., 83, 1743, (1961)
- (12) J.F.J.Engbersen, J.B.F.N.Engberts, J.Am.Chem.Soc., 97, 1563, (1975)
- (13) H.A.J.Holterman, J.B.F.N.Engberts, J.Am.Chem.Soc., 104, 6382, (1982)
- (14) H.A.J.Holterman, J.B.F.N.Engberts, J.Org.Chem., 48, 4025, (1983)
- (15) J.B.F.N.Engberts, "Water a Comprehensive Treatise", Vol.6, Ed. F.Franks, New York, (1979)
- (16) B.Briggs, PhD Thesis, University of Leicester (1985)
- (17) M.J.Blandamer, M.F.Fox, Chem.Revs., 70, 59, (1970)

- (18) T.Tien, J.Phys.Chem., 67, 532, (1963)
- (19) S.Lindenbaum, G.E.Boyd, J.Phys.Chem., 68, 911,  
(1964)
- (20) W.-Y.Wen, S.Saito, C.M.Lee, J.Phys.Chem., 70  
1244, (1966)
- (21) R.A.Robinson, R.H.Stokes, "Electrolyte  
Solutions", 2nd Ed., Butterworths, London,  
(1959)
- (22) R.W.Gurney, "Ionic Processes in Solution"  
McGraw-Hill, New York, (1953)



# CHAPTER 7

Pitzer's Equations for the activity  
coefficients of salts and the  
relationship between osmotic coefficients,  
activity coefficients and the Excess  
Gibbs function

## 7.1 Introduction

In the previous Chapter it was shown how the effects of added salt on rates of reactions between neutral species in dilute salt solutions can be accounted for using treatments based on the Debye-Huckel equations for the dependence of the activity coefficients of ions on ionic strength. It was also shown however, that the predictive power of these equations diminished as the effect of cosphere interactions and specific ion-ion interactions increased. In this Chapter the equations of Pitzer<sup>1,2,3</sup> are surveyed as a method of extending quantitative treatments to more concentrated salt solutions. In particular Pitzer's equations are used as a basis for calculating Savage-Wood parameters<sup>4,5,6,7</sup> characterising pairwise Gibbs function cosphere-cosphere interaction parameters. The stimulus for this study originated in the task of accounting for observed patterns in rate constants for chemical reactions in solutions containing added electrolytes<sup>8,9</sup>. In Chapter 9 the predictive power of Pitzer's equations and the Debye-Huckel treatment is examined for mixed electrolyte systems with reference to kinetic data describing the alkaline hydrolysis of the sodium salt of bromophenol blue<sup>10,11</sup> in the presence of various added salts.

### 7.2.1 Salt Solutions

By definition the chemical potential of an ion-*j* in solution is related to its molality  $m_j$  by equation [7.1].

$$\mu_j(\text{sln}; T; p) = \mu_j^\#(\text{sln}; T; p) + RT \ln \{ m_j \gamma_j / m^\circ \} \quad [7.1]$$

Where  $\gamma_j$  is the activity coefficient of ion-j;  $m^\circ = 1 \text{ mol kg}^{-1}$ ;  $\mu_j^\#(\text{sln}; T; p)$  is the chemical potential of ion-j in solution at the same T and p where  $m_j = 1$  and  $\gamma_j = 1$ .

The chemical potential of a salt is related to the chemical potential of cations and anions using equation [7.2].

$$\begin{aligned} \mu(\text{salt}; \text{sln}; T; p) &= v_m \mu(\text{M-cation}; \text{sln}; T; p) \\ &+ v_x \mu(\text{X-anion}; \text{sln}; T; p) \quad [7.2] \end{aligned}$$

Here one mole of salt forms on complete dissociation  $v_m$  moles of cations, M, and  $v_x$  moles of anions, X. Also for the salt in the reference state;

$$\begin{aligned} \mu^\#(\text{salt}; \text{sln}; T; p) &= v_m \mu^\#(\text{M-cation}; \text{sln}; T; p) \\ &+ v_x \mu^\#(\text{X-anion}; \text{sln}; T; p) \quad [7.3] \end{aligned}$$

By definition ;

$$v = v_{m+} + v_{x-} \quad [7.4]$$

$$\gamma_{\pm}^v = \gamma_{m+}^{v+} \gamma_{x-}^{v-} = \gamma_+^{v+} \gamma_-^{v-} \quad [7.5]$$

$$\text{and } m_{\pm}^v = m_+^{v+} m_-^{v-} \quad [7.6]$$

also  $m_+ = v_+ m_2$  and  $m_- = v_- m_2$  where  $m_2$  is the molality of the salt MX. Hence;

$$\begin{aligned} \mu(\text{sln}; \text{salt}; T; p) &= \mu^\#(\text{salt}; \text{sln}; T; p) + RT \ln \{ m_+^{v+} \gamma_+^{v+} / m^\circ \} \\ &+ RT \ln \{ m_-^{v-} \gamma_-^{v-} / m^\circ \} \quad [7.7] \end{aligned}$$

or alternatively;

$$\begin{aligned} \mu(\text{salt}; \text{sln}; T; p) &= \mu^\#(\text{salt}; \text{sln}; T; p) \\ &+ RT \ln \{ (v_+^{v+} v_-^{v-} m_2^v \gamma_{\pm}^v) / (m^\circ)^v \} \quad [7.8] \end{aligned}$$

By definition;  $Q^{\pm} = v_+^{v^+} v_-^{v^-}$

Hence;

$$\mu(\text{salt}; \text{sln}; T; p) = \mu^{\#}(\text{salt}; \text{sln}; T; p) + vRT \ln\{(Qm_2 \gamma_{\pm})/m^{\circ}\} \quad [7.9]$$

Where  $\lim(m_2 \rightarrow 0) \gamma_{\pm} = 1.0$  at all  $T$  and  $p$ . Then  $\mu(\text{salt}; \text{sln}; T; p)$  is the chemical potential of salt in solution at the same  $T$  and  $p$  where  $m_2 = 1.0$  and  $\gamma_{\pm} = 1.0$ .

By definition the chemical potential of the solvent is given by equation [7.10].

$$\mu_1(\text{sln}; T; p) = \mu_1^*(l; T; p) - v\phi RT m_1 m_2 \quad [7.10]$$

Where  $\phi$  is the practical osmotic coefficient, which for an ideal solution equals 1.0;  $\mu_1^*(l; T; p)$  is the chemical potential of pure liquid solvent at the same  $T$  and  $p$ .

### 7.2.2 Consideration of Excess Properties

According to equation [7.9] the chemical potential of a salt MX in ideal solution is given by equation [7.11].

$$\mu(\text{salt}; \text{id}; \text{sln}; T; p) = \mu^{\#}(\text{salt}; \text{sln}; T; p) + vRT \ln\{(Qm_2)/m^{\circ}\} \quad [7.11]$$

Hence the excess chemical potential of the salt  $\mu^E(\text{salt}; \text{sln}; T; p)$  is obtained from the difference  $\mu(\text{salt}; \text{sln}; T; p) - \mu(\text{salt}; \text{id}; \text{sln}; T; p)$ ;

$$\mu^E(\text{salt}; \text{sln}; T; p) = vRT \ln(\gamma_{\pm}) \quad [7.12]$$

The chemical potential of a solvent in an ideal solution is given by equation [7.13].

$$\mu_1(\text{id};\text{sln};T;p) = \mu_1^*(l;T;p) - vRTM_1m_2 \quad [7.13]$$

Hence the excess chemical potential of the solvent is given by equation [7.14].

$$\begin{aligned} \mu_1^E &= \mu_1(\text{sln};T;p) - \mu_1(\text{sln};\text{id};T;p) \\ \Rightarrow \mu_1^E &= vRTM_1m_2(1-\phi) \end{aligned} \quad [7.14]$$

### 7.2.3 The Solution

A given solution contains  $n_1$  moles of solvent and  $n_2$  (=  $M_1n_1m_2$ ) moles of salt MX. The excess Gibbs function of the system is given by equation [7.15].

$$\begin{aligned} G^E(\text{sln};T;p;n_1 \text{ moles solvent}) &= n_1 vRTM_1m_2(1-\phi) \\ &+ M_1n_1m_2RT \ln(\gamma_{\pm}) \end{aligned} \quad [7.15]$$

$$\begin{aligned} \Rightarrow G^E(\text{sln};T;p;n_1 \text{ moles solvent})/(n_1RT) &= \\ v m_2 M_1 [(1-\phi) + \ln(\gamma_{\pm})] \end{aligned} \quad [7.16]$$

By definition the excess Gibbs function of the salt MX in 1kg of solvent is described by equation [7.17].

$$G^E(\text{sln};T;p;w_1/\text{kg}=1) = G^E(\text{sln};T;p;n_1 \text{ moles solvent})/(n_1M_1) \quad [7.17]$$

$$\Rightarrow G^E(\text{sln};T;p;w_1/\text{kg}=1) = vRTm_2[(1-\phi) + \ln(\gamma_{\pm})] \quad [7.18]$$

Communication of the changes in chemical potential of

the salt and the solvent is obtained through the Gibbs-Duhem equation at fixed temperature and pressure.

$$n_1 d\mu_1(\text{sln}; T; p) + n_2 d\mu_2(\text{salt}; \text{sln}; T; p) = 0 \quad [7.19]$$

In a solution containing 1 kg of solvent;

$$\begin{aligned} (1/M_1) d\{\mu_1^*(1; T; p) - \phi RT v m_2 M_1\} + m_2 d\{\mu_2^\#(\text{sln}; T; p) \\ + v RT \ln(Q m_2 \gamma_\pm / m^\circ)\} = 0 \end{aligned}$$

Hence the Gibbs-Duhem equation for a salt solution can be written;

$$d[-m_2 \phi] + m_2 d[\ln(m_2 / m^\circ) + \ln(\gamma_\pm)] = 0 \quad [7.20]$$

This equation can be applied in two ways. If  $\ln \gamma_\pm$  is known as a function of  $m_2$ , then  $(1-\phi)$  can be calculated. Alternatively if  $(1-\phi)$  is known as a function of  $m_2$ , then  $\ln \gamma_\pm$  can be calculated. [N.B.  $d[m_2(1-\phi)] = d[m_2 - m_2 \phi] = 1 - d(m_2 \phi)$ ; further details are given in Appendix 3 Section 1.].

#### 7.2.4 Models for Salt Solutions

As described in Chapter 6 equation [6.3], the Debye-Huckel limiting law, (DHLL), describes the mean ionic activity coefficient as a function of the ionic strength<sup>12</sup>,  $I$ . The equations in Appendix 3 Section 2 are used to obtain an equation for the dependence of  $\phi$  on ionic strength. Hence;

$$\phi - 1 = -|z_+ z_-| (S_\gamma / 3) (m_2 / m^\circ)^{1/2} \quad [7.21]$$

A quantity  $S_\phi$  is defined by  $S_\phi = (S_\gamma/3)$ . Hence;

$$\phi-1 = -|z_+z_-|S_\phi(m_2/m^\circ)^{1/2} \quad [7.22]$$

The Debye-Huckel equation for the mean ionic activity coefficient of a salt in solution is given by equation [6.4] of Chapter 6. The equations in Appendix 3 Section 3 yield an equation for the corresponding dependence of  $\phi$  on ionic strength. Hence;

$$(1-\phi) = |z_+z_-|(S_\gamma/3)(I)^{1/2}\sigma(x) \quad [7.23]$$

where  $x = b(I)^{1/2}$  and  $\sigma(x) = (3/x^3)\{(1+x) - (1/[1+x]) + 2\ln(1+x)\}$ .

The equations described above are restricted to the DHLL and the full Debye-Huckel equation. In practice their success is modest. Bronsted<sup>13</sup> and Guggenheim<sup>14,15</sup> sought to extend the range in which  $\ln\gamma_\pm$  could be predicted by basing their theories on Debye-Huckel treatment and including terms which took account of specific ion-ion interactions. Pitzer argued that a better approach is through solution theory which leads to a virial equation for  $(\phi-1)$  in terms of solute-solute interactions. As shown earlier an equation for  $\ln\gamma_\pm$  can then be obtained through the Gibbs-Duhem equation.

### 7.2.5 Pitzer's Equations

Pitzer's equations are based on virial coefficients for  $(\phi-1)$  and hence for  $\ln\gamma_\pm$ . In summary form the equations for  $\phi-1$  and  $\ln\gamma_\pm$  are as shown in equations [7.24] and [7.25].

$$\phi-1 = |z_+z_-|f^\phi + m_2(2v_m v_x/v)B_{mx}^\phi + m_2^2\{2(v_m v_x)^{3/2}/v\}C_{mx}^\phi \quad [7.24]$$

$$\ln\gamma_\pm = |z_m z_x|f^\gamma + m_2(2v_m v_x/v)B_{mx}^\gamma + m_2^2\{2(v_m v_x)^{3/2}/v\}C_{mx}^\gamma \quad [7.25]$$

### 1. The Electrostatic f-Term

Pitzer considered various forms of this term, favouring that given in equation [7.26]

$$f_{DHO}^\phi = -A^\phi\{(I/m^\circ)^{1/2}/(1+b(I/m^\circ)^{1/2})\} \quad [7.26]$$

$A^\phi$  is the Debye-Huckel term (written above previously as  $S^\phi$ ). The equation for  $\ln\gamma_\pm$  corresponding to the equation for  $\phi$  based on  $f_{DHO}^\phi$  can be calculated using the Gibbs-Duhem equation; Appendix 3 Section 4. Hence;

$$\ln\gamma_\pm = -|z_+z_-|A^\phi\{[(I/m^\circ)^{1/2}/(1+b(I/m^\circ)^{1/2})] - (2/b)\ln(1+b(I/m^\circ)^{1/2})\} \quad [7.27]$$

where  $A^\phi = (A^\gamma/3)$ .

### 2. The B Term

The second virial coefficient in the equation for  $\phi$  was based on the following form;

$$B^\phi = \beta^\circ + \beta^1 \exp(-\alpha(I/m^\circ)^{1/2}) \quad [7.28]$$

This form was selected as a result of calculating the practical osmotic coefficient for a series of 1:1 and 2:1

salts from equations in which all forms of  $f^\phi$  and  $B^\phi$  were tested. According to Pitzer, this simple form has the desirable properties of (i) finite value at zero ionic strength (ii) a rapid change linear in  $I^{1/2}$  at low ionic strength and (iii) a smooth approach to a constant value at high ionic strength. The constant  $\alpha$  was independently varied throughout the analysis and best general agreement was obtained with  $\alpha = 2.0$ .

Pitzer<sup>1</sup> advanced arguments based on the results of Card and Valleau<sup>16</sup>. These require that  $\beta^0$  represents contributions from interactions between like and unlike charges whilst  $\beta^1$  represents short range interactions between unlike charged ions. Granted therefore that equation [7.28] defines  $B^\phi$  in terms of  $\beta^0$  and  $\beta^1$ , an integrated form of the Gibbs-Duhem equation yields  $B^\gamma$  also in terms of  $\beta^0$  and  $\beta^1$ ; Appendix 3 Section 5. Hence;

$$B_{mx}^\gamma = 2\beta^0 + (2\beta^1/\alpha^2 I)[1 - [1 + \alpha I^{1/2} - (\alpha^2 I/2)] \exp(-\alpha I^{1/2})] \quad [7.29]$$

where  $I = (I/m^0)$ . For higher valence salts the possibility arises that a  $\beta^{(2)}$  term is required, in which case<sup>17</sup>;

$$B^{\phi\beta(2)} = \beta^{(2)}_{mx} \exp(-\alpha(I/m^0)^{1/2}) \quad [7.30]$$

Consequently;

$$B^{\gamma\beta(2)} = (2\beta^{(2)}/\alpha^2 I)[1 - [1 + \alpha I^{1/2} - (\alpha^2 I/2)] \exp(-\alpha I^{1/2})] \quad [7.31]$$

where  $I = (I/m^0)$ . Thus equation [7.29] can be written in the form;

$$B_{mX}^{\gamma} = 2\beta^{\circ} + (2\beta^1/\alpha^2 I)[1-[1+\alpha I^{1/2}-(\alpha^2 I/2)]\exp(-\alpha I^{1/2})] \\ + (2\beta^{(2)}/\alpha^2 I)[1-[1+\alpha I^{1/2}-(\alpha^2 I/2)]\exp(-\alpha I^{1/2})] \quad [7.32]$$

where  $I = (I/m^{\circ})$ .

### 3. The C Term

The third virial coefficient,  $C^{\phi}$ , is specific for each salt MX. The corresponding  $C^{\gamma}$  term is again calculated using an integrated Gibbs-Duhem equation; Appendix 3 Section 6. Hence;

$$C^{\gamma} = (3/2)C^{\phi} \quad [7.33]$$

The various terms were drawn together by Pitzer to yield an equation for  $(\phi-1)$  and  $\ln\gamma_{\pm}$ .

$$\phi-1 = -|z_+z_-|A^{\phi}(m_2^{1/2}/(1+bm_2^{1/2})) + \\ 2m_2(v_m v_x/v)[\beta^{\circ} + \beta^1 \exp(-\alpha m_2^{1/2}) + \beta^{(2)} \exp(-\alpha m_2^{1/2})] + \\ m_2^2 [2(v_m v_x)^{3/2}/v]C_{mX}^{\phi} \quad [7.34]$$

$$\ln\gamma_{\pm} = -|z_+z_-|A^{\phi}(m_2^{1/2}/(1+bm_2^{1/2})) - |z_+z_-|A^{\phi}(2/b) \\ \ln(1+bm_2^{1/2}) + 2m_2[(2v_m v_x)/v]\beta^{\circ} + 2m_2[(v_m v_x)/v] \\ [(2\beta^1/\alpha^2 m_2)\{1-\exp(-\alpha m_2^{1/2})[1+\alpha m_2^{1/2}-(\alpha^2 m_2/2)]\}] \\ + 2m_2\{(v_m v_x)/v\}\{(2\beta^{(2)})/\alpha^2 m_2\}[1-[1+\alpha m_2^{1/2}-(\alpha^2 m_2)/2] \\ \exp(-\alpha m_2^{1/2})] + 2m_2^2\{(v_m v_x)^{3/2}/v\}(3/2)C^{\phi} \quad [7.35]$$

### 7.2.6 Extension of Analysis to Consideration of the Excess Gibbs Function.

Pitzer extended the analysis based on  $(\phi-1)$  to include equations for the excess Gibbs function,  $G^E$  (see Section

7.2.3).

In his analysis the excess Gibbs function is defined for a system in 1 kg of solvent as shown in equation [7.18] or;

$$(G^E/RT) = v_{m_2}[1-\phi + \ln\gamma_{\pm}] \quad [7.36]$$

Equation [7.36] is then expressed in an analogous form to equations [7.24] and [7.25];  $G^E = G^E(sln;T;p;w_1/kg=1)$

$$(G^E/RT) = f + m_2^2 [2(v_m v_x)(B_{mx}/m^\circ)] + m_2^3 [2v_m v_x (v_m z_m)] C_{mx}/(m^\circ)^2 \quad [7.37]$$

Parameters for the above equation can be obtained from the full equation for  $(\phi-1)$  and  $\ln\gamma_{\pm}$  given by equations [7.34] and [7.35] respectively; Appendix 3 Section 7. Hence;

$$(G^E/RT) = v_{m_2}[-|z_+ z_-| A^\phi (2/b) \ln(1+b(m_2^{1/2}/m^\circ))] + m_2^2 [2(v_m v_x) \{\beta^\circ + [2\beta^1/(\alpha^2 m_2)]\} \{1 - \exp(-\alpha m_2^{1/2})(1 + \alpha m_2^{1/2})\}] / m^\circ + m^3 [2(v_m v_x)(v_m z_m)] \{C_{mx}^\phi / 2 |z_m z_x|^{1/2}\} / (m^\circ)^2 \quad [7.38]$$

### 7.2.7 The Savage-Wood Link

In a study of the properties of neutral solutes in aqueous solutions Wood et al<sup>4,5,6,7</sup> express the osmotic coefficient as a power series in molality representing pairwise, triplet, quadruplet..... interactions. Data are fitted to an equation of the form;

$$(\phi-1)RT = g_2 m_2 + g_3 m_2^2 + g_4 m_2^3 + \dots + g_n m_2^{n-1} \quad [7.39]$$

Here  $g_2$  = pairwise interaction parameter,  $g_3$  = triplet interaction parameter .....

From the Gibbs-Duhem equation (see Appendix 3 Section 1);

$$\ln \gamma_2 = (1/RT) \{ [g_2 m_2 + g_3 m_2^2 + g_4 m_2^3 + \dots + g_n m_2^{n-1} + g_2 m_2 + g_3 (m_2^2/2) + g_4 (m_2^3/3) + \dots + g_n (m_2^{n-1}/n-1)] \} \quad [7.40]$$

Using equation [7.18];

$$\Rightarrow G^E = [g_2 m_2^2 + g_3 (m_2^3/2) + g_4 (m_2^4/3) + \dots + g_n (m_2^n/n-1)] \quad [7.41]$$

Considering all but the pairwise interaction parameters as being negligible, then in its simplest form equation [7.41] can be rewritten as;

$$G^E = g_2 m_2^2 \quad [7.42]$$

By analogy with the Savage-Wood approach, if Pitzer's electrostatic interaction term,  $f$ , is subtracted from the total excess Gibbs function then analogous pairwise interaction parameters can be obtained for salt solutions.

An excess Gibbs function characteristic of all pairwise ion-ion interactions except charge-charge interactions is defined by equation [7.43].

$$[G^E/RT]^{ne} = G^E/RT - f$$

$$\Rightarrow [G^E/RT]^{ne} = m_2^2 (2\nu_m \nu_x) \beta^\circ \quad [7.43]$$

In using only  $\beta^\circ$ , the above equation can be seen to

represent all interactions between like and unlike charges. Hence in the absence of a charge-charge interaction term a cosphere-cosphere interaction term has been identified. For a salt MX molality  $m_2$  in solution then the total molality of all solutes (cations + anions) is given by;

$$m_m + m_x = 2m_2$$

Then  $RT(\phi-1) = 2m_2 g_2 + 4m_2^2 g_3 + 8m_2^3 g_4 + \dots + 2^n m_2^n g_{n-1}$

And assuming all but pairwise interactions are negligible

$$\Rightarrow [G^E]^{ne} = g_2 (2m_2^2)$$

where;

$$g_2 = \left[ \frac{(g_{mm} m_m^2)}{(m_m + m_x)^2} \right] + 2g_{mx} \left[ \frac{(m_m m_x)}{(m_m + m_x)^2} \right] + \left[ \frac{(g_{xx} m_x^2)}{(m_m + m_x)^2} \right] \quad [7.44]$$

If MX is a 1:1 salt.

$$m_m = m_x = m_2$$

$$\Rightarrow g_2 = \left[ \frac{g_{mm} m_2^2}{2m_2^2} \right] + \left[ \frac{2g_{mx} m_2^2}{2m_2^2} \right] + \left[ \frac{g_{xx} m_2^2}{2m_2^2} \right] \quad [7.45]$$

$$\Rightarrow g_2 = (1/2) [g_{mm} + 2g_{mx} + g_{xx}] \quad [7.46]$$

Hence;

$$[G^E]^{ne} = m_2^2 [g_{mm} + 2g_{mx} + g_{xx}] \quad [7.47]$$

By combining equation [7.47] with [7.43] a link has been established between Pitzer's  $\beta^0$  parameters and pairwise cosphere-cosphere group interaction parameters.

$$[G^E/RT]^{ne} = \{m_2^2/RT\}[g_{mm}+2g_{mx}+g_{xx}] = 2m_2^2\beta^\circ$$

$$\Rightarrow 2\beta^\circ RT = [g_{mm} + 2g_{mx} + g_{xx}] \quad [7.48]$$

### 7.3 Summary

This Chapter has outlined methods of deriving equations for  $\ln\gamma_{\pm}$  and the excess Gibbs function,  $G^E$ , from Pitzers equation for  $(\phi-1)$  using the Gibbs-Duhem and equation [7.16]. The equation for the excess Gibbs function has been further developed using a Savage-Wood type approach, to produce an equation, [7.48], in which pairwise group interaction parameters for salts can be obtained using Pitzers  $\beta^\circ$  parameter. Thus  $\beta^\circ$  represents interactions between like and unlike charged species, after all electrostatic interactions have been removed - in effect a cosphere-cosphere interaction term.

Chapter 8 develops the theme of pairwise interactions and reports pairwise group interaction parameters based on the available osmotic data for a number of salts.

## References Chapter 7

- (1) K.S.Pitzer, J.Phys.Chem., 77, 268, (1973)
- (2) K.S.Pitzer, "Activity Coefficients in Electrolyte Solutions", Vol.1, Ed. R.M. Pytkowicz, CRC.Press, (1979)
- (3) R.C.Phutela, K.S.Pitzer, J.Phys.Chem., 90, 895, (1986)
- (4) J.J.Savage, R.H.Wood, J.Soln.Chem., 5, 733, (1976)
- (5) B.Y.Okamoto, R.H.Wood, P.T.Thompson, J.Chem. Soc., Faraday Trans. I, 74, 1990, (1978)
- (6) A.L.Harris, P.T.Thompson, R.H.Wood, J.Soln. Chem., 9, 305, (1980)
- (7) S.K.Suri, R.H.Wood, J.Soln.Chem., 15, 705, (1986)
- (8) M.J.Blandamer, B.Clark, J.Burgess, A.W.Hakin, J.B.F.N.Engberts, J.Chem.Soc., Chem.Comm, 414, (1985)
- (9) M.J.Blandamer, B.Clark, J.Burgess, A.W.Hakin, J.B.F.N.Engberts, J.Chem.Soc., Faraday Trans. I, 83, 865, (1987)
- (10) J.R.Velasco, F.S.Burgos, M.C.Carmona, J.H. Hidalgo, An.Quim., 80, 173, (1984)
- (11) L.Rudra, M.N.Das, J.Chem.Soc., A, 630, (1967)
- (12) R.A.Robinson, R.H.Stokes, "Electrolyte Solutions", 2nd Ed., Butterworths, London, (1959)
- (13) J.N.Bronsted, J.Am.Chem.Soc., 44, 938, (1922)
- (14) E.A.Guggenheim, Phil.Mag., 19, 588, (1935)
- (15) E.A.Guggenheim, J.C.Turgeon, Trans.Faraday Soc., 51, 747, (1955)
- (16) D.N.Card, J.P.Valleau, J.Chem.Phys., 81, 1822, (1970)
- (17) K.S.Pitzer, G.Mayorga, J.Soln.Chem., 3, 539, (1974)



# CHAPTER 8

Pairwise Gibbs function  
Cosphere-Cosphere Group  
Interaction Parameters

## 8.1 Introduction

The previous Chapter examined how osmotic coefficients, activity coefficients and excess Gibbs functions could be used to obtain pairwise Gibbs function cosphere-cosphere interaction parameters. This theme is continued here in a quantitative method for analysing the rates of reactions between ions in aqueous solution containing added electrolytes<sup>1,2</sup>. The analysis builds on the success of the Savage-Wood<sup>3</sup> additivity scheme, in which estimates of solute-solute pairwise interaction parameters have been successfully used in the analysis of kinetic data for systems in which the impact of neutral solutes on reactions involving neutral substrates are investigated.

This Chapter reports how osmotic coefficients for ammonium, alkylammonium and azoniaspiroalkane halides can be used to calculate pairwise group interaction parameters,  $g(i \rightleftharpoons j)$ , between the groups  $i$  and  $j$  where the symbols  $i$  and  $j$  refer to the  $\text{CH}_2$  group and ions  $\text{I}^-$ ,  $\text{Br}^-$ ,  $\text{Cl}^-$  and  $\text{F}^-$ .

Calculated pairwise interaction parameters are used in estimating cosphere-cosphere contributions to Setschenow coefficients for gaseous hydrocarbons dissolved in aqueous salt solutions.

For a typical 1:1 salt  $\text{M}^+\text{X}^-$  there are at least three separate interaction parameters i.e.  $(\text{M}^+ \rightleftharpoons \text{M}^+)$ ,  $(\text{M}^+ \rightleftharpoons \text{X}^-)$  and  $(\text{X}^- \rightleftharpoons \text{X}^-)$ . This highlights a problem. As one extends the number of salts in the analysis, so the number of unknowns (the pairwise Gibbs function cosphere-cosphere group interaction parameters) is always larger than the number of knowns (the number of sets of osmotic coefficient data). Fortunately one can overcome this setback by

developing an analysis using data for the alkylammonium halide salts. The key to breaking the known-unknown problem is the varying number of methylene groups around the positively charged nitrogen atom in each salt. The Wood et al<sup>7-9</sup> methylene-methylene interaction parameter,  $g(\text{CH}_2\text{<=>CH}_2)$ , is assumed common to both ionic and neutral solutes. For a given series of tetraalkylammonium halide salts, e.g.  $\text{R}_4\text{NCl}$  where  $\text{R} = \text{Me, Et, Pr and Bu}$ , sufficient equations are obtained which allow specific pairwise Gibbs function cosphere-cosphere parameters to be estimated.

## 8.2 Analysis

Input data to the analysis were published osmotic coefficients and molalities for aqueous solutions containing ammonium, alkylammonium and azoniaspiroalkane halide salts. These data were fitted using a linear least squares procedure to Pitzer's equation<sup>4</sup> modelling the dependence of the osmotic coefficient on molality (see Chapter 7 Section 7.4.2). Calculated estimates for  $\beta^0$ ,  $\beta^1$  and  $C$  were checked against Pitzers tabulated values<sup>4</sup>. However the calculation of pairwise interaction parameters needs only consideration of the calculated  $\beta^0$  parameters of each salt. A non-electrical cosphere<sup>5</sup> interaction term was identified by equation [8.1]. This equation was based on a procedure suggested by Guggenheim<sup>6</sup>; [refer to Chapter 7 Section 7.2.7 ]

$$[G^E/RT] = 2v_m v_x m_2^2 \beta^0 \quad [8.1]$$

This equation was used to obtain a quantity identified as

$g(\text{salt})$ , defined by equation [8.2], which is a function of pairwise ion-ion Gibbs function interaction parameters.

$$g(\text{salt}) = 2\beta^{\circ} RT \quad [8.2]$$

For a 1:1 salt of the type  $M^+X^-$ ,  $g(\text{salt})$  is expressed in terms of cation-cation, anion-anion and cation-anion interaction parameters.

$$g(\text{salt}) = g(M^+ \rightleftharpoons M^+) + 2g(M^+ \rightleftharpoons X^-) + g(X^- \rightleftharpoons X^-) \quad [8.3]$$

Hence;

$$2\beta^{\circ} RT = g(M^+ \rightleftharpoons M^+) + 2g(M^+ \rightleftharpoons X^-) + g(X^- \rightleftharpoons X^-) \quad [8.4]$$

In the case of a tetraalkylammonium halide salt,  $g(\text{salt})$  was broken down into pairwise interaction contributions using the Wood et al<sup>7-9</sup> interaction parameter for methylene-methylene interactions,  $g(\text{CH}_2 \rightleftharpoons \text{CH}_2)$ , and the assumption that a terminal methyl group,  $-\text{CH}_3$ , is equivalent to 1.5 methylene groups<sup>8,9</sup> (in the case of an ammonium halide salt the assumption was made that a hydrogen atom was equivalent to one half of a methylene group). Hence for tetrabutylammonium bromide;

$$\begin{aligned} g(\text{Bu}_4\text{NBr}) &= (4\text{CH}_3 + 12\text{CH}_2 + \text{N}^+ + \text{Br}^-) \\ &= (18\text{CH}_2 + \text{N}^+ + \text{Br}^-) \end{aligned}$$

$$\begin{aligned} \Rightarrow g(\text{Bu}_4\text{NBr}) &= 324g(\text{CH}_2 \rightleftharpoons \text{CH}_2) \\ &+ 36g(\text{CH}_2 \rightleftharpoons \text{N}^+) + g(\text{N}^+ \rightleftharpoons \text{N}^+) \\ &+ 36g(\text{CH}_2 \rightleftharpoons \text{Br}^-) + 2g(\text{N}^+ \rightleftharpoons \text{Br}^-) + g(\text{Br}^- \rightleftharpoons \text{Br}^-) \end{aligned}$$

In the scheme above only the  $(\text{CH}_2 \rightleftharpoons \text{CH}_2)$  Wood<sup>7-9</sup>

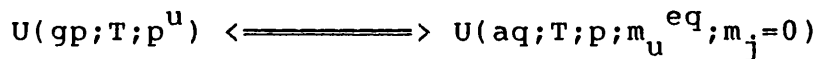
interaction parameter is known at this stage. Hence a residual  $Y$  can be calculated; equation [8.5].

$$Y = 2\beta^{\circ}RT - 324g(\text{CH}_2\rightleftharpoons\text{CH}_2) \quad [8.5]$$

The residual  $Y$  is related to the five unknowns ( $\text{CH}_2\rightleftharpoons\text{N}^+$ ), ( $\text{N}^+\rightleftharpoons\text{N}^+$ ), ( $\text{CH}_2\rightleftharpoons\text{Br}^-$ ), ( $\text{N}^+\rightleftharpoons\text{Br}^-$ ) and ( $\text{Br}^-\rightleftharpoons\text{Br}^-$ ). Further equations containing these properties were obtained using data for the tetraalkylammonium bromides i.e.  $\text{Pr}_4\text{NBr}$ ,  $\text{Et}_4\text{NBr}$ ,  $\text{Me}_4\text{NBr}$  and also using osmotic coefficient data for the cyclic azoniaspiroalkane bromides and ammonium bromide. Similar sets of equations were obtained for the fluoride, chloride and iodide salts. In the case of chloride salts the data set was supplemented using information describing the properties of aqueous solutions containing monomethyl, dimethyl and trimethylammonium chlorides. Each set of halide salts introduced three new unknowns i.e. ( $\text{CH}_2\rightleftharpoons\text{X}^-$ ), ( $\text{N}^+\rightleftharpoons\text{X}^-$ ) and ( $\text{X}^-\rightleftharpoons\text{X}^-$ ). In total there were twenty seven equations containing fourteen unknown pairwise interaction parameters which were estimated using a least squares procedure. A linear least squares procedure proved unsuccessful, in view of the structure of the input data. A column reporting the number of pairwise interaction parameters could be formed as a linear combination of one or more of the other columns. A minimisation technique was used in the form of a FORTRAN NAG library routine, (F04JDF). The outcome was a least squares estimate of pairwise interaction parameters. Standard errors were calculated using the output<sup>10</sup> from NAG routine F04JDF (see program listing presented in Appendix 4 Section 1).

### 8.2.1 Setschenow Coefficients and Their Relationship to the Excess Gibbs Function.

A given volatile substance U at temperature T and partial pressure  $p^u$  is in equilibrium with solute U in solution at temperature T and pressure p in (i) an aqueous solution in which the molality of added salt is zero, i.e.  $m_j = 0$  and the molality of U is  $m_u^{eq}$ .



and (ii) an aqueous solution in which the molality of added salt is  $m_j$  and the molality of substance U is  $m_u^{eq}$ .



At equilibrium the chemical potentials of substance U in these solutions are equal.

$$\mu_u^{eq}(aq;T;m_u^{eq};m_j=0) = \mu_u^{eq}(aq;T;m_u^{eq};m_j)$$

$$\begin{aligned} \Rightarrow \mu^\#(aq;T;p;id) + RT \ln[m_u^{eq}(m_j=0) \gamma_u^{eq}(m_j=0)/m^\circ] \\ = \mu^\#(aq;T;p;id) + RT \ln[m_u^{eq}(m_j) \gamma_u^{eq}(m_j)/m^\circ] \end{aligned} \quad [8.6]$$

Assuming substance U forms an ideal solution when  $m_j = 0$  i.e.  $\gamma_u^{eq}(m_j=0) = 1.0$ , then;

$$m_u^{eq}(m_j=0) = m_u^{eq}(m_j) \gamma_u^{eq}(m_j) \quad [8.7]$$

A Setschenow coefficient is obtained by experiment and is defined by equation [8.8].

$$\log_{10} (S^{\circ}/S) = k_u m_j \quad [8.8]$$

where  $k_u$  is the Setschenow coefficient of substance U,  $S^{\circ}$  is the solubility of the volatile substance U in an aqueous solution containing no added salt and S is the solubility of U in an aqueous solution containing  $m_j$  moles of added salt.

$$\text{i.e. } S^{\circ} = m_u^{\text{eq}}(m_j=0)$$

$$\text{and } S = m_u^{\text{eq}}(m_j)$$

Hence using equation [8.7];

$$\begin{aligned} \log_{10} [m_u^{\text{eq}}(m_j=0)/m_u^{\text{eq}}(m_j)] &= \log_{10} \gamma_u^{\text{eq}}(m_j) \\ \Rightarrow \log_{10} \gamma_u^{\text{eq}}(m_j) &= k_u m_j \\ \Rightarrow \ln \gamma_u^{\text{eq}}(m_j) &= 2.303 k_u m_j \end{aligned} \quad [8.9]$$

The total Gibbs function of a solution containing a 1:1 salt-j of molality  $m_j$  and a volatile substance U of molality  $m_u^{\text{eq}}$  in 1 kg of water is given by equation [8.10].

$$\begin{aligned} G(\text{total}) &= m_j [\mu_j^{\#}(s, l; T; p) + 2RT \ln [Q m_j \gamma_{\pm}^{\#}/m^{\circ}]] \\ &\quad + m_u^{\text{eq}} [\mu_u^{\#}(s, l; T; p) + RT \ln [m_u^{\text{eq}} \gamma_u^{\#}/m^{\circ}]] \\ &\quad + (1/M_1) [\mu^*(\text{H}_2\text{O}; l; T; p) - \phi RT M_1 [2m_j + m_u^{\text{eq}}]] \end{aligned} \quad [8.10]$$

Hence the excess Gibbs function of the system is given by equation [8.11].

$$\begin{aligned} G^E &= m_j [2RT \ln \gamma_{\pm}] + m_u^{\text{eq}} [RT (\ln \gamma_u)] + (1-\phi) RT [2m_j + m_u^{\text{eq}}] \\ \Rightarrow G^E/RT &= 2m_j \ln \gamma_{\pm} + m_u^{\text{eq}} \ln \gamma_u + (1-\phi) (2m_j + m_u^{\text{eq}}) \end{aligned} \quad [8.11]$$

At constant temperature, pressure and molality of added salt,  $m_j$ ;

$$(1/RT)[\partial G^E/\partial m_u^{eq}]_{T;p;m_j} = 2m_j[d\ln\gamma_{\pm}/dm_u^{eq}] + \ln\gamma_u^{eq} - 2(m_j+m_u^{eq})[d\phi/dm_u^{eq}] + (1-\phi) \quad [8.12]$$

According to the Gibbs-Duhem equation (at constant temperature and pressure)  $\sum n_i d\mu_i = 0$ . Hence;

$$-d[\phi(2m_j+m_u^{eq})] + 2m_j d\ln[Qm_j\gamma_{\pm}/m^\circ] + m_u^{eq} d\ln[m_u^{eq}\gamma_u^{eq}/m^\circ] = 0$$

$$\Rightarrow -(2m_j+m_u^{eq})d\phi - \phi + 2m_j d\ln\gamma_{\pm} + m_u^{eq} d\ln\gamma_u^{eq} + 1 = 0 \quad [8.13]$$

Differentiating with respect to  $m_u^{eq}$  yields equation [8.14].

$$\Rightarrow 2m_j[d\ln\gamma_{\pm}/dm_u^{eq}] - 2(m_j+m_u^{eq})[d\phi/dm_u^{eq}] + (1-\phi) = 0 \quad [8.14]$$

Substituting equation [8.14] back into equation [8.12] produces a simplified equation for the differential of the excess Gibbs function with respect to  $m_u^{eq}$ .

$$(1/RT)[\partial G^E/\partial m_u^{eq}]_{T;p;m_j} = \ln\gamma_u^{eq} \quad [8.15]$$

Hence the excess Gibbs function defined by the above equation can be linked to the Setschenow coefficient of the volatile solvent,  $k_u$ , through equation [8.9]. Hence;

$$(1/RT)[\partial G^E/\partial m_u^{eq}]_{T;p;m_j} = 2.303k_u m_j \quad [8.16]$$

Using the Savage-Wood type approach, outlined in Chapter 7 Section 7.2.7, an equation for the cosphere-cosphere interaction contribution of the excess Gibbs function can be developed for an aqueous salt solution containing trace amounts of volatile substance U.

For a solution containing a 1:1 salt  $M^+X^-$  where the molality of cations is  $m_j$ , the molality of the anions is  $m_j$  and the molality of U is  $m_u$  then a cosphere-cosphere interaction contribution to the excess Gibbs function can be defined using equation [8.17].

$$\begin{aligned}
 G^E(\text{sln}; T; p; \text{cosphere}) = & g(M^+ \rightleftharpoons M^+) m_j^2 + 2g(M^+ \rightleftharpoons X^-) m_j^2 \\
 & + g(M^+ \rightleftharpoons U) m_j m_u + g(X^- \rightleftharpoons X^-) m_j^2 + 2g(U \rightleftharpoons X^-) m_j m_u \\
 & + g(U \rightleftharpoons U) m_u^2 \qquad \qquad \qquad [8.17]
 \end{aligned}$$

The differential of the excess Gibbs function with respect to  $m_u$  at constant T, p and  $m_j$  can be written in the form;

$$\begin{aligned}
 [\partial G^E / \partial m_u]_{T; p; m_j} = & 2g(M^+ \rightleftharpoons U) m_j + 2g(U \rightleftharpoons X^-) m_j \\
 & + 2g(U \rightleftharpoons U) m_u \qquad \qquad \qquad [8.18]
 \end{aligned}$$

Hence using equation [8.15];

$$\ln \gamma_u^{eq} = (2/RT) [g(M^+ \rightleftharpoons U) m_j + g(U \rightleftharpoons X^-) m_j + g(U \rightleftharpoons U) m_u]$$

But only trace amounts of U are present;  $m_u \approx 0$

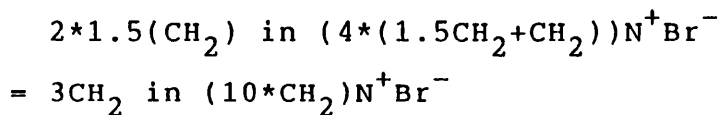
$$\Rightarrow \ln \gamma_u^{eq} = (2m_j/RT) [g(M^+ \rightleftharpoons U) + g(U \rightleftharpoons X^-)] \qquad [8.19]$$

Using equation [8.9] the interaction parameters can be

linked to the Setschenow coefficient of the volatile solute,  $k_u$ .

$$k_u = (2/2.303RT)[g(M^+ \rightleftharpoons U) + g(U \rightleftharpoons X^-)] \quad [8.20]$$

In one example the volatile substance U is ethane and the salt-j in solution is tetraethylammonium bromide i.e.  $C_2H_6$  in  $(CH_3CH_2)_4N^+Br^-$ . Using the procedures adopted earlier for terminal methyl groups, the situation can be reconsidered as;



$$\Rightarrow g(M^+ \rightleftharpoons U) = 30g(CH_2 \rightleftharpoons CH_2) + 3g(CH_2 \rightleftharpoons N^+)$$

$$\Rightarrow g(U \rightleftharpoons X^-) = 3g(CH_2 \rightleftharpoons Br^-)$$

Hence an estimate of the cosphere-cosphere interaction contribution to the Setschenow coefficient of ethane in a solution of tetraethylammonium bromide can be written as equation [8.21].

$$k_{\text{ethane}} = (2/2.303RT)[30g(CH_2 \rightleftharpoons CH_2) + 3g(CH_2 \rightleftharpoons N^+) \\ + 3g(CH_2 \rightleftharpoons Br^-)] \quad [8.21]$$

The pairwise cosphere-cosphere interaction parameters of equation [8.21] are obtained from the least squares minimisation technique described earlier.

### 8.3 Results

A FORTRAN program was written to access osmotic coefficient and molality data contained in data files for the twenty

seven salts studied<sup>11-17</sup>, see Table 8.1. Appendix 4 Section 1 contains a program listing. All data referred to a temperature of 298.15 K and were in the concentration range  $0 \leq m_j/\text{mol kg}^{-1} \leq 2.0$ . Of the three possible routes available to calculate Pitzer's  $\beta^\circ$  parameter, namely through (i)  $G^E$  (ii)  $\gamma_{\pm}$  and (iii)  $(\phi-1)$  [refer to Chapter 7] the third approach via the osmotic coefficient was used within the program. This method is in line with procedures adopted by Pitzer<sup>4</sup>. Estimates of  $\beta^\circ$  produced using a linear least squares fit of osmotic data and molality data to equation [8.22] were found to be in satisfactory agreement with those tabulated by Pitzer<sup>4</sup>.

$$(\phi-1) - f = m_2 [2v_m v_x / v] \{ \beta^\circ + \beta^1 \exp(-\alpha m_2^{1/2}) \} + m_2^2 [2(v_m v_x)^{3/2} / v] C_{mx}^\phi \quad [8.22]$$

where  $f$  represents a coulombic interaction contribution to the osmotic coefficient (refer to Chapter 7).

Figures 8.1 - 8.4 show plots of  $[(\phi-1)-f]_{\text{calc}}$  (calculated from the best fit parameters to equation [8.22]) against  $[(\phi-1)-f]_{\text{obs}}$  (calculated from the input osmotic coefficient data) for four different salts used in the analysis.

Table 8.2 reports the calculated  $\beta^\circ$  parameters for the twenty seven salts investigated in the analysis together with their standard errors. Deviations between  $\beta^\circ(\text{calc})$  and  $\beta^\circ(\text{lit})$  can be explained in part by the differing ranges of molalities covered in the calculation of the literature values. Values of  $g(\text{salt})$  for each salt

Table 8.1

Salts and references to data used in the calculation of pairwise cosphere-cosphere Gibbs function interaction parameters. All data refer to a temperature of 298K.

No.	Salt	Reference
1	$\text{NH}_4\text{Br}$	11
2	$(\text{CH}_3)_4\text{NBr}$	12
3	$(\text{C}_2\text{H}_5)_4\text{NBr}$	12
4	$(\text{C}_3\text{H}_7)_4\text{NBr}$	12
5	$(\text{C}_4\text{H}_9)_4\text{NBr}$	12
6 <sup>a</sup>	6,6A <sub>Br</sub>	13
7 <sup>b</sup>	4,4A <sub>Br</sub>	13
8 <sup>c</sup>	5,5A <sub>Br</sub>	13
9	$\text{NH}_4\text{Cl}$	14
10	$(\text{CH}_3)_3\text{H}_3\text{NCl}$	15
11	$(\text{CH}_3)_2\text{H}_2\text{NCl}$	15
12	$(\text{CH}_3)_3\text{HNCl}$	15
13	$(\text{CH}_3)_4\text{NCl}$	12
14	$(\text{C}_2\text{H}_5)_4\text{NCl}$	12
15	$(\text{C}_3\text{H}_7)_4\text{NCl}$	12
16	$(\text{C}_4\text{H}_9)_4\text{NCl}$	12
17 <sup>d</sup>	5,5A <sub>Cl</sub>	13
18 <sup>e</sup>	6,6A <sub>Cl</sub>	13
19	$(\text{CH}_3)_4\text{NF}$	16
20	$(\text{C}_2\text{H}_5)_4\text{NF}$	16
21	$(\text{C}_3\text{H}_7)_4\text{NF}$	16
22	$(\text{C}_4\text{H}_9)_4\text{NF}$	16
23	$\text{NH}_4\text{I}$	17
24	$(\text{CH}_3)_4\text{NI}$	12
25	$(\text{C}_2\text{H}_5)_4\text{NI}$	12
26	$(\text{C}_3\text{H}_7)_4\text{NI}$	12
27 <sup>f</sup>	5,5A <sub>I</sub>	13

- a - 6.6 azonspiroalkane Bromide
- b - 4.4 azonspiroalkane Bromide
- c - 5.5 azonspiroalkane Bromide
- d - 5.5 azonspiroalkane Chloride
- e - 6.6 azonspiroalkane Chloride
- f - 5.5 azonspiroalkane Iodide

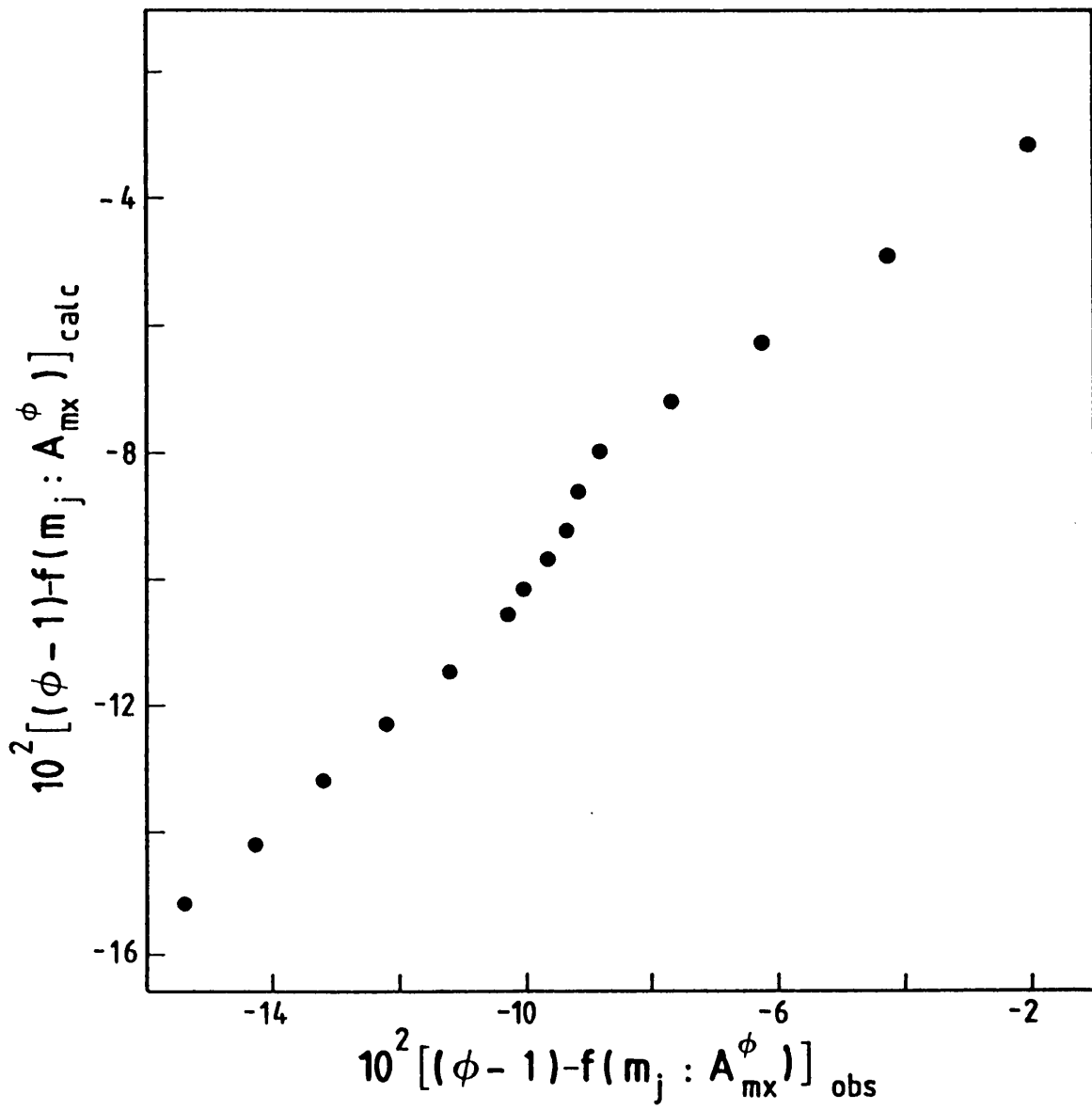


FIGURE 8.1

Comparison of observed and calculated  $[(\phi-1)-f(m_j; A_{mx}^\phi)]$  for  $Bu_4NBr$  in aqueous solution at 298.15 K and ambient pressure.

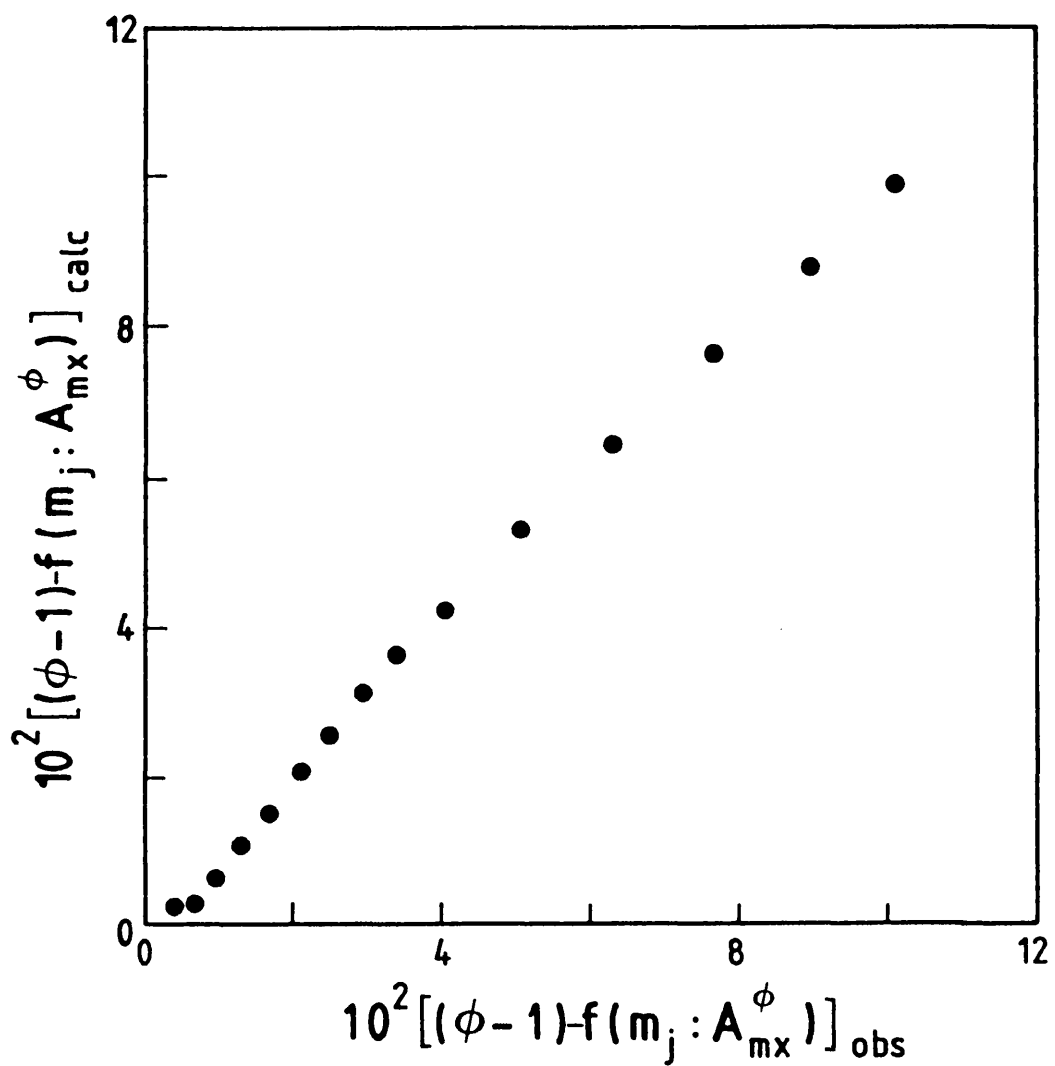


FIGURE 8.2

Comparison of observed and calculated  $[(\phi-1)-f(m_j; A_{mx}^\phi)]$  for  $\text{Me}_4\text{NCl}$  in aqueous solution at 298.15 K and ambient pressure.

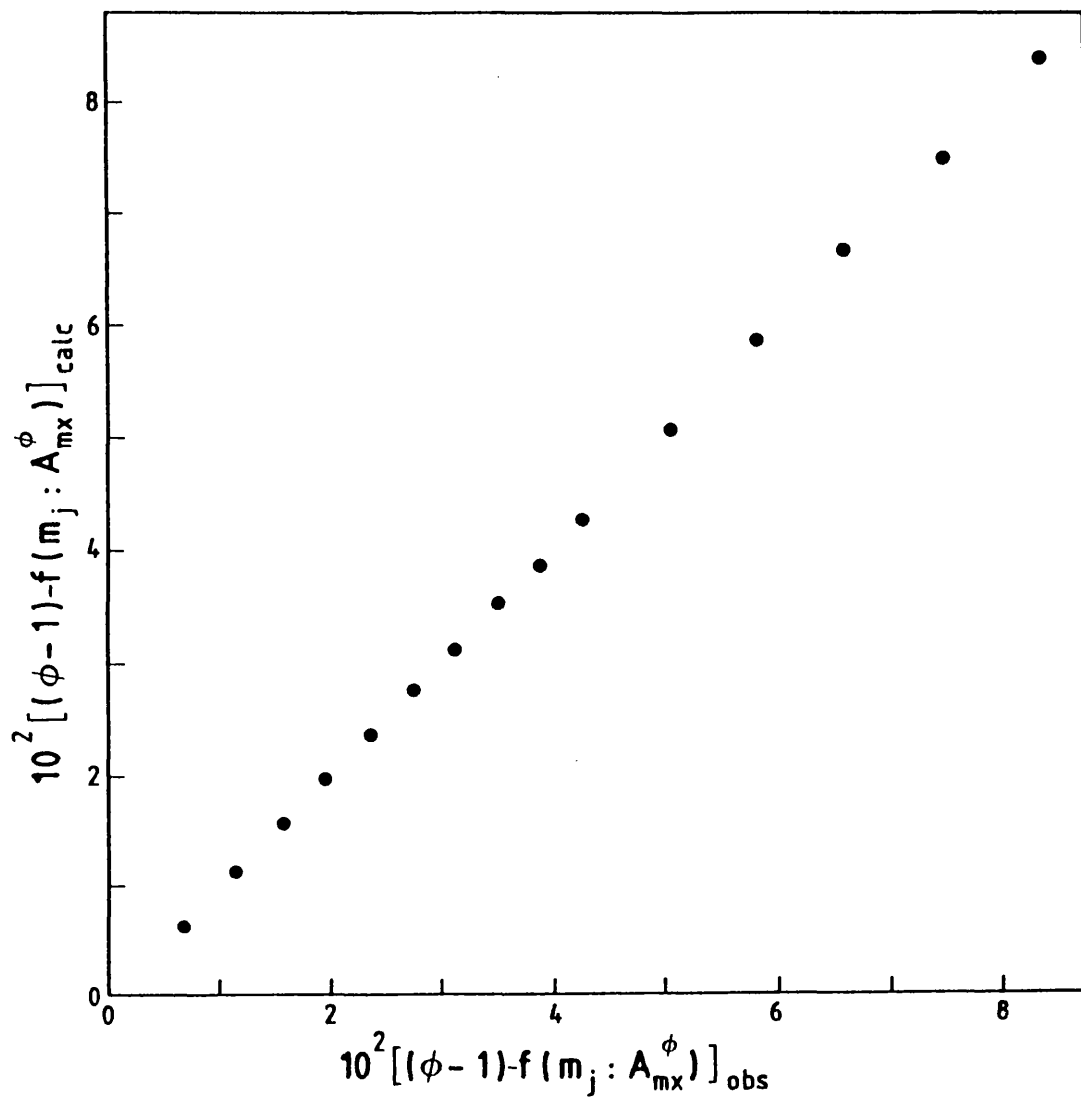


FIGURE 8.3

Comparison of observed and calculated  $[(\phi-1)-f(m_j; A_{mx}^\phi)]$  for  $\text{Et}_4\text{NF}$  in aqueous solution at 298.15 K and ambient pressure.

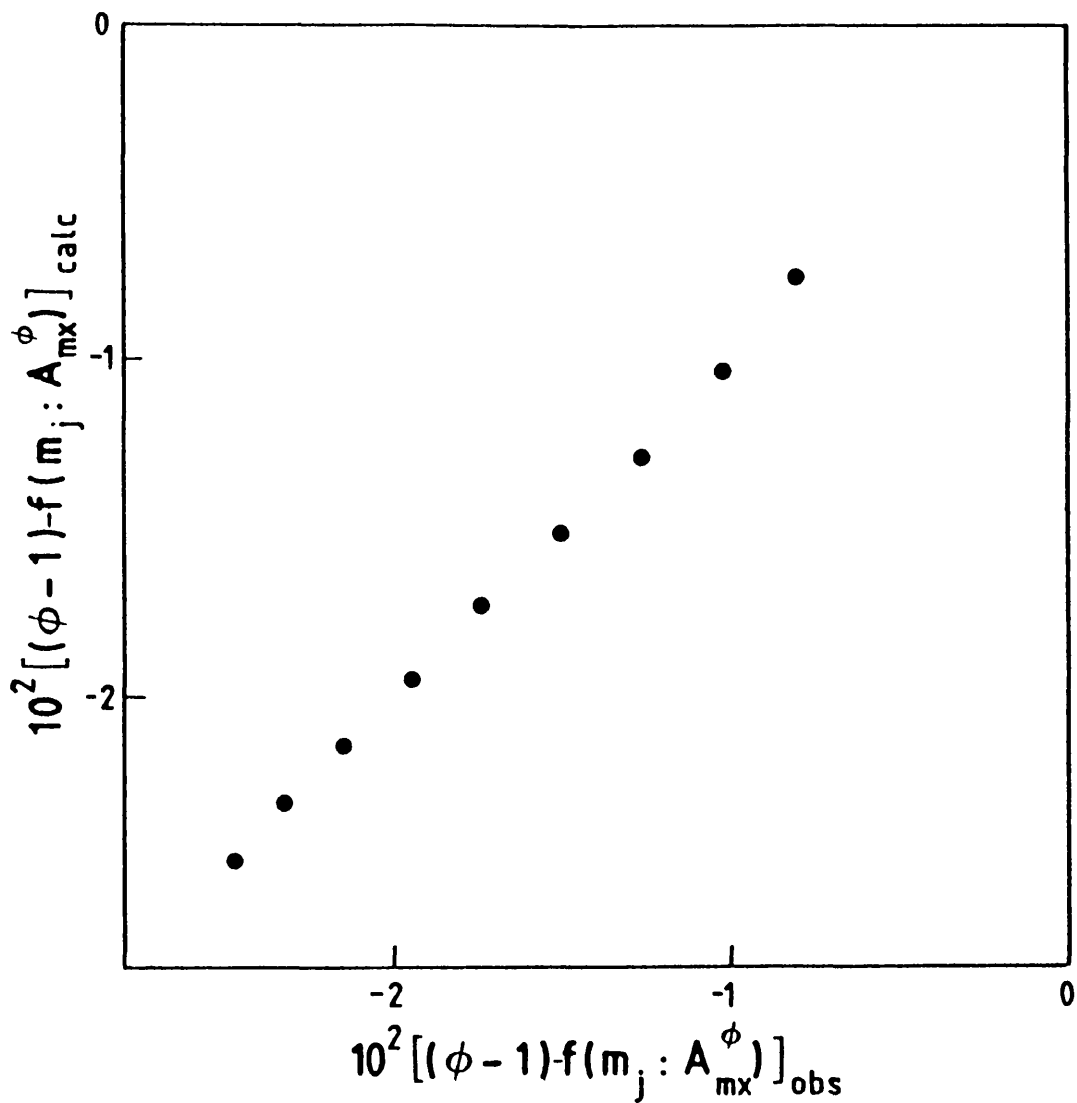


FIGURE 8.4

Comparison of observed and calculated  $[(\phi-1)-f(m_j; A_{mx}^\phi)]$  for  $\text{Pr}_4\text{NI}$  in aqueous solution at 298.15 K and ambient pressure.

Table 8.2

Derived  $\beta^\circ$  parameters for salts in aqueous solution at 298K and ambient pressure.

Salt	$10^2\beta^\circ$ (calc)	$10^2$ Standard error	$10^2\beta^\circ$ (lit)
NH <sub>4</sub> Br	6.037	0.214	6.24
(CH <sub>3</sub> ) <sub>4</sub> NBr	0.739	0.348	-0.82
(C <sub>2</sub> H <sub>5</sub> ) <sub>4</sub> NBr	0.416	0.260	-1.76
(C <sub>3</sub> H <sub>7</sub> ) <sub>4</sub> NBr	-5.120	0.996	3.90
(C <sub>4</sub> H <sub>9</sub> ) <sub>4</sub> NBr	-1.919	1.511	-2.77
6,6ABr	-14.007	1.099	-
4,4ABr	-4.174	0.062	-
5,5ABr	-9.963	0.030	-
NH <sub>4</sub> Cl	4.467	0.025	5.22
(CH <sub>3</sub> ) <sub>3</sub> H <sub>3</sub> NCl	6.539	0.104	-
(CH <sub>3</sub> ) <sub>2</sub> H <sub>2</sub> NCl	5.385	0.040	-
(CH <sub>3</sub> ) <sub>3</sub> HNC1	5.567	0.098	-
(CH <sub>3</sub> ) <sub>4</sub> NCl	5.576	0.128	4.30
(C <sub>2</sub> H <sub>5</sub> ) <sub>4</sub> NCl	8.939	0.285	6.17
(C <sub>3</sub> H <sub>7</sub> ) <sub>4</sub> NCl	8.808	0.992	13.46
(C <sub>4</sub> H <sub>9</sub> ) <sub>4</sub> NCl	22.386	1.377	23.39
5,5ACl	2.094	0.274	-
6,6ACl	-4.153	0.228	-
(CH <sub>3</sub> ) <sub>4</sub> NF	27.092	0.084	26.77
(C <sub>2</sub> H <sub>5</sub> ) <sub>4</sub> NF	31.397	0.569	31.13
(C <sub>3</sub> H <sub>7</sub> ) <sub>4</sub> NF	45.024	0.878	44.63
(C <sub>4</sub> H <sub>9</sub> ) <sub>4</sub> NF	56.690	0.377	60.92
NH <sub>4</sub> I	5.816	0.197	-
(CH <sub>3</sub> ) <sub>4</sub> NI	64.902	24.860	3.45
(C <sub>2</sub> H <sub>5</sub> ) <sub>4</sub> NI	-17.227	0.765	-17.90
(C <sub>3</sub> H <sub>7</sub> ) <sub>4</sub> NI	-27.862	1.229	-28.39
5,5AI	-24.401	0.106	-

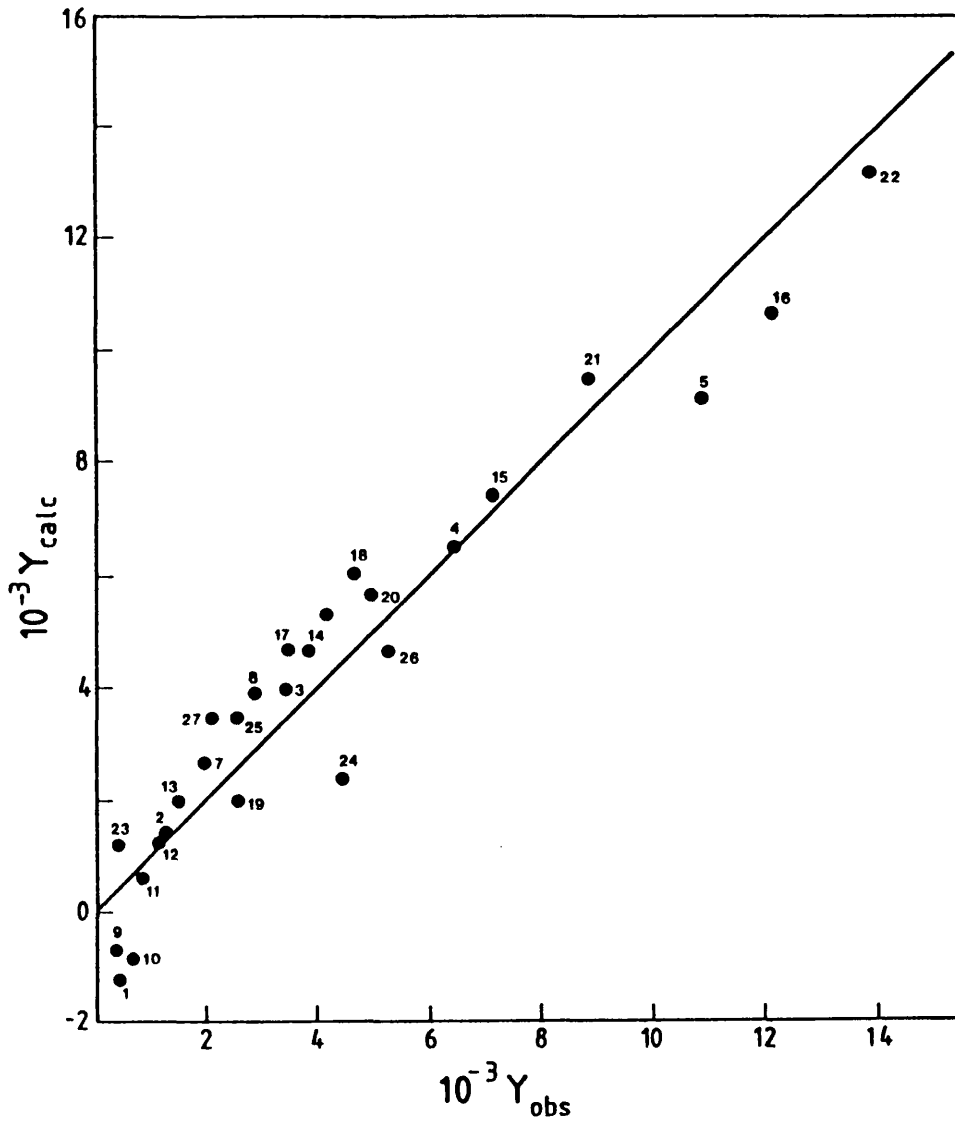
representing the effects of cosphere-cosphere overlap within the solution, were then calculated using equation [8.2]. Hence using Woods<sup>7-9</sup> estimate for the pairwise ( $\text{CH}_2 \rightleftharpoons \text{CH}_2$ ) interaction the twenty seven equations for the least squares minimisation technique were set up.

Figure 8.5 shows a plot of  $Y_{\text{obs}}$  (calculated for each salt using equations similar to [8.5]) against  $Y_{\text{calc}}$  (calculated from the least squares estimates of the cosphere-cosphere interaction parameters). The resulting pattern of the points indicates a satisfactory fit of the data.

The fourteen pairwise cosphere-cosphere group interaction parameters are reported in Table 8.3 in which the ( $\text{CH}_2 \rightleftharpoons \text{CH}_2$ ) interaction<sup>7-9</sup> parameter has been included to complete the matrix. The parameters contained in the latter Table were used to calculate the cosphere-cosphere interaction contribution to the Setschenow coefficients for a series of hydrocarbons in aqueous salt solutions using procedures outlined in Section 8.2.1. Tabulated values of these cosphere-cosphere contributions to the total Setschenow coefficient are reported together with their observed values<sup>18</sup> in Table 8.4. The same information is represented graphically in Figure 8.6.

#### 8.4 Discussion

The decision to use  $2 \text{ mol kg}^{-1}$  as a cut off point for input data to the analysis was based on the assumption that in more concentrated aqueous salt solutions triplet, quadruplet ion-ion interactions have an increased influence on the magnitude of the osmotic coefficient of each system.



**FIGURE 8.5**

Comparison of observed and calculated  $Y$  parameters (cf. equation [9.5]) for aqueous salt solutions at 298.15 K and ambient pressure. Numbers refer to the salts listed in Table 8.1. Perfect agreement between observed and calculated is represented by the straight line running through the origin at an angle of  $45^\circ$  to both axis.

Table 8.3

Pairwise cosphere-cosphere group Gibbs function interaction matrix calculated from osmotic data at 298K ( $\text{J MOL}^{-1}$ )

	CH <sub>2</sub>	N <sup>+</sup>	F <sup>-</sup>	Cl <sup>-</sup>	Br <sup>-</sup>	I <sup>-</sup>
CH <sub>2</sub>	-34.0					
N <sup>+</sup>	255.4	-871.0				
F <sup>-</sup>	216.1	-1153.1	-576.5			
Cl <sup>-</sup>	83.0	-498.2	-	-249.1		
Br <sup>-</sup>	68.8	-669.4	-	-	-334.7	
I <sup>-</sup>	-112.5	578.6	-	-	-	289.3

Table 8.4

Derived cosphere-cosphere contributions to Setschenow coefficients for a series of hydrocarbons dissolved in aqueous salt solutions at 298K. (Observed Setschenow coefficients were taken from reference 18)

System	$k_u$ (calc)	$k_u$ (obs)
1 CH <sub>4</sub> in NH <sub>4</sub> Br	0.090	0.054
2 CH <sub>4</sub> in Me <sub>4</sub> NBr	0.042	-0.017
3 CH <sub>4</sub> in Et <sub>4</sub> NBr	-0.006	-0.049
4 CH <sub>4</sub> in Pr <sub>4</sub> NBr	-0.053	-0.082
5 CH <sub>4</sub> in Bu <sub>4</sub> NBr	-0.101	-0.096
6 C <sub>2</sub> H <sub>6</sub> in NH <sub>4</sub> Br	0.135	0.065
7 C <sub>2</sub> H <sub>6</sub> in Me <sub>4</sub> NBr	0.063	-0.040
8 C <sub>2</sub> H <sub>6</sub> in Et <sub>4</sub> NBr	-0.008	-0.117
9 C <sub>2</sub> H <sub>6</sub> in Pr <sub>4</sub> NBr	-0.080	-0.141
10 C <sub>2</sub> H <sub>6</sub> in Bu <sub>4</sub> NBr	-0.151	-0.155
11 C <sub>3</sub> H <sub>8</sub> in NH <sub>4</sub> NBr	0.180	0.076
12 C <sub>3</sub> H <sub>8</sub> in Me <sub>4</sub> NBr	0.084	-0.059
13 C <sub>3</sub> H <sub>8</sub> in Et <sub>4</sub> NBr	-0.011	-0.158
14 C <sub>3</sub> H <sub>8</sub> in Pr <sub>4</sub> NBr	-0.106	-0.187
15 C <sub>3</sub> H <sub>8</sub> in Bu <sub>4</sub> NBr	-0.202	-0.248
16 C <sub>4</sub> H <sub>10</sub> in Me <sub>4</sub> NBr	0.105	-0.074
17 C <sub>4</sub> H <sub>10</sub> in Et <sub>4</sub> NBr	-0.014	-0.168
18 C <sub>4</sub> H <sub>10</sub> in Pr <sub>4</sub> NBr	-0.133	-0.227
19 C <sub>4</sub> H <sub>10</sub> in Bu <sub>4</sub> NBr	-0.252	-0.286

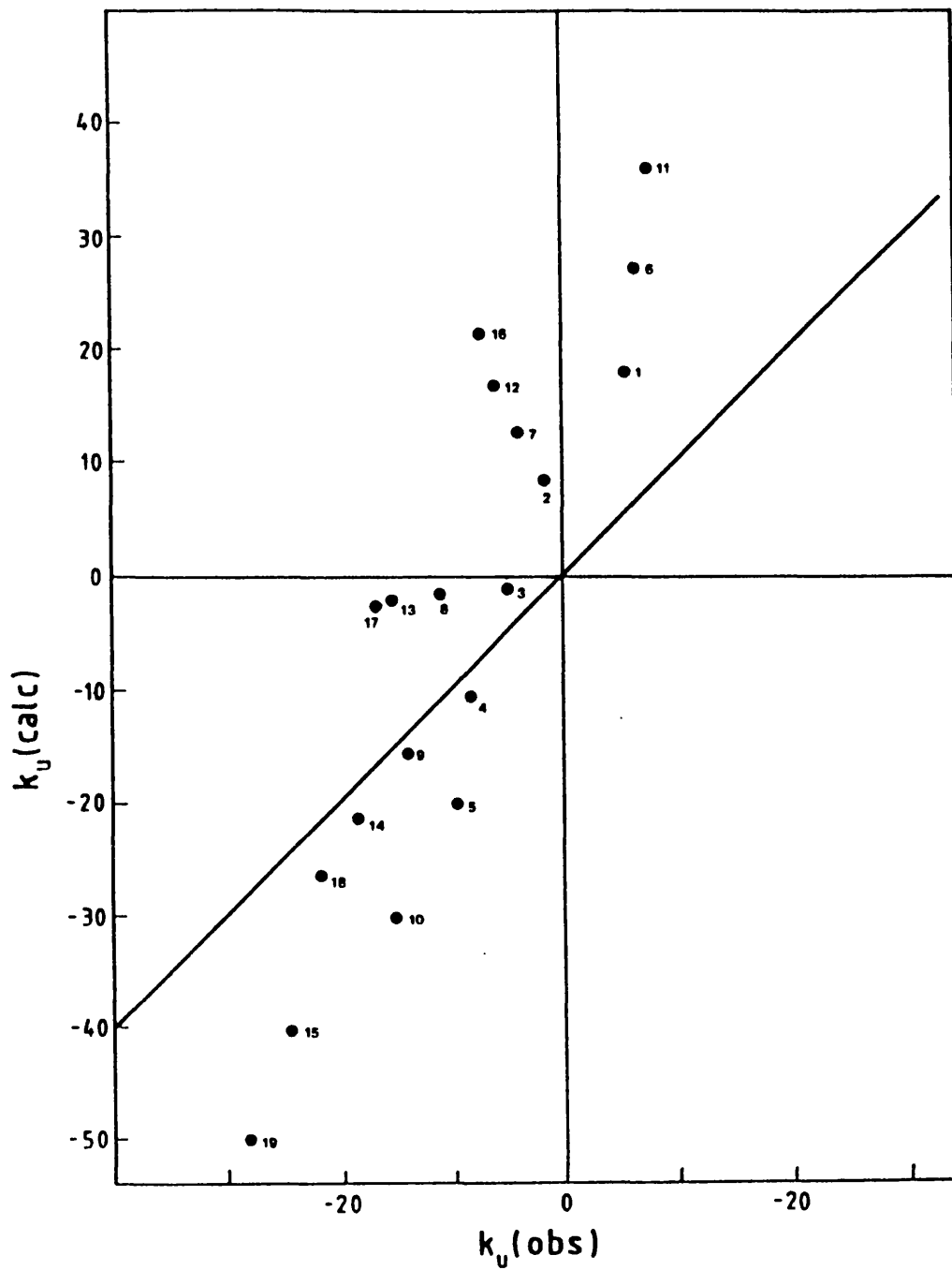


**FIGURE 8.6**

Comparison of calculated and observed Setschenow coefficients for hydrocarbons in aqueous salt solutions at 298.15 K. The numbers refer to the systems listed in Table 8.4.

The accuracy is therefore reduced to which  $\beta^\circ$  can be estimated from equation [8.22].

The Setschenow coefficients reported in Table 8.4 represent the non-electrostatic i.e. cosphere-cosphere interaction contribution to a total Setschenow coefficient. The contribution from coulombic type interactions is not a simple quantity. Long and McDevit<sup>19</sup> claim to describe in their treatment electrostatic interactions. Their equations use the molar and partial molar volumes of salts and the partial molar volume of the added volatile solutes. The observed trends in Setschenow coefficients are understood in terms of the occupation of solvent cavities i.e. a non-electrostatic contribution. As Conway<sup>20</sup> points out the Long-McDevit treatment includes in part a cosphere contribution. The data plotted in Figure 8.6 covers the range negative to positive i.e. from describing salting-in to salting-out. This observation suggests a basis for the conclusion that an understanding of the properties of aqueous salt solutions has been established in terms of group pairwise cosphere-cosphere<sup>5</sup> interaction<sup>21-23</sup> parameters. This conclusion is supported by a consideration of the properties of cosphere-cosphere overlap discussed in Chapter 6. The overlap of solute cospheres with similar hydration characteristics is attractive i.e. the cosphere-cosphere interaction parameter  $g(i \rightleftharpoons j) < 0$ . However the overlap of solute cospheres with dissimilar hydration characteristics is found to be repulsive i.e.  $g(i \rightleftharpoons j) > 0$ . Turning to Table 8.3 the large positive value of  $g(\text{CH}_2 \rightleftharpoons \text{F}^-)$  (= 216.1) and the large negative value of  $g(\text{F}^- \rightleftharpoons \text{F}^-)$  (= -576.5) are consistent with this

generalisation.

Appendix 4 Section 2 extends the interaction matrix, Table 8.3, to a consideration of the interactions of the potassium cation i.e.  $g(K^+ \rightleftharpoons K^+)$ ,  $g(K^+ \rightleftharpoons CH_2)$ ,  $g(K^+ \rightleftharpoons Cl^-)$ ,  $g(K^+ \rightleftharpoons Br^-)$ ,  $g(K^+ \rightleftharpoons F^-)$  and  $g(K^+ \rightleftharpoons N^+)$  using the mixed salt data of Wen et al<sup>24</sup>. Similar interaction parameters are calculated for the sodium cation using Rosenzweigs<sup>25</sup> data. The matrix is further extended by the calculation of the interaction parameters of the nitrate anion,  $NO_3^-$ , using Bonner's<sup>26</sup> compilation of osmotic and activity coefficient data of the tetraalkylammonium nitrates. Extensions of the matrix to include interaction parameters for other alkali metal cations and other ions, for example the  $ClO_4^-$  anion using the data of Bonner<sup>27</sup>, are expected.

### 8.5 A Look Forward

The success of a procedure based on the excess Gibbs function which yields pairwise interaction parameters of solutes in aqueous solution points towards procedures which use other thermodynamic functions for the same purpose. Recalling trends in partial molar volumes of alkylammonium salts discussed by Franks and Smith<sup>28</sup> and by Wen and Saito<sup>29</sup>, and the dependence on molalities of the partial molar heat capacities of salts discussed by Desnoyers et al<sup>30</sup> it would prove interesting to investigate trends in pairwise volume and heat capacity interaction parameters i.e.  $V(i \rightleftharpoons j)$  and  $C_p(i \rightleftharpoons j)$ .

## References Chapter 8

- (1) M.J.Blandamer, J.Burgess, P.P.Duce, S.J.Hamshere, J.J.Walker, J.Chem.Soc., Dalton Trans., 1809, (1980)
- (2) N.F.Ashford, M.J.Blandamer, J.Burgess, D.Laycock, M.Waters, P.Wellings, R.Woodhead, J.Chem.Soc., Dalton Trans., 869, (1979)
- (3) J.J.Savage, R.H.Wood, J.Soln.Chem., 5, 733, (1976)
- (4) K.S.Pitzer, "Activity Coefficients in Electrolyte Solutions" ed.R.M.Pytkowicz, CRC Press, Boca Raton, Florida, Vol.1, Chapt.7, (1979)
- (5) M.J.Blandamer, Adv.Phys.Org.Chem., 14, 203, (1977)
- (6) E.A.Guggenheim, Trans.Faraday Soc. I, 62, 3446, (1966)
- (7) S.K.Suri, J.J.Spitzer, R.H.Wood, E.G.Abel, P.T.Thompson, J.Soln.Chem., 14, 781, (1985)
- (8) J.J.Spitzer, S.K.Suri, R.H.Wood, J.Soln.Chem., 14, 571, (1985)
- (9) S.K.Suri, R.H.Wood, J.Soln.Chem., 15, 705, (1986)
- (10) K.Brodlie, Leicester University Computer Centre, *private communication* .
- (11) A.K.Covington, D.E.Irish, J.Chem.Eng.Data, 17, 175, (1972)
- (12) S.Lindenbaum, G.E.Boyd, J.Phys.Chem., 68, 911, (1964)
- (13) A.Losurdo, W.-Y.Wen, C.Jolicoeur, J.L.Fortier, J.Phys.Chem., 81, 1813, (1977)
- (14) R.S.Robinson, R.H.Stokes, "Electrolyte Solutions" , London, Butterworths, 2nd Edition, (1959)
- (15) J.B.Maskill, R.G.Bates, J.Soln.Chem., 15, 323, (1986)
- (16) W.-Y.Wen, S.Saito, C.Lee, J.Phys.Chem., 70, 1244 , (1966)
- (17) O.D.Bonner, J.Chem.Eng.Data, 21, 498, (1976)
- (18) W.-Y.Wen, J.Hung, J.Phys.Chem., 74, 170, (1970)

- (19) F.A.Long, W.F.McDevit, Chem.Revs., 51, 119, (1952)
- (20) B.E.Conway, D.M.Novak, L.Laliberte, J.Soln.Chem., 3, 683, (1974)
- (21) R.W.Gurney, "Ionic Processes in Solution", McGraw-Hill, New York, (1953)
- (22) J.E.Desnoyers, M.Arel, G.Perron, C.Jolicoeur, J.Phys.Chem., 73, 3346, (1969)
- (23) C.V.Krishnan, H.L.Friedman, "Water a Comprehensive Treatise" ed.F.Franks, Plenum Press, New York, Vol.3, Chapt.1, (1973)
- (24) W.-Y.Wen, K.Miyajima, A.Otsuka, J.Phys.Chem., 75, 2148, (1971)
- (25) D.Rosenzweig, J.Padova, Y.Marcus, J.Phys.Chem., 80, 601, (1976)
- (26) O.D.Bonner, J.Chem.End.Data, 21, 499, (1976)
- (27) O.D.Bonner, J.Chem.Eng.Data, 27, 63, (1982)
- (28) F.Franks, H.T.Smith, Trans.Faraday Soc., 63, 2586, (1967)
- (29) W.-Y.Wen, S.Saito, J.Phys.Chem., 68, 2639, (1964)
- (30) G.Perron, N.Desrosiers, J.E.Desnoyers, Can.J.Chem., 54, 2163, (1976)

❧  
CHAPTER  
9

Salt effects on the alkaline  
hydrolysis of Bromophenolblue

## 9.1 Introduction

Second order rate constants for the alkaline hydrolysis of the sodium salt of bromophenol blue<sup>1-4</sup> are dependent on the concentration of added potassium bromide and tetraalkylammonium halide salts,  $R_4NX$  where  $R = \text{Me}$  and  $\text{Et}$  and  $X = \text{F}^-$ ,  $\text{Cl}^-$ ,  $\text{Br}^-$  and  $\text{I}^-$ . The reactions were studied over an added salt concentration range  $0.10 \leq [\text{added salt}]/\text{mol dm}^{-3} \leq 2.0$  at 298.15 K.

Trends in  $\ln(k_2/k_0)$ , where  $k_0 = 3.507 \times 10^{-4} \text{ mol dm}^{-3} \text{ s}^{-1}$  is the second order rate constant at zero ionic strength (taken from the work of Panepinto and Kilpatrick<sup>1</sup>) and  $k_2$  is the calculated second order rate constant, were analysed in terms of dependences predicted by the Debye-Huckel Limiting Law (DHLL; see Chapter 6) and Pitzer's<sup>5</sup> equation for activity coefficients of single ions in aqueous salt solutions.

The results pointed towards the marked effect of cosphere overlap on both the bromophenol blue dianion and trinegative transition state. Moreover the success of Pitzer's equation indicated a dependence of reaction rate on ionic strength in contradiction to the theories reported by Rudra and Das<sup>3</sup>.

## 9.2 Experimental

The sodium salt of bromophenol blue was prepared using the method of Amis and La Mer<sup>6</sup>. A concentrated stock solution of the aqueous salt solution was prepared. The product of reaction was characterised by an intense absorption band in the visible region of the electromagnetic spectrum centered at  $\lambda_{\text{max}} = 510 \text{ nm}$  which corresponds to a  $\pi$  to  $\pi^*$  transition.

Reaction of bromophenol blue dianions with hydroxide ions produces a carbinol species<sup>2</sup> (see Figure 9.1).

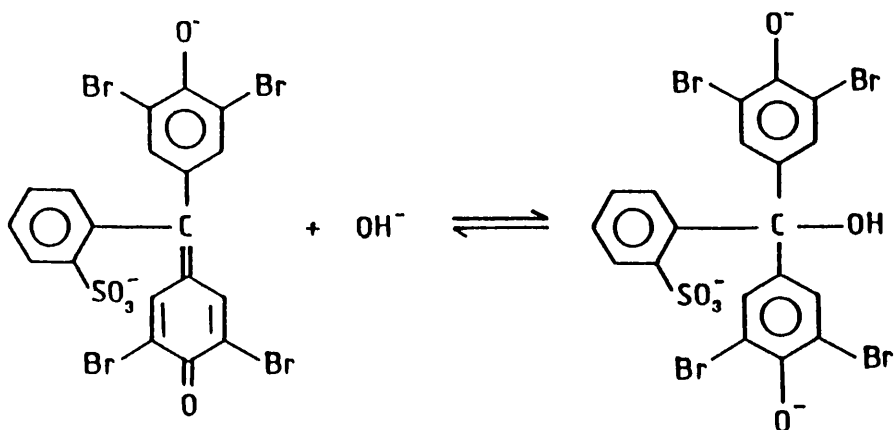


FIGURE 9.1

In a typical kinetic run, 2 cm<sup>3</sup> of an aqueous salt solution were added to 1 cm<sup>3</sup> of sodium hydroxide solution in a quartz cell such that the final concentration of added salt was in the range 0.1 to 2.0 mol dm<sup>-3</sup> and the final hydroxide concentration was 0.1 mol dm<sup>-3</sup> in the cell. The cell was placed in the cell holder of either the HP 8451A or Unicam SP 1800 spectrophotometers (see Chapter 2) and allowed to attain thermal equilibrium at 298.15 K over a period of approximately five minutes. The reaction was initiated by adding one drop of the concentrated sodium dye salt into the cell. After vigorous shaking, the disappearance of the dye band was monitored at  $\lambda_{\max}$  for at least 2.5 half lives. The reaction was overall second order. However by ensuring the concentration of hydroxide ions was in vast excess over the concentration of the bromophenol blue salt, it was possible to monitor the rate of reaction under pseudo first order conditions (see Chapter 2).

$$(dP/dt) = k' [\text{BPB}] \quad [9.1]$$

where  $k'$  is the pseudo first order rate constant.

$$\Rightarrow k' = k_2 [\text{NaOH}] \quad [9.2]$$

Analysis of the absorbance/time data used the method of non-linear least squares outlined in Chapter 2 and produced estimates of the pseudo first order rate constants  $k'/\text{s}^{-1}$  and hence estimates of the second order rate constants,  $k_2/\text{mol dm}^{-3} \text{s}^{-1}$ .

### 9.3 Details of Data Analysis

The dependence of ionic activity coefficients on ionic strength as predicted by the DHLL were calculated for hydroxide ions, the bromophenol blue dianions and the trinegative transition state using equations [9.3] to [9.5] respectively.

$$\ln \gamma(\text{OH}^-) = -S_\gamma z(\text{OH}^-)^2 (I/m^\circ)^{1/2} \quad [9.3]$$

$$\ln \gamma(\text{BPB}^{2-}) = -S_\gamma z(\text{BPB}^{2-})^2 (I/m^\circ)^{1/2} \quad [9.4]$$

$$\ln \gamma(\text{ts}^{3-}) = -S_\gamma z(\text{ts}^{3-})^2 (I/m^\circ)^{1/2} \quad [9.5]$$

where  $S_\gamma = 1.1763$ ,  $z$  is the charge number of the ion,  $I$  is the ionic strength and  $m^\circ = 1 \text{ mol kg}^{-1}$ . The ionic strength of the system was calculated from the definition used in equation [6.3] of Chapter 6. So for a typical reaction which contains added salt MX the ionic strength was

calculated using equation [9.6].

$$I = 0.5 \left[ m_{\text{OH}^-} z_{\text{OH}^-}^2 + m_{\text{Na}^+} z_{\text{Na}^+}^2 + m_{\text{M}^+} z_{\text{M}^+}^2 + m_{\text{X}^-} z_{\text{X}^-}^2 + m_{\text{Na}^+} z_{\text{Na}^+}^2 + m_{\text{BPB}^{2-}} z_{\text{BPB}^{2-}}^2 \right] \quad [9.6]$$

In practice the two terms originating from the sodium salt of bromophenol blue are small and so equation [9.6] can be simplified to the form shown in equation [9.7].

The dependence of the second order rate constant,  $k_2$ , on ionic strength can thus be written in the form;

$$\begin{aligned} \ln(k_2/k_0) &= \ln\gamma(\text{OH}^-) + \ln\gamma(\text{BPB}^{2-}) - \ln\gamma(\text{ts}^{3-}) \\ &= -S_{\gamma}(I/m^\circ)^{1/2} - 4S_{\gamma}(I/m^\circ)^{1/2} + 9S_{\gamma}(I/m^\circ)^{1/2} \end{aligned}$$

$$\Rightarrow \ln(k_2/k_0) = 4S_{\gamma}(I/m^\circ)^{1/2} \quad [9.7]$$

An alternative description of the role of charge-charge interactions used Pitzer's equation for a single ion activity coefficient<sup>5</sup>. For a single anion X, Pitzer's equation can be written in the form of equation [9.8].

$$\begin{aligned} \ln\gamma_X &= z_X^2 f^{\gamma} + 2 \sum m_c [B_{xc} + (\sum z) C_{xc}] + 2 \sum m_a^{\ominus} C_{ca} \\ &\quad \text{A} \qquad \qquad \qquad \text{B} \qquad \qquad \qquad \text{C} \\ &\quad + \sum \sum m_c m_a [z_X^2 B'_{ca} + z_X C_{ca}] \quad [9.8] \\ &\quad \qquad \qquad \qquad \qquad \qquad \text{D} \end{aligned}$$

c = cations of salts in system.

a = anions of salts in system.

### 9.3.1 Term A

$f^\gamma$  represents the contribution of charge-charge interactions and can be written in the form of equation [9.9].

$$\begin{aligned} \ln \gamma_x^{\text{elect}} &= z_x^2 f^\gamma \\ &= z_x^2 \{-A_\phi \{ (I^{1/2} / (1+bI^{1/2})) + (2/b) \ln(1+bI^{1/2}) \} \} \end{aligned} \quad [9.9]$$

where  $I = (I/m^\circ)$ ;  $A_\phi = S_\gamma/3 = 0.3903$  and  $b = 1.2$ . Equation [9.9] describes the electrical part of the single ion activity coefficient for the species involved in the reaction. Hence the sum of all the contributing terms defines a total electrical term,  $\ln \gamma^{\text{elect}}$ .

$$\ln \gamma^{\text{elect}} = \ln \gamma^{\text{elect}}(\text{OH}^-) + \ln \gamma^{\text{elect}}(\text{BPB}^{2-}) - \ln \gamma^{\text{elect}}(\text{ts}^{3-}) \quad [9.10]$$

In a similar fashion to the procedure used with respect to equation [9.7] equation [9.10] can be simplified to the form given in equation [9.11].

$$\begin{aligned} \ln \gamma^{\text{elect}} &= 4A_\phi \{ ((I/m^\circ)^{1/2} / (1+b(I/m^\circ)^{1/2})) \\ &\quad + (2/b) \ln(1+b(I/m^\circ)^{1/2}) \} \end{aligned} \quad [9.11]$$

### 9.3.2 Term B

The second term represents the effect of non-coulombic ion-ion interactions i.e. cosphere-cosphere interactions/overlap, on the activity coefficient. Within the context of the reaction under study this term describes the effect of sodium cations and added salt cations on the activity coefficient of hydroxide anions.

$$\{\text{OH}^- \text{cosph}\}^{\text{termB}} = 2\sum m_c [B_{xc} + (\sum z)C_{xc}] \quad [9.12]$$

where  $\sum z = \sum m_c z_c = \sum m_a z_a$ . For the reaction under investigation equation [9.12] can be written in the form of equation [9.13].

$$\{\text{OH}^- \text{cosph}\}^{\text{termB}} = 2[m_c [B_{\text{OH}-c} + m_c z_c C_{\text{OH}-c}] + m_{\text{Na}^+} [B_{\text{OH}-\text{Na}^+} + m_{\text{Na}^+} z_{\text{Na}^+} C_{\text{OH}-\text{Na}^+}]] \quad [9.13]$$

where  $B_{\text{OH}-c}$  and  $B_{\text{OH}-\text{Na}^+}$  represent equations [9.14] and [9.15].

$$B_{\text{OH}-c} = \beta^{\circ}_{\text{OH}-c} + [2\beta^1_{\text{OH}-c}/(\alpha^2 I)] [1 - (1 + \alpha I^{1/2}) \exp(-\alpha I^{1/2})] \quad [9.14]$$

$$B_{\text{OH}-\text{Na}^+} = \beta^{\circ}_{\text{OH}-\text{Na}^+} + [2\beta^1_{\text{OH}-\text{Na}^+}/(\alpha^2 I)] [1 - (1 + \alpha I^{1/2}) \exp(-\alpha I^{1/2})] \quad [9.15]$$

where  $I = (I/m^{\circ})$  and  $\beta$  parameters were taken from Tables compiled by Pitzer<sup>5</sup>. Where tetraalkylammonium salts were added to the reaction no data were available for tetraalkylammonium hydroxide salts and so the  $\beta$  and  $C$  terms for the chloride salts were used. This assumption was based on the the similarity in ion size between chloride and hydroxide anions<sup>7</sup>.

The terms  $C_{\text{OH}-c}$  and  $C_{\text{OH}-\text{Na}^+}$  used in equation [9.13] represent equations [9.16] and [9.17].

$$C_{\text{OH}-c} = C^{\phi}_{\text{OH}-c} / (2 |z_c z_{\text{OH}-}|^{1/2}) \quad [9.16]$$

$$C_{\text{OH-Na}^+} = C_{\text{OH-Na}^+}^{\phi} / (2 |z_{\text{Na}^+} z_{\text{OH}^-}|^{1/2}) \quad [9.17]$$

$C^{\phi}$  terms were taken from Tables compiled by Pitzer<sup>5</sup>.

A quantity delta,  $\Delta$ , was defined from the difference between the sum of the first and second Pitzer terms and  $\ln(k_2/k_0)$ .

$$\Delta = \ln(k_2/k_0) - \ln \gamma^{\text{elect}} - \{\text{OH}^- \text{cosph}\} \quad [9.18]$$

$$\Rightarrow \Delta = \{\text{BPB}^{2-} \text{cosph}\} - \{\text{ts}^{3-} \text{cosph}\} \quad [9.19]$$

As denoted in equation [9.19],  $\Delta$  represents the difference between the cosphere interaction effects of the bromophenol blue dianion and the trinegative transition state.

### 9.3.3 Term C

Relevant data were not available for the bromophenol blue dianion and the transition state trinegative anion. Hence in the absence of any data this term was assumed to be negligibly small and set equal to zero.

### 9.3.4 Term D

With the fourth term of Pitzer's equation it was only possible to investigate the effect of the anions and cations present in the system on the hydroxide anion. As with term C no relevant data for  $\text{BPB}^{2-}$  and  $\text{ts}^{3-}$  were available. If a salt MX is added to the reaction mixture, Pitzers fourth term can be written in the form of equation [9.20].

$$\begin{aligned} \ln \gamma_{\text{OH}^-}^{\text{termD}} = & m_{\text{M}} m_{\text{X}} [z_{\text{OH}^-}^2 B'_{\text{MX}} + z_{\text{OH}^-} C_{\text{MX}}] \\ & + m_{\text{Na}^+} m_{\text{X}} [z_{\text{OH}^-}^2 B'_{\text{NaX}} + z_{\text{OH}^-} C_{\text{NaX}}] \\ & + m_{\text{M}} m_{\text{OH}^-} [z_{\text{OH}^-}^2 B'_{\text{MOH}} + z_{\text{OH}^-} C_{\text{MOH}}] \\ & + m_{\text{Na}^+} m_{\text{OH}^-} [z_{\text{OH}^-}^2 B'_{\text{NaOH}} + z_{\text{OH}^-} C_{\text{NaOH}}] \quad [9.20] \end{aligned}$$

where  $B'_{\text{MX}}$  and  $C_{\text{MX}}$  are used to represent equations [9.21] and [9.22].

$$\begin{aligned} B'_{\text{MX}} = & [2\beta_{\text{MX}}^1 / (\alpha_1^2 I^2)] [(1 + \alpha_1 I^{1/2} + 0.5\alpha_1^2 I) \exp(-\alpha_1 I^{1/2}) - 1] \\ & + [2\beta_{\text{MX}}^{(2)} / (\alpha_2^2 I^2)] [(1 + \alpha_2 I^{1/2} + 0.5\alpha_2^2 I) \exp(-\alpha_2 I^{1/2}) - 1] \quad [9.21] \end{aligned}$$

$$C_{\text{MX}} = C_{\text{MX}}^\phi / (2 |z_{\text{M}^+} z_{\text{X}^-}|^{1/2}) \quad [9.22]$$

where  $I = (I/m^\circ)$  and Tables compiled by Pitzer<sup>5</sup> yielded  $\beta^1$ ,  $\beta^{(2)}$  and  $C$ . The constants  $\alpha_1$  and  $\alpha_2$  equal 2.0 and 0.0 respectively in line with the suggestions of Pitzer and Mayogra<sup>8</sup>.

The final equation based on Pitzer's equation was obtained as the sum of the four terms described above.

#### 9.4 Results

Table 9.1 reports second order rate constants for reaction solutions containing added salts KBr and  $\text{R}_4\text{NX}$  (where  $\text{R} = \text{Me}$  and  $\text{Et}$  and  $\text{X} = \text{F}^-$ ,  $\text{Cl}^-$ ,  $\text{Br}^-$  and  $\text{I}^-$ ) over the concentration range  $0.1 \leq c/\text{mol dm}^{-3} \leq 2.0$ . The results are summarised in Figure 9.2 as a plot of  $\ln(k_2/k_0)$  against ionic strength. The tetramethylammonium salts accelerated the reaction rate whilst the tetraethylammonium salts retarded the reaction rate. The nature of the anion of the added salt had a

Table 9.1

Second order rate constants for the alkaline hydrolysis of the sodium salt of bromophenolblue in the presence of known concentrations of aqueous salt solutions at 298K.

Molarity /mol dm <sup>-3</sup>	Me <sub>4</sub> NF	Me <sub>4</sub> NCl	Me <sub>4</sub> NBr
	$10^3 k_2 / \text{dm}^3 \text{mol}^{-1} \text{s}^{-1}$		
0.00	0.656	0.656	0.656
0.25	1.089	1.012	0.943
0.50	1.334	1.133	1.001
0.75	1.526	1.226	1.014
1.00	1.679	1.309	1.026
1.50	2.102	1.435	1.056
2.00	2.533	1.588	1.077

Molarity /mol dm <sup>-3</sup>	Et <sub>4</sub> NI	Et <sub>4</sub> NBr	KBr
	$10^4 k_2 / \text{dm}^3 \text{mol}^{-1} \text{s}^{-1}$		
0.00	6.559	6.559	6.559
0.10	6.412	-	-
0.25	5.343	6.362	8.990
0.40	4.207	-	-
0.50	3.760	5.762	9.656
0.60	3.187	-	-
0.75	2.677	5.193	10.137
1.00	-	4.549	10.317
1.50	-	3.971	10.562
2.00	-	3.532	10.853

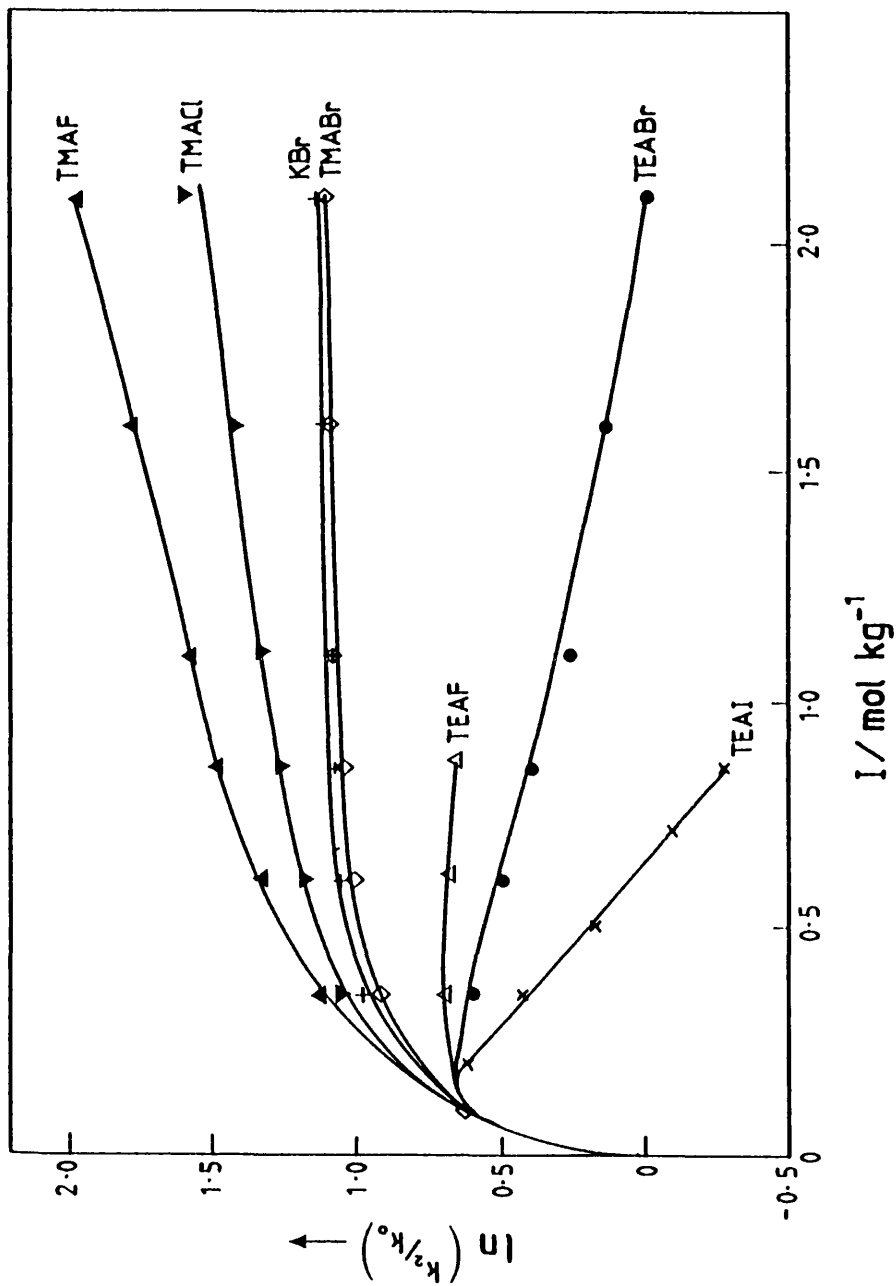


FIGURE 9.2  
Effect of added salts on the rate constant for reaction of the sodium salt of bromophenolblue with hydroxide ions at 298.15 K in aqueous solutions.

specific effect on reaction rate<sup>1</sup>. For both the tetramethylammonium and tetraethylammonium halides the reaction rate increased in the order;



Potassium bromide had an effect on reaction rate very similar to that produced by tetramethylammonium bromide.

A FORTRAN program analysed the kinetic data using the methods described in Section 9.3. Appendix 5 contains a listing of the program.

### 9.5 Discussion

The Debye-Huckel treatment of activity coefficients for all added salts predicts a positive salt effect on the alkaline hydrolysis reaction under consideration. This can be understood in terms of the greater stabilisation of the transition state of the reaction (charge -3) compared to the stabilisation of the initial states (i.e.  $\text{OH}^- + \text{BPB}^{2-}$  ions). The stabilisation effect predicted by the Debye-Huckel equation and calculated in the FORTRAN program (Appendix 5) is illustrated in Figure 9.3. The Debye-Huckel equation predicts an increase in reaction rate with increase in ionic strength due to an increased stabilisation of the transition state and hence a decrease in the Gibbs function for activation.

In Pitzer's equation the fourth term for each added salt is negligible in comparison to the first two terms of the equation for  $\ln \gamma_j$ . The electrostatic, first term of the full equation, for all added salts, predicted a positive salt effect on reaction rate in a similar manner to the trend predicted by the Debye-Huckel equation. Again the

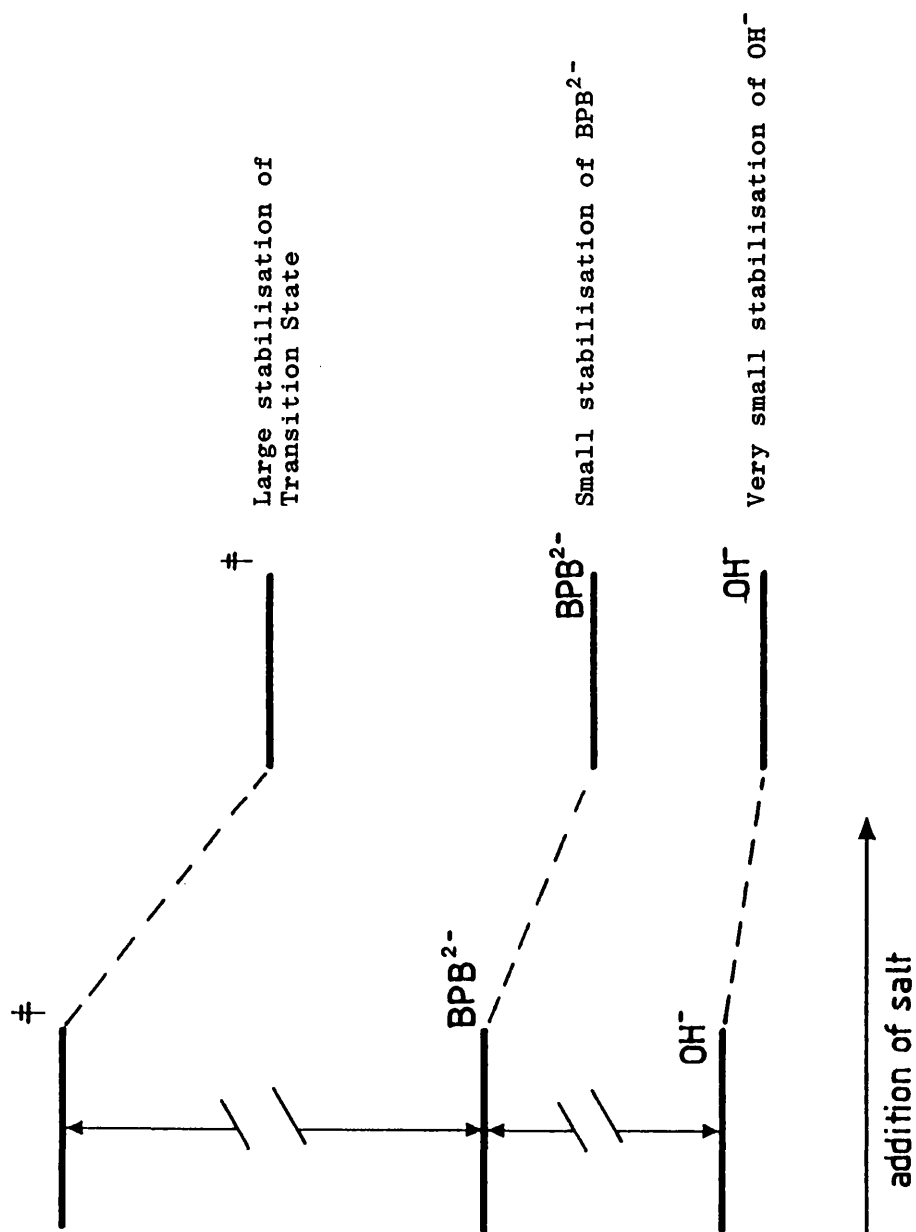


**FIGURE 9.3**

Predicted Debye-Hückel stabilisation of the initial and transition states for the addition of added salt to the alkaline hydrolysis of bromphenolblue at 298.15 K.

trend can be understood in terms of the increased stabilisation of the trinegative transition state compared to the initial state contributions. However, the magnitude of the positive salt effect predicted by Pitzer's electrostatic term was smaller than that predicted by the Debye-Huckel treatment. In comparison to the first term the effect of Pitzer's second term on  $\ln(k_2/k_0)$  is small. However, the nature of the added salt has, for the first time, been taken into consideration. Although not having a dramatic effect on the overall pattern produced by Pitzer's full equation the second term follows the observed trends in  $\ln(k_2/k_0)$ . For example, in the case of added tetramethylammonium fluoride a positive salt effect is observed and this is mirrored by a positive second term. However in the case of tetraethylammonium bromide a negative salt effect was observed in the kinetics and in this situation the second term of Pitzer's equation was negative.

Pitzer's full equation predicts an overall positive salt effect for the reaction under consideration over the range of salts investigated, in line with the predictions of the Debye-Huckel equation. Figure 9.4 reports predicted trends in  $\ln(k_2/k_0)$  calculated from the DHLL and Pitzer's full equation together with the experimental results for the addition of KBr to the alkaline hydrolysis reaction of the sodium salt of bromophenol blue. However in calculating this trend two important terms are ignored by the analysis, namely the second term contributions to Pitzer's full equation which describes the effects of non-electrostatic, charged species interactions (i.e. cosphere-cosphere

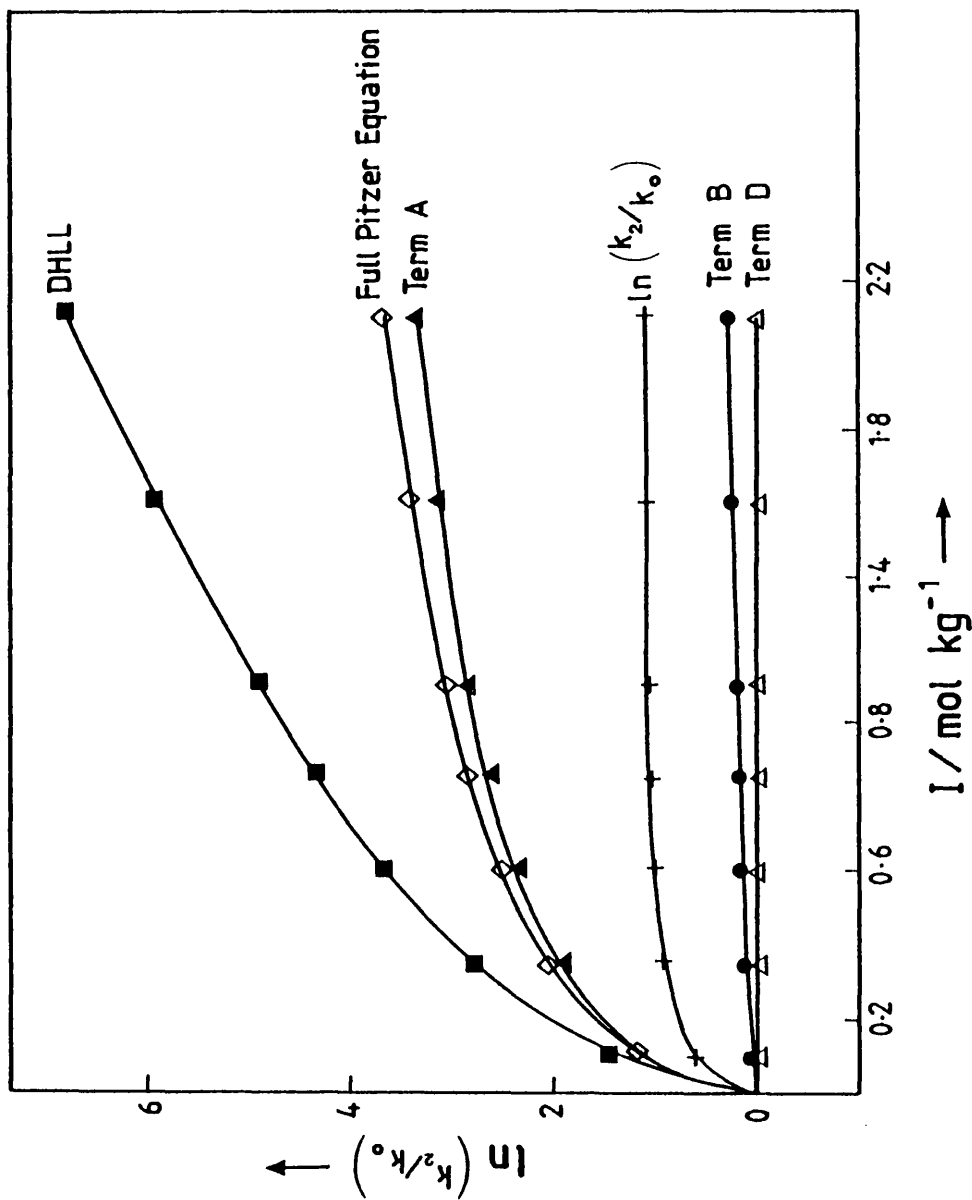


FIGURE 9.4

$\ln(k_2/k_0)$  against ionic strength for the alkaline hydrolysis of bromophenol blue at 298.15 K in the presence of various concentrations of potassium bromide. The figure reports both the experimental results and the trends predicted by Pitzer's equation and the DHLL. Terms A, B and D are separate contributions to the full Pitzer equation.

interactions) for both the dinegative bromophenol blue anion and the trinegative transition state. For Pitzer's full equation to accurately predict the observed trends in  $\ln(k_2/k_0)$  for various added salts the magnitude of the difference between  $\{BPB^{2-}\text{-cosph}\}-\{ts^{3-}\text{-cosph}\}$  must be equal to the quantity  $\Delta$  defined by equation [9.18]. In real terms this difference cannot be accurately calculated because no  $\beta$  or  $C$  terms are available. However estimates of this difference can be obtained using  $\beta^0$ ,  $\beta^1$  and  $C$  parameters which cover the complete range recorded by Pitzer for 3:1 and 2:1 salts. Using these ranges of estimates the cosphere contributions of both the bromophenol blue dianion and trinegative transition state were estimated using equations similar to equation [9.13] which defines the  $OH^-$  cosphere contribution. Using this technique, (subroutine cosphere of the program contained in Appendix 5) it was found that the magnitude of the difference between the cosphere terms of the dianion and the trinegative transition state was sufficient to explain the differences between the observed trend in  $\ln(k_2/k_0)$  and that predicted by the full Pitzer equation. Figure 9.5 reports the range of  $\ln(k_2/k_0)$  the dianion and transition state cosphere terms cover based on approximations for  $\beta^0$ ,  $\beta^1$  and  $C$ -terms taken from Pitzer's<sup>5</sup> tabulated values for 2:1 and 3:1 salts.

The apparent success of Pitzer's equation in modelling the effect of added salt on the rate constant, using equations containing ionic strength casts doubt on the suggestions of Rudra and Das<sup>3</sup>. Based on the addition of a number of salts to the same alkaline hydrolysis reaction, they concluded the reaction was a demonstration of the

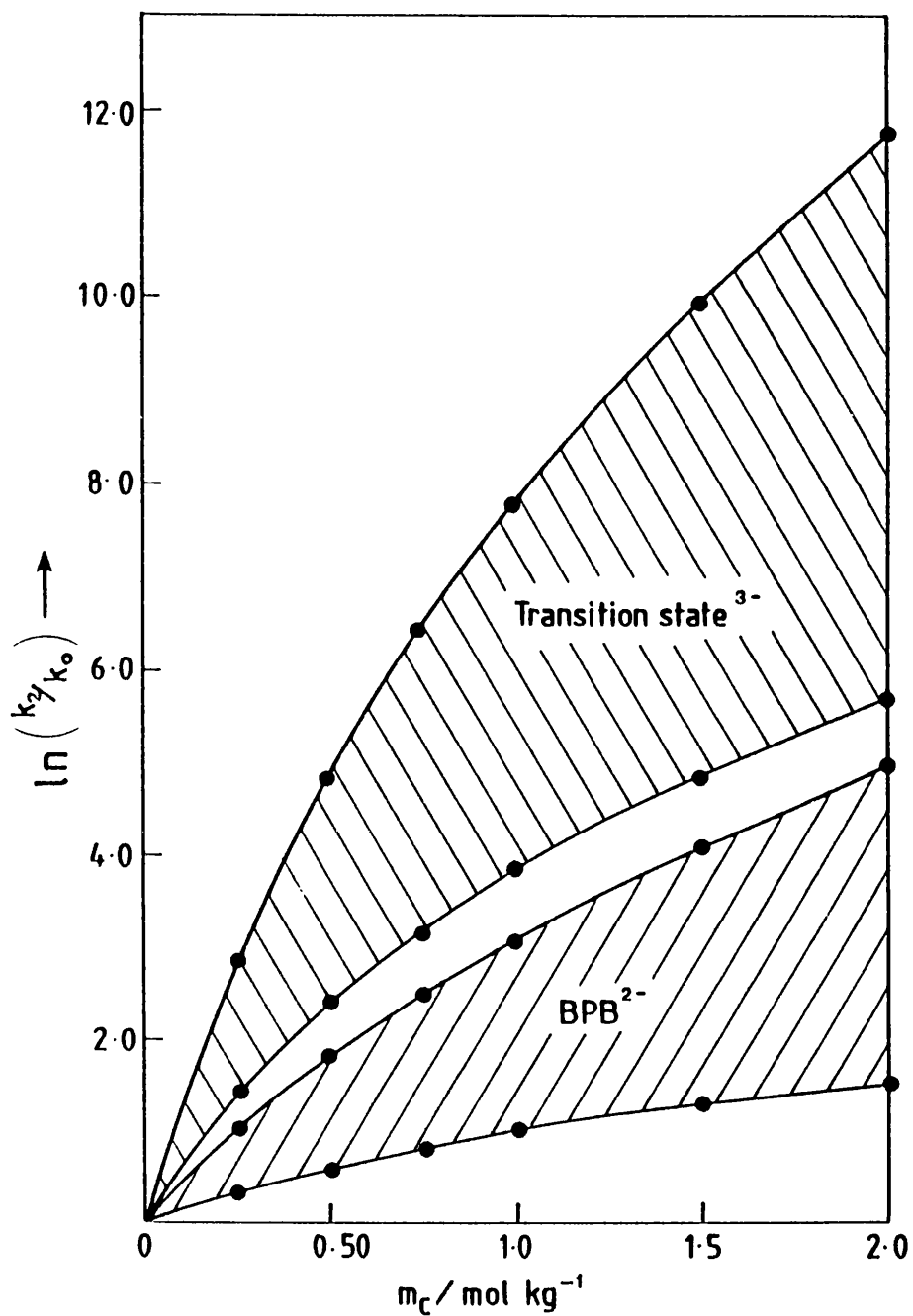


FIGURE 9.5

Trends in  $\ln(k_2/k_0)$  at 298.15 K, calculated for the bromophenolblue dianion and the tri-negative transition state as predicted by Pitzer's equation using a range of  $\beta^0$  and  $\beta^1$  values for 2:1 and 3:1 salts, plotted against the molality of added cation,  $m_c / \text{mol kg}^{-1}$ .

Olson-Simonsen effect, in which ionic strength is of no consequence to the rate of disappearance of the bromophenol blue dianion. This is certainly not the situation observed at the concentrations of added salt investigated in this study. This conclusion is backed up by the work of Carmona<sup>1</sup> et al who also found a dependence on ionic strength.

Turning now to the observed specific anion effect identified from the reported second order rate constants. According to the analysis described above this contribution is catered for in Pitzer's full equation by the third term. However this was assumed to be zero. Ideally a plot of  $\ln(k_2/k_0) - \Delta$  against the molality of the cation of the added salt produces a straight line of gradient defined by the difference between the  $B_{BPB2-c}$  dianion term and the  $B_{ts3-c}$  transition state term (see equations [9.14] and [9.15]). However using the analysis described above the pattern reported in Figure 9.6 emerges. This pattern points to the importance the third term of Pitzer's equation and identifies a method from which more precise estimates of  $\beta$  parameters could be calculated in future work.

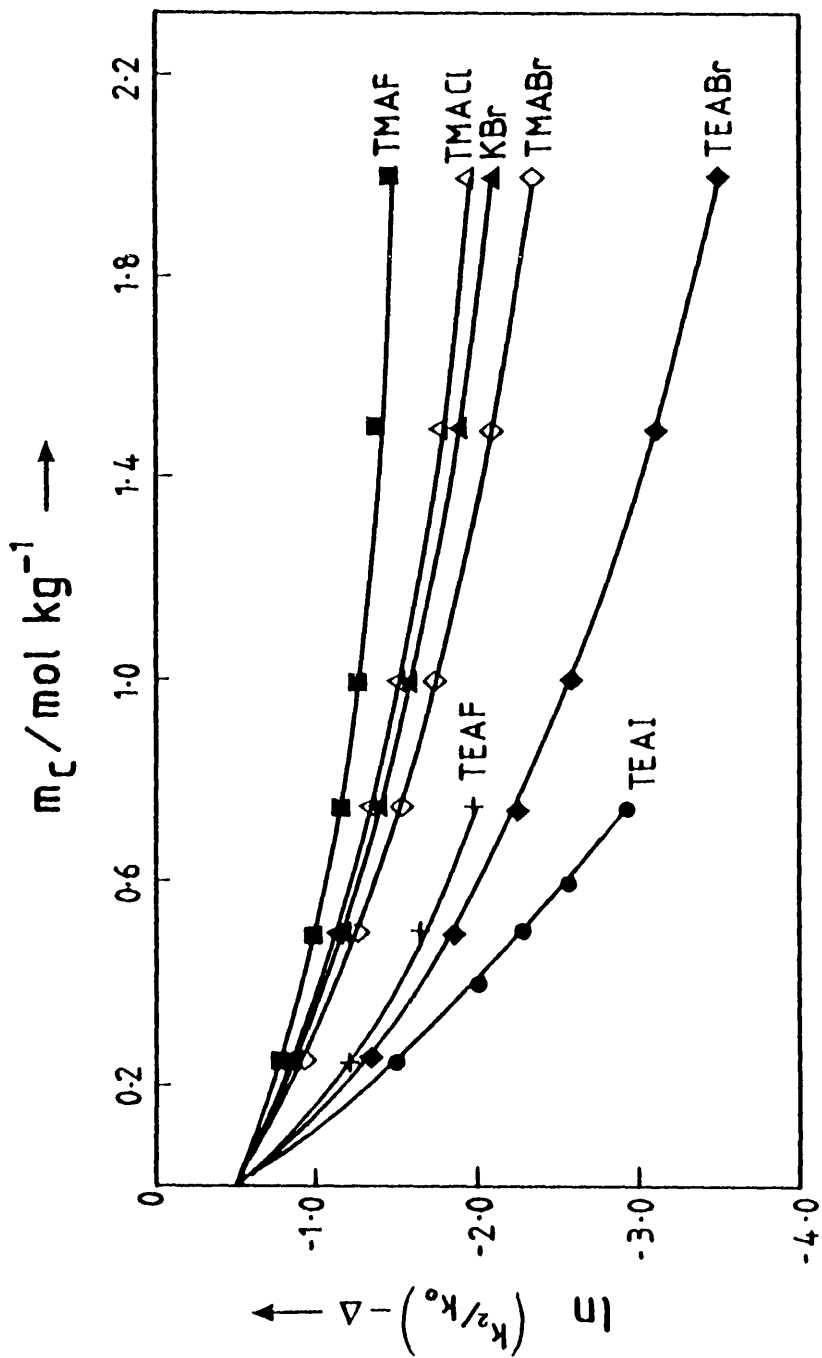


FIGURE 9.6

$\ln(k_2/k_0) - \Delta$  (see equations [9.19] and [9.20]) against molality of the cation of the added salt,  $m_c / \text{mol kg}^{-1}$ , for the alkaline hydrolysis of bromophenolblue at 298.15 K in the presence of known concentrations of various added salts.

## References Chapter 9

- (1) J.R.Velasco, F.S.Burgos, M.C.Carmona, J.H.Toledo, *An.Quim.*, 80, 173, (1984)
- (2) E.S.Amis, R.T.Overman, *J.Am.Chem.Soc.*, 66, 941, (1944)
- (3) L.Rudra, M.N.Das, *J.Chem.Soc.A*, 630, (1967)
- (4) F.W.Panepinto, M.Kilpatrick, *J.Am.Chem.Soc.*, 59, 1871, (1937)
- (5) K.S.Pitzer, "Activity Coefficients in Electrolyte Solutions", Vol.1, Ed. R.M.Pytkowicz, CRC Press, (1979)
- (6) E.S.Amis, V.K.Lamer, *J.Am.Chem.Soc.*, 61, 905, (1939)
- (7) M.J.Blandamer, J.Burgess, *Coord.Chem.Revs.*, 31, 93, (1980)
- (8) K.S.Pitzer, G.Mayorga, *J.Phys.Chem.*, 77, 268, (1973)



# CHAPTER 10

Internal Pressures of Water  
and Deuterium Oxide

## 10.1 Introduction

This Chapter reports equations which describe the internal pressure<sup>1</sup>,  $\Pi_i$ , as a function of temperature and pressure, in the ranges  $273.15 \leq T/K \leq 373.15$  and  $0 \leq P/\text{bar} \leq 1000$ , for water and deuterium oxide. Quadratic equations which model the pressure dependence of (i) the temperature at which  $\Pi_i$  is equal to zero and (ii) the temperature of maximum density (TMD) are reported for both systems and the distinction between equilibrium internal pressure  $\Pi_i(A=0)$  and an instantaneous/frozen internal pressure  $\Pi_i(\xi)$  is discussed in terms of the structuredness of water in conjunction with the Lumry two-state model<sup>2</sup> (see Chapter 12).

Interest in internal pressure arose from work reported in Chapters 4 and 5 which dealt with kinetics of reactions in binary liquid mixtures. Solvent-solvent interactions in such systems play a large part in influencing the magnitude and sign of kinetic parameters and so quantities which probe such interactions may provide a handle for predicting trends in these parameters. Internal pressures can shed light on the structuredness of solvent mixtures as demonstrated by the work of Leyendekker<sup>3,4</sup> and also Hyne et al<sup>5</sup>. By examining the internal pressure of water and deuterium oxide it was hoped to go some way towards establishing a quantitative method of examining kinetic parameters for reactions carried out in binary mixtures.

## 10.2 Definition and Methods of Obtaining Internal Pressure

The internal pressure of a system can be defined by

equation [10.1].

$$\Pi_i = T(\partial p / \partial T)_V - p \quad [10.1]$$

T = temperature /K

$(\partial p / \partial T)_V$  = Rate of change of pressure with temperature at constant volume, V.

p = external pressure /bar

According to Frank <sup>7</sup> equation [10.1] portrays the external pressure, p, as a 'residual squeeze' which must be applied in order to balance the expansive tendency represented by the equilibrium thermal pressure  $T(\partial p / \partial T)_V$  with the contractive nature of  $\Pi_i$ . The internal pressure is the weaker force.

Equation [10.1] can be developed using the isobaric expansibility,  $\alpha$ , and the isothermal compressibility,  $\kappa_T$  which are defined by equations [10.2] and [10.3] respectively.

$$\alpha = (1/V)(\partial V / \partial T)_p \quad [10.2]$$

i.e. the rate of change of volume with temperature per unit volume at constant pressure.

$$\kappa_T = -(1/V)(\partial V / \partial p)_T \quad [10.3]$$

i.e. the rate of change of volume with pressure per unit volume at constant temperature. The negative sign makes  $\kappa_T$  a positive quantity. When the pressure is increased the volume of all stable phases decreases and so  $(\partial V / \partial p)_T$  is always negative.

Combination of equations [10.2] and [10.3] leads to an expression for  $(\partial p/\partial T)_V$  which is substituted into equation [10.1] to form the more widely used expression for  $\Pi_i$ ; equation [10.4].

$$\begin{aligned} \alpha/\kappa_T &= \{(1/V)(\partial V/\partial T)_p\}/\{(-1/V)(\partial V/\partial p)_T\} \\ &= (\partial p/\partial T)_V \end{aligned}$$

$$\Rightarrow \Pi_i = T(\alpha/\kappa_T) - p \quad [10.4]$$

The isothermal compressibility is closely related to the isentropic compressibility,  $\kappa_S$ , which is defined by equation [10.5].

$$\kappa_S = -(1/V)(\partial V/\partial p)_S \quad [10.5]$$

i.e. the rate of change of volume with pressure per unit volume at constant entropy, S.

The isentropic compressibility is a relatively simple quantity to establish experimentally. It is calculated from sound velocity, c, using the relationship described by equation [10.6].

$$c^2 = 1/(\kappa_S \rho) \quad [10.6]$$

c = speed of sound /m s<sup>-1</sup>

$\rho$  = density /kg m<sup>-3</sup>

$\kappa_S$  = isentropic compressibility /N m<sup>-2</sup>

The relationship between  $\kappa_S$  and  $\kappa_T$  uses the mathematical expression shown below in equation [10.7] which transposes the conditions on a partial differential.

$$(\partial Z/\partial X)_U = (\partial Z/\partial X)_Y - (\partial U/\partial X)_Y (\partial Y/\partial U)_X (\partial Z/\partial Y)_X \quad [10.7]$$

By applying this to  $\kappa_S$  and  $\kappa_T$ ;

$$(\partial V/\partial p)_S = (\partial V/\partial p)_T - (\partial S/\partial p)_T (\partial T/\partial S)_p (\partial V/\partial T)_p \quad [10.8]$$

From a Maxwell relationship;

$$-(\partial S/\partial p)_T = (\partial V/\partial T)_p$$

Also  $(\partial S/\partial T)_p = (C_p/T)$  where  $C_p$  is the isobaric heat capacity. Hence;

$$(\partial V/\partial p)_S = (\partial V/\partial p)_T + (\partial V/\partial T)_p (T/C_p) (\partial V/\partial T)_p \quad [10.9]$$

Multiplying both sides by  $-(1/V)$  yields equation [10.10].

$$\begin{aligned} \Rightarrow \quad -(1/V)(\partial V/\partial p)_S &= -(1/V)(\partial V/\partial p)_T \\ &\quad - (1/V)(\partial V/\partial T)_p (T/C_p) (\partial V/\partial T)_p \end{aligned} \quad [10.10]$$

Using equations [10.3] and [10.5], equation [10.10] can be written in the form of equation [10.11].

$$\kappa_S = \kappa_T - (1/V)(\partial V/\partial T)_p (T/C_p) (\partial V/\partial T)_p \quad [10.11]$$

From equation [10.2];

$$\begin{aligned} \alpha &= (1/V)(\partial V/\partial T)_p \\ \Rightarrow \quad \alpha V &= (\partial V/\partial T)_p \end{aligned} \quad [10.12]$$

Hence, equation [10.11] can be written in the form;

$$\kappa_S = \kappa_T - [(TV\alpha^2)/C_p] \quad [10.13]$$

or alternatively;

$$\kappa_S = \kappa_T - [(T\alpha^2)/(C_p/V)] \quad [10.14]$$

Where  $(C_p/V)$  is the isobaric heat capacity per unit volume  $/J \text{ K}^{-1} \text{ m}^{-3}$ . Combination of equations [10.6] and [10.14] leads to an equation from which  $\kappa_T$  can be directly calculated from sound velocity data.

$$\kappa_T = [1/(c^2\rho)] + [(T\alpha^2)/(C_p/V)] \quad [10.15]$$

The expansibility,  $\alpha$ , is usually obtained from density measurements over a series of temperatures at set pressure.

### 10.3 Experimental

Estimates of  $\alpha$  and  $\kappa_T$  were taken from the papers published by Fine and Millero<sup>8,9</sup> who based the calculation of these quantities on recast forms of equation [10.16].

$$PV^0/(V^0 - V^P) = B + A_1P + A_2P^2 \quad [10.16]$$

where  $P$  = the gauge pressure (p-1) atmospheres

$V^0$  = volume of liquid at gauge pressure 0 (i.e 1 atm.)

$V^P$  = volume of liquid at gauge pressure  $P$

$B, A_1, A_2$  = temperature dependent parameters

Equations for  $V^0$  were taken from the work of Kell<sup>10</sup>. By

rearranging equation [10.16] into a form which defines  $v^P$  it is possible to obtain equations for  $\alpha$  and  $\kappa_T$ .

$$v^P = (v^O - v^O_P)/(B + A_1P + A_2P^2) \quad [10.17]$$

From equation [10.2]  $\alpha = (1/v)(\partial v/\partial T)_p$ . Hence by differentiating [10.17] with respect to temperature and multiplying by  $(1/v^P)$  an expression for  $\alpha$  is derived in terms of  $v^O$ ,  $v^P$ ,  $B$ ,  $A_1$ ,  $A_2$  and  $P$ .

$$\begin{aligned} \alpha / K^{-1} &= (1/v^P)(\partial v^O/\partial T)_p - (P(\partial v^O/\partial T))/(v^P(B+A_1P+A_2P^2)) \\ &\quad - PV^O[(\partial B/\partial T)+P(\partial A_1/\partial T)+P^2(\partial A_2/\partial T)] \\ &\quad / (v^PB + A_1P + A_2P^2)^2 \end{aligned} \quad [10.18]$$

According to equation [10.3].

$$\kappa_T = -(1/v^P)(\partial v^P/\partial p)_T$$

Therefore differentiating equation [10.17] with respect to pressure yields the isothermal compressibility; equation [10.19].

$$\kappa_T/\text{bar}^{-1} = (v^O(B-A_2P^2))/(v^P(B + A_1P + A_2P^2)^2) \quad [10.19]$$

A FORTRAN program was written which modelled equations [10.17], [10.18] and [10.19] to produce values of  $v$ ,  $\alpha$  and  $\kappa_T$  and then went on to calculate internal pressures using equation [10.4], over the range  $273.15 \leq T/K \leq 373.15$  and  $0 \leq p/\text{bar} \leq 100$ . Internal pressures were fitted using a linear least squares technique<sup>11</sup> to equation [10.20], which is

based on a Taylor expansion about internal pressure  $\Pi_i(\pi, \theta)$  at temperature  $T = \theta$  and pressure  $p = \pi$ .

$$\begin{aligned} \Pi_i(T, p)/\text{bar} = & \Pi_i(\pi, \theta) + a_2(/K)(T-\theta) + a_3(/bar)(p-\pi) \\ & + a_4(/K^2)(T-\theta)^2 + a_5(/K \text{ bar})(T-\theta)(p-\pi) \\ & + a_6(/K^2 \text{ bar})(T-\theta)^2(p-\pi) \\ & + a_7(/K \text{ bar}^2)(T-\theta)(p-\pi)^2 \\ & + a_8(/bar^2)(p-\pi)^2 + a_9(/K^3)(T-\theta)^3 \end{aligned} \quad [10.20]$$

The parameters  $\theta$  and  $\pi$  were set to 323.15 K and 500 bar respectively. This method differs from that used by Leyendekker<sup>12</sup> who based an analysis on the Tait equation written in logarithmic form<sup>13</sup>.

A listing of the FORTRAN program is included in Appendix 6 Section 1. A separate FORTRAN program, included as Appendix 6 Section 2, calculated temperatures and pressures at which  $V$  is at a minimum i.e. the temperature of maximum density (TMD). These data were fitted by the method of linear least squares to equation [10.21].

$$\text{TMD} = \text{TMD}(273.15 \text{ K}; P=0) + a_1(/bar)P + a_2(/bar^2)P^2 \quad [10.21]$$

The latter program could be modified to calculate the temperature at which for a set pressure the internal pressure is equal to zero. These data were fitted using the method of linear least squares to equation [10.22].

$$\begin{aligned} T(\Pi_i=0)(/K) = & a_0(/K) + a_1(/bar)P + a_2(/bar^2)P^2 \\ & + a_3(/bar^3)P^3 \end{aligned} \quad [10.22]$$

#### 10.4 Results

Tables of internal pressures for water and deuterium oxide are included as Tables 10.1 and 10.2 respectively. Figures 10.1 and 10.2 reproduce these data as plots of internal pressure as functions of temperature and pressure. Alternatively the temperature/pressure surfaces of the internal pressure for both systems are included as Figures 10.3 and 10.4. A most interesting trend is marked by negative internal pressure at low temperatures. This can be understood at various levels. In the first explanation, negative internal pressures are simply a consequence of negative expansibilities. Water below the TMD contracts with an increase in temperature. The second view point, stresses an explanation in terms of molecular organisation as discussed in a later section. At low temperatures  $\Pi_i$  increases but at high temperature the internal pressure decreases with an increase in pressure. Hence, at around 313 K for water and 318 K for deuterium oxide  $\Pi_i$  is particularly insensitive to pressure.

The validity of derived parameters with respect to equation [10.20] was decided using F-tests<sup>14</sup> of the variance at the 95% confidence limit. For water only the first seven terms proved to be significant whilst for deuterium oxide nine parameters were needed to accurately model the temperature/pressure surface. These parameters are reported in Tables 10.3 and 10.4 together with their standard errors calculated from the diagonal of the variance/covariance matrix.

Internal pressures calculated using equation [10.20] were subtracted from the internal pressures calculated from

Table 10.1

Internal pressures for water over the ranges  $273.15 \leq T/K \leq 373.15$   
and  $0 < P/\text{bar} < 1000$  calculated using equation [10.4]<sup>a</sup>

<i>t</i>	<i>P</i> /bar										
	0	100	200	300	400	500	600	700	800	900	1000
0	-367	-274	-184	-94	-64	79	163	243	321	396	467
0.5	-320	-230	-140	-53	33	117	199	278	355	428	498
1.0	-273	-185	-98	-12	72	155	235	313	388	460	429
1.5	-227	-141	-55	29	111	192	271	348	422	492	560
2.0	-181	-97	-13	69	150	230	307	382	455	524	590
2.5	-135	-53	29	110	189	267	343	416	487	556	621
3.0	-90	-9	71	150	227	304	378	450	520	587	651
3.5	-44	34	112	189	266	340	413	484	553	619	681
4.0	(0.4)	77	153	229	304	377	448	518	585	649	712
4.5	45	120	194	268	341	413	483	551	617	681	741
5.0	89	162	235	308	379	449	518	585	650	711	771
5.5	133	205	276	347	416	485	552	618	682	743	801
10	520	576	632	689	746	802	858	912	964	1015	1064
15	928	970	1012	1055	1099	1143	1186	1229	1270	1310	1349
20	1319	1347	1377	1408	1440	1473	1505	1537	1569	1599	1628
25	1693	1710	1729	1750	1771	1794	1816	1839	1862	1883	1904
30	2052	2059	2069	2080	2092	2106	2120	2134	2149	2162	2175
35	2396	2395	2396	2399	2404	2410	2416	2423	2430	2436	2442
40	2727	2718	2713	2709	2706	2705	2705	2705	2705	2705	2705
45	3044	3029	3018	3007	2999	2992	2985	2980	2974	2968	2962
50	3348	3328	3311	3296	3282	3270	3258	3247	3236	3225	3214
55	3639	3615	3593	3574	3555	3538	3522	3506	3491	3476	3460
60	3917	3889	3864	3841	3818	3797	3777	3758	3738	3719	3699
65	4182	4152	4124	4097	4072	4047	4023	4000	3977	3954	3930
70	4436	4403	4372	4343	4314	4287	4260	4234	4207	4181	4154
75	4677	4642	4609	4577	4546	4516	4487	4458	4429	4399	4370
80	4906	4870	4825	4801	4768	4735	4704	4672	4640	4608	4576
85	5124	5086	5049	5013	4978	4944	4910	4876	4842	4807	4773
90	5330	5291	5252	5215	5178	5141	5105	5069	5032	4996	4958
95	5525	5484	5444	5405	5366	5327	5289	5250	5211	5172	5133
100	5709	5666	5624	5583	5542	5501	5460	5420	5378	5336	5294

<sup>a</sup>  $t \equiv (T - 273.15)/K$ ; internal pressures recorded in bar.

Table 10.2

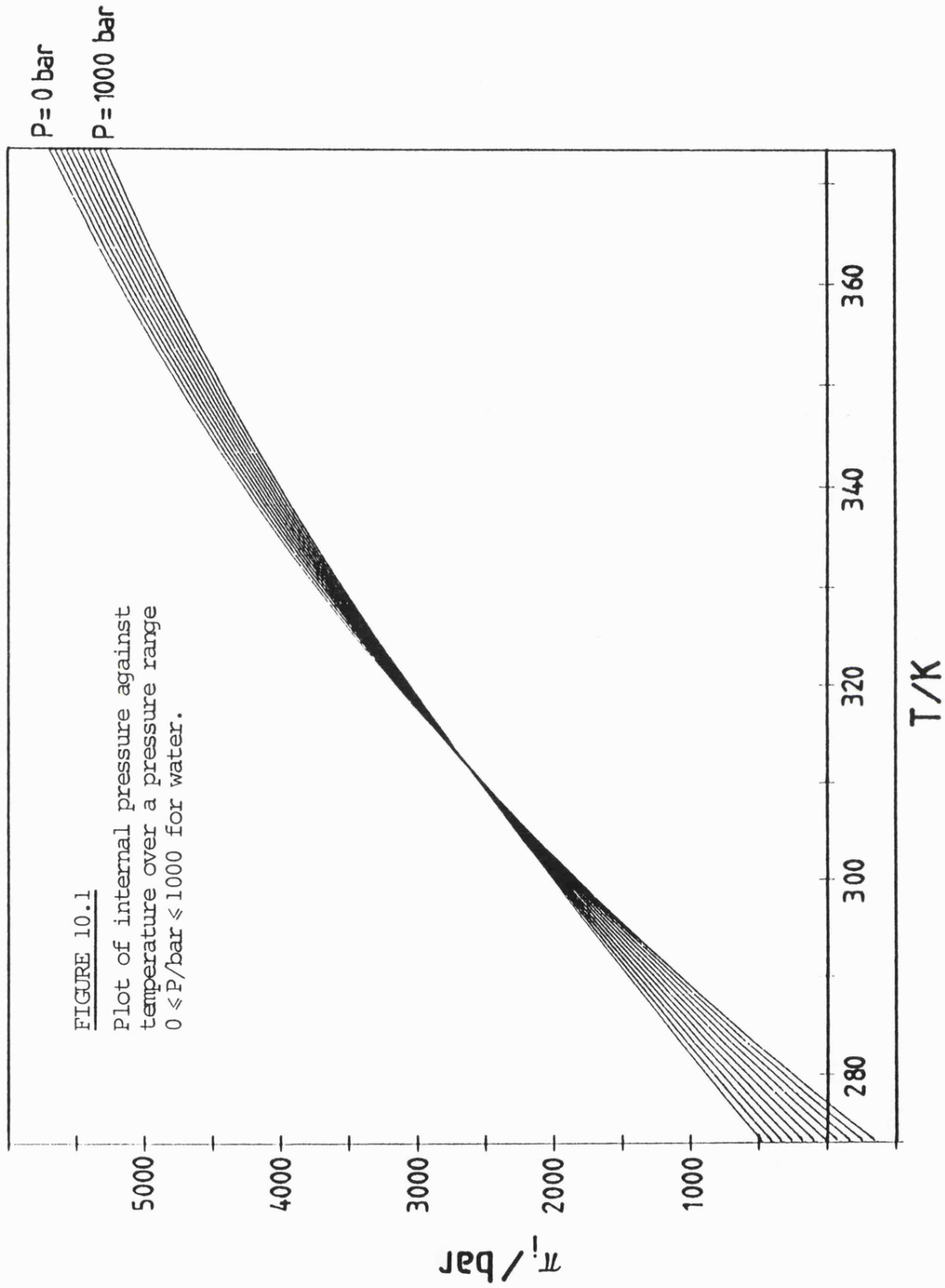
Internal pressures for deuterium oxide over the ranges  $273.15 \leq T/K \leq 373.15$  and  $0 < P/\text{bar} < 1000$  calculated using equation [10.4]<sup>a</sup>

$t$	P/bar										
	0	100	200	300	400	500	600	700	800	900	1000
5	-617	-524	-432	-342	-251	-163	-75	12	97	180	262
10	-115	-43	30	103	177	250	322	394	465	535	604
15	357	411	468	525	583	642	700	759	817	874	931
20	804	843	884	927	972	1017	1063	1110	1156	1202	1247
25	1229	1255	1283	1314	1346	1380	1414	1449	1485	1520	1554
30	1635	1649	1666	1685	1707	1730	1754	1779	1805	1830	1855
35	2023	2027	2034	2044	2055	2069	2084	2100	2116	2133	2149
40	2394	2389	2388	2389	2392	2397	2404	2412	2420	2428	2437
45	2749	2737	2727	2721	2717	2715	2714	2715	2716	2717	2718
50	3087	3069	3054	3041	3030	3022	3015	3009	3003	2998	2993
55	3410	3387	3366	3348	3332	3318	3305	3294	3283	3272	3261
60	3717	3690	3665	3642	3622	3603	3585	3569	3553	3528	3523
65	4009	3978	3950	3924	3899	3877	3855	3835	3815	3796	3777
70	4286	4252	4221	4192	4165	4139	4114	4091	4068	4046	4024
75	4547	4512	4479	4448	4418	4390	4363	4370	4312	4287	4263
80	4794	4758	4723	4691	4660	4630	4601	4573	4547	4521	4495
85	5026	4989	4954	4921	4889	4858	4829	4800	4773	4746	4720
90	5244	5207	5172	5139	5107	5076	5047	5018	4990	4964	4938
95	5447	5412	5378	5345	5314	5284	5255	5227	5200	5174	5149
100	5638	5604	5571	5540	5510	5481	5454	5428	5402	5378	5354

<sup>a</sup>  $t \equiv (T - 273.15)/K$ ; internal pressures recorded in bar.

FIGURE 10.1

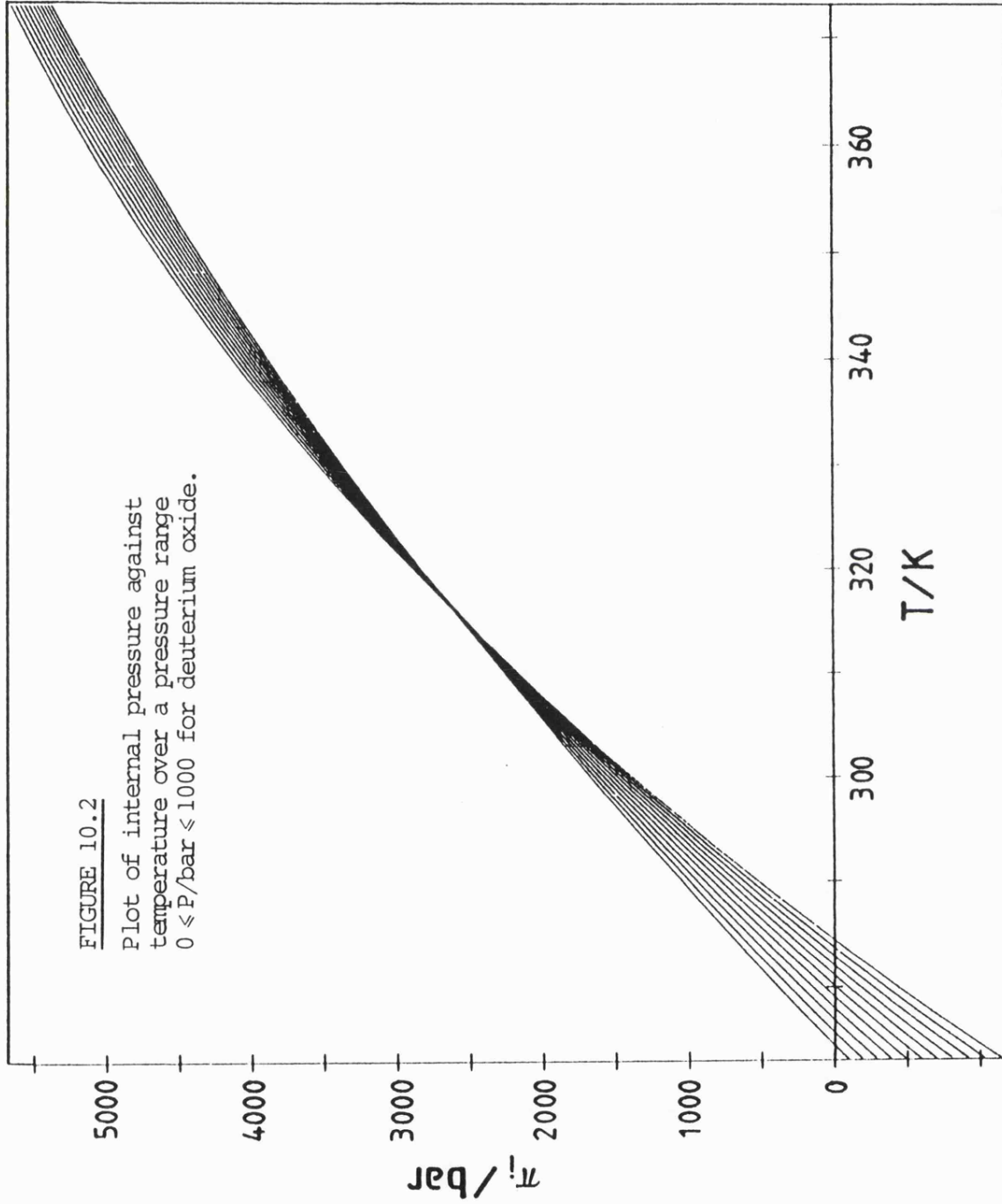
Plot of internal pressure against temperature over a pressure range  $0 \leq P/\text{bar} \leq 1000$  for water.



P = 0 bar  
P = 1000 bar

FIGURE 10.2

Plot of internal pressure against temperature over a pressure range  $0 \leq P/\text{bar} \leq 1000$  for deuterium oxide.



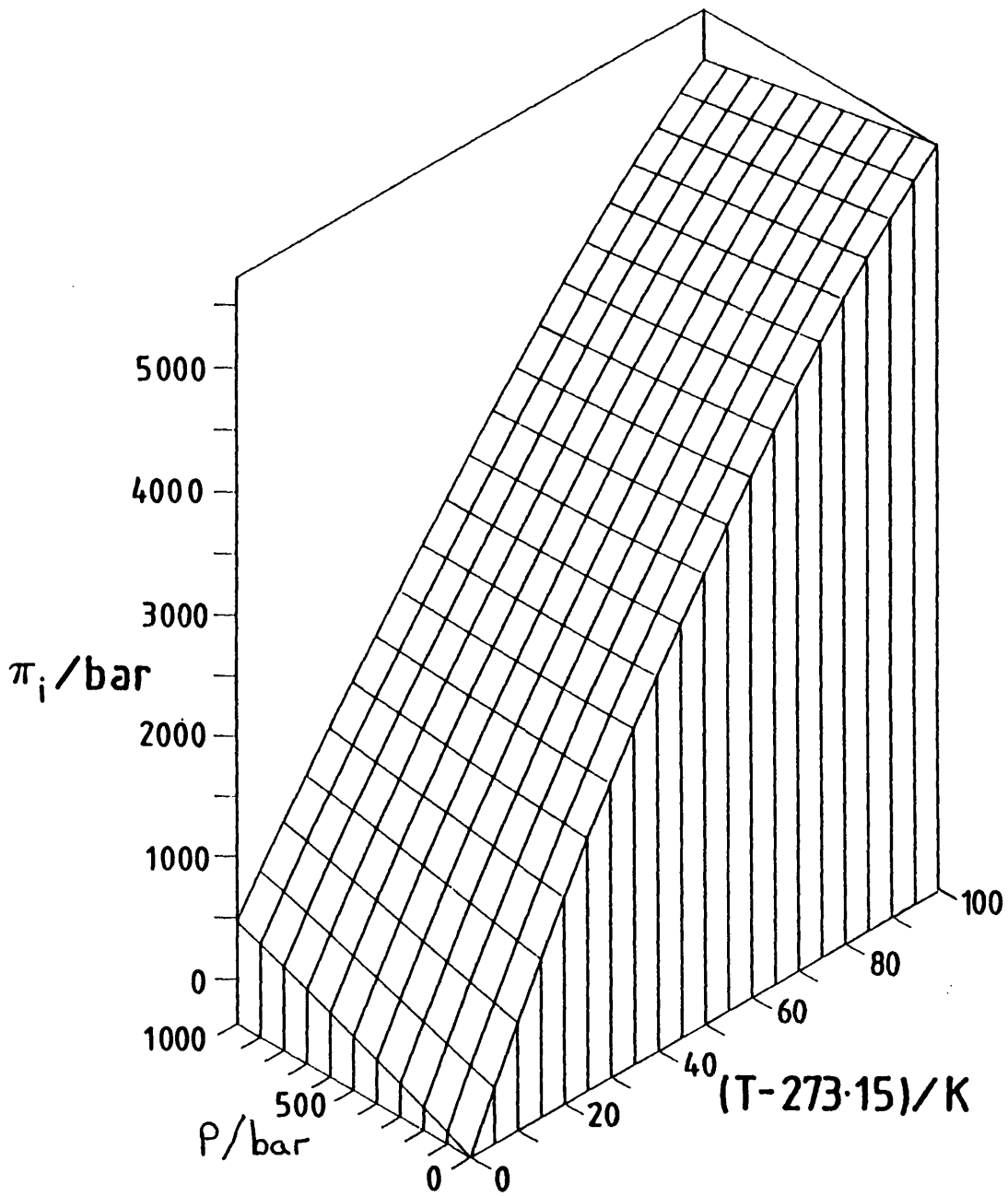


**FIGURE 10.3**

Temperature, pressure surface of the internal pressure for water.

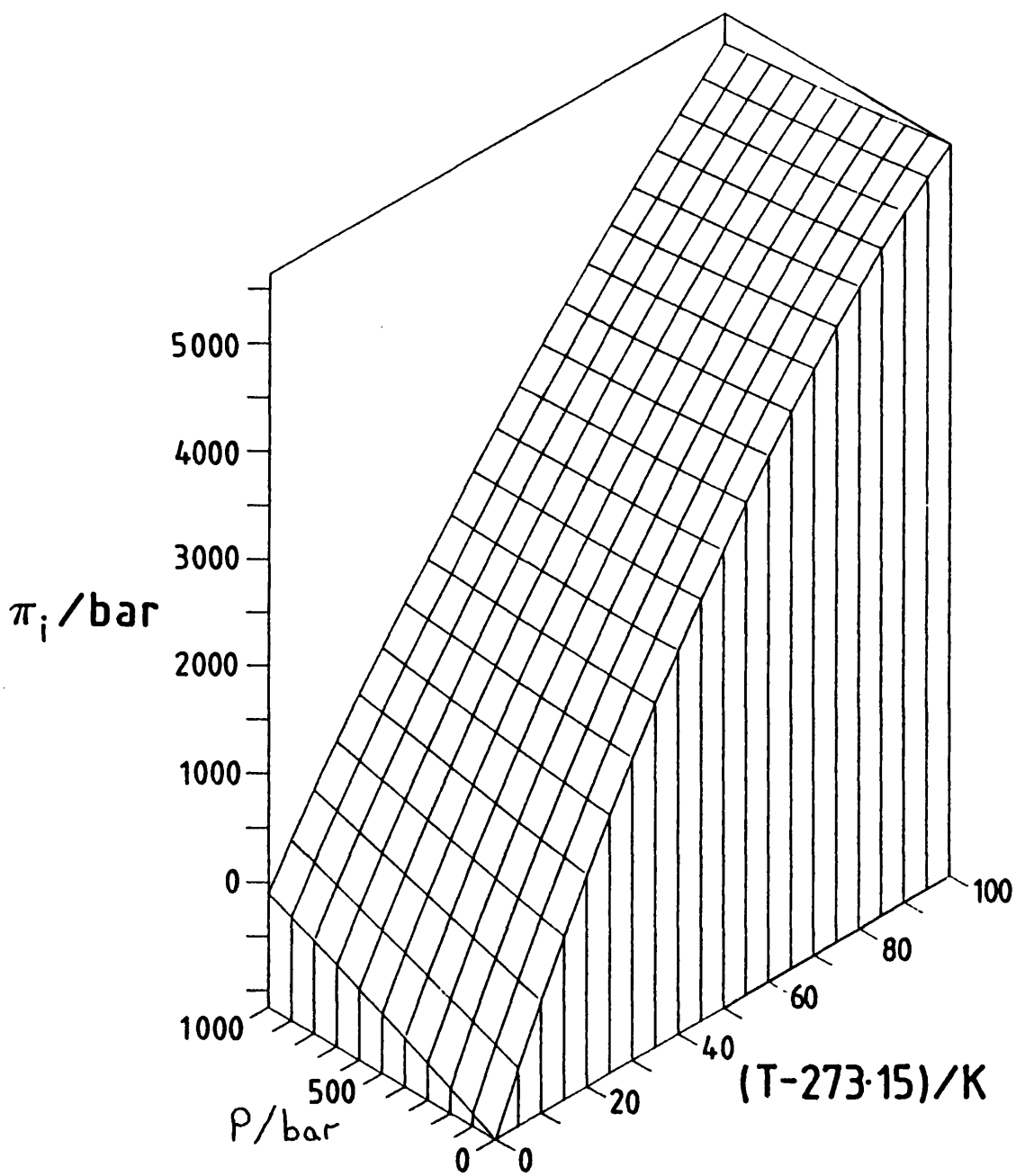


FIGURE 10.4

Temperature, pressure surface of the internal pressure for deuterium oxide.

Table 10.3

Derived parameters and their standard errors for equation [10.20] which predicts the internal pressure of water over the ranges  $273.15 \leq T/K \leq 373.15$  and  $0 \leq P/\text{bar} \leq 1000$ .

Parameter	Estimate	Standard Error
$a_1$	$3.2772 \times 10^3$	$8.514 \times 10^{-1}$
$a_2/K$	$5.4214 \times 10^1$	$2.173 \times 10^{-2}$
$a_3/\text{bar}$	$-1.3345 \times 10^{-1}$	$2.692 \times 10^{-3}$
$a_4/K^2$	$-1.9429 \times 10^{-1}$	$5.822 \times 10^{-4}$
$a_5/K \text{ bar}$	$-1.1732 \times 10^{-2}$	$5.055 \times 10^{-5}$
$a_6/K^2 \text{ bar}$	$1.4494 \times 10^{-4}$	$1.841 \times 10^{-6}$
$a_7/K \text{ bar}^2$	$1.3946 \times 10^{-6}$	$1.472 \times 10^{-7}$

Table 10.4

Derived parameters and their standard errors for equation [10.20] which predicts the internal pressure of deuterium oxide over the ranges  $273.15 \leq T/K \leq 373.15$  and  $0 \leq P/\text{bar} \leq 1000$ .

Parameter	Estimate	Standard Error
$a_1$	$3.0317 \times 10^3$	$9.408 \times 10^{-1}$
$a_2/K$	$5.9693 \times 10^1$	$4.461 \times 10^{-2}$
$a_3/\text{bar}$	$-9.4450 \times 10^{-2}$	$2.435 \times 10^{-3}$
$a_4/K^2$	$-2.3523 \times 10^{-1}$	$5.489 \times 10^{-4}$
$a_5/K \text{ bar}$	$-1.2970 \times 10^{-2}$	$4.572 \times 10^{-5}$
$a_6/K^2 \text{ bar}$	$1.9410 \times 10^{-4}$	$1.665 \times 10^{-6}$
$a_7/K \text{ bar}^2$	$1.6969 \times 10^{-6}$	$1.464 \times 10^{-7}$
$a_8/\text{bar}^2$	$2.8231 \times 10^{-5}$	$5.360 \times 10^{-6}$
$a_9/K^3$	$4.3171 \times 10^{-4}$	$2.175 \times 10^{-5}$

the data of Fine and Millero<sup>8,9</sup> to produce plots of the residuals at each temperature and pressure for each system (Figures 10.5 and 10.6).

A maximum error of  $\pm 35$  bar was reported on equation [10.20] for both water and deuterium oxide systems.

The temperature of maximum density decreases in an almost linear fashion with increase in pressure; Figure 10.7. The derived parameters to equation [10.21] with their standard errors are presented in Table 10.5. A similar situation is observed for the dependence of pressure on temperatures corresponding to the condition that  $\Pi_i = 0$ ; Figure 10.8. A Table of the linear least squares fitted parameters to equation [10.21] together with their standard errors are included as Table 10.6.

### 10.5 Discussion

For a closed single phase system the First and Second Laws of Thermodynamics describe the change in thermodynamic energy,  $dU$ , by equation [10.23].

$$dU = TdS - pdV - Ad\xi \quad [10.23]$$

$TdS$  describes the change in entropy,  $dS$ , at temperature  $T$ ;  $pdV$  describes the change in volume,  $dV$ , at pressure  $p$  and  $Ad\xi$  is the product of the affinity for spontaneous change,  $A$ , and the change in composition/organisation,  $d\xi$ .

In most cases interest is restricted to closed systems at fixed temperatures and pressures in a state of thermodynamic equilibrium. A corresponding minimum in the Gibbs function,  $G$ ; the latter is defined by equation

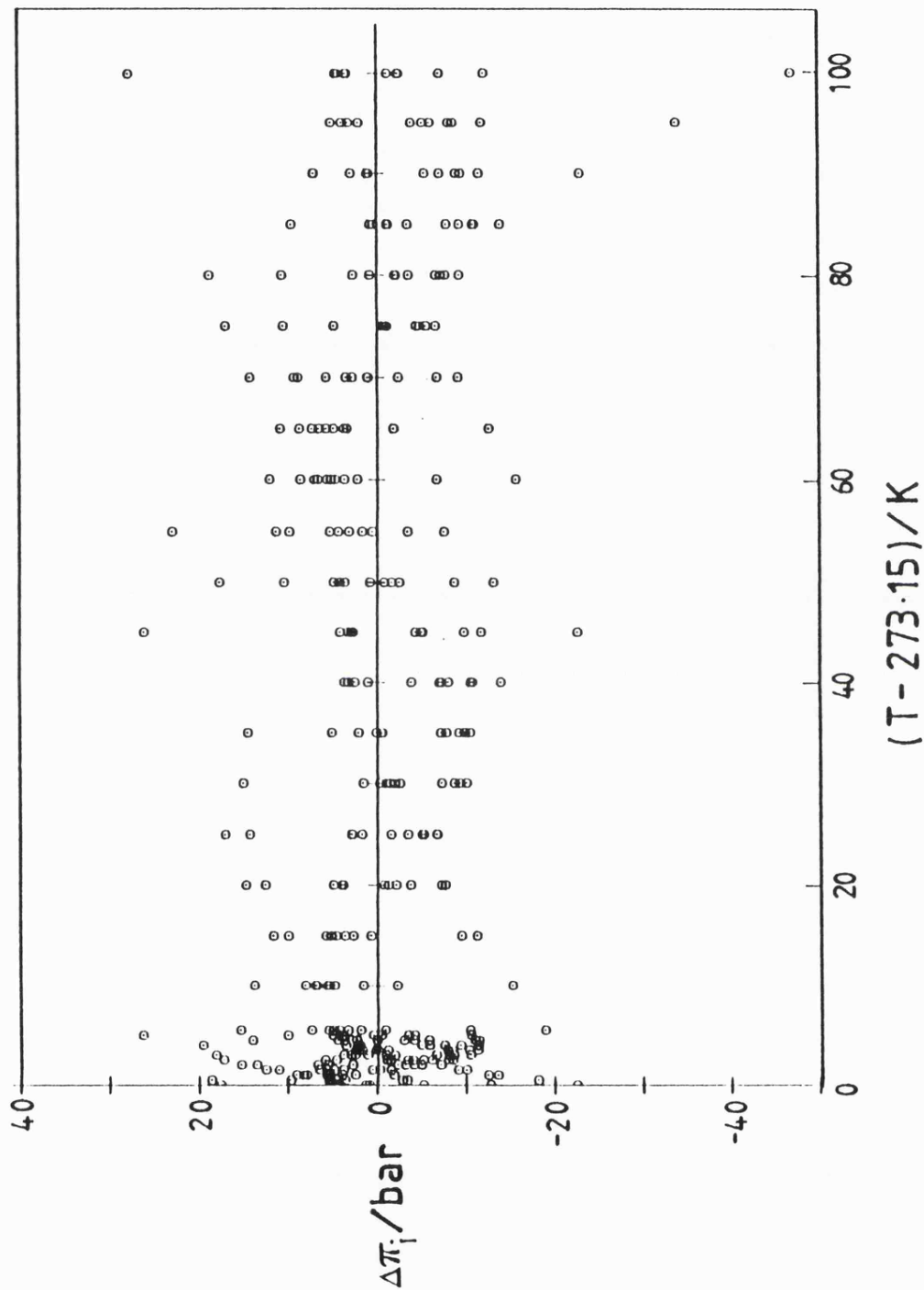


FIGURE 10.5

$\pi_1(\text{obs}) - \pi_1(\text{calc})$  against temperature over the range of pressures  $0 \leq P/\text{bar} \leq 1000$  for water.

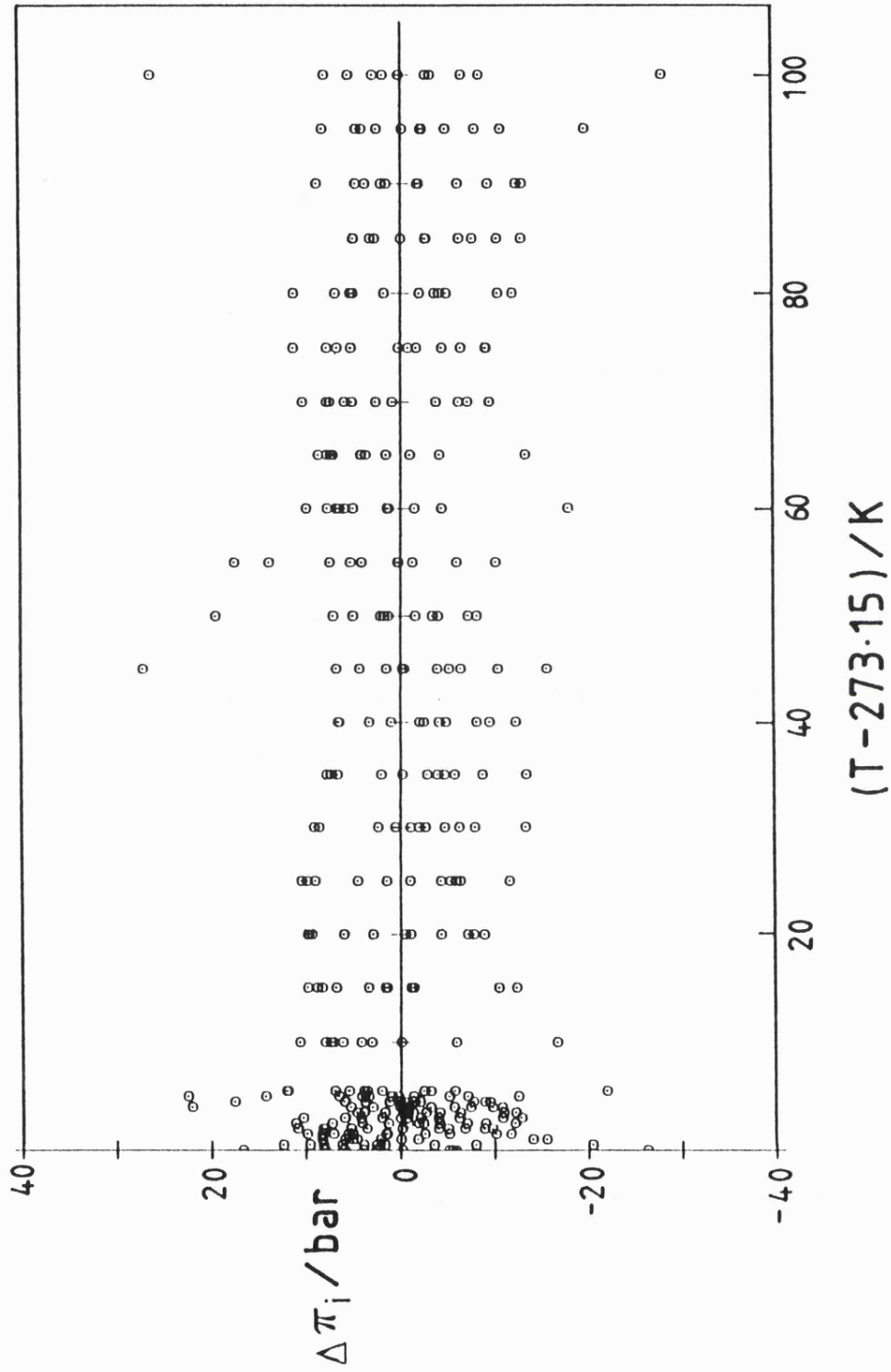


FIGURE 10.6

$\pi_i(\text{obs}) - \pi_i(\text{calc})$  against temperature over the range of pressures  $0 \leq P/\text{bar} \leq 1000$  for deuterium oxide.

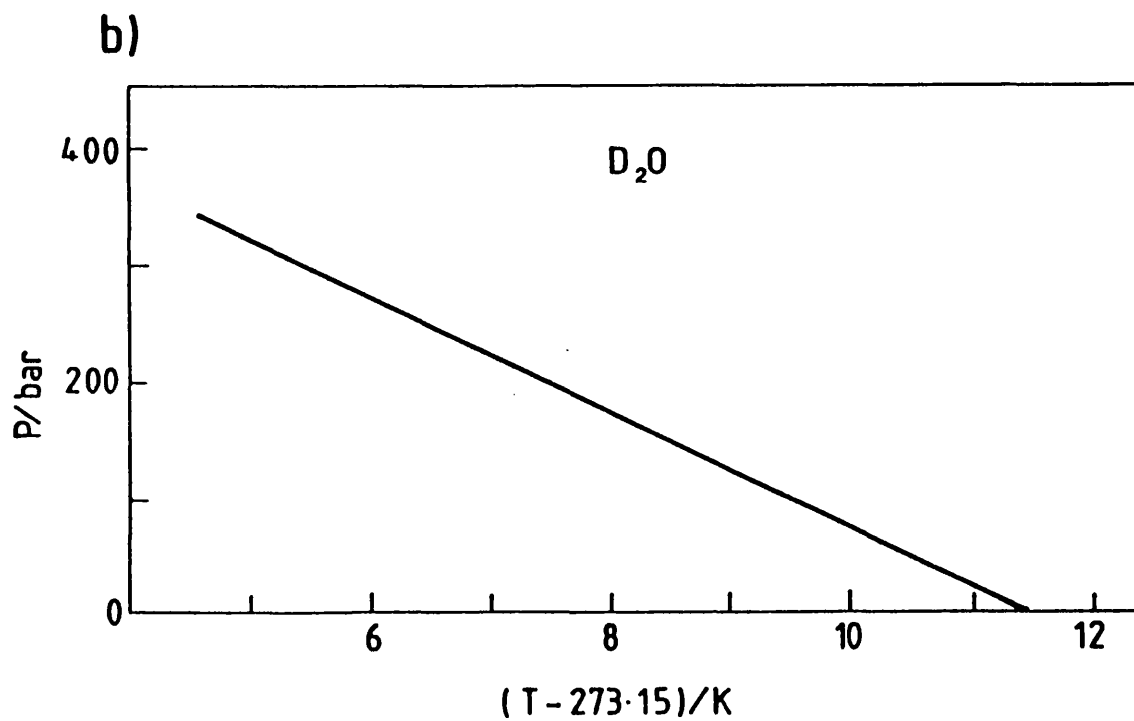
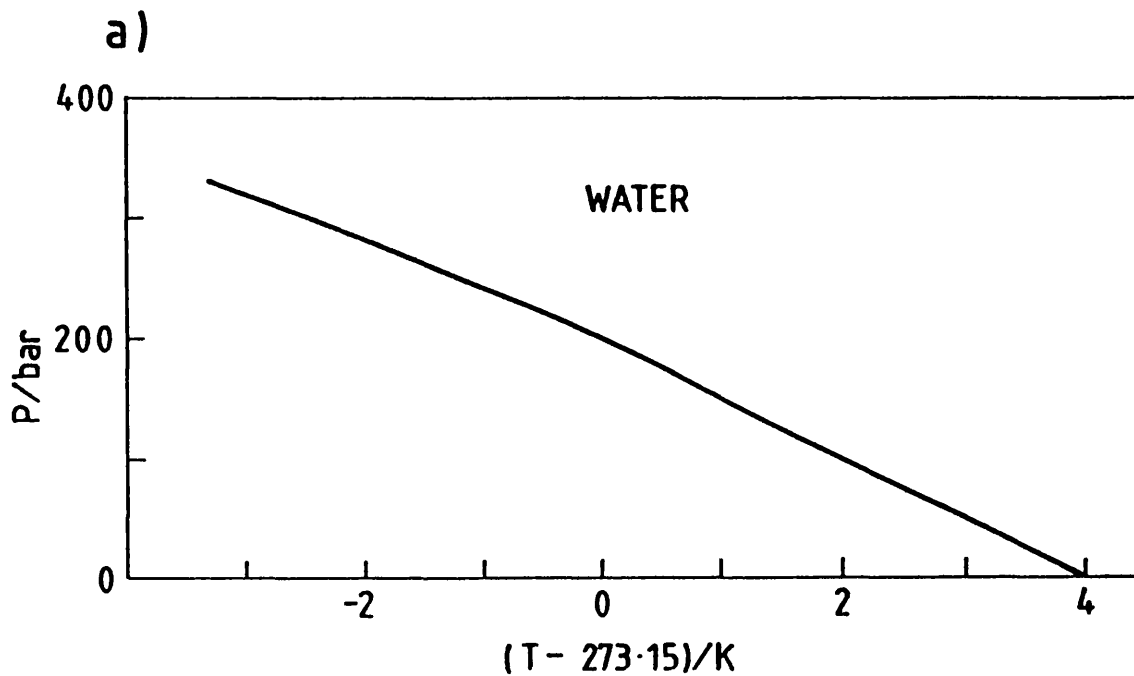


FIGURE 10.7

Temperature of maximum density, calculated using equation [10.21] against temperature for (a) water and (b) deuterium oxide.

Table 10.5

Derived parameters and their standard errors for equation [10.21] which predicts the temperature of maximum density with change in pressure for water and deuterium oxide.

Parameter	water	deuterium oxide
t.m.d(P=0)/celsius	3.9852 ± 0.0012	11.4161 ± 0.0323
10 <sup>2</sup> a <sub>1</sub> /bar	-1.9964 ± 0.0018	-1.9543 ± 0.0322
10 <sup>6</sup> a <sub>2</sub> /bar <sup>2</sup>	-5.5560 ± 0.0528	-1.9843 ± 0.7315
Standard error on t.m.d/celsius	0.0014	0.0340

Table 10.6

Derived parameters and their standard errors for equation [10.22] which predicts the temperature at which  $\Pi_i=0$  with change in pressure for both water and deuterium oxide.

Parameter	water	deuterium oxide
a <sub>0</sub> /K	277.1337 ± 0.0002	284.3354 ± 0.0002
10 <sup>2</sup> a <sub>1</sub> /bar	-1.9882 ± 0.0007	-1.7630 ± 0.0005
10 <sup>6</sup> a <sub>2</sub> /bar <sup>2</sup>	-6.2307 ± 0.0514	-5.8061 ± 0.0312
10 <sup>9</sup> a <sub>3</sub> /bar <sup>3</sup>	1.3899 ± 0.1049	9.4678 ± 0.0518
10 <sup>4</sup> Standard error on T( $\pi_i=0$ )/K	2.4701	2.7018

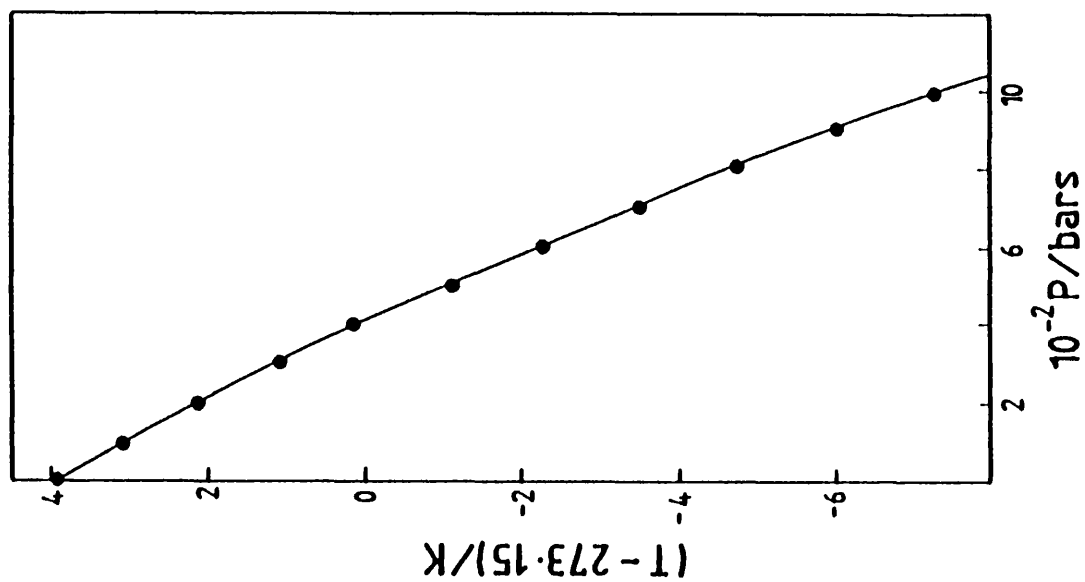
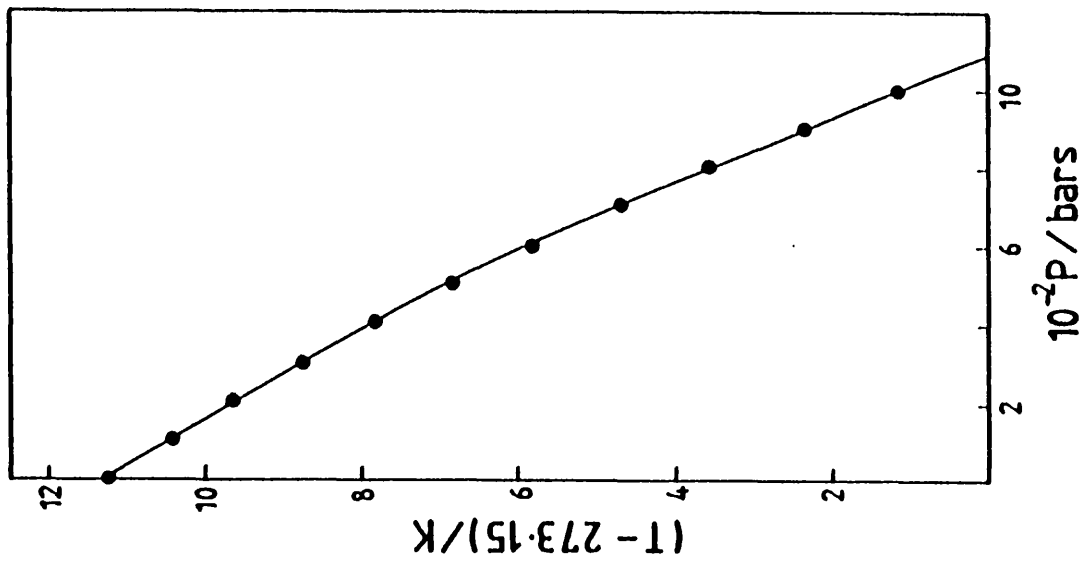


**FIGURE 10.8**  
 Temperature against pressure plot corresponding to the condition that internal pressure is equal to zero for (a) water and (b) deuterium oxide.

[10.4].

$$G = U + pV - T.S \quad [10.24]$$

At equilibrium the affinity for spontaneous change,  $A$ , and the change of composition/organisation,  $d\xi$ , are zero.

In displacing a given system from a state of equilibrium (I) to a nearby state (II) there are two limiting pathways which need consideration. (i) The affinity for spontaneous change remains constant at zero and the change in composition/organisation of the system is characterised by  $\xi^{eq(I)} \rightarrow \xi^{eq(II)}$  where  $A$  is zero in both states i.e. constant  $A$ ; an equilibrium transformation. (ii) There is no change in composition / organisation and the affinity for spontaneous change is displaced  $A^{eq(I)} \rightarrow A(II)$  i.e. an instantaneous/frozen process at fixed  $\xi$ , where  $d\xi = 0$ .

This point establishes two separate definitions which describe the internal pressure in such situations;

$$(i) \Pi_i(A=0) \quad (\partial U / \partial V)_{T, A=0} = T(\alpha(A=0) / \kappa_T(A=0)) - p \quad [10.25]$$

and

$$(ii) \Pi_i(\xi) \quad (\partial U / \partial V)_{T, \xi} = T(\alpha(\xi) / \kappa_T(\xi)) - p \quad [10.26]$$

Equation [10.25] defines the equilibrium internal pressure using the equilibrium expansibility and equilibrium isothermal compressibility. The latter quantities are those reported by Fine and Millero<sup>8,9</sup> and used as the basis of the preceding analysis. Equation [10.26] however, defines the instantaneous/frozen internal

pressure calculated from the corresponding instantaneous/frozen expansibilities and isothermal compressibilities. Unlike  $\alpha(A=0)$  and  $\kappa_T(A=0)$ ,  $\alpha(\xi)$  and  $\kappa_T(\xi)$  are not readily available. However  $\kappa_T(\xi)$  can be obtained from ultrasonic data through the closely related property,  $\kappa_S(\xi)$  the instantaneous isentropic compressibility. The latter is identified by  $\lim_{\nu \rightarrow \infty} \kappa_S$  where  $\nu$  is the frequency of the sound wave. Endo<sup>15</sup> estimates  $\kappa_T(\xi)$  at ten degree intervals over the range  $273.15 \leq T/K \leq 373.15$  at ambient pressure together with estimates of  $\alpha(\xi)$  for both water and deuterium oxide ( $\alpha(\xi)[H_2O] = 1.1822 \times 10^{-3} K^{-1}$  and  $\alpha(\xi)[D_2O] = 1.03244 \times 10^{-3} K^{-1}$ ). Using these values and equation [10.26],  $\Pi_i(\xi)$  is calculated, and the resulting trend with temperature, at ambient  $p$ , is included as Figure 10.9 together with plots of  $\Pi_i(A=0)$  over the same range. A third quantity, the relaxational internal pressure,  $\Pi_i(\text{relax})$ , is defined by equation [10.27].

$$\Pi_i(\text{relax}) = \Pi_i(A=0) - \Pi_i(\xi) \quad [10.27]$$

$\Pi_i(\text{relax})$  can be regarded as being the configurational/relaxational component of the equilibrium internal pressure. For both systems  $\Pi_i(A=0)$  approaches  $\Pi_i(\xi)$  with increase in temperature i.e. the relaxational component of  $\Pi_i(A=0)$  increases with increase in temperature. This points to the fact that structural changes, most likely due to H-bonding, occur in the two systems which can be understood if  $\Pi_i(\xi)$  is regarded as representing the attractive component of H-bonding and  $\Pi_i(\text{relax})$  as representing the

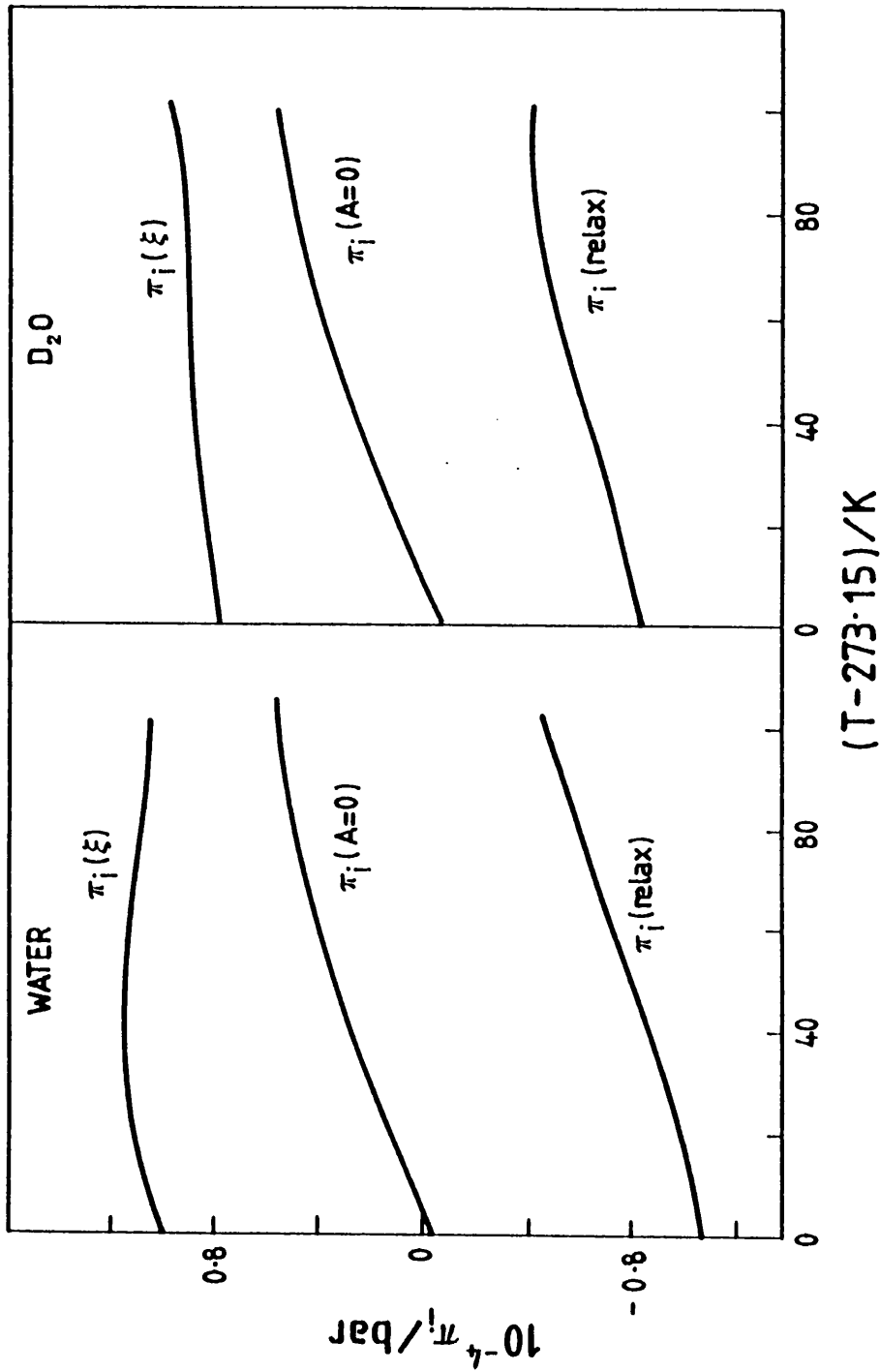


**FIGURE 10.9**

Dependence of  $\pi_i(A=0)$ ,  $\pi_i(\xi)$  and  $\pi_i(\text{relax})$  on temperature at ambient pressure for water and deuterium oxide.

repulsive part of H-bonding.

Water at low temperatures has most of its hydrogen bonding framework intact. From this it could be argued that in this situation the hydrogen bonds are repulsive in nature i.e. when a hydrogen bond is formed between two water molecules their centres of mass are pushed apart. In this situation  $\Pi_i(\text{relax})$  dominates  $\Pi_i(A=0)$  leading to an overall negative equilibrium internal pressure. However as the temperature is increased, so there is a decrease in the number of hydrogen bonds i.e.  $\Pi_i(\text{relax})$  becomes more positive as the attractive component of H-bonding begins to dominate - giving increasingly positive equilibrium internal pressures.

This explanation is in agreement with the Lumry two-state model of water<sup>2</sup> (see Chapter 12 Section 12.2). At lower temperatures the short-bonded form with its stiff, repulsive bonds is most abundant. With increase in temperature, increases in the degree of bending, librational and rotational freedoms of the H-bonds, causes more H-bond breaking and a subsequent domination of the long-bond form.

This explanation also helps to explain the trends of  $\Pi_i(A=0)$  in Figures 10.1 and 10.2 respectively.

The trend of TMD moving to lower temperatures with an increase in pressure is also consistent with the Lumry model. The two-state equilibrium between the short-bonded and long-bonded structures moves over to favour the long-bonded, low volume, high density state in a similar manner to the effect of an increase in temperature at fixed pressure, as described earlier. Confirmation of this

conclusion comes from the fact that there is an increase in nearest-neighbour O-O co-ordination number with an increase in pressure<sup>16</sup>, as determined by X-ray diffraction methods.

From a kinetics point of view this work has pointed towards using  $\Pi_i$  isobars as a reference state for reactions in aqueous solutions. Usually reactions in aqueous solution are followed to obtain rate constants as a function of temperature and pressure. A criticism of this approach is that water at temperature  $T_1$ , (at constant pressure), is a different media from water at temperature  $T_2$ , (at constant pressure), merely from the extent of hydrogen bonding present in each system. As examined in this Chapter an interesting  $\Pi_i$  isobar to use as a reference state would be that at which  $\Pi_i(A=0)$  is equal to zero. This then describes states in which the external pressure,  $p$ , is equal to the equilibrium thermal pressure,  $T(\partial P/\partial T)_{V,A=0}$  at constant volume and affinity equal to zero. There is however, at present a distinct lack of kinetic data along the  $\Pi_i(A=0)$  isotherm.

Preliminary investigations into the possibility of using  $\Pi_i$  as a reference state for aqueous solutions are promising, as demonstrated by Figure 10.10 which shows a plot of  $\ln k_{obs}$  against  $\Pi_i(A=0)$  for the neutral hydrolysis of phenyldichloroacetate. The relationship is linear and demonstrates that the hydrolysis reaction is a function of the organisation of the solvent structure.

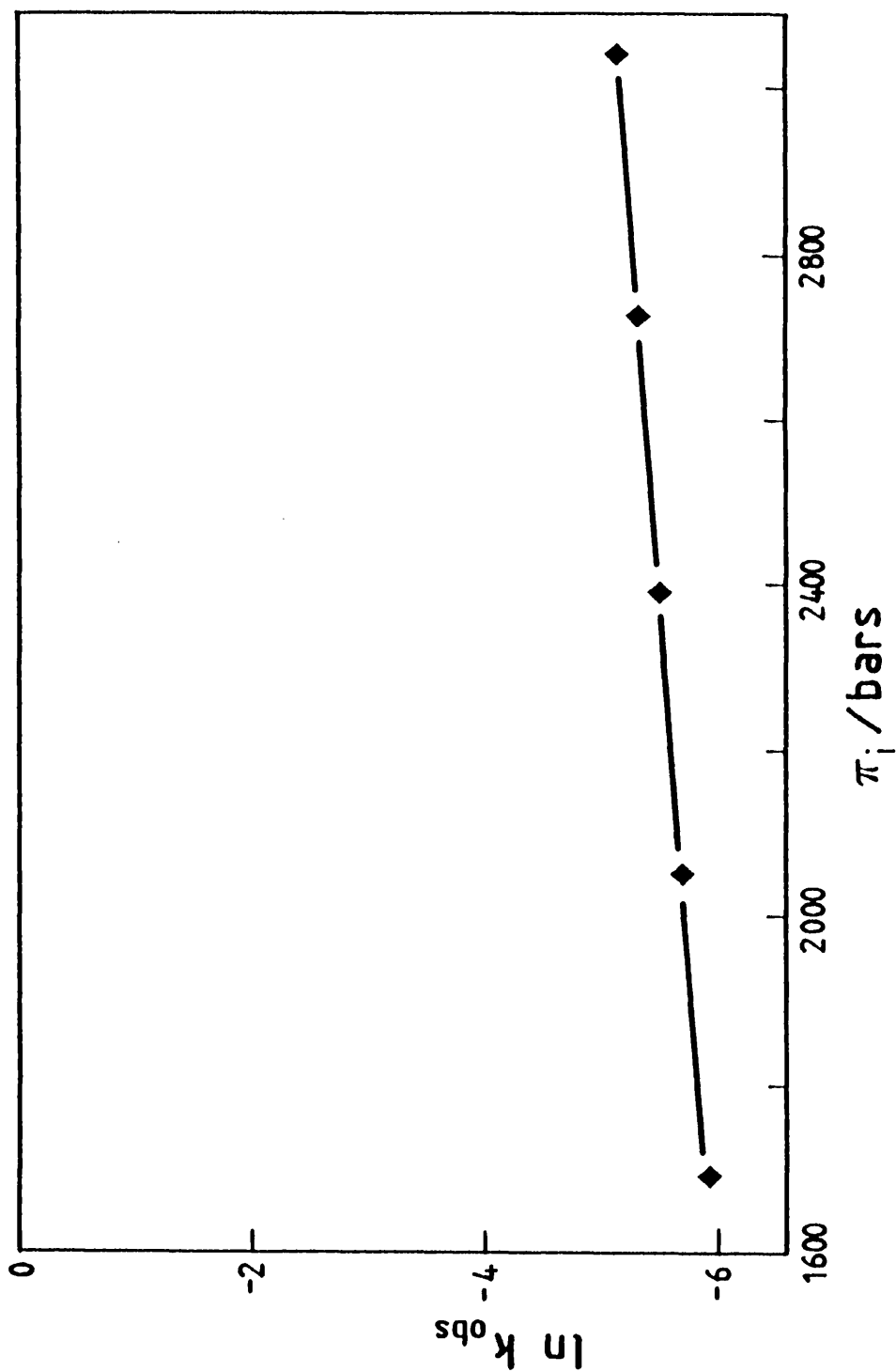


**FIGURE 10.10**  
 Dependence of rate constant on the internal pressure of water for the neutral hydrolysis of para-methoxyphenyldichloroacetate at 298 K and ambient pressure.

## References - Chapter 10

- (1) J.H.Hildebrand, R.L.Scott, "Solubility of Non-Electrolytes", Reinhold, New York, (1950)
- (2) R.Lumry, E.Battistel and C.Jolicoeur, Faraday Symp.Chem.Soc., 17, 93, (1982)
- (3) J.V.Leyendekker, J.Phys.Chem., 87, 3327, (1983)
- (4) J.V.Leyendekker, J.Chem.Soc., Faraday Trans. I, 82, 1663, (1986)
- (5) D.D.Macdonald, J.B.Hyne, F.L.Swinton, J.Am.Chem.Soc., 92, 6355, (1970)
- (6) M.J.Blandamer, J.Burgess, J.B.F.N.Engberts, Chem.Soc.Revs., 14, 237, (1985)
- (7) H.S.Frank *private communication*
- (8) R.A.Fine, F.J.Millero, J.Chem.Phys., 59, 5529, (1973)
- (9) R.A.Fine, F.J.Millero, J.Chem.Phys., 63, 89, (1975)
- (10) G.S.Kell, J.Chem.Eng.Dat., 12, 66, (1967)
- (11) D.Z.Arbritton, A.L.Schmeltekoptf, "Modern Spectroscopy, Modern Research II", Ed.K.N.Rao, Academic Press, New York, (1976)
- (12) J.V.Leyendekker, "The Thermodynamics of Seawater", Part 1. M.Dekker, New York, (1976)
- (13) G.S.Kell, "Water a Comprehensive Treatise", Ed. F.Franks, Vol. 1, New York, (1973)
- (14) C.J.Brookes, I.G.Betteley, S.M.Loxston, "Fundamentals of Mathematics and Statistics", J. Wiley, Chichester, (1979)
- (15) H.Endo, J.Chem.Phys., 76, 4578, (1982)
- (16) G.A.Gaballa, G.W.Neilson, Mol.Phys., 50, 97, (1986)



# CHAPTER 11

Excess Pressures for Aqueous Solutions

## 11.1 Introduction

The task of accounting for trends in kinetic parameters for reactions in aqueous solution in the presence of electrolytes<sup>1,2</sup> provided the stimulus for work presented in this Chapter. Many authors comment on the intense pressures operating on solvents in salt solutions, usually aqueous solutions. However the basis for this statement is not always clear and hence the aim of this study was to examine the definition of this 'excess pressure'. For the most part, Gibson's<sup>3</sup> concept of an excess pressure, discussed by Harned and Owen<sup>4</sup>, is applied in the analysis of the properties of solutions containing salts. The definition used by Gibson is examined below, together with definitions of excess pressures,  $p^E$ , used by Leyendekker<sup>5,6</sup>.

Originally an excess pressure was related to solvent-solute interactions in solution. Tamman (cf. refs. 3 - 6) suggested that water in an aqueous salt solution is subject to an additional pressure,  $p^E$ , dependent on solute type and concentration. However both the sign and magnitude of an excess pressure are shown to depend on the definition of reference volumes of the solvent and the solute. At one extreme  $p^E$  characterises solute-solute interactions whilst at the other  $p^E$  takes account of solvent-solute interactions. Therefore the main aim of the work described here was to explore different methods for calculating excess pressures. These pressures express in different ways the impact of solute-solvent and solute-solute interactions in solution.

In developing this subject it is useful to examine volumetric properties of solutions and to define a

volumetric property, identified by the symbol 'O' and called the occupied volume.

### 11.2.1 The Occupied Volume, O

The underlying hypothesis can be summarised in the following terms. Within a given solution each mole of solute occupies a volume  $O_j(\text{sln};T;p)$  and each mole of solvent occupies a volume  $O_1(\text{sln};T;p)$ . The occupied volume for the pure liquid solvent is assumed equal to the molar volume of the pure liquid solvent.

$$O_1(l;T;p) = V_1^*(l;T;p) \quad [11.1]$$

In a solution molality  $m_j$ ,  $\lim(m_j \rightarrow 0) O_1(\text{sln};T;p) = V_1^*(l;T;p)$ . One aim of this Chapter is to show that a calculated excess pressure depends strongly on the definition adopted for occupied volumes.

### 11.2.2 Volumetric Properties

In terms of a thermodynamic description, the volume of a solution prepared using 1 kg of solvent and  $m_j$  moles of solute-j is given by equation [11.2].

$$V(\text{sln};T;p;w_1/\text{kg}=1) = (1/M_1)V_1(\text{sln};T;p) + m_j V_j(\text{sln};T;p) \quad [11.2]$$

$M_1$  is the molar mass of the solvent;  $V_1$  is the partial molar volume of the solvent and  $V_j$  is the partial molar volume of the solute. The latter two properties are defined by the partial derivatives;

$$V_1(\text{sln}; T; p) = [\partial V(\text{sln}; T; p) / \partial n_1]_{n_j; T; p} \quad [11.3]$$

$$V_j(\text{sln}; T; p) = [\partial V(\text{sln}; T; p) / \partial n_j]_{n_1; T; p} \quad [11.4]$$

$V_1(\text{sln}; T; p)$  is the differential change in the volume of the system when  $dn_1$  moles of solvent are added and  $V_j(\text{sln}; T; p)$  is the change in the volume of the system when  $dn_j$  moles of solute are added. The following definitions are important to equation [11.2].

$$\begin{aligned} \text{limit}(m_j \rightarrow 0) V_j(\text{sln}; T; p) &= V_j^\infty(\text{sln}; T; p) \\ \text{and} \quad \text{limit}(m_j \rightarrow 0) V_1(\text{sln}; T; p) &= V_1^*(l; T; p) \end{aligned} \quad [11.5]$$

Hence for an ideal solution;

$$V(\text{sln}; T; p; id; w_1/kg=1) = (1/M_1)V_1^*(l; T; p) + m_j V_j^\infty(\text{sln}; T; p) \quad [11.6]$$

$V_1^*(l; T; p)$  and  $V_j^\infty(\text{sln}; T; p)$  are reference volumetric properties for the solvent 1 and solute-j respectively. The quantities  $V_1(\text{sln}; T; p)$ ,  $V_j(\text{sln}; T; p)$ ,  $V_1^*(l; T; p)$  and  $V_j^\infty(\text{sln}; T; p)$  are unambiguous and properly defined thermodynamic variables.

### 11.2.3 Apparent Molar Volumes

The apparent molar volume of solute-j in a solution containing 1 kg of solvent,  $\phi(v_j)$ , is defined by equation [11.7].

$$V(\text{sln}; T; p; w_1/kg=1) = (1/M_1)V_1^*(l; T; p) + m_j \phi(v_j) \quad [11.7]$$

where by definition  $\text{limit}(m_j \rightarrow 0) \phi(v_j) = \phi(v_j)^\infty = V_j^\infty(\text{sln}; T; p)$ . In equation [11.7] the non-ideal properties

of the solution are loaded onto the solute. If the solution is ideal then  $\phi(v_j)$  is replaced by  $\phi(v_j)^\infty$  or  $V_j^\infty$ . In other words the non-ideal properties of the system are described by the difference  $\phi(v_j) - \phi(v_j)^\infty$ . Alternatively an equation can be written to load the non-ideality of the solution onto the solvent using  $\phi(v_1)$ , the apparent molar volume of the solvent.

$$V(\text{sln}; T; p; w_1/\text{kg}=1) = (1/M_1)\phi(v_1) + m_j V_j^\infty(\text{sln}; T; p) \quad [11.8]$$

The partial molar volume of solute-j and the apparent molar volume of the solute are linked through equation [11.9]. (This is obtained as the differential of equation [11.7] with respect to  $m_j$ )

$$V_j(\text{sln}; T; p) = \phi(v_j) + m_j [\partial \phi(v_j) / \partial m_j]_{T; p} \quad [11.9]$$

#### 11.2.4 Calculation of an Excess Pressure, $p^E$ , Using the Tait Equation.

A given solution contains solvent and solute, molality  $m_j$ . As a starting hypothesis, it is assumed that one mole of solvent in this solution occupies a volume  $O_1(\text{sln}; T; p)$ . The question of how  $O_1(\text{sln}; T; p)$  is defined is left for the moment. It is also assumed that for a given solution  $O_1(\text{sln}; T; p)$  differs from the molar volume  $V_1^*(\text{sln}; T; p)$ . Therefore the excess pressure is calculated from the pressure  $(p+p^E)$  at which the molar volume of pure solvent,  $V_1^*(1; T; p+p^E)$  equals  $O_1(\text{sln}; T; p)$ . Hence an equation of state is required for the solvent - and this role is generally filled by the logarithmic form<sup>7</sup> of the Tait

equation. In the case of water and aqueous solutions;

$$-\{v_1^*(l;T;\pi)-v_1^*(l;T;p)\} = d_1 \ln[(d_2+\pi)/(d_2+p)] \quad [11.10]$$

This equation is satisfactory for water at 298 K over the pressure range 1 to 1001 bar.

In the definitions of excess pressure explored later in this Chapter the Tait equation is used in a form which includes the occupied volume of the solvent in a given solution.

$$-\{O_1(sln;T;p)-v_1^*(l;T;p)\} = d_1 \ln[(d_2+p+p^E)/(d_2+p)] \quad [11.11]$$

The parameters  $d_1$  and  $d_2$  were calculated using Fine and Millero's<sup>8</sup> molar volume data for water over the range  $1 \leq p/\text{bar} \leq 1001$  at 298.15 K. The calculation was based on equation [11.10] using a FORTRAN program written by Dr.M.J.Blandamer. The program used a Gauss-Newton minimisation technique to obtain estimates of  $d_1$  and  $d_2$ . ( $2.46696 \times 10^{-6} \text{ m}^3 \text{ mol}^{-1}$  and  $2.99339 \times 10^3 \text{ bar}$  respectively) These estimates are close to those reported by Leyendekker<sup>6</sup>.

### 11.2.5 Solutions

Combination of equations [11.2] and [11.7] yields equation [11.12].

$$-[V_1(sln;T;p)-v_1^*(l;T;p)] = m_j M_1 [V_j(sln;T;p) - \phi(v_j)] \quad [11.12]$$

This interesting equation links the properties of solvent

and solute in a given solution, molality  $m_j$ . In the limit ( $m_j \rightarrow 0$ ) both sides of equation [11.12] tend to zero. For an ideal solution  $V_1(\text{sln}; T; p) = V_1^*(l; T; p)$ . If the occupied volume for the solvent is the same as the molar volume, the Tait equation (equation [11.10]) predicts zero excess pressure for an ideal solution. This conclusion is inconsistent with the concept of  $p^E$  discussed by Gibson and hence other methods of defining volumetric properties of both solute and solvent are required.

Turning to equations [11.2], [11.7] and [11.8] it is interesting to note that  $V(\text{sln}; T; p; w_1/\text{kg}=1)$  has been defined in three separate ways, each description taking account of the solute and solvent in different ways. Stepping outside the terms of reference of classical thermodynamics the situation can be summarised in the form shown in equation [11.13].

$$V(\text{sln}; T; p; w_1/\text{kg}=1) = (1/M_1)V_1(?) + m_j V_j(?) \quad [11.13]$$

Equation [11.13] does not describe how the volumetric properties of the solvent or solute are defined. Granted that this representation is possible then an excess pressure can be calculated from the equation;

$$-[V_1(?) - V_1^*(?)] = d_1 \ln[(d_2 + p + p^E)/(d_2 + p)] \quad [11.14]$$

Clearly the size and magnitude of  $p^E$  must depend on the particular definition adopted for  $V_j(?)$ .

### 11.2.6 Addition of Solute to Solvent

The limiting partial molar volume,  $V_j^\infty$ , is independent of solute molality,  $m_j$ , solution and hence remains constant as more solute is added to 1 kg of solvent. However, consider the situation in which a solute-j is added gradually to 1 kg of solvent. In nearly all instances the molar volume of the solvent is likely to change. The extent of this change is directly linked to the intensity of solute-solvent interactions within the system. The change in volume can be understood in terms of incorporation of solvent into solute cospheres<sup>9</sup>. Hence as the molality of solute increases the occupied volume of the solvent changes and so referring back to the Tait equation the excess pressure  $p^E$  reflects the solvation characteristics of the solute.

For an ideal solution the volume occupied by the solvent is described by the symbol  $O_1(\text{sln};T;p;id)$ . Hence for an ideal solution with a given  $V(\text{sln};T;p;id;w_1/kg=1)$  and defined  $O_1(\text{sln};T;p;id)$  the occupied volume of the solute,  $O_j(\text{sln};T;p;id)$ , can be calculated through simple arithmetic.

$$V(\text{sln};T;p;id;w_1/kg=1) = (1/M_1)O_1(\text{sln};T;p;id) + m_j O_j(\text{sln};T;P;id) \quad [11.15]$$

An excess pressure  $p^E$  is calculated through the difference  $[O_1(\text{sln};T;p) - V_1^*(l;T;p)]$  and to obtain this difference an estimate of the occupied volume of the solute,  $O_j(\text{sln};T;p)$ , is required. In some treatments it is assumed that the occupied volume of the solute is independent of molality i.e. the same for real and ideal solutions.

$$\text{i.e. } O_j(\text{sln};T;p;\text{id}) = O_j(\text{sln};T;p) \quad [11.16]$$

Thus for a real solution equation [11.15] can be rewritten in the form;

$$V(\text{sln};T;p;w_1/\text{kg}=1) = (1/M_1)O_1(\text{sln};T;p) + m_j O_j(\text{sln};T;p) \quad [11.17]$$

Hence for a real solution combination of equations [11.7] and [11.17] yields equation [11.18].

$$-[O_1(\text{sln};T;p)-V_1^*(1;T;p)] = m_j M_1 [O_j(\text{sln};T;p)-\phi(v_j)] \quad [11.18]$$

Deviations of the volumetric properties from ideal are accounted for in terms of  $O_1(\text{sln};T;p)$  on the left hand side of the equation and by  $\phi(v_j)$  on the right hand side of the equation. This equation highlights a contribution to the excess pressure arising from non-ideal solute-solute interactions as well as the solute-solvent interactions within the system. If all solute-solute interactions could be turned off, then this would result in a pressure  $p^E(\text{id})$ . Turning to equation [11.18] if  $p^E$  is related to the difference  $[O_j(\text{sln};T;p)-\phi(v_j)]$  then the corresponding  $p^E(\text{id})$  quantity could be calculated from the difference  $[O_j(\text{sln};T;p)-\phi(v_j)^\infty]$ . In effect the difference in the excess pressure caused by solute-solute interactions (i.e.  $p^E-p^E(\text{id})$ ) is directly related to  $[\phi(v_j)-\phi(v_j)^\infty]$ .

### 11.3 Methods of Obtaining Excess Pressures

#### 11.3.1 Gibsons Procedures

Gibson<sup>3,10</sup> identified two procedures for calculating

excess pressures. The first approach takes into account contributions made by the volumes of solvent  $V_1$  and solute  $V_2$  in a solution prepared from  $w_1$  kg of solvent and  $w_j$  kg of solution.  $V_1$  represents the volume of pure liquid at a pressure  $(1+p^E)/\text{bar}$  and  $V_j$  represents the volume which 1 kg of solute contributes to the volume at a pressure  $p/\text{bar} = 1.0$ .  $V_1^*(1;T;w_1/\text{kg}=1;p/\text{bar}=1.0+p^E)$  is the volume of 1 kg of pure liquid 1 at temperature  $T$  and a pressure  $1.0+p^E$ . An equation for the volume of the solution can be written;

$$V(\text{sln};T;p/\text{bar}=1.0;w_1+w_j) = w_1 V_1^*(1;T;w_1/\text{kg}=1;p/\text{bar}=1.0+p^E) + w_j V_j(\text{sln};T;w_j/\text{kg}=1;p/\text{bar}=1) \quad [11.19]$$

If this solution had a total mass of 1 kg then equation [11.19] can be written in the form;

$$V(\text{sln};T;p/\text{bar}=1.0;(w_1+w_j)/\text{kg}=1) = [w_1/(w_1+w_j)] V_1^*(1;w_1/\text{kg}=1;T;p/\text{bar}=1+p^E) + [w_j/(w_j+w_1)] V_j(\text{sln};T;w_j/\text{kg}=1;p/\text{bar}=1) \quad [11.20]$$

If the excess pressure,  $p^E$ , is independent of pressure,  $p$ , then equation [11.20] can be written for a solution under an external pressure of 1000 bar.

$$V(\text{sln};T;p/\text{bar}=10^3;(w_1+w_j)/\text{kg}=1) = [w_1/(w_1+w_j)] V_1^*(1;T;w_1/\text{kg}=1;p/\text{bar}=10^3+p^E) + [w_j/(w_j+w_1)] V_j(\text{sln};T;w_j/\text{kg}=1;p/\text{bar}=10^3) \quad [11.21]$$

The difference in volumes of the solutions at  $p/\text{bar} = 1.0$  and  $p/\text{bar} = 1000$  is given by equation [11.22].

$$\begin{aligned} \Delta_p V(\text{sln}; T; (w_1 + w_j)/kg=1) = \\ [w_1/(w_1 + w_j)] \Delta_p V_1^*(1; T; w_1/kg=1) \\ + [w_j/(w_j + w_1)] \Delta_p Y_j(\text{sln}; T; w_j/kg=1) \quad [11.22] \end{aligned}$$

where;

$$\begin{aligned} \Delta_p V_1^*(1; T; w_1/kg=1) = V_1^*(1; T; w_1/kg=1; p/\text{bar}=10^3 + p^E) \\ - V_1^*(1; T; w_1/kg=1; p/\text{bar}=1 + p^E) \quad [11.23] \end{aligned}$$

and

$$\begin{aligned} \Delta_p Y_j(\text{sln}; T; w_j/kg=1) = Y_j(\text{sln}; T; w_j/kg=1; p/\text{bar}=1000) \\ - Y_j(\text{sln}; T; w_j/kg=1; p/\text{bar}=1) \quad [11.24] \end{aligned}$$

Gibson developed this first analysis from two standpoints; (1) the difference in compression of the solution and (2) the difference in compression of the solvent. The first method is the more direct and is based on equation [11.22].  $\Delta_p Y_j(\text{sln}; T; w_j/kg=1)$ , the compression of the solute is replaced by  $\Delta_p V_j^*(\text{sln}; T; w_j/kg=1)$ , the compression of the pure solute, and then on the basis that this term is negligibly small compared to the compression of the solution and solvent, is set equal to zero. Hence if the change of volume of the solution is known for a pressure change of 1 to 1000 bar, the excess pressure is calculated from the Tait parameters.

$$\Delta_p V(\text{sln}; T; (w_1 + w_j)/kg=1) = d_1 \ln[(d_2 + p + p^E(G1))/(d_2 + p)] \quad [11.25]$$

$$\Rightarrow p^E(G1) = [(d_2 + p) \exp\{\Delta_p V(\text{sln}; T; (w_1 + w_j)/kg=1)/d_1\}] - (d_2 + p) \quad [11.26]$$

However in the absence of satisfactory data, describing the

volume of solutions with change in pressure, an independent estimate of the occupied volume of the solute,  $O_j$ , is required. Equation [11.2], which characterises the volume of the solution, is rewritten in terms of the occupied volumes of both the solvent and solute.

$$V(\text{sln}; T; w_1/\text{kg}=1) = (1/M_1)O_1(\text{sln}; T; p; G_2) + m_j O_j(\text{sln}; T; p; G_2) \quad [11.27]$$

According to Gibsons<sup>second</sup> method,  $O_j(\text{sln}; T; p; G_2)$  is based on the assumption that a solute melts on going into solution and expands by 10%. Hence the volume of the solute in solution using Gibsons second approach is assumed to be 10% greater than the volume of the pure solute.

$$O_j(\text{sln}; T; p; G_2) = 1.10[V_j^*(s; T; p)] \quad [11.28]$$

This approach reflects Gibsons interest in the properties of salt solutions. However there is no reason why this approach cannot be applied to liquid solutes in solution e.g. DMSO. For consistency it is assumed that the occupied volume of a given liquid solute is equal to the volume of the corresponding pure liquid.

$$O_j(\text{sln}; T; p; G_2) = V_j^*(l; T; p) \quad [11.29]$$

Equation [11.28] is based on the assumption that for all systems  $V_j^*(l; T; p) = 1.10[V_j(s; T; p)]$ . Alternatively the volume of the solution can be expressed in terms of the apparent molar volume  $\phi(v_j)$ , see equation [11.7]. Combining equations [11.7] and [11.27] produces equation [11.30].

$$-[O_1(\text{sln}; T; p; G_2) - v_1^*(1; T; p)] = m_j M_1 [O_j(\text{sln}; T; p; G_2) - \phi(v_j)] \quad [11.30]$$

Hence from the Tait equation;

$$m_j M_1 [O_j(\text{sln}; T; p; G_2) - \phi(v_j)] = d_1 \ln[(d_2 + p + p^E(G_2)) / (d_2 + p)] \quad [11.31]$$

and

$$p^E(G_2) = (d_2 + p) (\exp[m_j M_1 [O_j(\text{sln}; T; p; G_2) - \phi(v_j)] / d_1] - 1) \quad [11.32]$$

The excess pressure for a real solution,  $p^E(G_2)$ , assumed to be pressure independent is calculated using equation [11.32]. An ideal excess pressure  $p^E(G_2; id)$  can be calculated from equation [11.33] in which the apparent molar volume  $\phi(v_j)$  is replaced by the apparent molar volume at infinite dilution  $\phi(v_j)^\infty$ .

$$p^E(G_2; id) = (d_2 + p) [\exp\{m_j M_1 [O_j(\text{sln}; T; p; G_2; id) - \phi(v_j)^\infty] / d_1\} - 1] \quad [11.33]$$

Both  $p^E(G_2)$  and  $p^E(G_2; id)$  depend on the molality of the solute and a plot of  $p^E(G_2)$  against molality of added solute,  $m_j$ , is almost linear; Figures 11.1 to 11.6.

### 11.3.2 Relationship of the Partial Molar Volume $v_j(\text{sln}; T; p)$ to the Excess Pressure $p^E(G_2)$ .

Equation [11.27] can be written in the form<sup>4</sup>;

$$V(\text{sln}; T; p; w_1/\text{kg}=1) = (1/M_1) [O_1(\text{sln}; T; p; G_2) - v_1^*(1; T; p)] + (1/M_1) v_1^*(1; T; p) + m_j O_j(\text{sln}; T; p; G_2) \quad [11.34]$$

Using the Tait equation;

$$V(\text{sln}; T; p; w_1/\text{kg}=1) = (1/M_1)V_1^*(1; T; p) + m_j O_j(\text{sln}; T; p; G_2) \\ - (d_1/M_1) \ln[(d_2 + p^E(G_2) + p)/(d_2 + p)] \quad [11.35]$$

Differentiation of equation [11.35] with respect to the molality of the solute,  $m_j$ , at constant  $T$  and  $p$  yields an expression for the partial molar volume of the solute in terms of the excess pressure  $p^E(G_2)$ . The occupied volume of the solute,  $O_j$ , is assumed to be independent of solute molality.

$$V_j(\text{sln}; T; p) = -[(d_1/M_1)/(d_2 + p^E(G_2) + p)] [\partial p^E(G_2)/\partial m_j]_{T; p} \\ + O_j(\text{sln}; T; p; G_2) \quad [11.36]$$

where  $[\partial p^E(G_2)/\partial m_j]_{T; p}$  is calculated from the gradient of the plot of  $p^E(G_2)$  against  $m_j$  i.e. the differential of equation [11.33] with respect to the molality of the solute. From equations [11.9] and [11.29];

$$[\partial p^E(G_2)/\partial m_j]_{T; p} = (d_2 + p) [(M_1/d_1) \{V_j^*(1; T; p) - V_j(\text{sln}; T; p) \\ \exp\{m_j M_1 \{V_j^*(1; T; p) - \phi(v_j)\}/d_1\}] \quad [11.37]$$

By replacing  $O_j(\text{sln}; T; p; G_2)$  with  $V_j^*(1; T; p)$  (see equation [11.29]) a relative partial molar volume is obtained using equation [11.36].

$$V_j(\text{sln}; T; p) - V_j^*(1; T; p) = -[(d_1/M_1)/(d_2 + p + p^E(G_2))] \\ [\partial p^E(G_2)/\partial m_j]_{T; p} \quad [11.38]$$

### 11.3.3 Compressions of Solutions, $K(\text{sln}; T; p; w_1/\text{kg}=1)$ and the Excess Pressure, $p^E(G_2)$ .

Differentiating equation [11.37] with respect to pressure

at constant temperature,  $T$ , and molality of solute,  $m_j$ , leads to an equation relating the compression of the solution and the solute to the excess pressure  $p^E(G2)$ . In this case the occupied volume of the solute,  $O_j(\text{sln};T;p;G2)$ , is assumed independent of pressure. The excess pressure  $p^E(G2)$  is also assumed to be pressure independent. Then;

$$\begin{aligned} [\partial V(\text{sln};T;p;w_1/\text{kg}=1)/\partial p]_{T;m_j} &= (1/M_1)[\partial v_1^*(1;T;p)/\partial p]_{T;m_j} \\ &- [(d_1/M_1)/(d_2+p+p^E(G2))] + [(d_1/M_1)/(d_2+p)] \\ &+ m_j[\partial O_j(\text{sln};T;p;G2)/\partial p]_{T;m_j} \end{aligned} \quad [11.39]$$

The assumption that  $p^E(G2)$  is pressure independent is an approximation on the grounds that  $p^E(G2)$  is related to the partial molar volume of the solute,  $V_j(\text{sln};T;p)$  by equation [11.38]. An obvious difficulty arises concerning the assumption which sets  $O_j(\text{sln};T;p;G2)$  independent of pressure. If Gibsons arguments are accepted whereby  $O_j(\text{sln};T;p;G2)$  is replaced by  $v_j^*(1;T;p)$  then it is a poor assumption which sets this differential equal to zero. This is supported by the realisation that the basis of the analysis is the dependence of  $v_1^*(1;T;p)$  on pressure (see the Tait equation, equation [11.10]). Yet the procedures require the dependence on  $p$  of  $O_j(\text{sln};T;p;G2)$  is equal to zero. However accepting these assumptions equation [11.39] can be written in the form;

$$\begin{aligned} -[(d_1/M_1)/(d_2+p+p^E(G2))] &= [\partial V(\text{sln};T;p;w_1/\text{kg}=1)/\partial p]_{T;m_j} \\ &- (1/M_1)[\partial v_1^*(1;p)/\partial p]_T - [(d_1/M_1)/(d_2+p)] \end{aligned} \quad [11.40]$$

Hence an equation can be written in terms of the compression of the solution and the solute.

$$-\left[\frac{d_1/M_1}{d_2+p+p^E(G2)}\right] = -K(\text{sln};T;w_1/\text{kg}=1) + (1/M_1)K_1^*(1;T;p) - \left[\frac{d_1/M_1}{d_2+p}\right] \quad [11.41]$$

where;

$$K(\text{sln};T;p;w_1/\text{kg}=1) = -[\partial V(\text{sln};T;p;w_1/\text{kg}=1)/\partial p]_{T;m_j} \quad [11.42]$$

and;

$$K_1^*(1;T;p) = -[\partial V_1^*(1;T;p)/\partial p]_T \quad [11.43]$$

Using the compressions of the solutions, and equation [11.41], the dependence of  $p^E(G2)$  on solute molality,  $m_j$ , can be obtained. Using the partial molar volume of the solute  $V_j(\text{sln};T;p)$  (see equation [11.36]) an 'estimate' of the occupied volume<sup>4</sup>  $O_j(\text{sln};T;p;G2)$  can be obtained without the need of any predefinition.

#### 11.3.4 Procedures Used by Leyendekker

Leyendekker obtained an excess pressure  $p^E(L)$  based on an equation similar to equation [11.36].

$$V_j(\text{sln};T;p) = O_j(\text{sln};T;p;L) - \left[\frac{d_1/M_1}{d_2+p+p^E(L)}\right] \left[\frac{\partial p^E(L)}{\partial m_j}\right]_{T;p} \quad [11.44]$$

where  $O_j(\text{sln};T;p;L)$  is the occupied volume of the solute according to Leyendekker and where  $O_j(\text{sln};T;p;L)$  and  $p^E(L)$  are both assumed to be pressure independent<sup>5</sup>. By definition the compression of the solute is defined by equation

[11.45].

$$K_j(\text{sln}; T; p) = -[\partial V_j(\text{sln}; T; p) / \partial p]_{T; m_j} \quad [11.45]$$

where  $\lim(m_j \rightarrow 0) K_j(\text{sln}; T; p) = K_j^\infty(\text{sln}; T; p)$ . Hence differentiating equation [11.44] with respect to pressure at constant temperature and molality provides an alternative description of the compression of the solute.

$$K_j(\text{sln}; T; p) = -[(d_1/M_1)/(d_2+p+p^E(L))^2][\partial p^E(L)/\partial m_j]_{T; p} \quad [11.46]$$

Therefore<sup>11</sup>;

$$K_j^\infty(\text{sln}; T; p) = -[(d_1/M_1)/(d_2+p)^2][\partial p^E(L)/\partial m_j]^\infty_{T; p} \quad [11.47]$$

Both equations demand that at fixed temperature and pressure  $\lim(m_j \rightarrow 0) [\partial p^E(L)/\partial m_j]_{T; p} \neq 0$ . Further,  $\lim(m_j \rightarrow 0) V_j(\text{sln}; T; p) - O_j(\text{sln}; T; p; L) = V_j^\infty(\text{sln}; T; p) - O_j(\text{sln}; T; p; L)$ . Equation [11.44] can thus be rewritten in the form;

$$O_j(\text{sln}; T; p; L) = V_j^\infty(\text{sln}; T; p) - (d_2+p)K_j^\infty(\text{sln}; T; p) \quad [11.48]$$

Equation [11.48] thus provides a definition for the occupied volume of the solute in terms of the limiting partial molar volume and its partial differential with respect to pressure, the limiting compression of the solute<sup>12,13</sup>,  $K_j^\infty$ . There is an element of uncertainty involving the above definition of the occupied volume of the solute, particularly the pressure independence of the said quantity. However, this definition does provide a way

forward to obtain the excess pressure  $p^E(L)$ . From equations [11.30] and [11.31];

$$\begin{aligned} -[O_1(\text{sln}; T; p; L) - V_1^*(l; T; p)] &= m_j M_1 [O_j(\text{sln}; T; p; L) - \phi(v_j)] \\ &= d_1 \ln[(d_2 + p + p^E(L)) / (d_2 + p)] \quad [11.49] \end{aligned}$$

Hence using equation [11.48];

$$\begin{aligned} m_j M_1 [V_j^\infty(\text{sln}; T; p) - (d_2 + p) K_j^\infty(\text{sln}; T; p) - \phi(v_j)] \\ = d_1 \ln[(d_2 + p + p^E(L)) / (d_2 + p)] \quad [11.50] \end{aligned}$$

Therefore the excess pressure  $p^E(L)$  is defined by equation [11.51].

$$\begin{aligned} p^E(L) &= (d_2 + p) \{ \exp\{m_j M_1 [V_j^\infty(\text{sln}; T; p) \\ &\quad - (d_2 + p) K_j^\infty(\text{sln}; T; p) - \phi(v_j)] / d_1\} - 1 \} \quad [11.51] \end{aligned}$$

The gradient of a graph of  $p^E(L)$  against molality is defined by the differential of equation [11.51] with respect to molality,  $m_j$ , at fixed temperature and pressure.

$$\begin{aligned} [\partial p^E(L) / \partial m_j]_{T; p} &= [M_1 \{V_j^\infty(\text{sln}; T; p) - V_j(\text{sln}; T; p) \\ &\quad - (d_2 + p) K_j^\infty(\text{sln}; T; p)\} / \{d_1 / (d_2 + p + p^E(L))\}] \quad [11.52] \end{aligned}$$

Hence  $\lim(m_j \rightarrow 0)$

$$[\partial p^E(L) / \partial m_j]_{T; p} = [-M_1 (d_2 + p)^2 K_j^\infty(\text{sln}; T; p)] / d_1 \quad [11.53]$$

A second procedure used by Leyendekker to obtain an excess pressure  $p^E(L_2)$  also uses equation [11.49]. The method uses

the difference between the partial molar volumes at 1 and 1000 bars and assumes that the occupied volume,  $O_j(\text{sln}; T; p; L2)$  and the excess pressure  $p^E(L2)$  are pressure independent.

$$\begin{aligned} \phi(v_j; p/\text{bar}=10^3) - \phi(v_j; p/\text{bar}=1) = \\ (d_1/m_j M_1) \ln \left[ \frac{(d_2+1+p^E(L2))(d_2+10^3)}{(d_2+10^3+p^E(L2))(d_2+1)} \right] \end{aligned} \quad [11.54]$$

Hence an excess pressure  $p^E(L2)$  is defined by equation [11.55].

$$p^E(L2) = [d_2^2(x-1) + 1001d_2(x-1) + 1000(x-1)] / [d_2 + 1000 - d_2x - x] \quad [11.55]$$

where  $x$  is given by;

$$x = \exp[m_j M_1 \{ \phi(v_j; p/\text{bar}=10^3) - \phi(v_j; p/\text{bar}=1) \} / d_1] \quad [11.56]$$

### 11.3.5 Alternative Methods of Obtaining Excess Pressures

So far in this Chapter the methods of obtaining excess pressures have depended on the prior calculation of a volumetric property of the solute i.e. the occupied volume of the solute  $O_j(\text{sln}; T; p)$ . However in this Section an attempt is made to calculate an excess pressure using no a priori calculations.

#### (i) $p^E(\phi-v_j)$

Combination of equations [11.2] and [11.9] leads to an equation for the volume of the solution in terms of the partial molar volume of the solute.

$$V(\text{sln}; T; p; w_1/k_g=1) = (1/M_1)V_1(\text{sln}; T; p) + m_j[\phi(v_j) + m_j[\partial\phi(v_j)/\partial m_j]_{T;p}] \quad [11.57]$$

In addition the volume of solution,  $V(\text{sln}; T; p; w_1/k_g=1)$ , and the partial molar volume,  $\phi(v_j)$ , are related to the reference volume of the solvent,  $V_1^*(1; T; p)$ , by equation [11.7].

$$V_1^*(1; T; p) = (1/M_1)[V(\text{sln}; T; p; w_1/k_g=1) - m_j\phi(v_j)] \quad [11.58]$$

Combining the latter two equations yields an equation in the form of the Tait equation.

$$-[V_1(\text{sln}; T; p) - V_1^*(1; T; p)] = M_1 m_j^2 [\partial\phi(v_j)/\partial m_j]_{T;p} \quad [11.59]$$

Hence using equation [11.10];

$$M_1 m_j^2 [\partial\phi(v_j)/\partial m_j]_{T;p} = d_1 \ln[(d_2 + p^E(\phi - v_j) + p)/(d_2 + p)] \quad [11.60]$$

or alternatively;

$$p^E(\phi - v_j) = (d_2 + p) [\exp\{(M_1 m_j^2 [\partial\phi(v_j)/\partial m_j]_{T;p})/d_1\} - 1] \quad [11.61]$$

This definition is precise and as an added advantage the difference  $V_1(\text{sln}; T; p) - V_1^*(1; T; p)$  is an unambiguous thermodynamic property the excess volume of the solvent in solution,  $V_1^E(\text{sln}; T; p)$ . If  $V_1^E(\text{sln}; T; p) < 0$  then the solvent is compressed because  $p^E(\phi - v_j) > 0$  due to solute-solute interactions. Similarly if  $V_1^E(\text{sln}; T; p) > 0$  then the excess pressure is less than zero and the solvent has expanded due to solute-solute interactions.

(ii)  $p^E(\phi-v_1)$

A second procedure obtains an excess pressure,  $p^E(\phi-v_1)$ , through the apparent molar volume of the solvent,  $\phi(v_1)$ . The volume of the solution is expressed by two equations one in which the non-ideality of the solution is loaded onto the solute and the other in which the non-ideal properties of the solution are placed onto the solvent (c.f. equations [11.7] and [11.8]).

$$(1/M_1)\phi(v_1) + m_j v_j^\infty(\text{sln}; T; p) = (1/M_1)v_1^*(1; T; p) + m_j \phi(v_j) \quad [11.62]$$

$$\Rightarrow \phi(v_1) - v_1^*(1; T; p) = m_j M_1 [\phi(v_j) - v_j^\infty(\text{sln}; T; p)] \quad [11.63]$$

Hence using equation [11.14];

$$m_j M_1 [\phi(v_j) - v_j^\infty(\text{sln}; T; p)] = d_1 \ln[(d_2 + p + p^E(\phi-v_1))/(d_2 + p)] \quad [11.64]$$

Therefore the excess pressure  $p^E(\phi-v_1)$  is defined by equation [11.65].

$$p^E(\phi-v_1) = (d_2 + p) [\exp\{M_1 m_j [\phi(v_j) - v_j^\infty(\text{sln}; T; p)]/d_1\} - 1] \quad [11.65]$$

The effect of solute-solute interactions is measured in the above equation by the difference  $[\phi(v_j) - v_j^\infty(\text{sln}; T; p)]$ . In the limit ( $m_j \rightarrow 0$ )  $[\phi(v_j) - v_j^\infty(\text{sln}; T; p)] = 0$  and  $p^E(\phi-v_1) = 0$ . A plot of  $p^E(\phi-v_1)$  against molality is thus predicted to have a gradient given by equation [11.66] at fixed temperature and pressure.

$$M_1 [\phi(v_j) + m_j [\partial \phi(v_j) / \partial m_j]_{T; p} - v_j^\infty(\text{sln}; T; p)] = [d_1 [\partial p^E(\phi-v_1) / \partial m_j]_{T; p}] / (d_2 + p^E(\phi-v_1) + p)$$

Hence using equation [11.9];

$$\left[ \frac{\partial p^E(\phi-v_1)}{\partial m_j} \right]_{T;p} = \frac{(M_1/d_1) [V_j^\infty(\text{sln};T;p) - V_j(\text{sln};T;p)]}{[d_2 + p^E(\phi-v_1) + p]} \quad [11.66]$$

In the limit ( $m_j \rightarrow 0$ )  $\left[ \frac{\partial p^E(\phi-v_1)}{\partial m_j} \right]_{T;p} = 0$  and hence a plot of  $p^E(\phi-v_1)$  against  $m_j$  passes through the origin and the  $m_j$  axis is a tangent to the curve.

Equation [11.64] yields an equation for the apparent molar volume in terms of the partial molar volume at infinite dilution,  $V_j^\infty$ , and the excess pressure  $p^E(\phi-v_1)$ .

$$\phi(v_j) = V_j^\infty(\text{sln};T;p) - \left[ \frac{d_1}{m_j M_1} \right] \ln \left[ \frac{d_2 + p^E(\phi-v_1) + p}{d_2 + p} \right] \quad [11.67]$$

The volume of the solution can be defined using equation [11.68].

$$V(\text{sln};T;p;w_1/\text{kg}=1) = \left( \frac{1}{M_1} \right) V_1^*(1;T;p) + m_j V_j^\infty - \left( \frac{d_1}{M_1} \right) \ln \left[ \frac{d_2 + p^E(\phi-v_1) + p}{d_2 + p} \right] \quad [11.68]$$

The ideal properties of the solvent and the solute are represented by the first two terms on the right hand side of the equation above. This suggests that the non-ideal properties of the solution are accounted for by the excess pressure,  $p^E(\phi-v_1)$ . Differentiation of equation [11.68] with respect to molality,  $m_j$ , at constant temperature and pressure yields an equation for the partial molar volume,  $V_j(\text{sln};T;p)$ .

$$V_j(\text{sln};T;p) = V_j^\infty(\text{sln};T;p) - \left( \frac{d_1}{M_1} \right) \left[ \frac{1}{[d_2 + p^E(\phi-v_1) + p]} \right] \left[ \frac{\partial p^E(\phi-v_1)}{\partial m_j} \right]_{T;p} \quad [11.69]$$

Differentiation of the partial molar volume with respect to pressure at constant temperature and assuming  $d_1$ ,  $d_2$  and  $p^E(\phi-v_1)$  are pressure independent gives an equation for  $K_j(\text{sln};T;p)$ .

$$K_j(\text{sln};T;p) = K_j^\infty(\text{sln};T;p) + (d_1/M_1) \left[ 1/(d_2 + p^E(\phi-v_1) + p)^2 \right] \left[ \partial p^E(\phi-v_1) / \partial m_j \right]_{T;p} \quad [11.70]$$

Equations [11.69] and [11.70] resemble equations [11.44] and [11.46] used by Leyendekker. The difference lies in equation [11.69] which contains  $v_j^\infty$  in place of the occupied volume  $O_j(\text{sln};T;p;L)$  used in equation [11.44]. On differentiation with respect to pressure  $v_j^\infty(\text{sln};T;p)$  produces  $K_j^\infty(\text{sln};T;p)$ . Leyendekker assumes  $O_j(\text{sln};T;p;L)$  is independent of pressure, and hence such a procedure produces an element of doubt in the derivation of the occupied volume, equation [11.48].

#### 11.4 Applications of Excess Pressures

In this Section the four excess pressures  $p^E(G2)$ ,  $p^E(L)$ ,  $p^E(\phi-v_j)$  and  $p^E(\phi-v_1)$  are calculated for a range of aqueous solutions. A Hewlett Packard BASIC program written to perform such calculations is included in Appendix 7. The example shown is set up for aqueous urea solutions.

##### (a) NaCl(aq)

The occupied volume,  $O_j(\text{sln};T;p;G2)$ , required by Gibson's second method was calculated using equation [11.28] in which the molar volume of the pure salt<sup>14</sup>  $v_j^*(\text{sln};T;p) = 27.009 \text{ cm}^3 \text{ mol}^{-1}$ . Hence  $O_j(\text{sln};T;p;G2) = 29.71 \text{ cm}^3 \text{ mol}^{-1}$ . Apparent molar volumes were calculated using an equation

given by Desnoyers et al<sup>15</sup>.

$$\begin{aligned} \phi(v_j)/\text{cm}^3 \text{ mol}^{-1} &= 17.2928 + 0.074893m_j^{1/2} + 1.658657m_j \\ &\quad - 0.581723m_j^{3/2} \end{aligned} \quad [11.71]$$

where  $m_j = (m_j/m^\circ)$  and the apparent molar volume at infinite dilution  $\phi(v_j)^\infty = 17.2928 \text{ cm}^3 \text{ mol}^{-1}$ . The partial molar compression at infinite dilution,  $\kappa_j^\infty$ , used to calculate  $O_j(\text{sln};T;p;L)$  was taken from the work of Mathieson and Conway<sup>16</sup>;  $\kappa_j^\infty(\text{aq};\text{NaCl}) = -49.6 \times 10^{-4} \text{ cm}^3 \text{ mol}^{-1} \text{ bar}^{-1}$ . Hence the occupied volume  $O_j(\text{aq};T;p;L)$  calculated in equation [11.48] equals  $32.14 \text{ cm}^3 \text{ mol}^{-1}$  which is close to the volume used by Leyendekker, namely  $30.15 \text{ cm}^3 \text{ mol}^{-1}$ .

Figure 11.1 shows plots of the four excess pressures for NaCl(aq) mentioned at the start of this section. The excess pressure  $p^E(\text{G2})$  is positive, because  $O_j(\text{sln};T;p;\text{G2}) > \phi(v_j)$  and is in close agreement to that predicted by Gibson<sup>3</sup>. The excess pressure  $p^E(\text{L})$  is in very close agreement to  $p^E(\text{G2})$  being positive because  $O_j(\text{sln};T;p;L) > \phi(v_j)$ . Similarly the excess pressure  $p^E(\phi-v_j)$  is predicted to be positive over the range  $0 \leq m_j/\text{mol kg}^{-1} \leq 2.3$  because  $[\partial\phi(v_j)/\partial m_j]_{T;p} > 0$ . However  $p^E(\phi-v_1)$  is negative over the same range because  $\phi(v_j) > \phi(v_j)^\infty$  i.e. the non-ideal properties of the solute increase in importance with increasing molality.

#### (b) Bu<sub>4</sub>NBr(aq)

Figure 11.2 reports plots of excess pressure against molality where  $p^E$  is calculated from equations for  $p^E(\text{G2})$ ,  $p^E(\text{L})$ ,  $p^E(\phi-v_j)$  and  $p^E(\phi-v_1)$ . The apparent molar volume

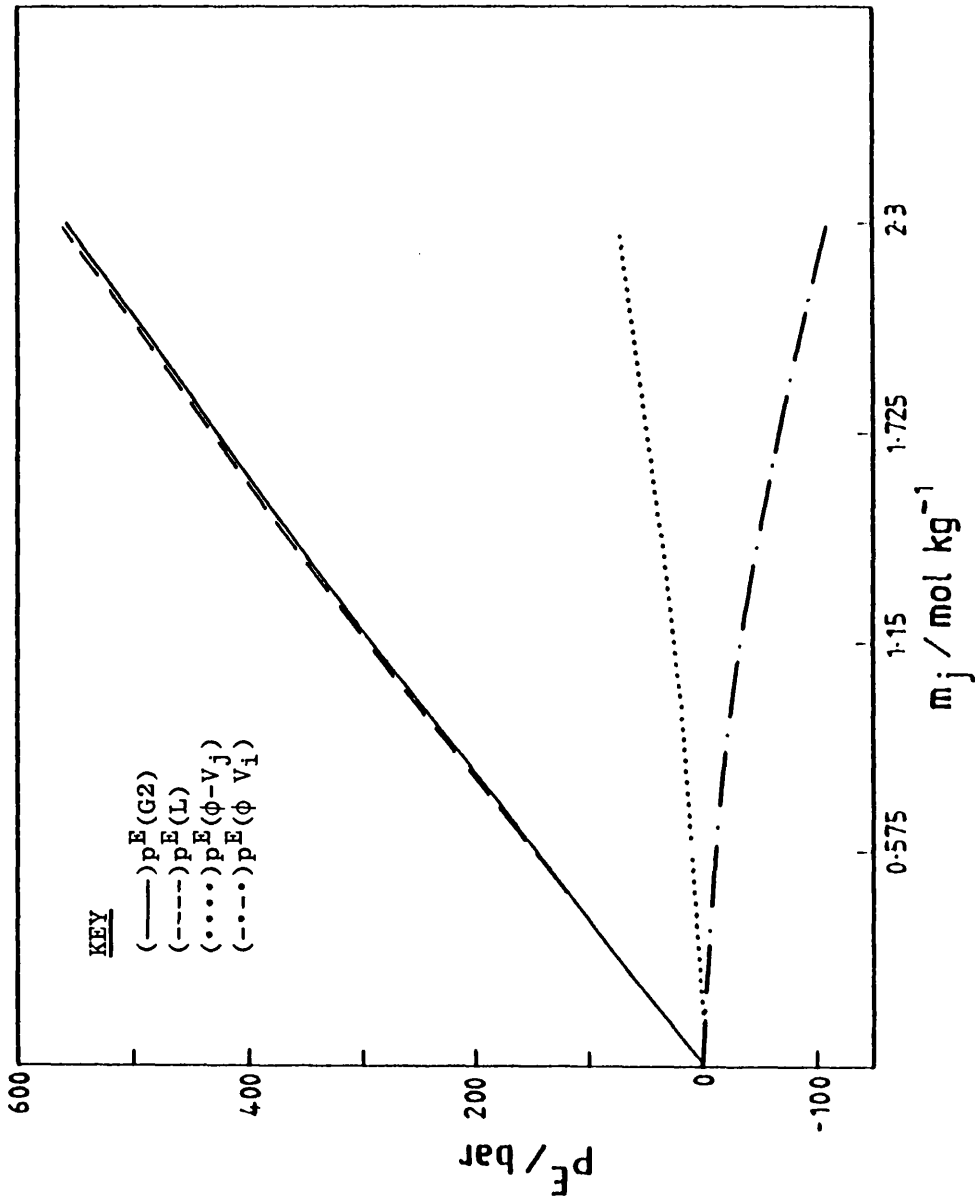
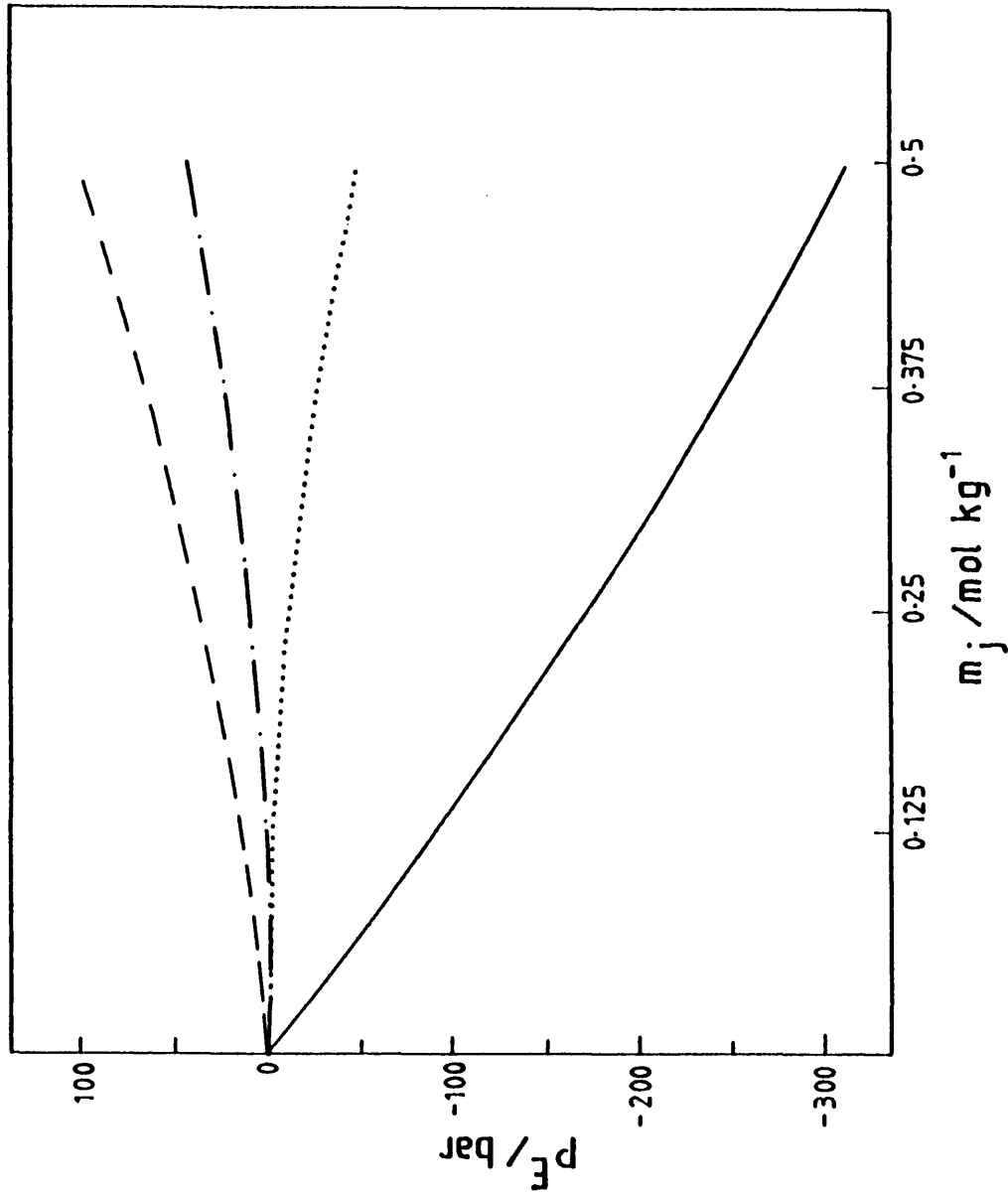


FIGURE 11.1

Dependences of excess pressure,  $p^E$ , on molality of solute,  $m_j$ , in aqueous solution at 298 K and ambient pressure where the solute is sodium chloride.



**FIGURE 11.2**

Dependences of excess pressure,  $p^E$ , on molality of solute,  $m_j$ , in aqueous solution at 298 K and ambient pressure where the solute is tetrabutylammonium bromide. [Key as in Fig. 11.1]

$\phi(v_j)$  is related to molality by the equation<sup>17</sup>;

$$\phi(v_j)/\text{cm}^3 \text{ mol}^{-1} = 300.40 + 1.865m_j^{1/2} - 10.60m_j \quad [11.72]$$

where  $m_j = (m_j/m^\circ)$  and  $\phi(v_j)^\infty = 300.40 \text{ cm}^3 \text{ mol}^{-1}$ . The occupied volume of the solute calculated from the density of the solid<sup>14</sup> and equation [11.28] equals  $266.63 \text{ cm}^3 \text{ mol}^{-1}$ . Combination of limiting compressions of  $\text{Bu}_4\text{N}^+$  and  $\text{Br}^-$  ions<sup>16</sup> sets  $K_j^\infty/\text{m}^3 \text{ mol}^{-1} \text{ bar}^{-1} = -17.3$ . Hence the occupied volume  $O_j(\text{sln};T;p;L)$  is calculated through equation [11.48] to equal  $305.58 \text{ cm}^3 \text{ mol}^{-1}$ . Inspection of these figures indicates the excess pressures predicted for  $\text{Bu}_4\text{NBr}(\text{aq})$  must differ considerably from those predicted for  $\text{NaCl}(\text{aq})$ . The excess pressure  $p^E(\text{G2})$  is negative over the range  $0 \leq m_j/\text{mol kg}^{-1} \leq 0.5$  because  $\phi(v_j) > O_j(\text{sln};T;p)$ ;  $p^E(\text{L})$  is positive and of lower magnitude over the same molality range because  $O_j(\text{sln};T;p;L) > \phi(v_j)$ . This arises from the large negative value of  $K_j^\infty$  for  $\text{Bu}_4\text{NBr}$  which goes to form  $O_j(\text{sln};T;p;L)$ .  $p^E(\phi-v_1)$  is also positive over the same molality range. However  $p^E(\phi-v_j)$  is negative, a pattern attributable to the dominant third term of the equation for the apparent molar volume.

### (c) Urea

Urea is included for study as an example of a neutral solute which is a solid at 298.15 K and ambient pressure. The dependences of apparent molar volume on molality<sup>18</sup> is predicted by equation [11.73].

$$\phi(v_j)/\text{cm}^3 \text{ mol}^{-1} = 44.20 + 0.126m_j - 0.004m_j^2 \quad [11.73]$$

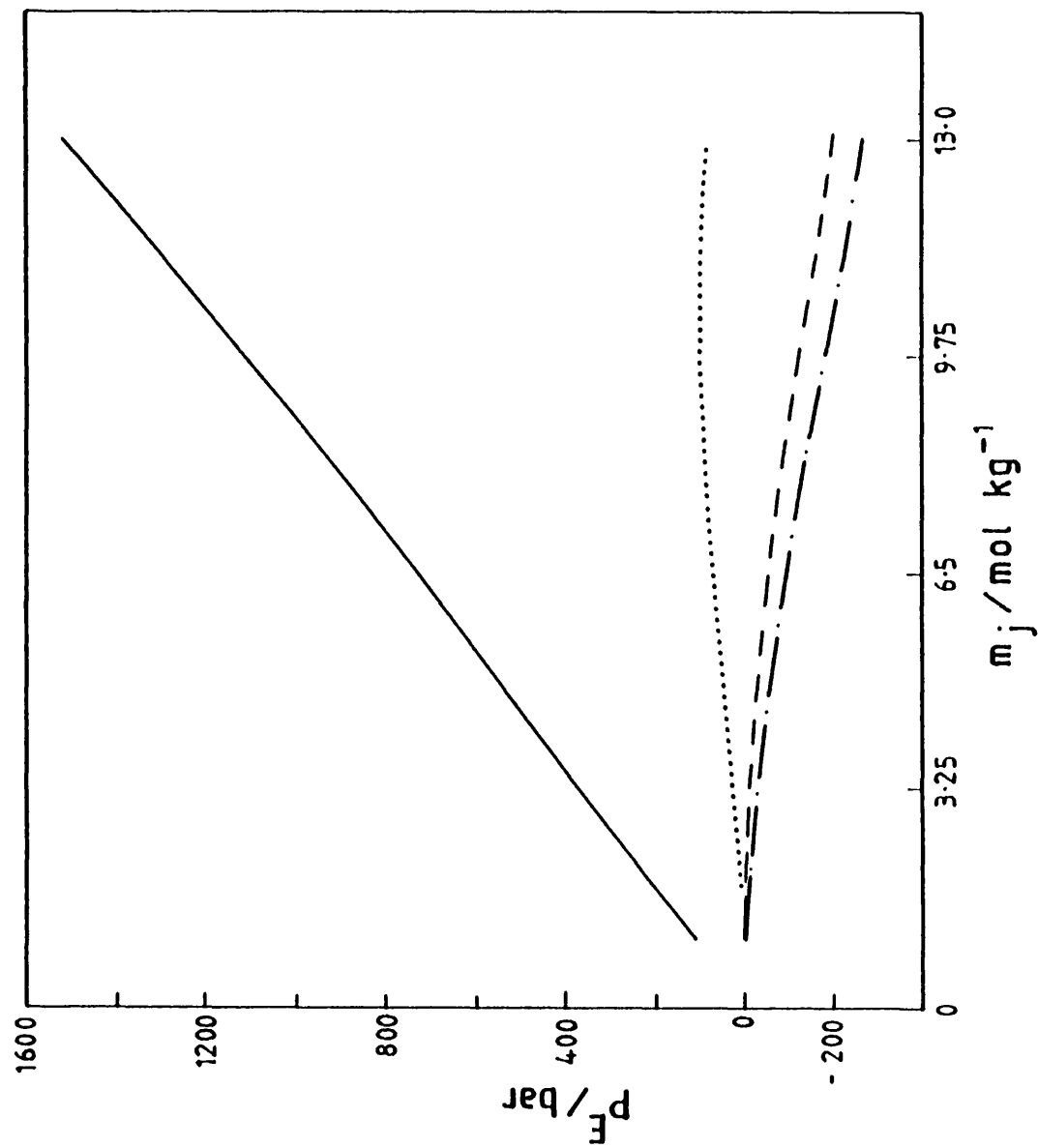


**FIGURE 11.3**

Dependences of excess pressure,  $p^E$ , on molality of solute,  $m_j$ , in aqueous solution at 298 K and ambient pressure where the solute is urea. [Key as in Fig. 11.1]

where  $m_j = (m_j/m^\circ)$  and  $\phi(v_j)^\infty/\text{cm}^3 \text{ mol}^{-1} = 44.20$ . The occupied volume  $O_j(\text{sln};T;p;G2)$  calculated from the density of the solid<sup>14</sup> and equation [11.28] equals  $49.49 \text{ cm}^3 \text{ mol}^{-1}$  and the limiting compression of the solute was taken from the work of Desnoyers et al<sup>18</sup>,  $K_j^\infty/\text{m}^3 \text{ mol}^{-1} \text{ bar}^{-1} = -0.90 \times 10^{-10}$ . Hence  $O_j(\text{sln};T;p;L)$  equals  $44.47 \text{ cm}^3 \text{ mol}^{-1}$ . In Figure 11.3  $p^E(G2)$  is large and positive over the molality range  $0 \leq m_j/\text{mol kg}^{-1} \leq 13$  because  $O_j(\text{sln};T;p;G2) - \phi(v_j) > 0$ . However  $p^E(L)$  proceeds through a maximum at  $m_j = 1.1 \text{ mol kg}^{-1}$  where  $p^E(L)/\text{bar} = 3.2$ . Up to this point the difference  $O_j(\text{sln};T;p;L) - \phi(v_j)$  is positive. However with increasing molality the second and third terms of equation [11.73] begin to dominate until the difference  $O_j(\text{sln};T;p;L) - \phi(v_j) < 0$ . Hence a negative excess pressure is predicted. Plots of  $p^E(\phi-v_j)$  and  $p^E(\phi-v_1)$  against molality are similarly dependent on equation [11.73] and hence both a positive and negative excess pressure are predicted by equations [11.61] and [11.65] respectively.

#### (d) t-Butyl alcohol

The properties of aqueous solutions for this liquid (at 298.15 K and ambient pressure) fall under the Typically Aqueous category<sup>19</sup>. Using equation [11.29] the occupied volume of the solute  $O_j(\text{sln};T;p;G2)$  equals the molar volume of the liquid,  $94.96 \text{ cm}^3 \text{ mol}^{-1}$ . The dependence of  $\phi(v_j)$  on molality up to  $0.38 \text{ mol kg}^{-1}$  is given by equation [11.74]<sup>20,11</sup>.

$$\phi(v_j)/\text{cm}^3 \text{ mol}^{-1} = 87.76 - 12.89(m_j/m^\circ) \quad [11.74]$$

Using values from Lara and Desnoyers<sup>21</sup> the calculated<sup>22</sup>  $K_j^\infty / m_j \text{ mol}^{-1} \text{ bar}^{-1} = 0.375 \times 10^{-9}$  and hence the occupied volume  $O_j(\text{sln}; T; p; L)$  equals  $86.63 \text{ cm}^3 \text{ mol}^{-1}$ , using equation [11.48]. Figure 11.4 reports plots of excess pressures against molality over the range  $0 \leq m_j / \text{mol kg}^{-1} \leq 0.38$  where the excess pressures are calculated from equations for  $p^E(\text{G2})$ ,  $p^E(\text{L})$ ,  $p^E(\phi-v_1)$  and  $p^E(\phi-v_j)$  respectively. As a consequence of  $\phi(v_j)$  decreasing with increased molality the difference  $O_j(\text{sln}; T; p; \text{G2}) - \phi(v_j)$  is positive producing a small but positive  $p^E(\text{G2})$  at 298.15 K. However  $p^E(\text{L})$  is negative because  $O_j(\text{sln}; T; p; L)$  is smaller than  $\phi(v_j)$  over the studied molality range. The difference between  $O_j(\text{sln}; T; p; \text{G2})$  and  $O_j(\text{sln}; T; p; L)$  is demonstrated by these two plots. The excess pressures  $p^E(\phi-v_1)$  and  $p^E(\phi-v_j)$  follow similar patterns to those predicted for  $\text{Bu}_4\text{NBr}(\text{aq})$ . These similarities can be understood in terms of the hydrophobic character of the solutes.

#### (e) DMSO and H<sub>2</sub>O<sub>2</sub>

Dimethylsulphoxide and hydrogen peroxide are included as examples in which there are strong solute-solvent interactions. For DMSO the molar volume of the liquid  $v_j^*(l; T; p)$  and hence  $O_j(\text{sln}; T; p; \text{G2})$  was taken from the work of Desnoyers et al<sup>23</sup>;  $v_j^*(l; T; p) / \text{cm}^3 \text{ mol}^{-1} = 71.29$ . The dependence of  $\phi(v_j)$  on molality over the region  $0 \leq m_j / \text{mol kg}^{-1} \leq 10.0$  was calculated from equation [11.75].

$$\phi(v_j) / \text{cm}^3 \text{ mol}^{-1} = 68.92 - 0.262m_j + 0.0515m_j^2 \quad [11.75]$$

where  $m_j = (m_j / m^\circ)$  and  $\phi(v_j)^\infty / \text{cm}^3 \text{ mol}^{-1} = 68.92$ . For

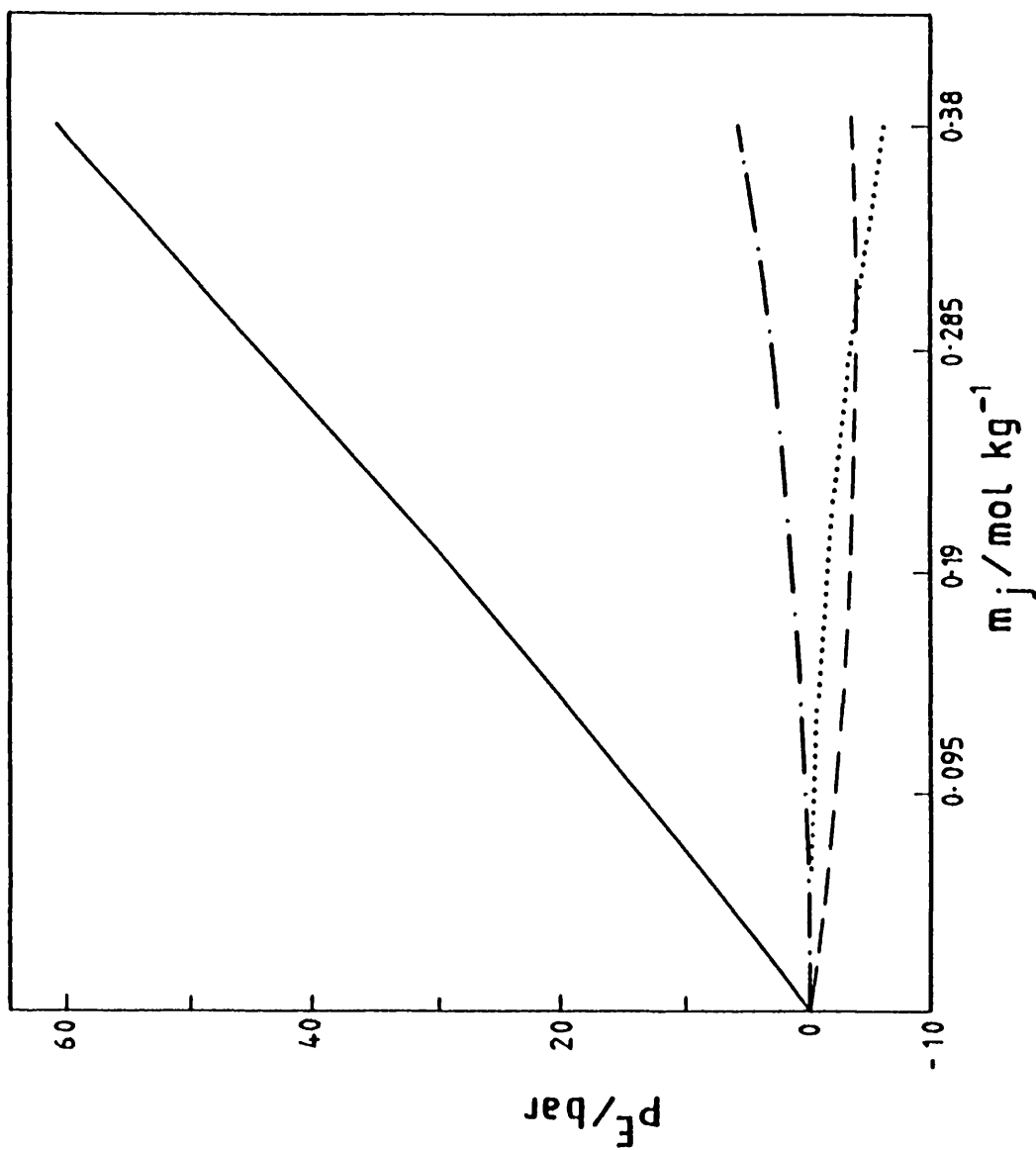


**FIGURE 11.4**

Dependences of excess pressure,  $p^E$ , on molality of solute,  $m_j$ , in aqueous solution at 298 K and ambient pressure where the solute is t-butyl alcohol. [Key as in Fig. 11.1]

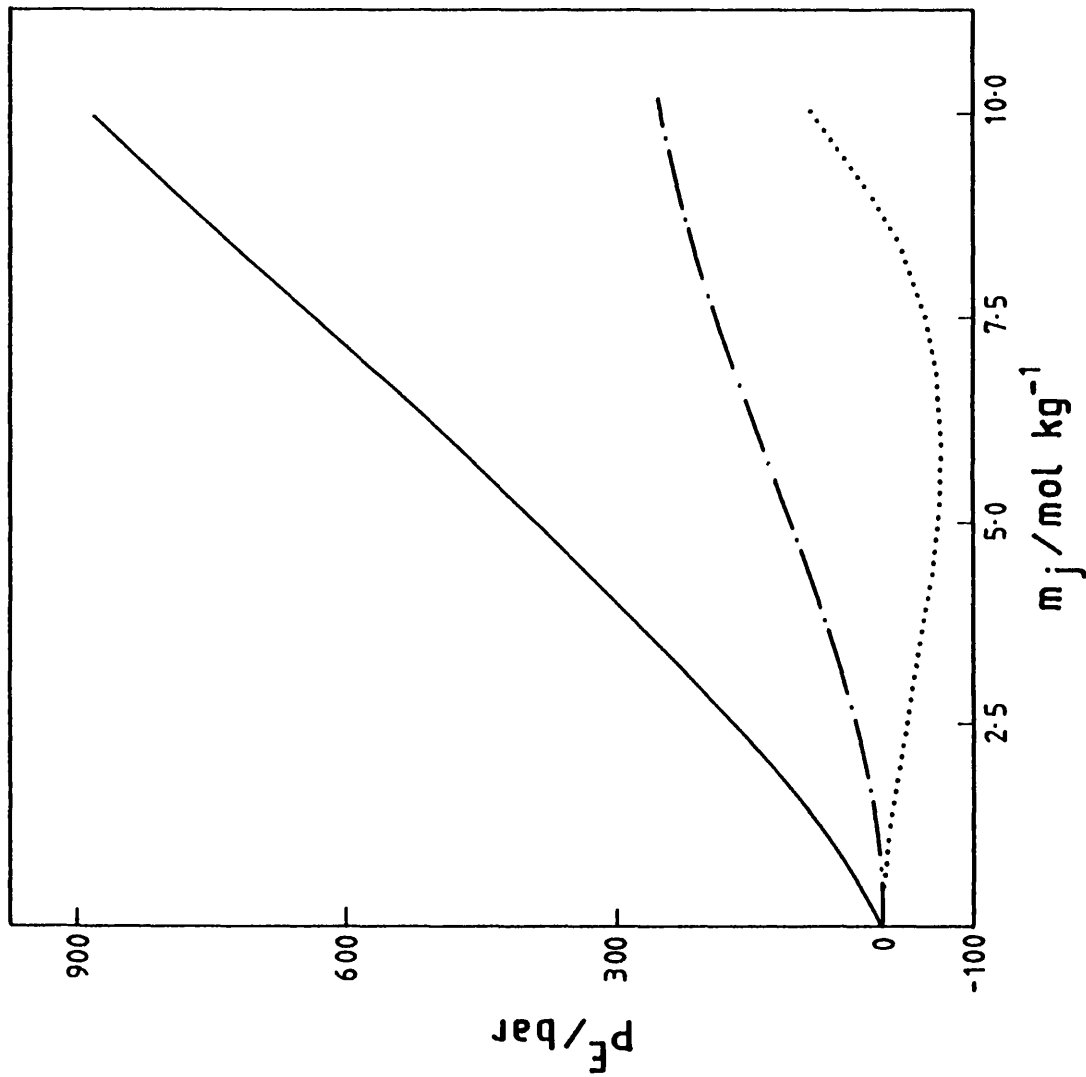


**FIGURE 11.5**  
 Dependences of excess pressure,  $P^E$ , on molality of solute,  $m_j$ , in aqueous solution at 298 K and ambient pressure where the solute is dimethylsulphoxide. [Key as in Fig. 11.1]

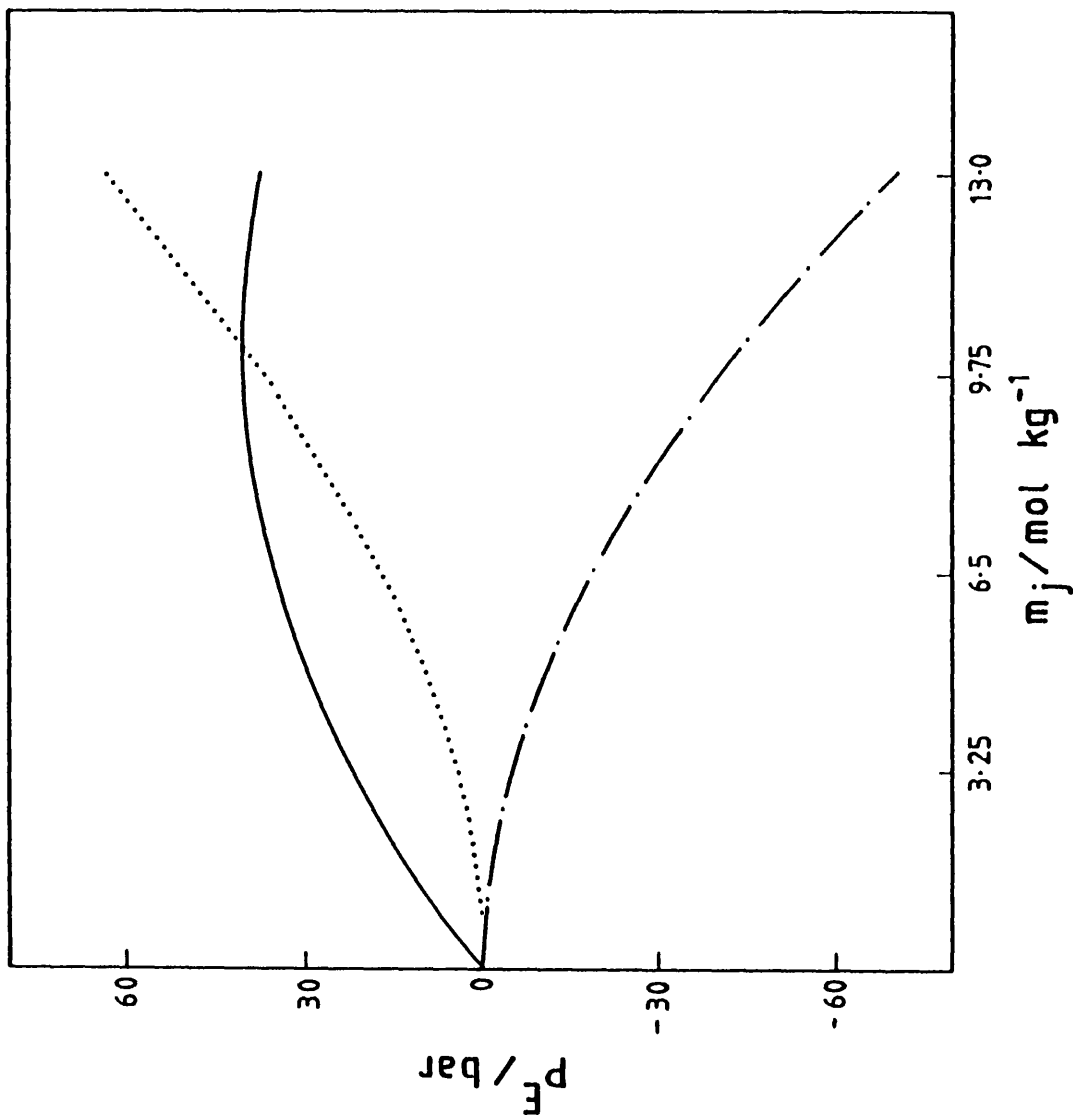


FIGURE 11.6

Dependences of excess pressure,  $P^E$ , on molality of solute,  $m_j$ , in aqueous solution at 298 K and ambient pressure where the solute is hydrogen peroxide. [Key as in Fig. 11.1]

hydrogen peroxide<sup>14,24</sup>  $v_j^*/\text{cm}^3 \text{ mol}^{-1} \approx 23.78$  and the dependence of  $\phi(v_j)$  on molality<sup>24</sup> in the region  $0 \leq m_j/\text{mol kg}^{-1} \leq 13.0$  was given by equation [11.76].

$$\phi(v_j)/\text{cm}^3 \text{ mol}^{-1} = 22.4378 + 0.0204m_j - 1.128 \times 10^{-4} m_j^2 \quad [11.76]$$

The dependences of the compressions of the solutes on molality and hence values of  $K_j^\infty(\text{sln}; T; p)$  could not be located for either solute. Hence values of  $O_j(\text{sln}; T; p; L)$  and therefore  $p^E(L)$  could not be calculated. The excess pressure  $p^E(G2)$  for both solutes is positive. However for  $\text{H}_2\text{O}_2$  the increasing importance of the second and third terms of equation [11.76] at higher molalities is pinpointed by the curved nature of the dependence. These contributions are also reflected in the plots of  $p^E(\phi-v_1)$  and  $p^E(\phi-v_j)$  against molality for both solutes. It is however the third term of equation [11.75] which is responsible for the cross over, negative to positive, for the  $p^E(\phi-v_j)$  curve of DMSO.

### 11.5 Discussion

The effect of solute on solvent can be analysed by at least two pathways. The first can be traced to the work of Bernal and Fowler<sup>25</sup> who used the concept of a structural temperature for a solvent in solution. An extension of this method uses the related extensive variable, the entropy, which uses order-disorder concepts to explain the impact of solute on water-water interactions. Such explanations lead to terms such as structure-forming and structure-breaking which are rarely quantitatively defined<sup>26</sup>. This method has

been used to the near exclusion of the methods adopted by Gibson.

Gibson's<sup>3</sup> route can be seen to be based on the intensive variable pressure, which is used to define an excess pressure. The problems with this method centre on the corresponding extensive variable volume and on the definitions of reference volumes for solvent and solute. For example there is no simple definition for the occupied volume of the solute,  $O_j$ , which one can use. However, given these problems it is still surprising to note that so few authors have taken up the challenge of pursuing the ideas of Tamman and Gibson to obtain a quantitative approach to the understanding of the effect of added solute on a solvent.

The plots shown in Figures 11.1 - 11.6 highlight the fact that the calculated excess pressure depends on the definition used to describe it. In particular this feature is highlighted by the occupied volume,  $O_j$ , where it has been shown depending on which definition is used, either  $O_j(\text{sln}; T; p; G_2)$  or  $O_j(\text{sln}; T; p; L)$ , a different excess pressure results. However the various definitions of excess pressures analysed in this Chapter do not weaken the overall approach. In fact it could be argued that these different definitions set out to highlight specific key features of the solute-solvent systems studied. Nevertheless statements concerning the pressure operating on solvents in salt solutions should be viewed with caution if the statement is not accompanied by definitions of the volumetric parameters. As a conclusion from this work, it is suggested that the excess pressure defined by equation

[11.65] i.e.  $p^E(\phi-v_1)$  points a way forward in this field.  
This is because the method utilises parameters which are  
rigorously defined.

## References Chapter 11

- (1) M.J.Blandamer, J.Burgess, B.Clark, J.B.F.N. Engberts, A.W.Hakin, J.Chem.Soc.Chem.Comm., 416, (1985)
- (2) M.J.Blandamer, J.Burgess, B.Clark, J.B.F.N. Engberts, A.W.Hakin, J.Chem.Soc., Faraday Trans. I, 83, 865, (1987)
- (3) R.E.Gibson, J.Am.Chem.Soc., 56, 4, (1934)
- (4) H.S.Harned, B.B.Owen, "The Physical Chemistry of Electrolyte Solutions", Reinhold, New York, (1943)
- (5) J.V.Leyendekker, J.Chem.Soc., Faraday Trans. I, 77, 1529, (1981)
- (6) J.V.Leyendekker, "Thermodynamics of Seawater as a Multicomponent Electrolyte Solution" M. Dekker, New York, part 1, (1976)
- (7) G.S.Kell, "Water A Comprehensive Treatise" Chap 10, Vol.1, Ed. F.Franks, Plenum Press, New York, (1973)
- (8) R.A.Fine, F.J.Millero, J.Chem.Phys., 59, 5529 (1973)
- (9) R.W.Gurney, "Ionic Processes in Solution" McGraw-Hill, New York, (1955)
- (10) R.E.Gibson, J.Am.Chem.Soc., 57, 284, (1935)
- (11) C.de Vissier, G.Perron, J.E.Desnoyers, Can.J. Chem., 55, 856, (1977)
- (12) J.V.Leyendekker, J.Chem.Soc., Faraday Trans. I, 79, 1109, (1983)
- (13) J.V.Leyendekker, Aust.J.Chem., 34, 1785, (1981)
- (14) J.D.Donnay, G.Donnay, E.G.Cox, O.Kennard, M.V.King, "Crystal Data : Determinative Tables" number 5, American Crystallographic Assoc., New York, (1963)
- (15) G.Perron, A.Roux, J.E.Desnoyers, Can.J.Chem., 59, 3049, (1981)
- (16) J.G.Mathieson, B.E.Conway, J.Soln.Chem., 3, 455, (1974)
- (17) G.Perron, N.Desrosiers, J.E.Desnoyers, Can.J. Chem., 54, 2163, (1974)

- (18) N.Desrosiers, G.Perron, J.G.Mathieson, B.E. Conway, J.E.Desnoyers, J.Soln.Chem., 3, 789, (1974)
- (19) M.J.Blandamer, R.E.Robertson, J.M.W.Scott, Prog.Phys.Org.Chem., 5, 149, (1985)
- (20) G.Roux, D.Roberts, G.Perron, J.E.Desnoyers, J.Soln.Chem., 9, 629, (1980)
- (21) J.Lara, J.E.Desnoyers, J.Soln.Chem., 10, 465, (1981)
- (22) J.E.Desnoyers, P.R.Philip, Can.J.Chem., 50, 1094, (1972)
- (23) O.Kiyohara, G.Perron, J.E.Desnoyers, Can.J.Chem., 53, 3263, (1975)
- (24) N.F.Easton, A.G.Mitchell, W.F.K.Wynne-Jones, Trans.Faraday Soc., 48, 796, (1952)
- (25) J.D.Bernal, R.H.Fowler, J.Chem.Phys., 1, 515 (1933)
- (26) M.J.Blandamer, Adv.Phys.Org.Chem., 70, 203, (1977)



# CHAPTER

# 12

Partial molar volumes and isobaric  
heat capacities of solutes in  
Aqueous Solution

## 12.1 Introduction

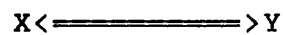
The calculations reported in this Chapter were prompted by controversy concerning isobaric heat capacities of activation,  $\Delta^\ddagger C_p^\infty$ , for the solvolysis of alkyl halides in water<sup>1</sup>. According to Robertson<sup>3</sup> the measured first order rate constant describes a single activation process and hence  $\Delta^\ddagger C_p^\infty$  measures the difference between partial molar isobaric heat capacities of the initial and transition states:  $\Delta^\ddagger C_p^\infty(\text{aq}) = C_p^\infty(\ddagger;\text{aq}) - C_p^\infty(\text{RX};\text{aq})$ . But according to Albery and Robinson<sup>2</sup> the reaction is two stage such that  $\Delta^\ddagger C_p^\infty$  calculated from the dependence of  $k(\text{obs})$  on temperature is not a true heat capacity of activation. Recently Robertson<sup>1</sup> has considered this possibility but the argument is not overwhelming because it ignores the role of the solvent and the significant partial molar heat capacities for solutes in aqueous solution. The possibility has been raised that  $\Delta^\ddagger C_p^\infty$  measures a contribution from a coupled solvent reaction<sup>4</sup>. This interpretation is examined in this Chapter. The partial molar isobaric heat capacities and volumes of apolar and ionic solutes, Z, are examined in this Chapter for a system in which substance Z is a solute in aqueous solution in which there exists an equilibrium between two states of water X and Y. Estimates are obtained of the partial molar heat capacities of initial state Z and transition state  $Z^\ddagger$  in a first order unimolecular solvolysis reaction. Hence by difference an estimate is calculated for the isobaric heat capacity of activation. The pattern in the dependence on temperature of the heat capacity of activation is shown to resemble that calculated on the basis of the Albery-Robinson<sup>2</sup> mechanism for

solvolytic reactions.

The model describes a given system at constant temperature and pressure containing X, Y and Z. Substances X and Y are in chemical equilibrium. This general model provides a basis for understanding the effects of added inert solute, Z, on the solvent equilibrium envisaged in the Lumry two-state model for water<sup>6</sup>.

## 12.2 The Solvent Equilibrium - Lumry's Two-state Model

The solvent, water, within the aqueous solution of substance Z is described in terms of an equilibrium between two states<sup>5</sup>;



The substances X and Y describe domains of water as described by Lumry's model<sup>6</sup>.

The model describes water in terms of a random network of hydrogen bonded water molecules. Embedded within this system are water clusters which have the correct geometry to allow cooperative electronic and nuclear rearrangements into short lived tetrameric hydrogen bonded units. The minimum cluster size is the symmetrical pentamer or tetrameric fragments both of which allow decreased bond length with increased bond strength to the central water molecule. The term 'geometric relaxation' is applied to the fluctuation described by the shift between the long and short bonded forms of water. Figure 12.1 gives a structural representation of the geometric relaxation of the pentameric cluster.

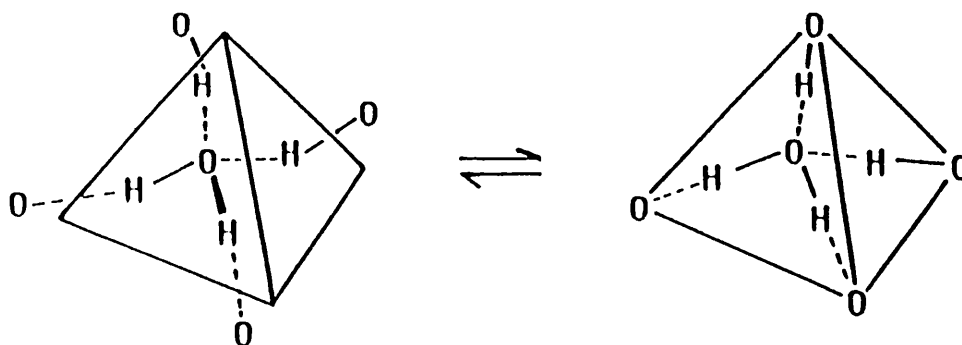


FIGURE 12.1

Structural representation of the geometric relaxation of a pentameric cluster neglecting effects of neighbouring molecules [Ref. 6].

#### Short bonded form

This pentameric unit holds five water molecules which are linked by stiff, linear H-bonds in which torsional and rotational freedom is severely restricted. Because of its rigid nature this form has high molar volume (low density). The molar entropy and molar enthalpy of such a unit is low and much of the free volume associated with this species is available to solutes.

#### Long bonded form

As the hydrogen bond length increases, the degrees of rotational and torsional freedom of the system increases. The tetrahedral constraint diminishes such that cluster cooperativity is replaced by the simple pairwise hydrogen bonds. The cluster has low molar volume (high density) and the local free volume is utilised by water and becomes less available to solutes.

In the equilibrium, substance X describes the short bonded form and substance Y describes the long bonded form of water. Lumry<sup>6</sup> suggested parameters which describe this equilibrium.  $\Delta_r H^*/kJ \text{ mol}^{-1} = 10.0$  and  $\Delta_r C_p^*/JK^{-1} \text{ mol}^{-1} =$

8.0. An estimate for  $\Delta_r V^*$  ( $= v_Y^*(1;T;p) - v_X^*(1;T;p)$ ) is not offered by Lumry. However estimates of a similar volumetric quantities based on two-state models for water are given by other authors<sup>20,21</sup>. In the calculation described in this Chapter  $\Delta_r V^*/\text{cm}^3 \text{ mol}^{-1}$  is set equal to -6.4 in line with the suggestions of Davis and Litovitz<sup>7</sup>. In a later communication, Lumry<sup>8</sup> suggests that  $\Delta_r V^* = -7.0 \text{ cm}^3 \text{ mol}^{-1}$ . This small difference produces an insignificant effect on the final pattern which emerged from the calculations.

### 12.3 Grunwalds Extrathermodynamic Hypothesis

The impact of a chemically inert solute Z on the solvent equilibrium between substances X and Y was analysed using Grunwalds extrathermodynamic hypothesis<sup>9</sup>.

The chemical potential of species X is related to the mole fraction composition of the equilibrium using equation [12.1].

$$\mu_X(\text{system};T;p) = \mu_X^\circ(1;T) + RT \ln(x_X f_X) + \int_{p^\circ}^p [v_X^*(1;T;p) dp] \quad [12.1]$$

where by definition in the limit ( $x_X \rightarrow 1.0$ )  $f_X = 1$  at all temperatures and pressures. The standard state for species X is the pure liquid at temperature T and pressure  $p^\circ$ . Similarly, the chemical potential of substance Y can be written;

$$\mu_Y(\text{system};T;p) = \mu_Y^\circ(1;T) + RT \ln(x_Y f_Y) + \int_{p^\circ}^p [v_Y^*(1;T;p) dp] \quad [12.2]$$

where the standard state for substance Y is the pure liquid at temperature T and pressure  $p^\circ$  and where by definition

limit( $x_y \rightarrow 1.0$ )  $f_y = 1.0$ . The chemical potential of solute Z is related to molality,  $m_z$ , by equation [12.3].

$$\mu_z(\text{system}; T; p) = \mu_z^\circ(\text{sln}; T) + RT \ln(m_z \gamma_z / m^\circ) + \int_{p^\circ}^p [V_z^\infty(\text{sln}; T; p) dp] \quad [12.3]$$

The standard state for substance Z is a solution in a solvent comprising an equilibrium mixture of X and Y where  $m_z = 1$  and  $\gamma_z = 1$  at temperature T and pressure  $p^\circ$ . Limit( $m_z \rightarrow 0$ )  $\gamma_z = 1.0$  at all temperatures and pressures;  $m^\circ = 1 \text{ mol kg}^{-1}$ .

According to Grunwalds hypothesis<sup>9</sup> the activity coefficients of substances X and Y are related to the molality  $m_z$  of the solute Z in solution. The procedure is adopted in which both  $\ln f_x$  and  $\ln f_y$  are linear functions of  $m_z$ .

$$\begin{aligned} \ln f_x &= \beta_x m_z / m^\circ \\ \ln f_y &= \beta_y m_z / m^\circ \\ \Rightarrow \ln(f_y / f_x) &= \beta m_z / m^\circ \quad \text{where } \beta = \beta_y - \beta_x \end{aligned} \quad [12.4]$$

It is assumed that Z is an ideal solute in the equilibrium solvent at all temperatures and pressures i.e.  $\gamma_z = 1$ . Hence derived parameters for solute Z in solution where  $m_z = 1$  are the corresponding molar properties.

#### 12.4 Analysis of a Unimolecular Solvolytic Process

In considering the equilibrium between the solvent species there are two limiting cases to examine. (i) There are no changes in organisation of the solvent i.e.  $\xi$  is held constant. (ii) the affinity for spontaneous change A is

held constant.

The chemical potential of solute Z measures the change in the Gibbs function,  $dG$ , when  $dn_z$  moles of Z are added to the system. The chemical potentials for both of the above limiting cases are related through equation [10.7] of Chapter 10. Therefore;

$$\left[\frac{\partial G}{\partial n_z}\right]_{ns;T;p;A} = \left[\frac{\partial G}{\partial n_z}\right]_{ns;T;p;\xi} - \left[\frac{\partial A}{\partial n_z}\right]_{\xi;T;p;ns} \left[\frac{\partial \xi}{\partial A}\right]_{T;p;ns;nz} \left[\frac{\partial G}{\partial \xi}\right]_{T;p;ns;nz} \quad [12.5]$$

The stability function states  $[\partial A/\partial \xi] < 0$ . In the region near chemical equilibrium and at thermodynamic equilibrium the affinity for spontaneous change,  $A$  ( $= -[\partial G/\partial \xi]_{T;p}$ ), is zero. Hence at equilibrium the triple product term on the right hand side of equation [12.5] is zero and the equation can be rewritten in the form;

$$\left[\frac{\partial G}{\partial n_z}\right]_{ns;T;p;A=0} = \left[\frac{\partial G}{\partial n_z}\right]_{ns;T;p;\xi} \quad [12.6]$$

For a system in a state of thermodynamic equilibrium the Gibbs function,  $G$ , is not a very sensitive test bed for molecular models and descriptions. However, the partial derivatives of  $G$  with respect to temperature,  $T$ , and pressure,  $p$ , provide more critical tests of a molecular model. In such situations the triple product term of the corresponding equations are no longer equal to zero. The differential of the Gibbs function with respect to pressure yields the volume,  $V$ , and the the differential of  $(G/T)$  with respect to temperature yields the enthalpy,  $H$ . Equation [12.5] can be rewritten in terms of both of these

quantities.

$$[\partial V/\partial n_z]_{T;p;ns;A} = [\partial V/\partial n_z]_{T;p;ns;\xi} - [\partial A/\partial n_z]_{T;p;ns;\xi} \\ [\partial \xi/\partial A]_{T;p;ns;nz} [\partial V/\partial \xi]_{T;p;ns;nz} \quad [12.7]$$

$$[\partial H/\partial n_z]_{T;p;ns;A} = [\partial H/\partial n_z]_{T;p;ns;\xi} - [\partial A/\partial n_z]_{T;p;ns;\xi} \\ [\partial \xi/\partial A]_{T;p;ns;nz} [\partial H/\partial \xi]_{T;p;ns;nz} \quad [12.8]$$

At equilibrium the triple product terms of equations [12.7] and [12.8] are non-zero because  $[\partial V/\partial \xi]_{T;p;ns;nz}$  and  $[\partial H/\partial \xi]_{T;p;ns;nz}$  are non-zero.

#### 12.4.1 Calculation of the Triple Product Term of Equation [12.7]

The affinity for spontaneous change within the solvent is given by equation [12.9].

$$A = -[\mu_y(\text{system};T;p) - \mu_x(\text{system};T;p)] \quad [12.9]$$

For a solution dilute in solute Z (with  $dn_z = v_j d\xi$  where  $v_i$  is the stoichiometry, which is positive for products and negative for reactants)

$$X_y = n_y/(n_s+n_z) \approx \xi/n_s \quad [12.10]$$

and similarly;

$$X_x = (n_s - \xi)/n_s \quad [12.11]$$

Using equations [12.1], [12.2] and [12.9] - [12.11].

$$[\partial A/\partial \xi]_{T;p;ns;nz} = -RT\{[\partial \ln(\xi/n_s)/\partial \xi] - [\partial \ln(n_s - (\xi/n_s))/\partial \xi] + [\partial \ln(f_y/f_x)/\partial \xi]\}_{T;p;ns;nz} \quad [12.12]$$

$$= -RT\{(n_s/\xi n_s) + (n_s/(n_s(n_s - \xi)))\} \\ = -RT\{n_s/(\xi(n_s - \xi))\} \quad [12.13]$$

or alternatively;

$$[\partial A/\partial \xi]_{T;p;ns;nz} = -RT/(n_s X_Y (1 - X_Y)) \quad [12.14]$$

The second term of the triple product can be written;

$$[\partial A/\partial n_z]_{T;p;ns;\xi} = -RT[d \ln(f_y/f_x)/dn_z] \quad [12.15]$$

Using Grunwalds hypothesis<sup>9</sup> equation [12.15] can be written in the form;

$$[\partial A/\partial n_z]_{T;p;ns;\xi} = -RT[d\beta(m_z/m^\circ)/dn_z] \quad [12.16]$$

For a solution dilute in solute Z an expression for  $m_z$  is given by equation [12.17].

$$m_z = \{n_z/(n_x M_x + n_y M_y)\} \quad [12.17]$$

where  $M_x$  and  $M_y$  are the molar masses of substances X and Y.

$$\Rightarrow [\partial A/\partial n_z]_{T;p;ns;\xi} = -RT[d(\beta n_z/((n_x M_x + n_y M_y)/m^\circ))/dn_z] \quad [12.18]$$

$$= -RT\beta/m^\circ (n_x M_x + n_y M_y) \quad [12.19]$$

$$= -RT\beta/m^\circ W \quad [12.20]$$

where W is the mass of the solvent.

The third term of the triple product can be written;

$$[\partial V/\partial \xi]_{T;p;ns;nz} = (V_Y^* - V_X^*) = \Delta_r V^* \quad [12.21]$$

where  $V_Y^*$  and  $V_X^*$  are the molar volumes of pure substances X and Y at temperature T and pressure p.

Combining equations [12.14], [12.20] and [12.21] yields the triple product term of equation [12.7]; equation [12.22].

$$= \{\beta(\xi/(1-\xi))\Delta_r V^*\}/m^\circ W \quad [12.22]$$

Hence by rewriting  $\xi(1-\xi)$  in the form  $x_Y^{eq}(1-x_Y^{eq})n_S$  equation [12.7] can be rewritten as;

$$[\partial V/\partial n_Z]_{T;p;ns;A=0} = [\partial V/\partial n_Z]_{T;p;ns;\xi} - [n_S \beta/m^\circ W] x_Y^{eq}(1-x_Y^{eq}) \Delta_r V^* \quad [12.23]$$

Alternatively equation [12.23] can be written in the form;

$$V_Z(A=0) = V_Z(\xi^{eq}) + V_Z^\# \quad [12.24]$$

where  $V_Z(A=0)$  describes the equilibrium partial molar volume,  $[\partial V/\partial n_Z]_{T;p;ns;A=0}$ ,  $V_Z(\xi^{eq})$  describes the instantaneous/frozen partial molar volume,  $[\partial V/\partial n_Z]_{T;p;ns;\xi}$  and  $V_Z^\#$  describes the configurational partial molar volume and registers the sensitivity to a change in composition of the solvent i.e.  $[n_S \beta/m^\circ W] x_Y^{eq}(1-x_Y^{eq}) \Delta_r V^*$ .

### 12.4.2 Calculation of the Triple Product Term of Equation

[12.8]

The triple product term of equation [12.8] can be calculated in a similar fashion to the method described above for equation [12.7].

The third term of the triple product of equation [12.8] is given by equation [12.25].

$$[\partial H / \partial \xi]_{T;p;ns;nz} = (H_Y^* - H_X^*) = \Delta_r H^* \quad [12.25]$$

where  $H_X^*$  and  $H_Y^*$  are the molar enthalpies of the pure substances X and Y.

Combining equations [12.14], [12.20] and [12.25] it is possible to write the triple product term in the form;

$$= \{ \beta (\xi / (1 - \xi)) \Delta_r H^* \} / m^{\circ} W \quad [12.26]$$

At equilibrium  $\xi / (1 - \xi)$  can be written as  $x_Y^{eq} (1 - x_Y^{eq})$ . Hence equation [12.8] can be written;

$$[\partial H / \partial n_z]_{T;p;ns;A=0} = [\partial H / \partial n_z]_{T;p;ns;\xi} - [n_s \beta / m^{\circ} W] x_Y^{eq} (1 - x_Y^{eq}) \Delta_r H^* \quad [12.27]$$

or in the alternative form;

$$H_z(A=0) = H_z(\xi^{eq}) - [n_s \beta / m^{\circ} W] x_Y^{eq} (1 - x_Y^{eq}) \Delta_r H^* \quad [12.28]$$

The differential of equation [12.28] with respect to temperature yields the equilibrium partial molar isobaric heat capacity of substance Z.

$$C_{pz}(A=0) = C_{pz}(\xi^{eq}) - [n_s \beta / m^{\circ} W] [d(x_Y^{eq}(1-x_Y^{eq}) \Delta_r H^*) / dT] \quad [12.29]$$

where  $C_{pz}(\xi^{eq})$  is the equilibrium frozen partial molar heat capacity. Equation [12.29] can be simplified by carrying out a product differentiation and allowing  $\phi = (n_s \beta / m^{\circ} W)$ . Hence equation [12.30].

$$C_{pz}(A=0) = C_{pz}(\xi^{eq}) - \phi \Delta_r C_p^* x_Y^{eq}(1-x_Y^{eq}) - \phi \Delta_r H^* (1-2x_Y^{eq})(dx_Y^{eq}/dT) \quad [12.30]$$

where the third term on the right hand side of equation [12.31], which later defines  $C_{pz}^{##}$ , registers the sensitivity of the solvent reaction to a change in temperature. The second term reflects the contribution of the solvent reaction to the equilibrium partial molar isobaric heat capacity.

The molar enthalpies of substances X and Y are assumed to be independent of pressure. Equation [12.30] can be simplified further by assuming that ambient pressure,  $p$ , is equal to the standard pressure  $p^{\circ}$ . Therefore  $\Delta_r H^{\circ} = H_Y^{\circ} - H_X^{\circ} = \Delta_r H^*$ . The equilibrium constant for the reaction is defined by equation [12.31].

$$K^{\circ}(T) = \xi^{eq} / (n_s - \xi^{eq}) \quad [12.31]$$

$$\text{where } \Delta_r G^{\circ}(T) = -RT \ln K^{\circ}(T) \quad [12.32]$$

$$= \mu_Y^{\circ}(1;T) - \mu_X^{\circ}(1;T) \quad [12.33]$$

$$\text{at } p^{\circ} \quad \Delta_r H^{\circ} = H_Y^{\circ}(1;T) - H_X^{\circ}(1;T) \quad [12.34]$$

$$\text{Then } [d\xi^{eq}/dT] = [n_s K^{\circ}(T) / (1+K^{\circ}(T))^2] \Delta_r H^{\circ} / RT^2 \quad [12.35]$$

$$\Rightarrow C_{pz}^{\#\#} = -\{\phi(1-2x_Y^{eq})K^{\circ}(T)/[1+K^{\circ}(T)]^2\}\Delta_r H^{\circ 2}/RT^2 \quad [12.36]$$

Using equation [12.31];

$$K^{\circ}(T)/[1+K^{\circ}(T)]^2 = x_Y^{eq}(1-x_Y^{eq}) \quad [12.37]$$

$$\Rightarrow C_{pz}^{\#\#} = -\{\phi(1-2x_Y^{eq})x_Y^{eq}(1-x_Y^{eq})[\Delta_r H^{\circ 2}/RT^2]\} \quad [12.38]$$

Hence equation [12.29] can be written in its final form as equation [12.39].

$$C_{pz}(A=0) = C_{pz}(\xi^{eq}) + C_{pz}^{\#} \quad [12.39]$$

$$\text{where } C_{pz}^{\#} = -\phi x_Y^{eq}(1-x_Y^{eq})\Delta_r C_{pz}^* - \phi x_Y^{eq}(1-x_Y^{eq})(1-2x_Y^{eq})\Delta_r H^{\circ 2}/RT^2 \quad [12.40]$$

$C_{pz}^{\#}$  is known as the configurational isobaric partial molar heat capacity.

### 12.4.3 Isobaric Heat Capacities of Activation

For the first order unimolecular solvation of solute Z, a transition state is passed through which can be labelled  $Z^{\ddagger}$ . The molar isobaric heat capacity of activation,  $\Delta^{\ddagger}C_{pz}$ , is given by equation [12.41].

$$\Delta^{\ddagger}C_{pz} = C_p(Z^{\ddagger};A=0) - C_p(Z;A=0) \quad [12.41]$$

Hence using equation [12.39],  $\Delta^{\ddagger}C_{pz}$  can be re-expressed in terms of the instantaneous and configurational isobaric heat capacity contributions.

$$\begin{aligned} \Delta^\ddagger C_{pz} &= [C_p(z^\ddagger; \xi^{eq}) + C_{pz}^\#(z^\ddagger)] - [C_p(z; \xi^{eq}) + C_{pz}^\#(z)] \\ &= [C_p^\#(z^\ddagger) - C_p^\#(z)] + [C_p(z^\ddagger; \xi^{eq}) - C_p(z; \xi^{eq})] \quad [12.42] \end{aligned}$$

Using equation [12.41] the difference  $[C_p^\#(z^\ddagger) - C_p^\#(z)]$  can be calculated as a function of temperature using  $\beta$  parameters. In calculating this difference, which characterises the effect of the initial and transition state on the solvent equilibrium, it is assumed that the impact registered by the difference between the initial and transition states of the instantaneous/frozen isobaric partial molar heat capacities is negligible.

## 12.5 Results

The dependence of  $C_{pz}^\#$  on  $\beta$  in the range  $-1.0 \leq \beta \leq 1.0$  at 298.15 K was analysed using a BASIC program written for an HP 85 minicomputer. This program is included in Appendix 8. Figure 12.2 summarises the results obtained from computer analysis in graphical form. Estimates, by Perron and Desnoyers<sup>10</sup>, of the standard partial molar isobaric heat capacities of neutral solutes in terms of group contributions are included on the same figure.

Figures 12.3 and 12.4 show plots of the dependence of  $C_{pz}^\infty$  on  $\beta$  at 298.15 K on which single ion partial molar isobaric heat capacities, proposed by Hepler<sup>11-13</sup> et al have been superimposed. In these plots it should be noted that  $C_{pz}^\infty(H^+)$  has been set equal to zero. If this assumption was modified then the observed positions and orders of the single ion values on the plots would be altered.

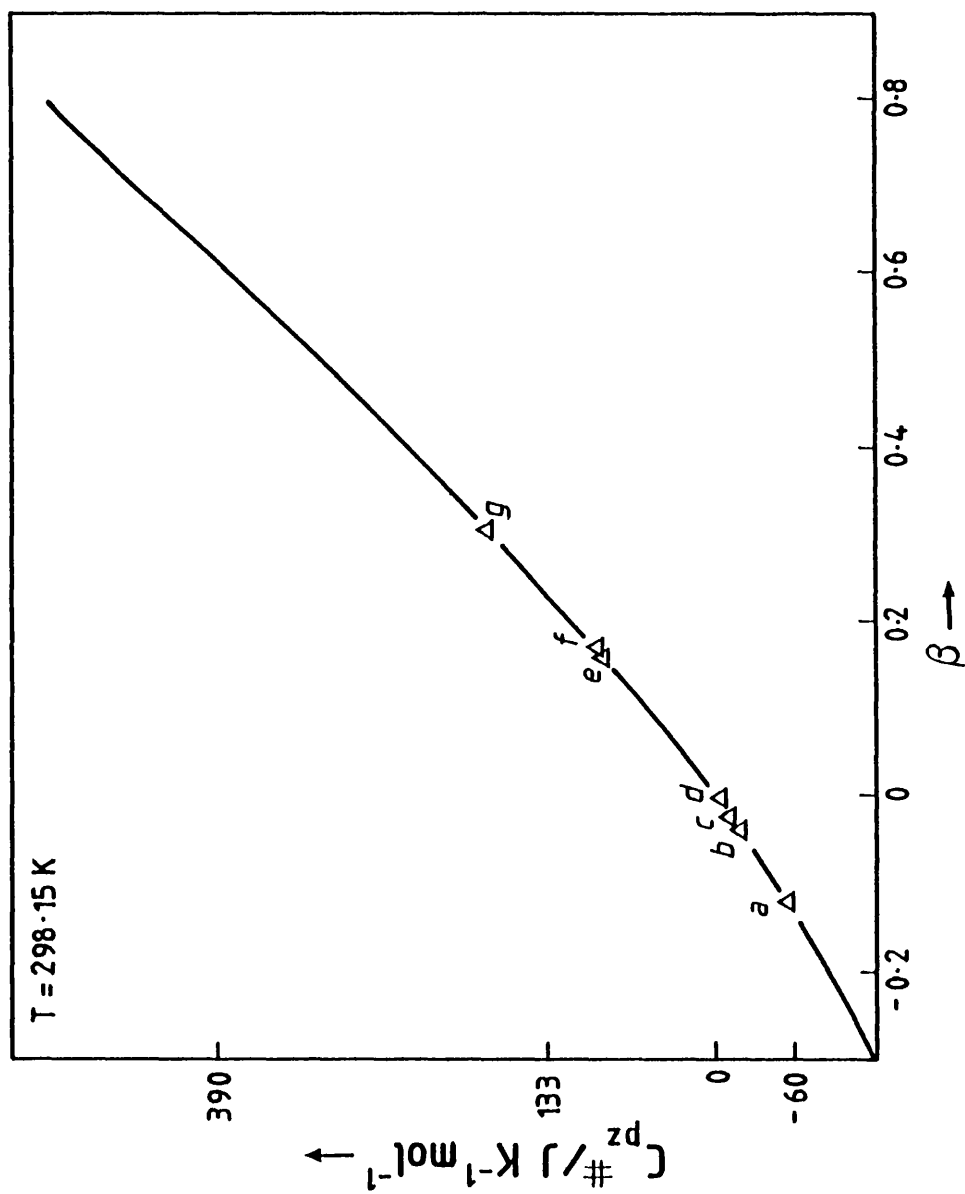


**FIGURE 12.2**

Dependence on  $\beta$  of the configurational partial molar isobaric heat capacity of a solute in aqueous solution at 298 K; comparison with group contributions for neutral aliphatic solutes (a) -O-, (b) -NH<sub>2</sub>, (c) -COOH, (d) -OH, (e) -CH<sub>2</sub>, (f) -H, (g) -CH<sub>3</sub>.

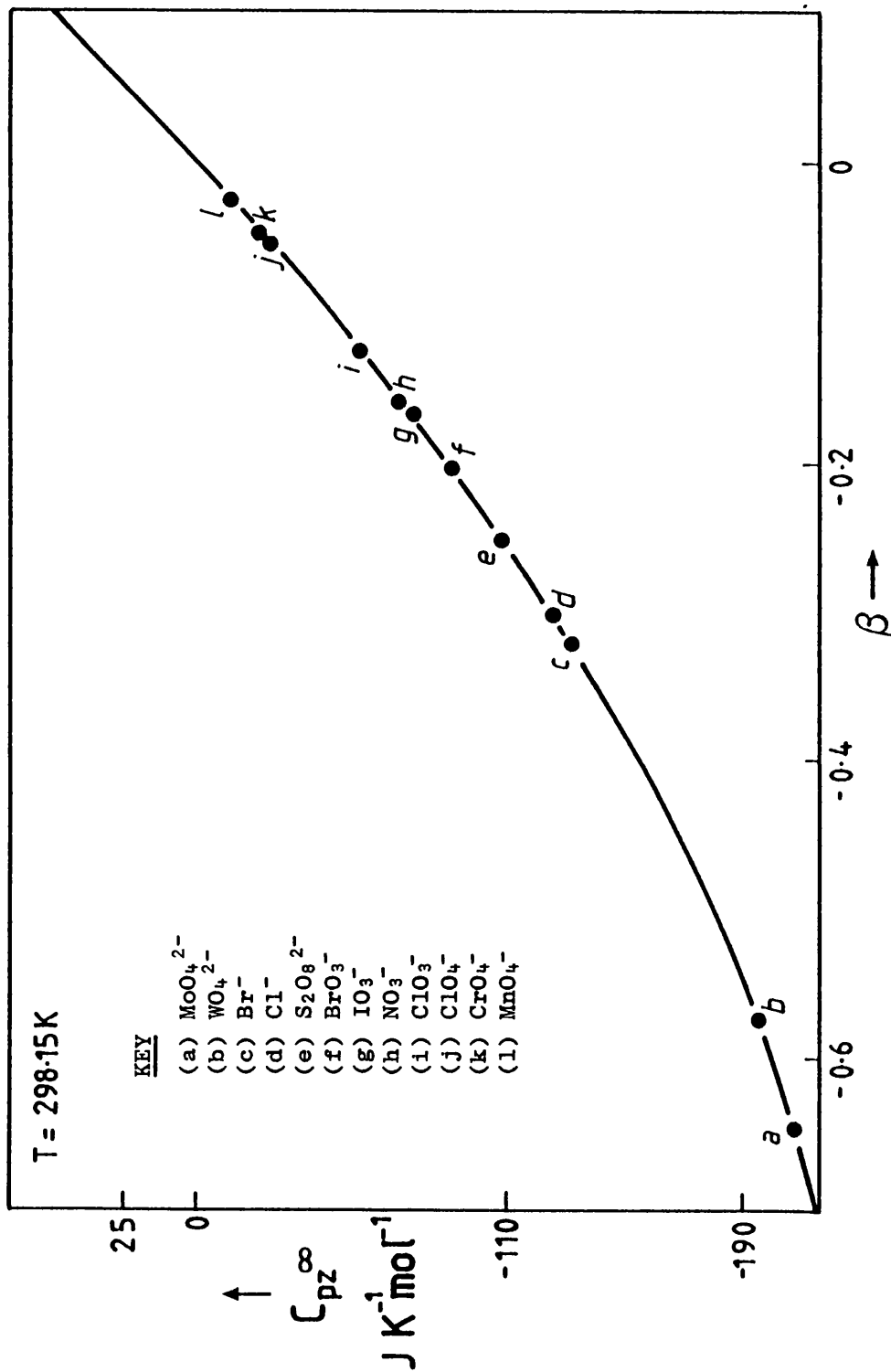


FIGURE 12.3

Dependence on  $\beta$  of the configurational partial molar isobaric heat capacity of a solute in an aqueous solution at 298 K; comparison with relative partial molar heat capacities for ions where  $C_p^{\infty}(\text{H}^+; \text{aq}; 298\text{ K})$  is set equal to zero.

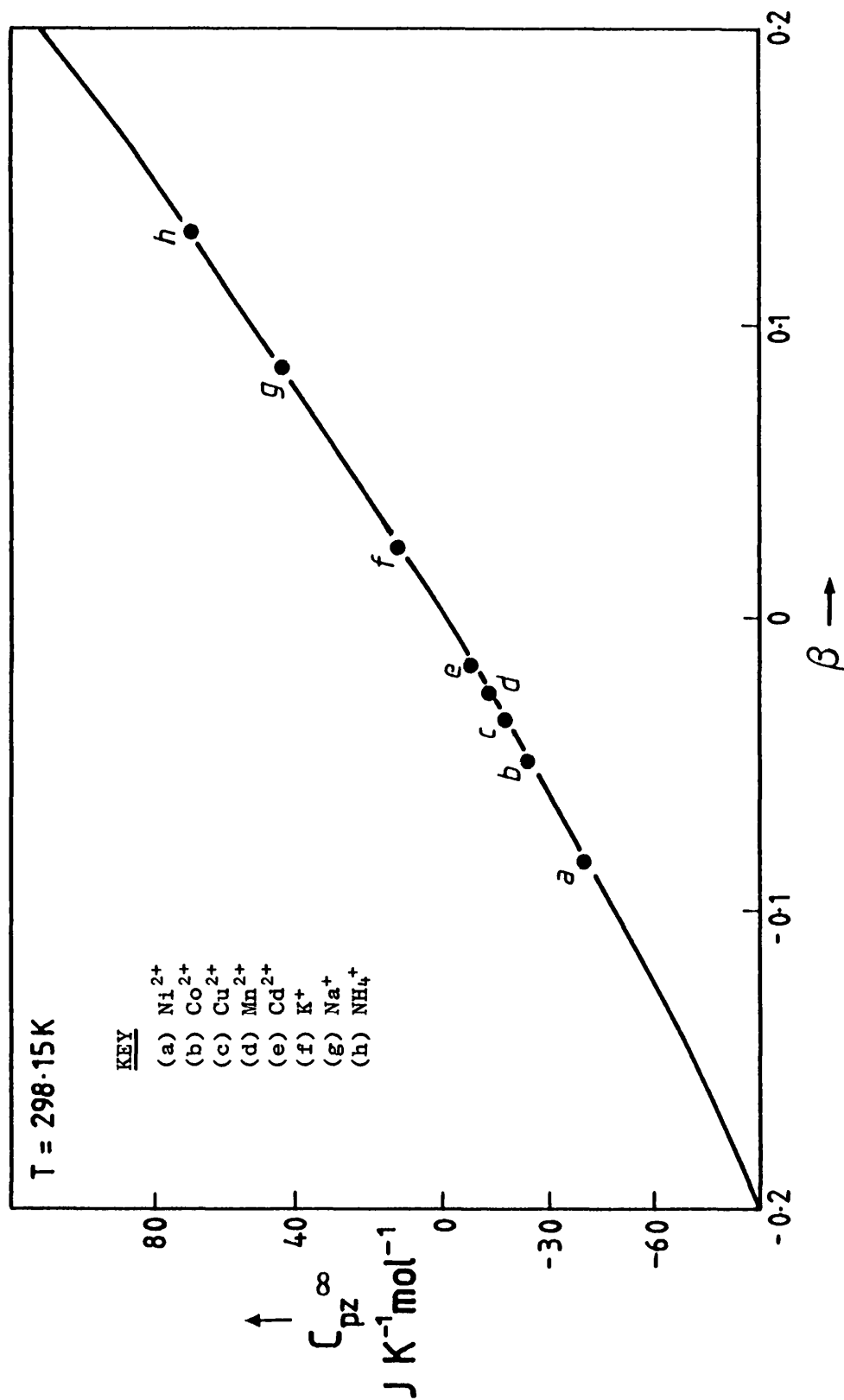


FIGURE 12.4

Dependence on  $\beta$  of the configurational partial molar isobaric heat capacity of a solute in aqueous solution at 298 K; comparison with relative partial molar heat capacities for ions where  $C_p^{\infty}(\text{H}^+; \text{aq}; 298 \text{ K})$  is set equal to zero.

The dependence of  $C_{pz}^\ddagger$  on temperature,  $273.15 \leq T/K \leq 373.15$  over a range of  $\beta$  values was obtained from a FORTRAN program, based on the BASIC program shown in Appendix 8. The  $C_{pz}^\ddagger$ , temperature/ $\beta$  surface has been included as Figure 12.5 and a program listing is given in Appendix 8.

When  $\beta < 0$ ,  $C_{pz}^\ddagger$  can be seen to increase with increase in temperature, however the effect of temperature steadily decreases to the point at which for all temperatures,  $\beta$  and  $C_{pz}^\ddagger$  are equal to zero. In the region  $0 \leq \beta \leq 1.0$ ,  $C_{pz}^\ddagger$  can be seen to decrease with increase in temperature, however when  $\beta > 1.0$  the trend is once again reversed.

A second BASIC program for the HP 85 minicomputer (Appendix 8) was written to calculate the difference  $C_{pz}^\ddagger(z^\ddagger) - C_p^\ddagger(z)$  using various combinations of  $\beta^\ddagger$  and  $\beta$ . Figure 12.6 shows the dependence on temperature of the configurational partial molar isobaric heat capacities for both the initial and transition states together with the difference i.e. the dependence on temperature on the molar isobaric heat capacity of activation,  $\Delta^\ddagger C_p^\ddagger(\text{aq})$ . The plotted curves are based on a calculation in which  $\beta^\ddagger$  and  $\beta$  have been arbitrarily set equal to  $-0.2$  and  $1.0$  respectively. This Figure illustrates how a maxima in  $\Delta^\ddagger C_p^\ddagger(\text{aq})$  emerges.

In a similar fashion to the above a BASIC program was written which modelled the dependence of  $v_z^\ddagger$  (i.e.  $v_z(A=0) - v_z(\xi^{\text{eq}})$ ) on  $\beta$  in the range  $-1.0 \leq \beta \leq 1.0$  using the relationship described in equation [12.24]. Figure 12.7 gives a graphical representation of this calculation on which estimates of  $v_z^\ddagger$  for neutral aliphatic solutes in

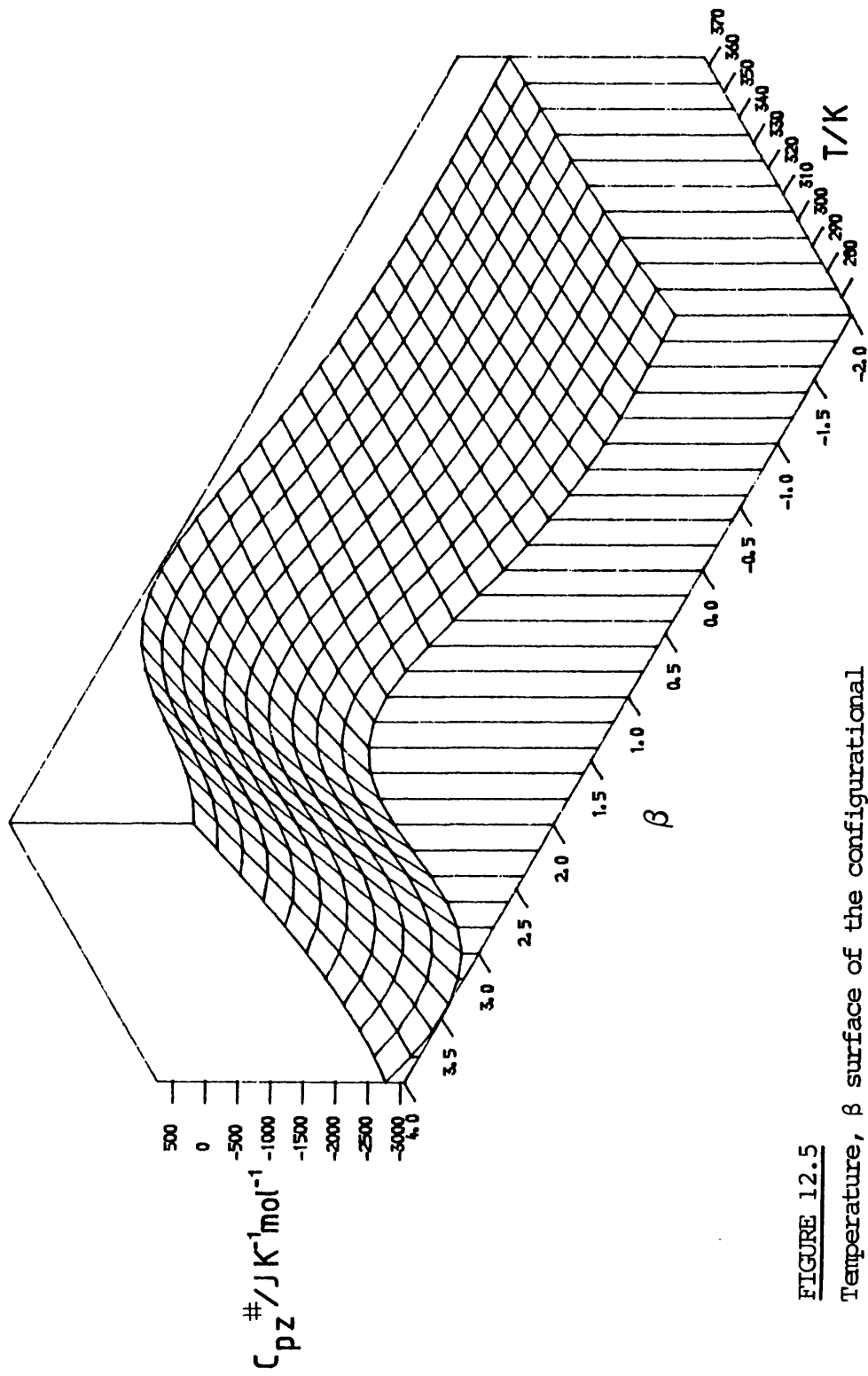


**FIGURE 12.5**

Temperature,  $\beta$  surface of the configurational partial molar isobaric heat capacity of a solute in aqueous solution.

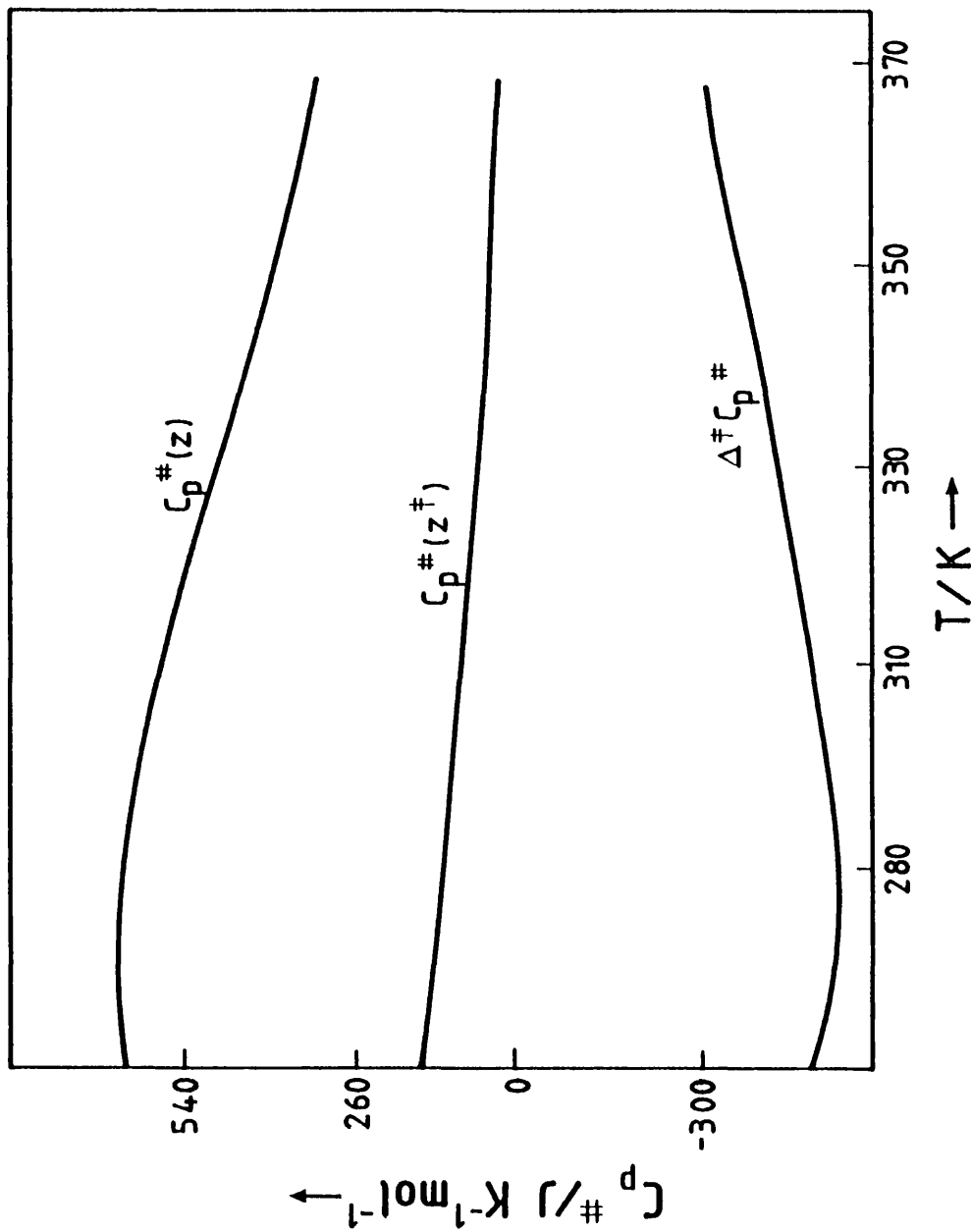


FIGURE 12.6

Dependence on temperature of configurational isobaric heat capacities for initial state,  $C_p^\#(z)$ , transition state  $C_p^\#(z^\ddagger)$  and activation  $\Delta^\ddagger C_p^\#$ ;  $\beta(z) = 1.0$  and  $\beta(z^\ddagger) = -0.2$ .

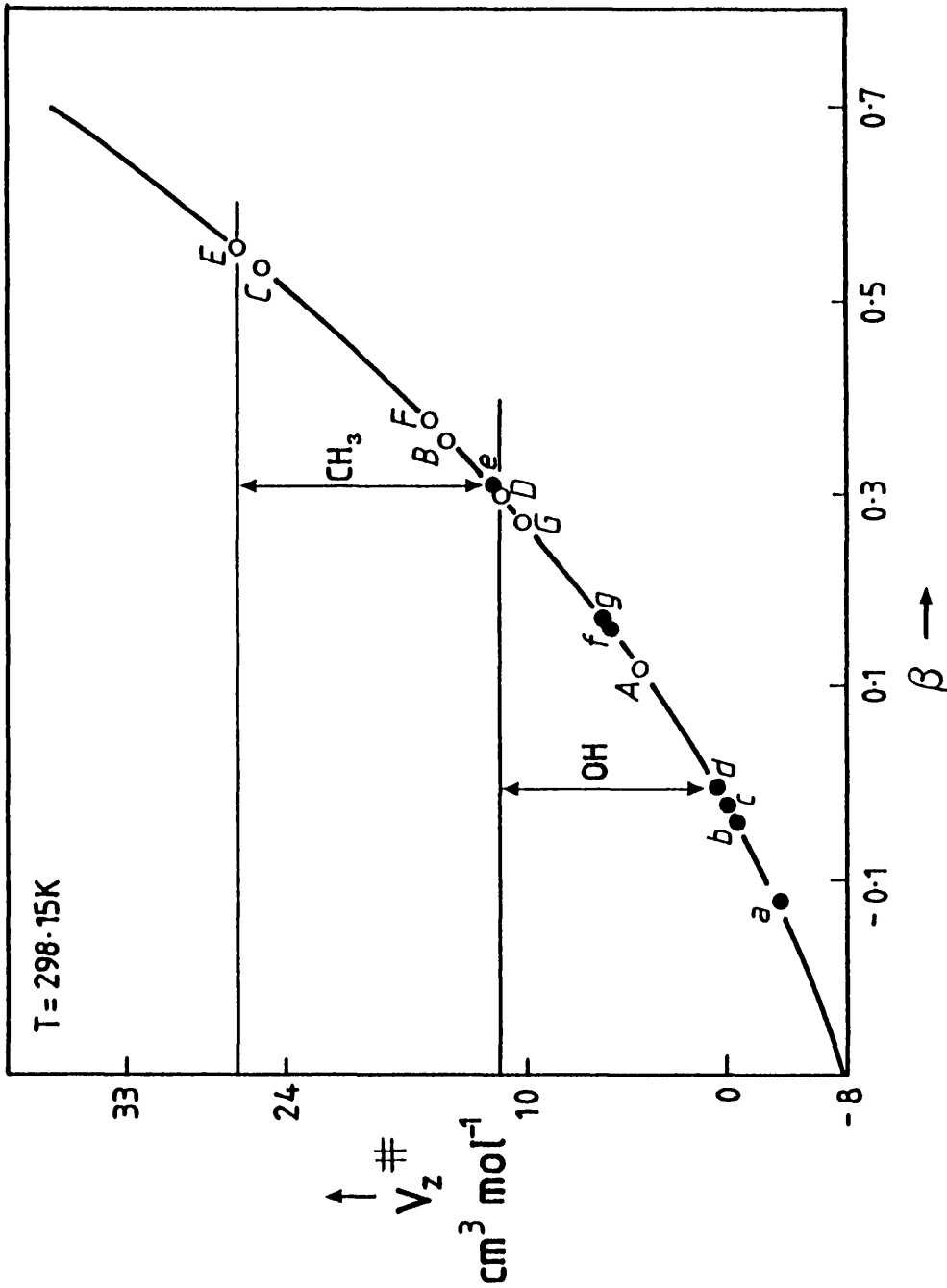


FIGURE 12.7

Dependence on  $\beta$  of  $V_z^\#$  (aq; 298 K). Plot includes estimates of  $V_z^\#$  for groups in aliphatic solutes calculated from partial molar volume data (O) and estimates of  $V_z^\#$  calculated (●) using  $\beta$  quantities predicted by a  $C_{pz}^\#$  versus  $\beta$  plot; (1) a and A, -O-, (2) b and B, -NH<sub>2</sub>, (3) c and C, -COOH, (4) d and D, -OH, (5) e and E, -CH<sub>3</sub>, (6) f and F, -CH<sub>2</sub>-, (7) g and G, -H.

terms of group contributions<sup>10</sup> have been superimposed. In addition to this, the  $\beta$  values obtained from Figure 12.2 from the  $C_{pz}^\#$  values of the same groups, have been added to the plot. In all cases a shift along the  $\beta$  axis is noted.

## 12.6 Discussion

In discussing the trend observed in Figure 12.2 it is of interest to note the experimental estimates of  $C_{pz}^\#$  in terms of group contributions of neutral aliphatic solutes scatter across  $\beta = 0$ . For the unimolecular solvolytic reaction under discussion if  $\beta < 0$  then the solvent equilibrium shifts to favour the short bonded form, X water species, whereas if  $\beta > 0$  the solvent equilibrium shifts to favour the long bonded form, Y water species. It is however too great a generalisation to suggest that if  $\beta < 0$  then a structure breaking influence has been identified, likewise if  $\beta > 0$  a structure forming influence has been identified. This is because the  $\beta$  parameter consists of two contributing terms i.e.  $\beta = \beta_Y - \beta_X$ . For example in a situation in which  $\beta > 0$ , one can imagine two separate situations which could arise. (i)  $\beta_Y > 0$  and  $|\beta_X| < |\beta_Y|$  and (ii)  $\beta_X < 0$  and  $|\beta_X| > |\beta_Y|$ . In general terms  $C_{pz}^\#$  reflects the extent to which both forms of water are stabilised and destabilised. Similar comments are valid for Figures 12.3 and 12.4 where once again experimental data,  $C_{pz}^\infty$ , straddles across  $\beta = 0$ .

Figure 12.7 shows the poor agreement between  $\beta$  parameters obtained from experimental  $V_z^\infty$  and those obtained from  $C_{pz}^\infty$ . This poor agreement is understandable, because in identifying  $V_z^\infty$  with  $V_z^\#(aq)$  it has been assumed

that  $v_{z\infty}(\xi^{eq})$  is negligible. However,  $v_z^\infty(\xi^{eq})$  is an intrinsic part of the molar volume and as such cannot be regarded as negligible. A similar state of affairs is identified with  $C_{pz}(\xi^{eq})$ .

An attempt to derive an absolute scale for the heat capacities of ions in solution from ionic volumes<sup>14</sup> based on  $v_z^\infty(H^+;aq;298.15K) = -5 \text{ cm}^3 \text{ mol}^{-1}$  proved unsuccessful, the calculated heat capacities giving unacceptably large values for  $\beta$ .

In comparing  $\beta$  values produced by the above quantities one is effectively comparing a first derivative and a second derivative of the chemical potential, the parent quantity itself being a first derivative property of the Gibbs function. The problem of comparison lies in the increasing degree of complexity required to define a quantity each time one differentiates away from the central property the Gibbs function.

A similar argument can be extended to the work of Abraham and Marcus<sup>15</sup> who have attempted to separate partial molar heat capacities of salts in solution into their contributing single ion values, using the TATB and TPTB (see Chapters 3,4 and 5) assumptions in which;

$$\begin{aligned} C_{pz}^\infty(\text{Ph}_4\text{P}^+;aq;298 \text{ K}) &= C_{pz}^\infty(\text{Ph}_4\text{B}^-;aq;298 \text{ K}) \\ &= C_{pz}^\infty(\text{Ph}_4\text{As}^+;aq;298 \text{ K}) \end{aligned}$$

Granted the success of such sub-divisions in obtaining single ion values for  $v_z^\infty$ <sup>14,16</sup>,  $\mu_j^\circ$ <sup>17</sup>, and viscosity  $B$  coefficients<sup>18,19</sup> (see also Chapters 3,4 and 5) one hesitates in developing such a broad treatment to the

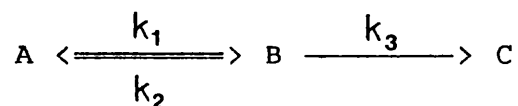
isobaric heat capacity of salts in solution.

Turning to Figure 12.6 in which a calculation of the molar isobaric heat capacity of solution has been attempted. The values of  $\beta^\ddagger$  and  $\beta$  used in the analysis were set such that  $\beta^\ddagger$  is small and  $\beta > 0$  which corresponds to a polar transition state and an apolar initial state. In describing the observed negative trend in the molar isobaric heat capacity of activation  $\Delta^\ddagger C_{pz}^\#(aq)$  for the unimolecular solvolysis of a solute Z two models have been suggested.

Robertson<sup>3</sup> model used a three term equation, known as the Valentier equation to calculate  $\Delta^\ddagger C_{pz}^\#$  from collected kinetic data.

$$\ln k = a_1 + a_2/T + a_3 \ln T \quad [12.43]$$

where  $a_1$ ,  $a_2$ , and  $a_3$  are used to calculate  $\Delta^\ddagger S^\#(T)$ ,  $\Delta^\ddagger H^\#(T)$  and  $\Delta^\ddagger C_{pz}^\#$  respectively at temperature T. Hence  $\Delta^\ddagger C_{pz}^\#$  is obtained from the linear least squares fit of the kinetic data to the above equation. The trends observed in Figure 12.6 emerge from a dominant, positive  $C_{pz}^\infty(Z)$ . If in the limit  $C_p^\infty(Z^\ddagger;aq) = 0$  and  $C_p^\infty(Z;aq) > 0$  then  $\Delta^\ddagger C_{pz}^\infty(aq) < 0$ . Albery and Robinson<sup>2</sup> argued, the isobaric heat capacity of activation is a temperature dependent phenomena and thus the three parameter Valentier equation used by Robertson was not strictly accurate. The argument progressed to suggest the reaction does not take place through a mechanism with one rate determining step. Rather it proceeded through an intermediate e.g. an ion pair. The following scheme was proposed;



Then  $k_{\text{obs}} = k_1/(1+\alpha)$  where  $\alpha = (k_2/k_3)$ . This scheme leads to an apparent  $\Delta^\ddagger C_{\text{pz}}^\#$  which is negative and depends on temperature.

In the calculation shown in Figure 12.6 the sign and magnitude of  $\Delta^\ddagger C_{\text{pz}}^\#$  together with inverted bell shape of the plot appear to agree with trends in  $\Delta^\ddagger C_{\text{pz}}^\infty(\text{aq};T;p)$  calculated from the kinetic data using the Alberly-Robinson<sup>2</sup> model. However it is difficult to ignore the role of the solvent in determining both the sign and magnitude of the molar isobaric heat capacity of activation. This gives rise to the possibility that both the solvent equilibrium and complexity in mechanism contribute to the observed trends in  $\Delta^\ddagger C_{\text{pz}}^\#$ , neither models accounting for trends observed in the experimental data.

The calculations presented in this Chapter point to a method of understanding the effects of solvent on the isobaric heat capacity of activation.

## References Chapter 12

- (1) R.E.Robertson, M.J.Blandamer, J.M.W.Scott, "Progress in Physical Organic Chemistry", ed.R.W. Taft, Vol.15, J.Wiley & Sons, New York, (1985)
- (2) J.Albery, R.H.Robinson, Trans.Faraday Soc., 65, 980, (1969)
- (3) R.E.Robertson, Progr.Phys.Org.Chem., 4, 203, (1967)
- (4) M.J.Blandamer, J.Burgess, A.W.Hakin, J.M.W.Scott, "Water and Aqueous Solutions", ed. G.W.Neilson, J.E.Enderby, Bristol, Adam Hilgar, 137, (1986)
- (5) H.S.Franks, "Water a Comprehensive Treatise", ed. F.Franks, Plenum Press, New York, Vol.1, Chapt 14, (1973)
- (6) R.Lumry, E.Battistel, C.Jolicoeur, Faraday Soc. Disc., 17, 93, (1982)
- (7) C.M.Davis, T.A.Litovitz, J.Chem.Phys., 42, 2563, (1965)
- (8) R.Lumry *private communication*
- (9) E.Grunwald, J.Am.Chem.Soc., 106, 5414, (1984)
- (10) G.Perron, J.E.Desnoyers, Fluid Phase Equilibria, 2, 239, (1979)
- (11) A.Roux, G.M.Musbally, G.Perron, J.E.Desnoyers, P.P.Singh, E.M.Wooley, L.G.Hepler, Can.J.Chem., 56, 24, (1978)
- (12) J.J.Spitzer, I.V.Olofsson, P.P.Singh, L.G.Hepler, Thermochem.Acta., 28, 155, (1979)
- (13) I.V.Olofsson, J.J.Spitzer, L.G.Hepler, Can.J. Chem., 56, 1871, (1978)
- (14) F.J.Millero, Chem.Revs., 71, 147, (1971)
- (15) M.H.Abraham, Y.Marcus *private communication*
- (16) B.E.Conway, J.Soln.Chem., 7, 721, (1978)
- (17) M.J.Blandamer, J.Burgess, B.Clark, A.W.Hakin, N. Gossal, S.Radulovic, P.P.Duce, P.Guardado, F. Sanchez, C.D.Hubbard, E-E.A.Abu-Gharib, J.Chem. Soc., Faraday Trans. I, 82, 1471, (1985)
- (18) K.G.Lawrence, A.Sacco, J.Chem.Soc., Faraday Trans. I, 79, 614, (1983)

- (19) K.G.Lawrence, R.T.M.Bickbell, A.Sacco,  
A.Dell'Atti, J.Chem.Soc.,Faraday Trans. I, 81,  
1133, (1985)
- (20) R.P.Marchi, H.Eyering, J.Phys.Chem.,Ithaca, 68,  
221, (1964)
- (21) G.Wada, Bull.Chem.Soc.Japan, 34, 955, (1961)



# Appendix

1

## Section 1

Program MJB3 is written in Hewlett Packard BASIC for the HP 8451A diode array spectrophotometer. The program was used for the collection of absorbance and time data for kinetic analysis. The key to the arrays in line 70 is as follows:

- P(5,100) - Dimensions array space for a maximum of 100 absorbance readings at up to 5 separate wavelengths.
- T(5,100) - Dimensions array space for the time readings at which absorbance readings were taken for each of the 5 wavelengths.
- C(5) - Array contains the time step, C(1) i.e. the time between each absorbance reading and the total run time, C(2).
- L(5) - Contains the wavelengths to be analysed.
- N(20) - Dimensions array space for the number of readings, N(1), and the wavelength limits between which the spectrophotometer scans. Lower limit N(19) and upper limit N(20).

A summary of the main features of the program is given below.

Line 80 is an error trap. If an error occurs when the program is running then subroutine ERROR at line 870 is invoked. This routine prints out the line number at which the error has occurred and the error number. It also terminates any measuring process.

Line 100 takes the user to a section of the program (lines 480 - 780) in which the necessary information to

conduct a run is entered into the spectrophotometer. The user is prompted to answer a number of questions. Line 530 inquires how many wavelengths are to be analysed? Line 570 asks what are the wavelengths to be analysed? Line 610 asks for the duration in seconds between absorbance readings? Finally lines 700 to 750 ask what are the wavelength boundaries inside which the spectrophotometer should operate?

Lines 110 to 180 instruct the user to take a suitable reference run. This spectrum is automatically stored and subtracted from the spectra of the sample under study.

Lines 190 to 310 ensure the absorbance reading of the sample is taken at the specified wavelength (or wavelengths), at the interval dictated by the time step for the duration of the run calculated by the program as C(2). Absorbance and time readings are entered into arrays P and T respectively.

Line 320 terminates the absorbance and time measuring process.

Line 330 gives a copy of the sample spectra on the in-built thermal printer.

Lines 360 to 400 print out (or display) the collected absorbance and time data.

Lines 410 to 440 copy the absorbance and time data onto disk.

```

10 : NJ83
20 ! FIRST ORDER; FIVE LAMBDA
30 ALPHA
40 ERASE STATUS
50 OPTION BASE 1
60 Y$="Y"
70 DIM P(5,100),T(5,100),N(20),
   C(5),L(5)
80 ON ERROR GOSUB 870
90 J=0
100 GOSUB 480
110 DISP "REFERENCE RUN?"
120 INPUT X$
130 IF X$#Y$ THEN 190
140 DISP "REFERENCE READY?"
150 INPUT X$
160 IF X$#Y$ THEN 140
170 REFERENCE
180 IF NMEAS=0 THEN 180
190 DISP "SAMPLE IN SYSTEM?"
200 INPUT X$
210 IF X$#Y$ THEN 190
220 OVERLAY N(19),N(20),0,2
230 MEASURE 1,C(1),0,C(2)
240 SETTIME 0,0
250 FOR I=0 TO N(1)-1
260 IF NMEAS=I THEN 260
270 J=J+1
280 FOR K=1 TO M @ P(K,J)=VALUE(
   L(K))
290 GOSUB 800
300 NEXT K
310 NEXT I
320 STOP MEASURE
330 COPY
335 N(19)=0
336 DISP "PRINT DATA?" @ INPUT X
   $
337 IF X$=Y$ THEN N(19)=1
340 DISP "DATA"
350 N(1)=N(1)-1
360 FOR K=1 TO M
370 FOR I=1 TO N(1) STEP 1
375 IF N(19)=1 THEN PRINT I,T(K,
   I),P(K,I)
380 DISP I,T(K,I),P(K,I)
390 NEXT I
400 NEXT K
410 VOLUME " :D701" IS "MIKE1"
420 ASSIGN# 1 TO "DATA.MIKE1"
430 PRINT# 1 ; N(),P(),T(),L()
440 ASSIGN# 1 TO *
450 PRINT "DATA ON DISC"
460 PRINT "THAT IS ALL, FOLKS"
470 END
480 CLEAR @ PRINT "HELLO"
490 PRINT "FIRST ORDER LOG"
500 DISP "SYSTEM"
510 INPUT A$
520 PRINT "SYSTEM=",A$
530 DISP "NUMBER OF WAVELENGTHS?"
   "
540 INPUT M
550 N(10)=M
560 FOR I=1 TO M
570 DISP "WAVELENGTH/NM ?"
580 INPUT L(I)
590 PRINT "WAVELENGTH = ",L(I)
600 NEXT I
610 DISP "TIME STEP ?"
620 INPUT C(1)
630 PRINT "TIME STEP=",C(1)
640 DISP "NUMBER OF READINGS?"
650 INPUT N(1)
660 C(2)=N(1)*C(1)
670 PRINT "RUN TIME=",C(2)
680 N(1)=INT(C(2)/C(1))+1
690 PRINT "NUMBER OF READINGS=",
   N(1)
700 DISP "WAVELENGTH RANGE"
710 DISP "LOWER LAMBDA="
720 INPUT N(19)
730 DISP "UPPER LAMBDA"
740 INPUT N(20)
750 PRINT "RANGE=",N(19),"TO",N(
   20)
760 DISP "OK?"
770 INPUT X$@ IF X$#Y$ THEN 700
780 RETURN
790 END
800 ! TIME
810 W=DATE
820 IF W=0 THEN T(K,J)=TIME @ RE
   TURN
830 V=TIME
840 T(K,J)=V+24*60*60*DATE
850 RETURN
860 END
870 ! ERROR
880 PRINT "ERRN=",ERRN
890 PRINT "ERRL=",ERRL
900 PRINT "STOP MEAS"
910 GOTO 320
920 END

```

## Section 2

Program MJB4 is written in Hewlett Packard BASIC. It's function was to read the absorbance/time data collected by program MJB3 and to use these data in a non-linear least squares analysis. From this analysis an estimated rate constant for reaction could be obtained. A brief summary of the main program routines is given below.

Lines 10 to 90 initialise the program and dimension array space for the data used in the analysis.

Lines 100 to 170 read absorbance and time data from a disk into the program (n.b. these data are those collected and stored by program MJB3).

Line 190 is a GOSUB statement which accesses lines 1110 to 1330 of the program. In this section the user is prompted for an estimated rate constant, a guessed  $P_0$  and a guessed  $P_\infty$ . These estimates are used in a non-linear least squares analysis (see Section 2.5 of Chapter 2). A facility for dropping data points from the analysis is also included in this section of the program.

Lines 200 to 270 set up arrays and variables for the data analysis.

Line 280 is a GOSUB statement which accesses lines 1350 to 1420 of the program. Line 1380 calculates  $P_t$  from the inputted guesses of  $P_0$ ,  $P_\infty$  and  $k$  (see equation [2.10] of Chapter 2) and line 1390 calculates the difference between an observed absorbance and the calculated absorbance,  $P_t$ . The sum of the square of the residuals is calculated in line 1400.

Lines 300 to 320 contain the first call to a plotting routine contained in lines 1620 to 2110 of the program.

This call produces a plot of absorbance against time of the experimental data.

Lines 330 to 670 contain the non-linear least squares analysis discussed in Section 2.5 of Chapter 2. The procedure is iterative and either continues for 10 cycles or comes out of the analysis cycle when the sum of the square of the residuals is less than  $1 \times 10^{-5}$ .

Lines 680 to 1090 output the information obtained from the analysis to the thermal printer. This includes the standard deviation on the absorbance, a rate constant and estimates of  $P_0$  and  $P_\infty$ . Two additional plots are available in this section of the program. They are called from line 830 and utilise the plot routine which starts at line 1620. The first plot compares the experimental absorbance/time curve with that predicted using the estimates of  $P_t$  calculated in the analysis. The second plot is a typical first order plot of  $\ln\{(P_\infty - P_0)/(P_\infty - P_t)\}$  against time for both the experimental data and data calculated from the results of the non-linear least squares analysis. Standard errors on all of the calculated parameters are printed out in lines 930 to 950.

```

10 ! MJ64
20 CLEAR
30 ALPHA
40 DISP "HI"
50 DISP "GETTING DATA"
60 Y$="Y"
70 ! DATA ANALYSIS; FIVE LAMBDA
80 OPTION BASE 1
90 DIM P(5,100),T(5,100),N(20),
L(5)
100 MASS STORAGE IS ":0701"
110 CRT OFF
120 VOLUME ":0701" IS "MIKE1"
130 ON ERROR GOSUB 1570
140 ASSIGN# 1 TO "DATA.MIKE1"
150 READ# 1 : N(),P(),T(),L()
160 ASSIGN# 1 TO *
170 CRT ON
180 DIM C(5),X(100,3),Q(100),Y(1
00),A(3),Z(1),V(3,3),W(3,100
)
190 GOSUB 1110
200 DISP "ANALYSIS UNDERWAY"
210 FOR B=1 TO N(10)
220 N(7)=0 @ N(8)=0
230 N(19)=0
240 IF L(B)=0 THEN 1090
250 PRINT "SET",E,"WAVELENGTH=",
L(B)
260 S=0
270 I=N(1)
280 GOSUB 1350
290 N(15)=0
300 REDIM X(I,3),Q(I),Y(I),W(3,I
)
310 DISP "PLOT DATA?" @ INPUT X$
320 IF X$=Y$ THEN GOSUB 1620
330 FOR K=1 TO 10
340 DISP "CYCLE",K
350 MAT Q=ZER@ MAT A=ZER
360 MAT X=ZER@ MAT Y=ZER
370 GOSUB 1350
380 FOR J=1 TO N(1)
390 U=EXP(-(R*T(B,J))) @ X(J,1)=
U
400 X(J,2)=1-U
410 X(J,3)=-((C(1)-C(2))*T(B,J)*
U)
420 NEXT J
430 MAT W=TRN(X)
440 MAT V=W*X
450 MAT W=INV(V)*W
460 MAT A=W*Y
470 G=R+A(3)
480 IF G>0 THEN 530
490 PRINT "NEG RATE CONSTANT",G
500 PRINT "INPUT WAS",R
510 DISP "FIT ABORT"
520 GOTO 190
530 R=G @ C(1)=C(1)+A(1) @ C(2)=
C(2)+A(2)
540 GOSUB 1350
550 DISP "RK=",R
560 DISP "SUM SQ RESID=",S
570 N(8)=S
580 F=ABS(N(8)-N(7))
590 F=100*F/N(8)
600 IF F<.1 THEN 670
610 N(7)=S
620 DISP "HAPPY"
630 INPUT X$
640 IF X$=Y$ THEN 670
650 IF S<.00001 THEN 670
660 NEXT K
670 DISP "FIT COMPLETE"
680 DISP "DATA SUMMARY?"
690 INPUT X$ @ M=0
700 IF X$=Y$ THEN M=1
710 DISP "PLOT RATE DATA?"
720 INPUT X$ @ L=0
730 IF X$=Y$ THEN L=1
740 IF M=0 THEN 780
750 FOR J=1 TO N(1)
760 PRINT J,T(J),P(J),Q(J),Y(J)
770 NEXT J
780 S=(S/(N(1)-3))^(1/2)
790 PRINT "ST DEV ON ABS=",S
800 PRINT "RATE CONSTANT=",R
810 PRINT "P-ZERO=",C(1)
820 PRINT "P-INF=",C(2)
830 IF L=1 THEN GOSUB 1440
840 MAT V=TRN(X)*X
850 MAT V=INV(V)
860 ! DISPERSION MATRIX
870 MAT Q=X*A
880 MAT Q=Y-Q
890 MAT Z=TRN(Q)*Q
900 Z(1)=Z(1)/(N(1)-3)
910 PRINT "ST DEV=",Z(1)^(1/2)
920 MAT V=(Z(1))*V
930 PRINT "ST ERROR ON P-ZERO=",
V(1,1)^(1/2)
940 PRINT "ST ERROR ON P-INFIN=",
V(2,2)^(1/2)
950 PRINT "ST ERROR ON K=",V(3,3
)^(1/2)
960 DISP "PRINT VAR-COVAR MAT?"
970 INPUT X$
980 IF X$=Y$ THEN MAT PRINT V
990 DISP "CORR. COEFF?"
1000 INPUT X$
1010 IF X$#Y$ THEN GOTO 1070
1020 FOR K=1 TO 3
1030 FOR L=1 TO 3
1040 S=V(K,L)/(V(K,K)*V(L,L))^(
/2)
1050 PRINT K,L,S
1060 NEXT L @ NEXT K
1070 NEXT B
1080 DISP "THAT IS ALL,FOLKS"
1090 PRINT "THAT IS ALL,FOLKS"

```

```

1100 END
1110 PRINT "HELLO AGAIN"
1120 DISP "RUN NUMBER?" @ INPUT
N(18)
1130 PRINT "NO. WAVELENGTHS=", N(1
0)
1140 PRINT "RUN =", N(18)
1150 PRINT "NUMBER OF DATA POINT
S=", N(1)
1160 DISP "GUESSED RK"
1170 INPUT R
1180 PRINT "EST K=", R
1190 DISP "GUESSED P-ZERO="
1200 INPUT C(1)
1210 DISP "GUESSED P=INFIN="
1220 INPUT C(2)
1230 PRINT "P-ZERO=", C(1), "P-INF
IN=", C(2)
1240 N(1)=N(1)-1
1250 DISP "DROP POINTS?"
1260 INPUT X$
1270 Q=0
1280 IF X$#Y$ THEN 1310
1290 DISP "POINTS DROPPED="
1300 INPUT Q
1310 N(1)=N(1)-Q
1320 I=N(1)
1330 RETURN
1340 END
1350 ! CALC
1360 S=0
1370 FOR J=1 TO N(1)
1380 Q(J)=(C(1)-C(2))*EXP(-(R*T(
B, J)))+C(2)
1390 Y(J)=P(B, J)-Q(J)
1400 S=S+Y(J)*Y(J)
1410 NEXT J
1420 RETURN
1430 END
1440 ! PLOT DATA
1450 N(19)=1
1460 N(15)=0
1470 DISP "COMPARISON PLOT?" @ I
NPUT X$
1480 IF X$#Y$ THEN 1510
1490 N(15)=0
1500 GOSUB 1620
1510 DISP "FIRST ORDER PLOT?" @
INPUT X$
1520 IF X$#Y$ THEN 1550
1530 N(15)=1
1540 GOSUB 1620
1550 RETURN
1560 END
1570 ! ERROR TRAP
1580 PRINT "ERRN=", ERRN
1590 PRINT "ERRL=", ERRL
1600 DISP "ERROR"
1610 STOP
1620 ! PLOT DATA

1630 M=B
1640 GCLEAR
1650 IF N(15)=0 THEN 1730
1660 DISP "FIRST ORDER PLOT"
1670 FOR K=1 TO I
1680 P(M, K)=(P(M, K)-C(2))/(C(1)-
C(2))
1681 IF P(M, K)<0 THEN P(M, K)=0 @
GOTO 1690
1682 P(M, K)=LOG(F(M, K))
1690 P(M, K)=ABS(F(M, K))
1700 Q(K)=(Q(K)-C(2))/(C(1)-C(2)
)
1701 IF Q(K)<0 THEN Q(K)=0 @ GOT
O 1710
1702 Q(K)=LOG(Q(K))
1710 Q(K)=ABS(Q(K))
1720 NEXT K
1730 G=AMAX(Q)
1740 LORG 5
1750 G=G+G/10
1760 SCALE -(T(M, I)/10), T(M, I)+T
(M, I)/10, -(G/10), G+G/10
1770 H=T(M, I)/10
1780 XAXIS 0, H, 0, T(M, I)
1790 H=G/5
1800 YAXIS 0, H, 0, G
1810 PENUP
1820 MOVE T(M, I), P(M, I)
1830 FOR K=1 TO I
1831 IF P(M, K)=0 THEN GOTO 1860
1840 MOVE T(M, K), P(M, K)
1850 LABEL "+"
1860 NEXT K @ PENUP
1870 IF N(19)=0 THEN 1920
1880 MOVE T(M, I), Q(1)
1890 LINETYPE 1
1900 FOR K=1 TO I
1901 IF Q(K)=0 THEN GOTO 1911
1910 DRAW T(M, K), Q(K)
1911 NEXT K
1920 PENUP
1930 LDIR 90
1940 H=T(M, I)/5
1950 FOR K=H TO T(M, I) STEP H
1960 MOVE K, .1
1970 Z=INT(K)
1980 LABEL VAL$(Z) @ NEXT K
1990 LDIR 0
2000 H=G/5
2010 FOR K=H TO G STEP H
2020 MOVE T(M, I)/10, K
2030 Z=INT(100*K)/100
2040 LABEL VAL$(Z)
2050 NEXT K
2060 SCALE 0, 100, 0, 100
2070 MOVE 50, 50
2080 LABEL "RUN NO.", VAL$(N(18))
2090 FRAME
2100 COPY

2110 ALPHA @ RETURN
2120 END

```

### Section 3

This HP BASIC program, AWH1, was written to run on the in-built HP 85A computer of the Hewlett Packard 8451A diode array spectrophotometer. It's purpose was to produce a scan of a given sample in the region 190 to 820 nm and to report the peak positions at which maximum absorbance occurred. Line 30 of the program initialises the spectrophotometer. Lines 50 to 110 give the user the option to take a scan of some suitable reference - this spectrum is automatically stored and then subtracted from the sample spectrum. Lines 120 to 170 take the spectrum of the sample under study. In lines 171 to 180 the PEAK# command is used to return the wavelength and absorbance readings of the 20 largest peaks within the spectrum. Finally line 190 gives a hard copy of the sample spectrum and the results of the PEAK# procedure on the in-built thermal printer.

```

10 ! AWH1
20 ! LAMBOA SCAN
30 ERASE STATUS
40 OPTION BASE 10 GOSUB 220
50 DISP "REFERENCE REQUIRED?"
60 INPUT Y$
70 IF Y$#"Y" THEN 130
80 DISP "REF CELL IN POSITION?"
85 INPUT Y$
90 IF Y$#"Y" THEN 80
100 REFERENCE
110 IF NMEAS=0 THEN 110
120 DISP "SAMPLE IN POSITION?"
130 DISP "CELL IN PLACE?"
140 INPUT Y$
150 IF Y$#"Y" THEN 120
160 MEASURE 1
164 PRINT "NO. "; " LAMBOA "; "ABSO
RBANCE"
170 IF NMEAS=0 THEN 170
171 PEAK FIND
172 CALCULATE
173 FOR X=1 TO PEAK#(0)
174 PRINT X;;;PEAK#(X);;;VALUE(P
EAK#(X))
176 NEXT X
180 STOP MEASURE
190 COPY
200 DISP "END OF RUN"
210 END
220 A$="HELLO"
230 CLEAR
240 PRINT A$
250 PRINT "AWH1"
260 DISP "SYSTEM IS "
270 INPUT B$
290 RETURN

```

#### Section 4

Program ANDY3 is written in HP BASIC and was used to give a linear least squares fit of a given set of data. In the example set up in the program below the equation  $y = a_1 + a_2x$  is solved for  $a_1$  and  $a_2$ . In matrix form this problem can be written as;

$$\begin{array}{c|c} \begin{array}{c} y_1 \\ y_2 \\ y_3 \\ \cdot \\ \cdot \\ y_n \end{array} & = & \begin{array}{c|c} \begin{array}{c} a_1 \\ a_2 \end{array} & \begin{array}{c} 1 \ x_1 \\ 1 \ x_2 \\ 1 \ x_3 \\ \cdot \ \cdot \\ \cdot \ \cdot \\ 1 \ x_n \end{array} \end{array}$$

$$Y = \beta X$$

where n sets of data are available for analysis.

$\beta$  can be calculated by performing the matrix operations shown in equation |1| on matrices X and Y.

$$\beta = (X^T X)^{-1} X^T Y \quad |1|$$

where  $X^T$  is the transpose of matrix X and  $( )^{-1}$  refers to the inversion of a matrix.

Turning back to the program, line 80 contains the data which is read by line 100 into matrix Y and line 90 contains the data which is read into matrix X. Lines 110 to 190 calculate matrix  $\beta$  using equation |1| and print out the results.

The variance of the fit can be calculated from equation |2|.

$$\sigma^2 = (n-\theta)^{-1}(Y-X\beta)^T(Y-X\beta) \quad |2|$$

where  $n$  refers to the numbers of data points in the analysis and  $\theta$  is the number of unknowns to be estimated. The standard deviation is thus given as the square root of the variance. Lines 200 to 340 of the program use equation 2 to produce an estimate of the standard deviation.

The variance-covariance matrix is used to find the variances of the estimated parameters. The matrix is calculated from equation |3|.

$$\theta = \sigma^2 V \quad |3|$$

where  $V$  is the dispersion matrix, which is defined by equation |4|.

$$V = (X^T X)^{-1} \quad |4|$$

The variances of the estimated parameters are obtained from the diagonal of the matrix  $\theta$ . Lines 350 to 450 of the program carry out these operations.

Finally lines 460 to 490 calculate the residuals i.e. the calculated  $Y$  values (obtained using the estimated parameters) are subtracted from the values entered into matrix  $Y$  at line 80.

```

10 ! ANDY 3
20 OPTION BASE 1
30 CLEAR
40 PRINT "LEAST SQUARES FITTING
"
50 PRINT
60 DIM Y(5),X(5,2),V(2,2)
70 DIM U(7,7),S(2),D(1),T(5)
80 DATA .000018248,.000096573,
.00019156,.0002788,.0003598
90 DATA 1,.001,1,.005,1,.01,1,
.015,1,.02
100 MAT READ Y,X
110 MAT U=ZERO MAT S=ZER
120 MAT U=TRN(X)*X
130 MAT U=INV(U)
140 MAT U=U*TRN(X)
150 MAT S=U*Y
160 PRINT "-----
"
170 PRINT "CALCULATED s"
180 MAT PRINT S
190 PRINT "-----
"
200 PRINT "ESTIMATED VARIANCE"
210 DISP "HOW MANY DATA POINTS?"
220 INPUT N
230 N=N-2
240 REDIM U(7,1)
250 MAT U=X*S
260 MAT U=Y-U
270 MAT D=TRN(U)*U
280 MAT D=(1/N)*D
290 MAT PRINT D
300 PRINT "-----
"
310 PRINT "STANDARD DEVIATION"
320 F=SQR(D(1))
330 PRINT F
340 PRINT "-----
"
350 PRINT "VARIANCE/COVARIANCE M
ATRIX"
360 MAT V=TRN(X)*X
370 MAT V=INV(V)
380 F=F^2
390 MAT V=(F)*V
400 FOR I=1 TO 2
410 Z=SQR(V(I,I))
420 PRINT
430 PRINT "STANDARD ERROR";I;Z
440 NEXT I
450 PRINT "-----
"
460 MAT T=X*S
470 MAT Y=Y-T
480 MAT PRINT Y
490 PRINT "-----
"
500 END

```

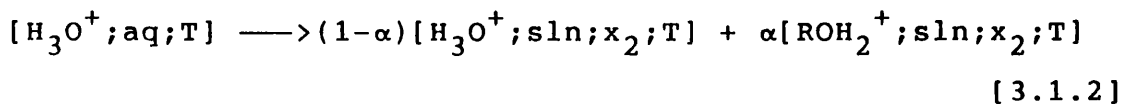
Appendix  
2

## Section 1

In calculating the transfer parameter for  $H^+$ , Wells imagines a solution containing 1 mole of  $H^+X^-$ ,  $n_1$  moles of water and  $n_2$  moles of alcohol, ROH. At equilibrium 1 mole of hydrogen ions is present in the form  $\alpha$  mole of  $ROH_2^+$  and  $(1-\alpha)$  mole of  $H_3O^+$ . If 1 =  $H_2O$  and 2 = ROH and  $H_3O^+$  is used to represent some solvated proton species then;

$$G(\text{system};T) = (n_1-1+\alpha)\mu_1(\text{system};T) + (n_2-\alpha)\mu_2(\text{system};T) \\ + \alpha\mu(ROH_2^+; \text{system};T) + (1-\alpha)\mu(H_3O^+; \text{system};T) \\ + \mu(X^-; \text{system};T) \quad [3.1.1]$$

The following hypothetical process is described for 1 mole of hydrogen ions.



Hence the transfer chemical potential describes the following comparison;

$$\mu^\#(H_3O^+; \text{aq}; T) \longrightarrow (1-\alpha)\mu^\#(H_3O^+; \text{sln}; \text{c-scale}; x_2; T) \\ + \alpha\mu^\#(ROH_2^+; \text{sln}; \text{c-scale}; x_2; T)$$

A transfer chemical potential can thus be written;

$$\Delta(\text{aq} \rightarrow x_2)\mu^\#(H_3O^+; \text{c-scale}; \text{sln}; T) = \\ [(1-\alpha)\mu^\#(H_3O^+; \text{sln}; \text{c-scale}; x_2; T) \\ + \alpha\mu^\#(ROH_2^+; \text{sln}; \text{c-scale}; x_2; T) \\ - \mu^\#(H_3O^+; \text{c-scale}; \text{aq}; T)]$$

$$\begin{aligned}
&= [\mu^\#(\text{H}_3\text{O}^+; \text{sln}; \text{c-scale}; x_2; T) - \mu^\#(\text{H}_3\text{O}^+; \text{c-scale}; \text{aq}; T)] \\
&\quad + \alpha [\mu^\#(\text{ROH}_2^+; \text{sln}; \text{c-scale}; x_2; T) - \mu^\#(\text{H}_3\text{O}^+; \text{sln}; \text{c-scale}; x_2; T)]
\end{aligned}
\tag{3.1.3}$$

In the absence of any chemical complexity  $\alpha$  is zero and hence the transfer quantity can be calculated using the Born equation to determine the first term on the right hand side of equation [3.1.3]. Hence<sup>4</sup>;

$$\begin{aligned}
\Delta(g \rightarrow \text{sln}) \mu^\#(\text{H}_3\text{O}^+; \text{Born}; \text{c-scale}; \text{sln}; T) \\
= -[(Nz_j^2 e^2) / (8\pi r_j^2 \epsilon_0)] (1 - (1/\epsilon_r))
\end{aligned}
\tag{3.1.4}$$

where  $N$  is Avogadro's number,  $z_j$  is the charge number of ion- $j$ ,  $e$  is the electronic charge,  $r_j$  is the radius of ion- $j$  and  $\epsilon_r$  is the relative permittivity of the solvent in which ion- $j$  is dissolved.

This however is only one contribution to the total transfer chemical potential of the ion, and attention in the analysis switches to the second term on the right hand side of equation [3.1.3]. Turning back to equation [3.1.1], if the system is dilute in  $\text{H}^+\text{X}^-$  then  $(n_1 - 1 + \alpha) \approx n_1$  and  $(n_2 - \alpha) \approx n_2$ . A chemical equilibrium involves  $\text{H}_3\text{O}^+$ ,  $\text{ROH}_2^+$ ,  $\text{H}_2\text{O}$  and  $\text{ROH}$ ;



$$\begin{aligned}
\Rightarrow \mu^{\text{eq}}(\text{H}_3\text{O}^+; \text{system}; T) + \mu^{\text{eq}}(\text{ROH}; \text{system}; T) \\
= \mu^{\text{eq}}(\text{ROH}_2^+; \text{system}; T) + \mu^{\text{eq}}(\text{H}_2\text{O}; \text{system}; T)
\end{aligned}
\tag{3.1.5}$$

The system can be described as a solution of solutes  $\text{ROH}_2^+\text{X}^-$  and  $\text{H}_3\text{O}^+\text{X}^-$  in a solvent comprising ' $\text{H}_2\text{O} + \text{ROH}$ '. If the system has volume  $V$  at fixed temperature  $T$  and pressure

$p(\approx p^\circ)$  then  $c(\text{ROH}_2^+) = [n(\text{ROH}_2^+)/V]$  and  $c(\text{H}_3\text{O}^+) = [n(\text{H}_3\text{O}^+)/V]$ . Hence using 1 mole of  $\text{H}^+\text{X}^-$ ,  $c(\text{ROH}_2^+) = (\alpha/V)$  and  $c(\text{H}_3\text{O}^+) = [(1-\alpha)/V]$ .

$$\begin{aligned} & \mu^\#(\text{H}_3\text{O}^+; \text{c-scale}; x_2; \text{sln}; T) + RT \ln[(1-\alpha)y(\text{H}_3\text{O}^+; x_2)/Vc_r] \\ & + \mu^\circ(\text{ROH}; 1; T) + RT \ln(x_2 f_2) = \\ & \mu^\#(\text{ROH}_2^+; \text{c-scale}; x_2; \text{sln}; T) + RT \ln[\alpha y(\text{ROH}_2^+; x_2)/Vc_r] \\ & + \mu^\circ(\text{H}_2\text{O}; 1; T) + RT \ln(x_1 f_1) \end{aligned} \quad [3.1.6]$$

By definition the change in the Gibbs function for equation [3.1.5] is given by equation [3.1.7].

$$\begin{aligned} \Delta_r G^\#(\text{c-scale}) &= \mu^\#(\text{ROH}_2^+; \text{c-scale}; x_2; T) + \mu^\circ(\text{H}_2\text{O}; 1; T) \\ & - \mu^\#(\text{H}_3\text{O}^+; \text{c-scale}; x_2; T) - \mu^\circ(\text{ROH}; 1; T) \quad [3.1.7] \\ &= -RT \ln K^\#(\text{c-scale}; \text{sln}; x_2; T) \end{aligned}$$

where  $K^\#(\text{c-scale}; \text{sln}; x_2; T)$  is an equilibrium constant. Hence;

$$\begin{aligned} & \mu^\#(\text{ROH}_2^+; \text{c-scale}; \text{sln}; x_2; T) - \mu^\#(\text{H}_3\text{O}^+; \text{c-scale}; \text{sln}; x_2; T) \\ &= -RT \ln K^\#(\text{c-scale}; \text{sln}; x_2; T) + [\mu^\circ(\text{ROH}; 1; T) - \mu^\circ(\text{H}_2\text{O}; 1; T)] \end{aligned} \quad [3.1.8]$$

Equation [3.1.8] describes the difference between the chemical potentials of the solutes  $\text{ROH}_2^+$  and  $\text{H}_3\text{O}^+$  in a solvent 'ROH +  $\text{H}_2\text{O}$ ' which contains  $x_2$  mole fraction ROH, and where  $c_j = 1$  and  $y_j = 1$  for  $j = \text{H}_3\text{O}^+$  and  $\text{ROH}_2^+$ .

$$\begin{aligned} K^\#(\text{c-scale}; \text{sln}; x_2; T) &= [\alpha y(\text{ROH}_2^+; x_2)(1-x_2)f(\text{H}_2\text{O})] \\ & / [(1-\alpha)y(\text{H}_3\text{O}^+; x_2)x_2 f(\text{ROH})] \quad [3.1.9] \end{aligned}$$

Turning now to equation [3.1.3] Wells uses equation [3.1.8] to calculate the difference between the chemical potentials of  $\text{ROH}_2^+$  and  $\text{H}_3\text{O}^+$  to provide a second part to the transfer chemical potential of  $\text{H}^+$ . However an extrathermodynamic assumption is made in which  $\mu^\circ(\text{ROH};1;\text{T})$  is set equal to  $\mu^\circ(\text{H}_2\text{O};1;\text{T})$ . Hence;

$$\begin{aligned} \mu^\#(\text{ROH}_2^+; \text{c-scale}; \text{sln}; x_2; \text{T}) - \mu^\#(\text{H}_3\text{O}^+; \text{c-scale}; \text{sln}; \text{T}) \\ = -RT \ln K^\#(\text{c-scale}; \text{sln}; x_2; \text{T}) \end{aligned} \quad [3.1.10]$$

Thus equation [3.1.3] can be rewritten in the form;

$$\begin{aligned} \Delta(\text{aq} \rightarrow x_2) \mu^\#(\text{H}_3\text{O}^+; \text{c-scale}; \text{sln}; x_2; \text{T}) = \\ \Delta(\text{aq} \rightarrow x_2) \mu^\#(\text{H}_3\text{O}^+; \text{Born}; \text{c-scale}; \text{sln}; \text{T}) \\ + \alpha \{-RT \ln K^\#(\text{c-scale}; \text{sln}; x_2; \text{T})\} \end{aligned} \quad [3.1.11]$$

The validity of this extrathermodynamic assumption is doubtful<sup>1</sup>.

## Section 2

Accepting the extrathermodynamic assumption identified in Section 1 of this Appendix, the next stage of the Wells analysis is to calculate  $\alpha$  and  $K^\#(c\text{-scale};sln;x_2;T)$  by experiment. A spectrophotometric approach is used to study solutions containing  $H^+X^-$ ,  $H_2O$ , and MeOH together with a base, B, p-nitro aniline. Two equilibria are envisaged in these solutions;



and



These equilibria can be described using two different approaches. Description 1 assumes that the system is an aqueous solution whilst description 2 identifies a situation in which the solutes  $H_3O^+$ ,  $ROH_2^+$  and B are in a solvent mixture composed of ' $H_2O + ROH$ '.

### Description 1

Equilibrium constants  $K^\#(c\text{-scale};sln;T)$  for (a) and (b) are defined using equations [3.2.1] and [3.2.2].

$$K^\#_1(c\text{-scale};sln;T)(a) = \frac{[c(B)c(H_3O^+)/c(BH^+)x_1(H_2O)]}{[Y^1(B)Y^1(H_3O^+)/Y^1(BH^+)f(H_2O)]} \quad [3.2.1]$$

$$K^\#_1(c\text{-scale};sln;T)(b) = \frac{[c(B)c(ROH_2^+)/c(BH^+)c(ROH)]}{[Y^1(B)Y^1(H_3O^+)/Y^1(BH^+)Y^1(ROH)]} \quad [3.2.2]$$

Activity coefficients for these equilibria under description 1 are thus defined as;

$$F^1(a) = [Y^1(B)Y^1(H_3O^+)/Y^1(BH^+)f(H_2O)] \quad [3.2.3]$$

$$F^1(b) = [Y^1(B)Y^1(ROH_2^+)/Y^1(BH^+)Y^1(ROH)] \quad [3.2.4]$$

The ratio of the equilibrium constants is given by equation [3.2.5].

$$K^{\#}_1(\text{sln}; \text{c-scale}; T)(b)/K^{\#}_1(\text{sln}; \text{c-scale}; T)(a) = \frac{[c(ROH_2^+)x_1(H_2O)/c(ROH)c(H_3O^+)]}{[Y^1(ROH_2^+)f(H_2O)/Y^1(ROH)Y^1(H_3O^+)]} \quad [3.2.5]$$

### Description 2

Equilibrium constants for (a) and (b) are defined under description 2 by equations [3.2.6] and [3.2.7].

$$K^{\#}_2(\text{c-scale}; \text{sln}; T)(a) = \frac{[c(B)c(H_3O^+)/c(BH^+)x_1(H_2O)]}{[Y^2(B)Y^2(H_3O^+)/Y^2(BH^+)f(H_2O)]} \quad [3.2.6]$$

$$K^{\#}_2(\text{c-scale}; \text{sln}; T)(b) = \frac{[c(B)c(ROH_2^+)/c(BH^+)x_2(ROH)]}{[Y^2(B)Y^2(H_3O^+)/Y^2(BH^+)f(ROH)]} \quad [3.2.7]$$

The activity coefficients are thus defined as;

$$F^2(a) = [Y^2(B)Y^2(H_3O^+)/Y^2(BH^+)f(H_2O)] \quad [3.2.8]$$

$$F^2(b) = [Y^2(B)Y^2(ROH_2^+)/Y^2(BH^+)f(ROH)] \quad [3.2.9]$$

The ratio of the equilibrium constants is given by equation [3.2.10].

$$K_2^\#(\text{sln}; \text{c-scale}; T)(b) / K_2^\#(\text{sln}; \text{c-scale}; T)(a) = \frac{[c(\text{ROH}_2^+)x_1(\text{H}_2\text{O})/x_2(\text{ROH})c(\text{H}_3\text{O}^+)]}{[y^2(\text{ROH}_2^+)f(\text{H}_2\text{O})/f(\text{ROH})y^2(\text{H}_3\text{O}^+)]} \quad [3.2.10]$$

Wells<sup>3</sup> defines two quantities;

$$F_1 = [f(\text{B})f(\text{H}_3\text{O}^+)/f(\text{BH}^+)f(\text{H}_2\text{O})] \quad [3.2.11]$$

and

$$F_2 = [f(\text{B})f(\text{ROH}_2^+)/f(\text{BH}^+)f(\text{ROH})] \quad [3.2.12]$$

The ratio  $(F_1/F_2)$  is thus defined by equation [3.2.13].

$$(F_1/F_2) = [f(\text{ROH})f(\text{H}_3\text{O}^+)/[f(\text{H}_2\text{O})f(\text{ROH}_2^+)]] \quad [3.2.13]$$

Using equations [3.2.3], [3.2.4], [3.2.8] and [3.2.9] the ratios of the activity coefficients for description 1 and for description 2 are given by equations [3.2.14] and [3.2.15] respectively.

$$(F^1(a)/F^1(b)) = [y^1(\text{ROH})y^1(\text{H}_3\text{O}^+)] / [f(\text{H}_2\text{O})y^1(\text{ROH}_2^+)] \quad [3.2.14]$$

$$(F^2(a)/F^2(b)) = [f(\text{ROH})y^2(\text{H}_3\text{O}^+)] / [f(\text{H}_2\text{O})y^2(\text{ROH}_2^+)] \quad [3.2.15]$$

Wells states that at low  $x_2$ ,  $F_1 \approx 1.0$  and  $(F_1/F_2)$  remains at unity. These assumptions are consistent with equation [3.2.14]. In a given system the ratio  $y^1(\text{H}_3\text{O}^+)/y^1(\text{ROH}_2^+) \approx 1.0$  and in dilute aqueous solution  $y(\text{ROH}) \approx 1.0$  and  $f(\text{H}_2\text{O}) \approx 1.0$ . Therefore Wells appears to have switched his description of the system to that of an aqueous solution from description 2, which he started with. In terms of

description 1  $K^\#(c\text{-scale};sln;T)$  and  $\Delta_r G^\#$  would be found to be independent of the amount of ROH in the system. Transfer chemical potentials can not be calculated using this description. Only description 2 is applicable. Furthermore at  $x(\text{ROH}) > 0.1$  the ratio  $(F_1/F_2)$  can no longer be unity, because  $y(\text{ROH})$  is no longer close to unity.



# Appendix

3

## Section 1

### Example (i)

From equation [8.20];

$$d[-m_2\phi] + 1 + m_2 d[\ln\gamma_{\pm}] = 0$$

or  $d[m_2(1-\phi)] + d[\ln\gamma_{\pm}] = 0$

$$\Rightarrow \int_0^{m_2} d[m_2(1-\phi)] = \int_0^{m_2} m_2 d[\ln\gamma_{\pm}]$$

or  $1-\phi = -(1/m_2) \int_0^{m_2} m_2 d[\ln\gamma_{\pm}]$

$$\Rightarrow \phi-1 = (1/m_2) \int_0^{m_2} m_2 d\ln\gamma_{\pm}$$

### Example (ii)

$$-d[m_2(\phi-1)] + m_2 d\ln\gamma_{\pm} = 0$$

or  $-(\phi-1)dm_2 - m_2 d\phi + m_2 d\ln\gamma_{\pm} = 0$

$$\Rightarrow -(\phi-1)(dm_2/m_2) - d\phi + d\ln\gamma_{\pm} = 0$$

$$\int_0^{m_2} d\ln\gamma_{\pm} = \int_0^{m_2} d\phi + \int_0^{m_2} (\phi-1)(dm_2/m_2)$$

$$\Rightarrow \ln\gamma_{\pm} = (\phi-1) + \int_0^{m_2} (\phi-1)d\ln m_2$$

Section 2

$$\phi-1 = (1/m_2) \int_0^{m_2} [-|z_+z_-| S_\gamma(I^{1/2}/m^\circ)]$$

For a 1:1 salt;

$$\phi-1 = [-|z_+z_-|/m_2] S_\gamma \int_0^{m_2} d(m_2^{1/2}/m^\circ)$$

Hence;

$$\phi-1 = [-|z_+z_-|/m_2] S_\gamma [m_2^{3/2}/3(m^\circ)^{1/2}]$$

### Section 3

Where  $\ln \gamma_{\pm}$  is defined by equation [7.24]; let  $x = b(m_2)^{1/2}$   
and  $k = |z_+ z_-| (S_{\gamma}/b)$ .

$$\begin{aligned} \Rightarrow \quad d \ln \gamma_{\pm} &= [-kx/(1+x)] dx \\ &= -k \left[ \frac{1}{(1+x)} - \frac{x}{(1+x)^2} \right] dx \\ &= -k dx / (1+x)^2 \end{aligned}$$

Hence;

$$(1-\phi) = (k/x^2) \int_0^x [x^2/(1+x)^2] dx$$

$$\Rightarrow \quad (1-\phi) = (k/x^2) [(1+x) - (1/(1+x)) + 2 \ln(1+x)]$$

In a form analogous to the limiting law;

$$(1-\phi) = (kx/3) \left[ \left( \frac{3}{x^3} \right) \left[ (1+x) - \frac{1}{(1+x)} + 2 \ln(1+x) \right] \right]$$

Hence;

$$(1-\phi) = \left[ \left( |z_+ z_-| S_{\gamma} \right) / 3b \right] \left[ b(m_2)^{1/2} / m^{\circ} \right] \sigma(x)$$

#### Section 4

$$\ln \gamma_{\pm} = (\phi - 1) + \int_0^{m_2} (\phi - 1) d \ln m$$

$$\text{with } (\phi - 1) = [-|z_+ z_-| A_{\phi} I^{1/2} / (1 + b I^{1/2})]$$

$$\begin{aligned} \Rightarrow \ln \gamma_{\pm} &= [-|z_+ z_-| A_{\phi} I^{1/2} / (1 + b I^{1/2})] \\ &+ \int_0^{m_2} [-|z_+ z_-| A_{\phi} I^{1/2} / (1 + b I^{1/2})] d \ln m \end{aligned}$$

$$\text{with } d \ln m = (dm/m) = (dI/I)$$

$$\begin{aligned} \Rightarrow \ln \gamma_{\pm} &= [-|z_+ z_-| A_{\phi} I^{1/2} / (1 + b I^{1/2})] \\ &- |z_+ z_-| A_{\phi} \int_0^I [I^{1/2} / (1 + b I^{1/2})] (dI/I) \end{aligned}$$

$$\text{Let } x = b I^{1/2} \text{ and } dx = (b/2) I^{1/2} dI$$

$$dI = (2/b) I^{1/2} dx = (2/b)(x/b) dx = (2/b^2) x dx$$

$$dI = \int_0^I [I^{1/2} / (1 + b I^{1/2})] [dI/I] = \int_0^I (1/I^{1/2}) (1/(1 + b I^{1/2})) dI$$

$$dI = \int_0^x (b/x) (1/(1+x)) (2/b^2) x dx$$

$$dI = (2/b) \int_0^x [dx/(1+x)] = (2/b) \ln(1+x)$$

$$dI = (2/b) \ln(1 + b I^{1/2})$$

Hence;

$$\begin{aligned} \ln \gamma_{\pm} &= [-|z_+ z_-| A_{\phi} I^{1/2} / (1 + b I^{1/2})] \\ &- |z_+ z_-| A_{\phi} (2/b) \ln(1 + b I^{1/2}) \end{aligned}$$

Section 5

For  $\beta^0$ ;

$$\ln \gamma_{\pm}(\beta^0) = (\phi-1)\beta^0 + \int_0^{m_2} (\phi-1) d \ln m_2$$

$$\begin{aligned} \Rightarrow \ln \gamma_{\pm}(\beta^0) &= m_2 [(2v_m v_x)/v] \beta^0 + \int_0^{m_2} m_2 [(2v_m v_x)/v] \beta^0 (dm_2/m_2) \\ &= 2m_2 [(2v_m v_x)/v] \beta^0 \end{aligned}$$

For  $\beta^1$ ;

$$(\phi-1)\beta^1 = 2m_2 (v_m v_x/v) \beta^1 \exp(-\alpha m_2^{1/2})$$

From Section 2;

$$\begin{aligned} \ln \gamma_{\pm}(\beta^1) &= 2m_2 (v_m v_x/v) \beta^1 \exp(-\alpha m_2^{1/2}) \\ &\quad + \int_0^{m_2} 2m_2 (v_m v_x/v) \beta^1 \exp(-\alpha m_2^{1/2}) d \ln m_2 \\ &= 2m_2 (v_m v_x/v) \beta^1 \exp(-\alpha m_2^{1/2}) \\ &\quad + 2(v_m v_x/v) \beta^1 \int_0^{m_2} \exp(-\alpha m_2^{1/2}) dm_2 \end{aligned}$$

$$\text{let } -\alpha m_2^{1/2} = -(1/2)x(\alpha/m_2^{1/2})dm = dx$$

$$\Rightarrow dm_2 = (-2/\alpha)m_2^{1/2}dx = (-2/\alpha)(-x/\alpha)dx = (2/\alpha^2)x dx$$

$$I = 2(v_m v_x/v) \beta^1 \int_0^x (2/\alpha^2)x \exp(x) dx$$

$$\Rightarrow I = 2(v_m v_x/v) \beta^1 (2/\alpha^2) [\exp(x)[x-1]]$$

$$\Rightarrow I = 2(v_m v_x/v) \beta^1 (2/\alpha^2) [\exp(-\alpha m_2^{1/2}) [-\alpha m_2^{1/2} - 1]]$$

$$\Rightarrow I = 2(v_m v_x / v) \beta^1 (2/\alpha^2) [\exp(-\alpha m_2^{1/2}) (-\alpha m_2^{1/2} - 1) + 1]$$

Applying this to the equation for  $\ln \gamma_{\pm}^{(\beta 1)}$ ;

$$\ln \gamma_{\pm}^{(\beta 1)} = 2m_2 (v_m v_x / v) \beta^1 \exp(-\alpha m_2^{1/2}) + 2(v_m v_x / v) \beta^1 (2/\alpha^2) [\exp(-\alpha m_2^{1/2}) (-\alpha m_2^{1/2} - 1) + 1]$$

$$= 2(v_m v_x / v) m_2 [\beta^1 \exp(-\alpha m_2^{1/2}) + \beta^1 (2/\alpha^2 m_2) [\exp(-\alpha m_2^{1/2}) (-\alpha m_2^{1/2} - 1) + 1]]$$

$$= 2(v_m v_x / v) m_2 [ (2\beta^1 / \alpha^2 m_2) \{1 - \exp(-\alpha m_2^{1/2}) [1 + \alpha m_2^{1/2} - (\alpha^2 m_2 / 2)]\} ]$$

## Section 6

From Section 1;

$$\ln \gamma_{\pm} = (\phi - 1) + \int_0^{m_2} (\phi - 1) d \ln m_2$$

$$\Rightarrow \ln \gamma_{\pm} = m_2^2 [2\{(v_m v_x)^{3/2}/v\}] C_{mx}^{\phi} + \int_0^{m_2} m_2^2 [2\{(v_m v_x)^{3/2}/v\}] C_{mx}^{\phi} d \ln m_2$$

$$= m_2^2 [2\{(v_m v_x)^{3/2}/v\}] C_{mx}^{\phi} + [2\{(v_m v_x)^{3/2}/v\}] C_{mx}^{\phi} \int_0^{m_2} m_2^2 dm_2$$

$$= (3/2) [m_2^2 [2\{(v_m v_x)^{3/2}/v\}] C_{mx}^{\phi}]$$

Then;

$$\ln \gamma_{\pm}^{C\gamma} = m_2^2 [2\{(v_m v_x)^{3/2}/v\}] C_{mx}^{\gamma}$$

## Section 7

### (i) The f term

From equation [7.38];

$$vm_2[1-\phi + \ln\gamma_{\pm}] = [G^E/RT]$$

Hence using equations [7.36] and [7.37];

$$\begin{aligned} \Rightarrow [G^E/RT]^{f\text{-term}} &= vm_2[|z_+z_-|A_{\phi}(m_2^{1/2}/(1+bm_2^{1/2})) \\ &\quad - |z_+z_-|A_{\phi}(m_2^{1/2}/(1+bm_2^{1/2})) \\ &\quad - |z_+z_-|A_{\phi}(2/b)\ln(1+bm_2^{1/2})] \\ &= vm_2[-|z_+z_-|A_{\phi}(2/b)\ln(1+bm_2^{1/2})] \end{aligned}$$

### (ii) The $\beta^{\circ}$ term

Using equations [7.38], [7.36] and [7.37];

$$[G_E/RT]\beta^{\circ} = vm_2[-2m_2\beta^{\circ}(v_m v_x/v) + 4m_2\beta^{\circ}(v_m v_x/v)]$$

Hence from equation [7.39];

$$\Rightarrow m_2^2[2v_m v_x]B_{mx}\beta^{\circ} = vm_2[2m_2\beta^{\circ}(v_m v_x/v)]$$

### (iii) The $\beta^1$ term

Using equations [7.38], [7.36] and [7.37];

$$\begin{aligned} [G^E/RT]\beta^1 &= vm_2[\{2m_2(v_m v_x/v)\beta^1 \exp(-\alpha m_2^{1/2})\} \\ &\quad \{2m_2(v_m v_x/v)\} \{ (2\beta^1/\alpha^2 m_2) \\ &\quad \{1 - \exp(-\alpha m_2^{1/2}) [1 + \alpha m_2^{1/2} - (\alpha^2 m_2/2)] \} \} \} \end{aligned}$$

$$= v m_2^2 (v_m v_x / v) \{ (2\beta^1 \alpha^2 m_2) \{ 1 - \exp(-\alpha m_2^{1/2}) [1 + \alpha m_2^{1/2}] \} \}$$

From equation [7.39];

$$m_2^2 B_{mx}^{\beta 1} (v_m v_x) = v m_2^2 (v_m v_x / v) \{ (2\beta^1 \alpha^2 m_2) \{ 1 - \exp(-\alpha m_2^{1/2}) [1 + \alpha m_2^{1/2}] \} \}$$

$$\Rightarrow B_{mx}^{\beta 1} = [2\beta^1 / \alpha^2 m_2] \{ 1 - \exp(-\alpha m_2^{1/2}) [1 + \alpha m_2^{1/2}] \}$$

In summary, the combination the two terms for  $B_{mx}^{\beta 0}$  and  $B_{mx}^{\beta 1}$  results in an overall  $B_{mx}$  term for the excess Gibbs function, equation [7.39].

$$B_{mx} = \beta^0 + [2\beta^1 / \alpha^2 m_2] \{ 1 - \exp(-\alpha m_2^{1/2}) [1 + \alpha m_2^{1/2}] \}$$

(iv) The C term

From equation [7.38];

$$v m_2 [1 - \phi + \ln \gamma_{\pm}] = [G^E / RT]$$

and from equation [7.39];

$$[G^E / RT]^C = m_2^3 [2v_m v_x (v_m z_m)] C_{mx}$$

Hence using equations [7.36] and [7.37];

$$m_2^3 [2v_m v_x (v_m z_m)] C_{mx} = v m_2 [-2m_2^2 \{ (v_m v_x)^{3/2} / v \} C_{mx}^{\phi} + 3m_2^2 \{ (v_m v_x)^{3/2} / v \} C_{mx}^{\phi}]$$

$$2m_2^3 v_m v_x (v_m z_m) C_{mx} = v m_2 [m_2^2 \{(v_m v_x)^{3/2} / v\} C_{mx}^\phi]$$

$$\Rightarrow C_{mx} = (C_{mx}^\phi / 2) \{(v_m v_x)^{1/2} / v_m z_m\}$$

But  $v_x |z_x| = v_m z_m$ ; then  $v_x |z_m z_x| = v_m z_m^2$

$$\Rightarrow |z_m z_x| = v_m z_m^2 / v_x = v_m^2 z_m^2 / v_m v_x$$

$$\Rightarrow \{(v_m v_x)^{1/2} / v_m z_m\} = 1 / |z_m z_x|^{1/2}$$

Hence;

$$C_{mx} = C_{mx}^\phi / 2 |z_m z_x|^{1/2}$$

The equation for the excess Gibbs function can thus be written in full as equation [7.40].



# Appendix

4

## Section 1

The listing below contains the main subroutines of the FORTRAN program PROJECT. This program was written to calculate pairwise group interaction parameters from osmotic coefficient data for ammonium, alkylammonium and azoniaspiroalkane halide salts.

The subroutine at the head of the program sets up key variables for the analysis and contains calls to other parts of the program. The main subroutine however is subroutine XION. Key arrays to be identified in this section are;

xm2(i) - contains the molality of the salt.

gam2(i) - contains the activity coefficients of the salt,  $\gamma_{\pm}$ .

xphi(i) - contains the osmotic coefficients of the salt,  $\phi$ .

xni(ict,i,j) - contains the number of known specific pairwise interaction parameters for each salt.

y(ict) - contains the Y matrix used in the minimal least squares analysis.

x(ict,i) - contains the X matrix used in the minimal least squares matrix.

In subroutine XION, shown in the listing below, only three salts, ammonium bromide, tetrabutylammonium bromide and 6.6 azoniaspiroalkane bromide have been included to give a feel of how the analysis was set up. In the full analysis subroutine XION contained 27 salts.

Consider the tetrabutylammonium bromide salt within this subroutine. The commented section details how the salt

can be broken down into its constituent pairwise interactions. The variable 'PIG' contains the name of the data file (in this example 'data5.dat') used in the call to subroutine SALT. This subroutine accesses the data file specific to tetrabutylammonium bromide which contains molality, activity coefficient and osmotic coefficient data for the salt in aqueous solution at 298 K. In the case of the azoniaspiroalkane halides subroutine WSALT is accessed. This subroutine differs from subroutine SALT only in the fact that osmotic and activity coefficient data has to be calculated from a set of equations. Hence data files for the azoniaspiroalkane halides contain parameters for these equations.

Within subroutine SALT (and WSALT) there is a call to subroutine PIZ. This subroutine is used to calculate Pitzers  $\beta^\circ$  parameter from the osmotic coefficient data (see equation [7.34] of Chapter 7) using the method of linear least squares, subroutine XLSQ. Hence on successful completion of subroutines SALT (or WSALT) and PIZ the program returns to subroutine XION with a value for  $\beta^\circ$ . Multiplying  $\beta^\circ$  by  $2RT$  gives  $g(\text{salt})$  (see equation [8.2] of Chapter 8) and once  $g(\text{salt})$  is known it is possible to form an equation for the unknown pairwise interactions. A Y matrix is formed by subtracting the known pairwise interaction parameters from  $g(\text{salt})$  (in this case the Savage-Wood interaction parameter for  $(\text{CH}_2-\text{CH}_2)$ , and for tetrabutylammonium bromide there are 324 such interactions). The X matrix is formed from the number of unknown pairwise interaction parameters for the salt.

In the full analysis this procedure is repeated for

each of the 27 salts. At the end of subroutine XION the Y and X matrices are solved for the unknown pairwise interaction parameters using a minimal least squares procedure, subroutine YLSQ. A linear least squares procedure proved unsuitable because of the structure of the data.

```

program project
implicit double precision(a-h,o-z)
common/linda/fiat
common/frog/flag
common/mike/xm2(40),ge(40),gam2(40),xphi(40),gs(40)
common/keith/beta0(100)
common/anne/rg,tk,int
common/andy/ai(50,50),xni(60,40,40),yi(50)

```

```

c *****
c *   beta0( ) in keith for beta0 parameter
c *   ge     = excess Gibbs function for
c *                               solution in 1 kg of water
c *   xphi   = osmotic coefficient
c *   xm2    = molality of salt
c *   gam2   = mean ionic activity coefficient
c *   ai(i,j) = total set of interaction parameters
c *   xni(i,j,k) = in solute i
c *                               number of group k-j interactions
c *****
c *   rg = gas constant          tk / kelvin = temperature
c *****
rg=8.31434
tk=298.15
fiat=0.0
call head
call xion
c *****
c *   subroutine xion analyses first 27 salts
c *****
c *   construct output array
c *****
write(6,90)
90  format(1h ,10x,'*** Output Data To Data File ***')
open(unit=7,file='apar.dat',status='old')
do 100 i=1,50
write (7,*) (ai(i,j),j=1,50)
100 continue
write(6,95)
95  format(1h,10x,'** Data Over To Data File **')
write(6,10)

```

```
10  format(1h ,20x,'That is all folks')  
    end
```

```

subroutine xion
implicit double precision(a-h,o-z)
  common/frog/flag
common/keith/beta0(100)
common/mike/xm2(40),ge(40),gam2(40),xphi(40),gs(40)
common/anne/rg,tk,int
common/andy/ai(50,50),xni(60,40,40),yi(50)
dimension y(200),x(200,40),a(40,1)
character*50 pig
c *****
c *   jan = 0   ; normal least squares
c *   jan = 1   ; special least squares for systems
c *
c *           with singular w-matrix
c *   enter jan here
c *****
c * y(i)  is input to least squares
c * x(i,j)      i= data points
c *           j = savage-wood parameter
c * xm1 = molar mass of water
c *****
  jan=1
  xm1= 0.01815
c *****
c *   clear arrays
c *****
  m=0
  jone=0
  do 10 i=1,50
  do 11 j=1,50
  ai(i,j)=0.0
11  continue
10  continue
  do 13 i=1,40
  xm2(i)=0.0
  gam2(i)=0.0
  xphi(i)=0.0
13  continue
  do 20 i=1,200
  y(i)=0.0
  do 21 j=1,40

```

```

x(i,j)=0.0
21  continue
20  continue
do 30 i=1,40
a(i,1)=0.0
30  continue
do 31 i=1,40
do 32 j=1,20
do 33 k=1,20
xni(i,j,k)=0.0
33  continue
32  continue
31  continue
c  *****
c  *  savage-wood  analysis
c  *  parameters from J.J.Spitzer; S.K.Suri; R.H.Wood
c  *  J.Soln.Chem., 1985,14,571.
c  *  store in ai( , )
c  *  1 = ch2          2 = oh
c  *  3 = conh        4 = o
c  *  5 = n           6 = n+
c  *  7 = f-          8 = cl-
c  *  9 = br-         10 = i-
c  *  11 = h+         12 =
c  *  13 =            14 = k+
c  *  15 = no3-       16 = clo4-
c  *  17 = Na+
c  *****
ai(1,1)=-34.0
ai(2,1)=29.0
ai(2,2)=-23.0
ai(3,1)=55.0
ai(3,2)=-31.0
ai(3,3)=-118.0
ai(4,1)=37.0
ai(4,2)=-22.0
ai(4,3)=-82.0
ai(4,4)=-57.0
ai(5,1)=46.0
ai(5,2)=-41.0

```

```
ai(5,3)=-42.0
ai(5,4)=-40.0
ai(5,5)=-27.0
```

```
c *****
c * MAKE MATRIX SYMMETRICAL *
c *****
do 107 i=1,5
do 108 j=1,i
ai(j,i)=ai(i,j)
108 continue
107 continue
write(6,112)
112 format(1h1,10x,'Savage - Wood Matrix')
write(6,113) (i,i=1,5)
113 format(1h ,5x,6(10x,i3))
do 114 i=1,5
write(6,115) i,(ai(i,j),j=1,5)
115 format(1h ,2x,i3,5(2x,1pe15.6))
114 continue
c *****
c * code for analysis
c * bromide set
c * a(1,1) = br-br- = ai(9,9)
c * a(2,1) = ch2n+ = ai(6,1)
c * a(3,1) = n+n+ = ai(6,6)
c * a(4,1) = ch2br- = ai(9,1)
c * a(5,1) = n+br- = ai(9,6)
c * chloride set
c * a(6,1) = cl-cl- = ai(8,8)
c * a(7,1) = ch2cl- = ai(8,1)
c * a(8,1) = n+cl- = ai(8,6)
c * fluoride set
c * a(9,1) = f-f- = ai(7,7)
c * a(10,1) = ch2f- = ai(7,1)
c * a(11,1) = n+f- = ai(7,6)
c * iodide set
c * a(12,1) = i-i- = ai(10,10)
c * a(13,1) = ch2i- = ai(10,1)
c * a(14,1) = n+i- = ai(10,6)
c *****
```

```

ict=0
*****
c   * use 'if(ict.gt.0) goto xxx' as a skip around a solute
c   *****
c   * call salts in turn
c   * test salt data by trapping to 999
c   * m = 1 beta0
c   * m = 2 plus betal
c   * m = 3 plus c-term
c   * m = 4 plus beta2 term (for high valence salts)
c   * use test to decide on m for each salt
c   * y(ict) is corrected ge(nonelec)
c   * minus known group interaction parameters
c   *****
c   * call salt(m,ict,pig)
c   * m = number of parameters in least squares
c   * ict = set number
c   * gs(ict) = returned gcorr which is required
c   * g(salt) + (r.t.ml)/2
c   * pig = data file
c   *****
c   * Ammonium Bromide
c   * g(nh4+br-) = 4h + n+ + br-
c   * = 4.(0.5*ch2) + n+ + br-
c   * g = 4.ch2ch2
c   * 2.ch2n+ + n+n+
c   * 2.ch2br- + n+br- + br-br-
c   * g = 4.ch2ch2 + 4.ch2n+ + n+n+
c   * 4.ch2br- + 2.n+br- + br-br-
c   *****
ict=ict+1
m=3
write(6,101) ict
101 format(1h1,10x,'Set count = ',3x,i4)
pig='data1.dat'
jone=3.0
call salt(m,ict,pig,jone)
beta0(ict)=2.0*rg*tk*beta0(ict)
write(6,1001) beta0(ict)
1001 format(1h ,10x,'g-salt = '1pe15.6)

```

```

write(6,2007)
2007 format(1h,'%%%%%%%%%%%%%%%%%%%%%%%%%%%%%%%%%%%%%%%%%%%%%%%%%%%%%%%%%%%%%%%%%%%%%%%%')
$%%%%%%%%%%%%%%%%%%%%%%%%%%%%%%%%%%%%%%%%%%%%%%%%%%%%%%%%%%%%%%%%%%%%%%%%
$%%%%%%%%%%%%%%%%%%%%%%%%%%%%%%%%%%%%%%%%%%%%%%%%%%%%%%%%%%%%%%%%%%%%%%%%' )
xni(ict,1,1)=4.0
y(ict)=beta0(ict)-(xni(ict,1,1)*ai(1,1))
x(ict,2)=4.0
x(ict,3)=1.0
x(ict,4)=4.0
x(ict,5)=2.0
x(ict,1)=1.0
c *****
c *      Tetrabutylammonium Bromide
c * g(bu4n+br-) = g(18*ch2 + n+ + br-)
c * g = 324(ch2ch2)
c *      18(ch2n+) + n+n+
c *      18(ch2br-) + n+br- + br-br-
c * g = 324(ch2ch2) + 36(ch2n+) + n+n+
c *      + 36 ch2br- + 2(n+br-) + br-br-
c *****
ict=ict+1
m=3
write(6,101) ict
pig='data5.dat'
jone=3.0
call salt(m,ict,pig,jone)
beta0(ict)=2.0*rg*tk*beta0(ict)
write(6,1001) beta0(ict)
write(6,2007)
xni(ict,1,1)=324.0
y(ict)=beta0(ict)-(xni(ict,1,1)*ai(1,1))
x(ict,2)=36.0
x(ict,3)=1.0
x(ict,4)=36.0
x(ict,5)=2.0
x(ict,1)=1.0
c *****
c *      6.6 Azonspiroalkane Bromide
c * g((ch2ch2)6n+6(ch2)br-) = g(12*ch2 + n+ + br-)
c * g = 144 ch2ch2

```

```

c      *          12 ch2n+      n+n+
c      *          12 ch2br-     n+br-      br-br-
c      * g = 144 ch2ch2 + 24 ch2n+ + n+n+
c      *          + 24 ch2br- + 2 n+br- + br-br-
c      *****
ict=ict+1
m=3
write(6,101) ict
  pig='data26.dat'
  jone=3.0
  call wsalt(m,ict,pig,jone)
  beta0(ict)=2.0*rg*tk*beta0(ict)
  write(6,1001) beta0(ict)
  write(6,2007)
  xni(ict,1,1)=144.0
  y(ict)=beta0(ict)-(xni(ict,1,1)*ai(1,1))
  x(ict,2)=24.0
  x(ict,3)=1.0
  x(ict,4)=24.0
  x(ict,5)=2.0
  x(ict,1)=1.0
c      *****
c      * input complete
c      *          End of Data Collection
c      *****
503  write(6,503) ict
      format(1h ,10x,'Number of Systems = ',i3)
c      *****
c      * Symmetrise the xni( , , ) matrix          *
c      * Set up for ipar                          *
c      *****
      ipar=14
      do 515 i=1,ict
      do 516 j=1,40
      do 517 k=1,j
      xni(i,k,j)=xni(i,j,k)
517  continue
516  continue
515  continue
write(6,500)

```

```

500  format(1h ,10x,'input complete')
      write(6,505)
505  format(1h ,20x,' input matrix ')
      write(6,501)
501  format(1h ,5x,'***** gsalt-residuals *****')
      do 177 j=1,ict
        write(6,178) j,y(j)
178  format(1h ,2x,i5,3x,1pe12.2)
177  continue
      write(6,179)
179  format(1h ,5x,'***** X Values *****')
      if(ipar.le.9) stump=1
      if(ipar.gt.9.and.ipar.le.18) stump=2
      if(ipar.gt.18.and.ipar.le.27) stump=3
      if(ipar.gt.27.and.ipar.le.36) stump=4
      dice=9
      if(stump.eq.1) dice=ipar
      write(6,506) (j,j=1,dice)
506  format(1h ,11x,i2,8(10x,i2))
      do 510 i=1,ict
        write(6,520) i,(x(i,j),j=1,dice)
520  format(1h ,i2,x,9(x,1pe10.1))
510  continue
      if(stump.eq.1) goto 546
      dice=18
      if(stump.eq.2) dice=ipar
      write(6,506) (j,j=10,dice)
      do 530 i=1,ict
        write(6,520) i,(x(i,j),j=10,dice)
530  continue
      if(stump.eq.2) goto 546
      dice=27
      if(stump.eq.3) dice=ipar
      write(6,506) (j,j=19,dice)
      do 540 i=1,ict
        write(6,520) i,(x(i,j),j=19,dice)
540  continue
      if(stump.eq.3) goto 546
      dice=27
      if(stump.eq.4) dice=ipar

```

```

write(6,506) (j,j=27,dice)
do 542 i=1,ict
write(6,520) i,(x(i,j),j=27,dice)
542 continue
546 continue
write(6,547)
547 format(1h , '*****')
$*****')
write(6,5006)
5006 format(1h ,10x, '*** Minimal Least Sq. So
$lution ***')
call ylsq(x,y,ict,ipar,a)
do 551 i=1,ipar
write(6,560) i,a(i,1)
560 format(1h ,10x, 'a ',10x,i4,10x,1pe15.6)
551 continue
write(6,580)
580 format(1h ,5x, 'Recalculation of gsalt residuals Using
$ Parameters from best fit')
write(6,590)
590 format(1h ,10x, 'comparison')
s=0.0
do 600 i=1,ict
dum=(xni(i,1,1)*ai(1,1)) + (xni(i,2,2)*ai(2,2))
$+(xni(i,1,2)*ai(1,2))
do 610 j=1,ipar
dum=dum+(x(i,j)*a(j,1))
610 continue
diff = beta0(i) - dum
s=s+(diff*diff)
xdiff=((beta0(i)-dum)/beta0(i))*100.0
write(6,650) i,beta0(i),dum,xdiff
650 format(1h ,10x,i3,3(3x,1pe15.6))
600 continue
s=dsqrt(s/(ict-1))
write(6,710) s
710 format(1h ,10x, 'standard error = ', 1pe15.6)
999 continue
1333 continue
write(6,585)

```

```

585   format(1h ,5x,'*****')
      $*****')
c     *****
c     * Convert matrix from local to global      *
c     *****
      ai(6,1)=a(2,1)
      ai(6,6)=a(3,1)
      ai(9,1)=a(4,1)
      ai(9,6)=a(5,1)
      ai(9,9)=a(1,1)
      ai(8,1)=a(7,1)
      ai(8,6)=a(8,1)
      ai(8,8)=a(6,1)
      ai(7,1)=a(10,1)
      ai(7,6)=a(11,1)
      ai(7,7)=a(9,1)
      ai(10,1)=a(13,1)
      ai(10,6)=a(14,1)
      ai(10,10)=a(12,1)
c     *****
c     * Symmetrise the ai( , ) matrix            *
c     *****
      do 800 i=6,10
      do 810 j=1,i
      ai(j,i)=ai(i,j)
810   continue
800   continue
c     *****
c     *      Print out interaction matrix      *
c     *****
      write(6,701)
701   format(1h ,10x,'interaction matrix')
      do 702 i=1,14
      do 703 j=1,i
      write(6,704) i,j,ai(i,j)
704   format(1h ,20x,i5,10x,i5,10x,1pe15.6)
703   continue
702   continue
      goto 997
9999  continue

```

```
write(6,996) ict
996 format(1h ,10x,'tape error at ict = ', i5)
997 continue
return
end
```

```

subroutine piz(ndata,ict,nup,nun,izp,izn,alpha,jone)
implicit double precision(a-h,o-z)
common/frog/flag
common/keith/beta0(100)
common/mike/xm2(40),ge(40),gam2(40),xphi(40),gs(40)
common/anne/rg,tk,int
dimension beta(200,30),yphi(200),a(30,1),ygam(200)
dimension yge(20)
write (6,7)nup,nun,izp,izn
7  format(1h ,10x,4(2x,i5))
write(6,8) alpha
8  format(1h ,10x,'alpha-gamma = ',1pe15.6)
c  *****
c  * subroutine to find terms in the pitzer equation
c  * Clear the Beta array
c  *****
do 2 i=1,200
yphi(i)=0.0
ygam(i)=0.0
do 4 j=1,30
beta(i,j)=0.0
4  continue
2  continue
c  *****
c  * STEP (1) Calculation of beta0 from osmotic
c  * coefficient equation.
c  *****
b=1.2
alpha=alpha/3.0
write(6,13)alpha
13 format(1h ,10x,'alpha-phi=',1pe15.6)
do 10 j=2,ndata
xionic= xm2(j)
one=xphi(j)-1.0
two=-alpha*(xionic**0.5)
three=1.0+(b*(xionic**0.5))
yphi(j)=one-(two/three)
vv=izp*izn
yphi(j)=dabs(vv)*yphi(j)
beta(j,1)=xm2(j)*(2.0*nup*nun/(nup+nun))

```

```

    beta(j,2)=xm2(j)*dexp(-2.0*xionic**0.5)
    $(2.0*nup*nun/(nup+nun))
    beta(j,3)=(xm2(j)**2.0)*((2.0*((nup*nun)**1.5))
    $/(nup+nun))
10    continue
    write(6,50)
50    format(1h ,10x,'Input')
    ipar=3.0
    write(6,150)
150   format(1h ,10x,'molality',10x,'yphi',10x,
    $ 'beta1',10x,'beta2',10x,'beta3')
    do 120 i=1,ndata
    write(6,110)xm2(i),yphi(i),(beta(i,j),j=1,ipar)
110   format(1h ,5(x,1pe15.6))
120   continue
    if(jone.eq.0) goto 111
    call xlsq(beta,yphi,ndata,jone,a)
    goto 112
111   continue
    do 121 i=1,3
    ipar=i
    call xlsq(beta,yphi,ndata,ipar,a)
    write(6,1007) a(1,1)
1007  format(1h ,10x,'beta0 =',1pe15.6)
121   continue
112   continue
    write(6,1007) a(1,1)
    if(ipar.eq.3) goto 1009
c     *****
c     * Step 2.....Calculation of beta0 parameter from
c     *           Pitzers In gamma+/- equation
c     *****
    write(6,208)
208   format(1h ,20x,'analysis two')
    do 200 j=2,ndata
    do 201 i=1,6
    beta(1,i)=0.0
201   continue
    xionic=xm2(j)
    one2=xionic/(1.0+(b*xionic**0.5))

```

```

two2=(2.0/b)*dlog(1.0+(b*xionic**0.5))
three2=-alpha*(one2+two2)*abs(izp*izn)
  ygam(j)=gam2(j)-three2
  beta(j,1)=2.0*xm2(j)
beta(j,1)=beta(j,1)*(2.0*nup*nun/(nup+nun))
dum1=dexp(-2.0*xionic**2)
dum2=1.0+(2.0*(xionic**0.5))-(0.5*4.0*xionic)
dum3=2.0/(4.0*xionic)
dum4=dum3*(1.0-(dum2*dum1))
beta(j,2)=dum4*(2.0*nup*nun/(nup+nun))*xionic
beta(j,3)=(xm2(j)**2)*(2.0*((nup*nun)**1.5))/(nup+nun)
200  continue
     write(6,50)
     write(6,205)
205  format(1h ,10x,'xm2',10x,'gamma',12x,'ygam',12x,
$'betal',12x,'beta2',10x,'beta3')
     do 220 i=1,ndata
       write(6,230)xm2(i),gam2(i), ygam(i),(beta(i,j),j=1,ipar)
230  format(1h ,6(x,1pe15.6))
220  continue
     if(jtwo.eq.0) goto 223
     call xlsq(beta,ygam,ndata,jtwo,a)
     goto 224
223  continue
     do 221 i=1,3
       ipar=i
       call xlsq(beta,ygam,ndata,ipar,a)
       write(6,1007) a(1,1)
221  continue
224  continue
     write(6,1007) a(1,1)
c     *****
c     * step3 calculation
c     * using ge
c     *****
     write (6,301)
301  format(1h ,10x,'analysis three')
     do 500 j=1,ndata
       xionic=xm2(j)
       one3=(4.0*xionic/b)

```

```

two3=dlog(1.0+(b*xionic**0.5))
yge(j)=ge(j)/(rg*tk)
three=-alpha*(one3*two3)
yge(j)=yge(j)-three
beta(j,1)=(xionic**2)*(2.0*nup*nun)
if(j.ne.1) goto 202
beta(1,2)=0.0
goto 203
202  continue
dum=2.0/(4.0*xionic)
dum1=(1.0+(2.0*xionic**0.5))*dexp(-2.0*xionic**0.5)
dum2=1.0-dum1
dum=dum*dum2
beta(j,2)=dum*(xionic**2)*(2.0*nup*nun)
203  continue
beta(j,3)=(xionic**3)*(2.0*nup*nun*nun*nup)
500  continue
write(6,50)
write(6,505)
505  format(1h ,10x,'xm2',10x,'ge',15x,'yge',14x,
$'beta1',10x'beta2',10x'beta3')
do520 i=1,ndata
write(6,230)xm2(i),ge(i),yge(i),(beta(i,j),j=1,3)
520  continue
if(jthree.eq.0) goto 523
call xlsq(beta,ygam,ndata,jthree,a)
goto 524
523  continue
do 521 i=1,3
ipar=i
call xlsq(beta,yge,ndata,ipar,a)
write(6,1007) a(1,1)
521  continue
524  continue
write(6,1007) a(1,1)
c *****
c * now put parameters together
c *****
1009  continue
beta0(ict)=a(1,1)

```

```
    write(6,406) beta0(ict)
406    format(1h ,20x,'returned Bo to common block keith =
$ ',1pe15.6)
    return
end
```

## Section 2

Extended pairwise cosphere-cosphere group Gibbs function interaction matrix calculated from osmotic coefficient data at 298 K. ( $\text{J MOL}^{-1}$ )

	$\text{K}^+$	$\text{Na}^+$	$\text{NO}_3^-$
$\text{CH}_2$	9.4	-5.3	-61
$\text{N}^+$	295	339	1.4
$\text{K}^+$	196	-	-
$\text{Na}^+$	-	31	-
$\text{F}^-$	324	-	-
$\text{Cl}^-$	174	-	-
$\text{Br}^-$	190	401	-
$\text{NO}_3^-$	-	-	-112



# Appendix

5

### Program BPB

This listing contains the main subroutines used in the FORTRAN program BPB. The program was used to generate the dependences on ionic strength of  $\ln(k/k_0)$  using the Debye-Huckel equation and Pitzer's equation for reaction between hydroxide ions and the sodium salt of bromophenol blue in the presence of various added salts.

The first subroutine at the head of the program contains the calls from which all subsequent subroutines are accessed. Rate data for each added salt and parameters necessary to Pitzer's equation were stored in separate data files and read into the main program using subroutine INPUT. The dependence of  $\ln(k/k_0)$  on ionic strength calculated using the Debye-Huckel equation was calculated in subroutine DEBYE whilst the same dependence predicted by Pitzer's equation was calculated from subroutines PELECT1, PELECT2 and PELECT4. The latter subroutines correspond to the equations represented by terms A, B and D of equation [9.8] discussed in Chapter 9. All of the data were collected in subroutine COLLECT and were set up to be printed out.

Subroutine COSPHERE represents an attempt to quantify the cosphere contribution to Pitzer's equation of the bromophenol blue dianion and the transition state trinegative ion. The calculation is based on  $\beta^0$  and  $\beta^1$  values for various 2:1 and 3:1 salts tabulated by Pitzer. Finally subroutine PLOT brings together all of the calculated data and produces plots of the dependence of  $\ln(k/k_0)$  on ionic strength for the experimental data, calculated using the Debye-Huckel equation, the individual

terms of Pitzer's equation and finally the full Pitzer equation.

```

program bpb
implicit double precision(a-h,o-z)
common/andy/xm2(30),xcons(30),pitzer(30)
common/linda/ndata,bo,bone3,btwo3,cterm3
common/answer/pe1(30),pe2(30),pe4(30),dh11(30),xi(30)
c *****
c *   rg = gas constant      tk / kelvin = temperature
c *****
c *
c *           EXPLANATION OF ARRAYS
c *   TITLE      POSITION      ASSIGNMENT
c *   xm2        andy         contains molarity of added salt
c *   xcons      andy         "      ln k/ko
c *   pitzer     andy         "      overall pitzer contr.
c *                                     pe1 + pe2 + pe4
c *   ndata     linda        " number of data points + 1
c *   b0        linda        "      beta0 for COH
c *                                     (C = added salt cation)
c *   bone3     linda        "      beta1 for COH
c *   btwo3     linda        "      beta2 for COH
c *   cterm3    linda        "      c term for COH
c *   pe1       answer       "      pitzers electrical term
c *   pe2       answer       "      pitzers second term
c *   pe4       answer       "      pitzers fourth term
c *   dh11     answer       "      total DHL contribution
c *   xi        answer       "      ionic strength
c *****
c   call paper(1)
c *****
c *   paper(1) is a set up for the plot routine
c *****
c   call head
c   call input
c   call debye
c   call Pelect1
c   call Pelect2
c   call Pelect4
c   call collect
c   call cosphere
c   call plot
c *****

```

```
c      * routine GREND ensures plot is finished
c      ****
      call grend
      write(6,10)
10     format(1h ,10x,'End of Program')
      end
```

```

subroutine debye
c *****
c * calculation of DHLL parameters for salts in aq sln.
c * x = c.c/{ F m^-1 J K^-1 K}
c * = A^2 s^2/(A^2 s^4 kg^-1 m^-2 kg m^2 s^-2
c * = 1
c * alpha = mol^-1 kg m^-3
c *****
implicit double precision(a-h,o-z)
common/andy/xm2(30),xcons(30),pitzer(30)
common/linda/ndata,bo,bone3,btwo3,cterm3
common/answer/pe1(30),pe2(30),pe4(30),dhll(30),xi(30)
common/huckel/dhllloh(30),dhllbb(30),dhllts(30)
c *****
c * EXPLANATION OF ARRAYS
c * TITLE POSITION ASSIGNMENT
c * dhllloh huckel contains hydroxide contribution to
c * total DHLL term
c * dhllbb huckel contains bpb anion contribution to
c * total DHLL term
c * dhllts huckel transition state contribution
c * to total DHLL term
c *****
rg=8.31434
tk=298.15
q=3.0/2.0
an=6.022169e23
bk=1.380622e-23
ez=8.854185e-12
zpi=3.14159
rho=997.045
er=78.30
pc=1.602191e-19
alpha=(2.0*zpi*an*rho)**(1.0/2.0)
x1=pc*pc/(4.0*zpi*ez*er*bk*tk)
x1=x1**(q)
alpha=alpha*x1
write(6,12) alpha
12 format(1h ,10x,'A-gamma = ',1pe15.6)
c *****

```

```

c      * A-gamma in pitzer
c      * A-gamma =1.173
c      *****
c      * calculation of the DHLL for each salt
c      * =4.A(gamma).I**0.5
c      *
c      *           where I is the ionic strength
c      *****
      write(6,5)
5      format(1h ,13x,'I.STRENGTH',10x,'OH-DHLL',10x,'BB-DHLL'
$,10x,'TS-DHLL',10x'TOTAL DEPENDENCE')
      do 10 j=1,ndata
      dh1loh(j)= -alpha * (xi(j)**0.5) * 1.0
      dh1lbb(j)= -alpha * (xi(j)**0.5) * 4.0
      dh1lts(j)= -alpha * (xi(j)**0.5) * 9.0
      dh1l(j) = dh1loh(j) + dh1lbb(j) - dh1lts(j)
      write(6,20) j,xi(j),dh1loh(j),dh1lbb(j),dh1lts(j)
$,dh1l(j)
20      format(1h ,2x,i5,5(2x,1pe15.6))
10      continue
      write(6,2007)
2007      format(1h,'%%%%%%%%%%%%%%%%%%%%%%%%%%%%%%%%%%%%%%%%%%%%%%%%%%%%%%%%%%%%%%%%%%%%%%%%%'
$'%%%%%%%%%%%%%%%%%%%%%%%%%%%%%%%%%%%%%%%%%%%%%%%%%%%%%%%%%%%%%%%%%%%%%%%%%'
$'%%%%%%%%%%%%%%%%%%%%%%%%%%%%%%%%%%%%%%%%%%%%%%%%%%%%%%%%%%%%%%%%%%%%%%%%%'
      return
      end

```

```

subroutine Pelect1
implicit double precision(a-h,o-z)
common/andy/xm2(30),xcons(30),pitzer(30)
common/linda/ndata,bo,bone3,btwo3,cterm3
common/answer/pel(30),pe2(30),pe4(30),dh11(30),xi(30)
common/elect1/peloh(30),pelts(30),pelbb(30)
c *****
c *
c *           EXPLANATION OF ARRAYS
c * TITLE      POSITION      ASSIGNMENT
c * peloh      elect1      hydroxide contribution to Pitzer
c *                               electrical term
c * pelts      elect1 transit. st. contribution to Pitzer
c *                               electrical term
c * pelbb      elect1      bpb contribution to Pitzer elect
c *                               term
c *****
c * This subroutine takes into account the first Pitzer
c * electrical term.
c * It is non salt specific, and is calculated from the
c * equation ;
c *  $Pe1 = 4 * \text{aphi} \{ [I^{0.5} / (1 + bI^{0.5})] + 2/b \cdot \ln(1 + b \cdot I^{0.5}) \}$ 
c *****
c b = 1.2
c aphi = 0.3903
c write(6,110)
110 format(1h ,16x,'I.STRENGTH',9x,'pelOH',13x,'pelBB'
$,13x,'pelTS',13x,'total pel')
do 10 j=1,ndata
part1 = xi(j)**0.5/(1+b*(xi(j)**0.5))
part2 = dlog(1.0+b*xi(j)**0.5)
part3 =(2/b)*part2
part4 = part1 + part3
peloh(j) = -1.0 * aphi * part4
pelbb(j) = -4.0 * aphi * part4
pelts(j) = -9.0 * aphi * part4
pel(j)   = peloh(j) + pelbb(j) - pelts(j)
write(6,20) j,xi(j),peloh(j),pelbb(j),pelts(j)
$,pel(j)
20 format(1h ,i5,3x,5(3x,1pe15.6))
10 continue

```

```
        write(6,2007)
2007  format(1h,'%%%%%%%%%%%%%%%%%%%%%%%%%%%%%%%%%%%%%%%%%%%%%%%%%%%%%%%%%%%%%%%%%%%%%%%%%'
           '$%%%%%%%%%%%%%%%%%%%%%%%%%%%%%%%%%%%%%%%%%%%%%%%%%%%%%%%%%%%%%%%%%%%%%%%%%'
           '$%%%%%%%%%%%%%%%%%%%%%%%%%%%%%%%%%%%%%%%%%%%%%%%%%%%%%%%%%%%%%%%%%%%%%%%%%'
           'return
           end
```

```

subroutine Pelect2
implicit double precision(a-h,o-z)
common/andy/xm2(30),xcons(30),pitzer(30)
common/linda/ndata,bo,bone3,btwo3,cterm3
common/answer/pe1(30),pe2(30),pe4(30),dh11(30),xi(30)
common/untidy/qx(30),qxx(30),pea(30)
common/elect2/bh(30),ch(30),bxc(30),cxc(30)

```

```

*****

```

```

*           EXPLANATION OF ARRAYS

```

```

*  TITLE           POSITION           ASSIGNMENT
*  bh              elect2           NaOH pitzer B term to Pitzer 2nd
*  ch              elect2           NaOH pitzer Cterm to Pitzer 2nd
*  bxc             elect2           COH pitzer B term to pitzer 2nd
*  cxc             elect2           COH pitzer C term to "      "
*  pea            untidy            bxc + cxc for COH
*  qxx            untidy            ln(k/ko)- pe1 - pe2
*  qx             untidy            a stage in qxx

```

```

*****

```

```

*salt specific routine, uses beta0 values calculated
* in the pairwise interactions program 'TEST'

```

```

*****

```

```

*  pe2 = 2.Mc[ Bxc + McZc.Cxc]

```

```

*

```

```

*  Bxc = b0xc + 2b1xc/alpha**2.I [ 1-(1+alpha.I**0.5)exp
*                                     (-alpha.I**0.5)]

```

```

*

```

```

*  Cxc(gamma) = Cxc(phi)/2|ZcZx|**0.5

```

```

*****

```

```

* N.B in this section X = OH-

```

```

*****

```

```

alpha = 2.0

```

```

pe2(1) = 0.0

```

```

bxc(1) = 0.0

```

```

cxc(1) = 2.5e-3

```

```

bh(1) = 0.0

```

```

ch(1) = 2.2e-3

```

```

pea(1) = 0.0

```

```

do 10 j=2,ndata

```

```

*****

```

```

*  pe2 = 2.Mc[ Bxc + McZc.Cxc]

```

```

c      *
c      * Bxc = b0xc + 2b1xc/alpha**2.I [ 1-(1+alpha.I**0.5)exp
c      *                                     (-alpha.I**0.5)]
c      *
c      * Cxc(gamma) = Cxc(phi)/2|ZcZx|**0.5
c      *****
c      * N.B in this section X = OH-
c      *****
c      *****
c      * Step 1: Calculation of Bxc
c      *****
term1 = dexp(-alpha*xi(j)**0.5)
term2 = 1 + alpha*xi(j)**0.5
term3 = 1 - (term2*term1)
if(xi(j).eq.0.0) goto 23
term4 = (2.0*bone3)/(alpha**2.0*xi(j))
if(xi(j).ne.0.0) goto 24
23 term4 = 0.0
24 continue
    bxc(j) = b0 + (term4 * term3)
c      *****
c      * Step 2: Calculation of Cxc
c      *
c      * nb. |ZxZc|**0.5 = |-1.1|**0.5 = 1.0
c      *****
cxc(j) = cterm3 / (2.0 * 1.0**0.5)
c      *****
c      * Step 3: Calculation of pitzer term for NaOH
c      *****
c      * NaOH beta0 b0h= 0.0864
c      * NaOH beta1 b1h= 0.253
c      * NaOH cterm coh=0.0044
c      * xmoh = molarity of hydroxide in system = 0.1 mol dm-3
c      *****
xmoh = 0.1
    b0h = 0.0864
    b1h = 0.253
    coh = 0.0044
c      *****
rem1 = dexp(-alpha*xi(j)**0.5)
rem2 = 1 + alpha*xi(j)**0.5

```

```

rem3 = 1 - (rem2*rem1)
if(xi(j).eq.0.0) goto 33
rem4 = (2.0*b1h)/(alpha**2.0*xi(j))
if(xi(j).ne.0.0) goto 34
33 rem4 = 0.0
34 continue
    bh(j) = b0h + (rem4 * rem3)
    ch(j) = coh / (2.0 * 1.0**0.5)
c *****
c * Step 4: Calculation of total Pe2
c *****
pea(j) =( xm2(j)*(bxc(j) + (xm2(j)*1.0*cxc(j))))
pe2(j) = 2.0 *(pea(j)+ (xmoh*(bh(j)+(xmoh*1.0*ch(j))))
10 continue
write(6,20)
20 format(1h ,17x,'I.STREN.',11x,'Boh',13x,'Coh'
$13x,'Bxc',13x,'Cxc')
do 30 i=1,ndata
write(6,40) i,xi(i),bh(i),ch(i),bxc(i),
$cxc(i)
40 format(1h ,2x,i5,5(3x,1pe15.6))
30 continue
write(6,81)
81 format(1h ,16x,'ionic str.',9x,'first-term'
$,7x'second term')
do 85 i=1,ndata
write(6,86) i,xi(i),pe1(i),pe2(i)
86 format(1h,2x,i5,3(4x,1pe15.6))
85 continue
write(6,2007)
2007 format(1h,'%%%%%%%%%%%%%%%%%%%%%%%%%%%%%%%%%%%%%%%%%%%%%%%%%%%%%%%%%%%%%%%%%%%%%%%%%'
$'%%%%%%%%%%%%%%%%%%%%%%%%%%%%%%%%%%%%%%%%%%%%%%%%%%%%%%%%%%%%%%%%%%%%%%%%%'
$'%%%%%%%%%%%%%%%%%%%%%%%%%%%%%%%%%%%%%%%%%%%%%%%%%%%%%%%%%%%%%%%%%%%%%%%%%')
c *****
c * Calculation of the Q quantity
c *****
write(6,90)
90 format(1h ,9x,'I.Strength',10x,'ln(k/ko) - Q')
do 100 j=1,ndata
qx(j) = pe2(j) + pe1(j)

```

```
    qxx(j) = xcons(j) - qx(j)
    write(6,95) xi(j),qxx(j)
95    format(1h ,4x,1pe15.6,5x,1pe15.6)
100   continue
    write(6,2007)
    return
end
```

```

subroutine Pelect4
implicit double precision(a-h,o-z)
common/andy/xm2(30),xcons(30),pitzer(30)
common/linda/ndata,bo,bone3,btwo3,cterm3
common/answer/pe1(30),pe2(30),pe4(30),dh11(30),xi(30)
common/flat/bone1,btwo1,cterm1
common/elect4/term(10,10),bone2,bone4,btwo2,btwo4
$,cterm2,cterm4
character*50 fox,check,name1,name2,name3,name4
*****
c
c      *           EXPLANATION OF ARRAYS
c
c      *  TITLE      POSITION      ASSIGNMENT
c
c      *  bone2      elect4      beta1 for NaOH
c
c      *  btwo2      elect4      beta2 for NaOH
c
c      *  cterm2     elect4      C term for NaOH
c
c      *  bone4      elect4      beta1 for NaA (A=anion added salt)
c
c      *  btwo4      elect4      beta2 for NaA
c
c      *  cterm4     elect4      C term for NaA
c
c      *  term       elect4      8 terms which form thePitzer 4th
c
c      *****
c
c      * Consider only added Cations and anions
c
c      *****
c
c      * pe(4) = Sum over all cations and anions of
c
c      *           M(c).M(a) [Zx**2.B'ca + ZxC'ca]
c
c      * where;
c
c      *   B'ca = 2.b1(ca)/alpha**2.I**2
c
c      *           [1+alpha.I**.5+0.5*alpha**2.I)
c
c      *           exp(-alpha.I**.5)-1] + 2.b2(ca)/alpha2**2.I**2
c
c      *           [1+alpha2.I**.5+0.5alpha2**2.I)exp(-alpha2.I**.5)-1]
c
c      * where ca is the salt added to the reaction
c
c      *****
c
c      * constants for analysis
c
c      *****
alpha = 2.0
alpha2 = 0.0
c
c      *****
c
c      * We need the sum over all cations and anions =>
c
c      * the expression has the following form
c
c      * ln(gamma) = 2[ m(Na).m(oh)Zx^2.B'(Na+OH-) +
c
c      * m(Na).m(OH).Zx.C(Na+OH-) + m(c).m(OH).Zx^2.B'(c-OH)

```

```

c      * +m(c).m(OH).Zx.C(cOH) + m(Na).m(a).Zx^2.B'(Na-a) +
c      * m(Na).m(a).Zx.C(Na-a) + m(c).m(a).Zx^2.B'(c-a) +
c      * m(c).m(a).Zx.C(c-a)
c      *
c      *      A total of eight terms
c      *****
c      * step1:  CALCULATION OF B' TERMS
c      *****
c      *      added salt  B'(ca) is term(1)
c      *                  B'(NaOH) is term(2)
c      *                  B'(cOH) is term(3)
c      *                  B'(Naa) is term(4)
c      *****
c      flag = 1
c      term(1,1) = 0.0
c      term(2,1) = 0.0
c      term(3,1) = 0.0
c      term(4,1) = 0.0
17  continue
c      do 100 j=2,ndata
c      part1 = 1+(alpha*xi(j)**0.5)+(0.5*alpha**2.0*xi(j))
c      part2 = (part1*dexp(-alpha*xi(j)**0.5))-1.0
c      part3 = (2.0/(alpha**2.0*xi(j)**2.0)) * part2
c      sect1 = 1+(alpha*xi(j)**0.5)+(0.5*alpha**2.0*xi(j))
c      sect2 = (sect1*dexp(-alpha*xi(j)**0.5))-1.0
c      sect3 = (2.0/(alpha**2.0*xi(j)**2.0)) * part2
c      if(flag.eq.1) dum1=bone1
c      if(flag.eq.1) dum2=btwo1
c      if(flag.eq.2) dum1=bone2
c      if(flag.eq.2) dum2=btwo2
c      if(flag.eq.3) dum1=bone3
c      if(flag.eq.3) dum2=btwo3
c      if(flag.eq.4) dum1=bone4
c      if(flag.eq.4) dum2=btwo4
c      part4 = dum1 * part3
c      sect4 = dum2 * sect3
c      term(flag,j) = part4 * sect4
100  continue
c      flag = flag + 1
c      if(flag.ne.5) goto 17

```

```

C      *****
C      *          END OF STEP 1
C      *****
C      * step 2:  CALCULATION OF C TERMS
C      *****
C      *      term(5)= C(ca)
C      *      term(6)= C(NaOH)
C      *      term(7)= c(cOH)
C      *      term(8)= C(Naa)
C      *****
do 21 j=1,ndata
term(5,j) = cterm1/(2.0*1.0)
term(6,j) = cterm2/(2.0*1.0)
term(7,j) = cterm3/(2.0*1.0)
term(8,j) = cterm4/(2.0*1.0)
21  continue
C      *****
C      *          END OF STEP 2
C      *****
C      * step3: Formation of the Pitzer fourth term
C      *****
C      * in this situation Zx=-1.0 = charge on OH-
C      * xmo = molarity of NaOH = 0.1 mol dm-3
C      *****
zx=-1.0
xmo=0.1
pe4(1)=0.0
write(6,2007)
2007 format(1h,'%%%%%%%%%%%%%%%%%%%%%%%%%%%%%%%%%%%%%%%%%%%%%%%%%%%%%%%%%%%%%%%%%%%%%%%%%'
$%%%%%%%%%'
$%%%%%%%%%' )
write(6,60)
60  format(1h ,16x,'I.Strength',9x'Fourth Term')
do 50 j=2,ndata
pe4(j)= (term(1,j)*zx**2.0*xm2(j)**2.0)
$(term(2,j)*zx**2.0*xmo**2.0)
$(term(3,j)*zx**2.0*xmo*xm2(j))
$(term(4,j)*zx**2.0*xmo*xm2(j))
$(term(5,j)*zx*xm2(j)**2.0)
$(term(6,j)*zx*xmo**2.0) + (term(7,j)*zx*xmo*xm2(j))

```

```
$(term(8,j)*zx*xmo*xm2(j))
  pe4(j)= 2.0 * pe4(j)
50  continue
    do 80 j=1,ndata
      write(6,70) j,xi(j),pe4(j)
70  format(1h,2x,i5,4x,1pe15.6,5x,1pe15.6)
80  continue
9999 continue
    return
  end
```

```

subroutine cosphere
implicit double precision(a-h,o-z)
common/andy/xm2(30),xcons(30),pitzer(30)
common/linda/ndata,bo,bone3,btwo3,cterm3
common/answer/pe1(30),pe2(30),pe4(30),dh11(30),xi(30)
common/fiat/bone1,btwo1,cterm1
c *****
c * pe2 = 2.Mc[ Bxc + McZc.Cxc]
c *
c * Bxc = b0xc + 2b1xc/alpha**2.I [ 1-(1+alpha.I**0.5)exp
c * (-alpha.I**0.5)]
c *
c * Cxc(gamma) = Cxc(phi)/2|ZcZx|**0.5
c *****
c * N.B in this section X = OH-
c *****
c * Step 1: Calculation of Bxc
c *****
alpha=2.0
WRITE(6,100)
100 format(1h ,5x,'THE TRINEGATIVE ANION')
do 2 j=2,ndata
write(6,14) xi(j)
14 format(1h ,10x,'NEW VALUE OF IONIC STRENGTH = ',1pe15.6)
do 4 b00=0.5,1.1,0.1
write(6,12) b00
12 format(1h ,10x,'NEW VALUE OF BETA0 =',1pe15.6)
do 6 b1 =5,10,0.2
term1 = dexp(-alpha*xi(j)**0.5)
term2 = 1 + alpha*xi(j)**0.5
term3 = 1 - (term2*term1)
term4 = (2.0*b1)/(alpha**2.0*xi(j))
bxcc = b00 + (term4 * term3)
write(6,10) j,b00,b1,bxcc,xi(j)
10 format(1h ,3x,i5,4(5x,1pe15.6))
6 continue
4 continue
2 continue
write(6,2007)
2007 format(1h,'%%%%%%%%%%%%%%%%%%%%%%%%%%%%%%%%%%%%%%%%%%%%%%%%%%%%%%%%%%%%%%%%%%%%%%%%')

```



```

subroutine plot
implicit double precision(a-h,o-z)
common/andy/xm2(30),xcons(30),pitzer(30)
common/linda/ndata,bo,bone3,btwo3,cterm3
common/answer/pe1(30),pe2(30),pe4(30),dh11(30),xi(30)
common/fiat/bone1,btwo1,cterm1
real*4 ionic(30),dh(30),one(30),two(30),four(30)
real*4 sconx(30),pitz(30)
c *****
c * Convert from double to single precision
c *****
do 10 j=1,30
ionic(j) = xi(j)
dh(j) = dh11(j)
one(j) = pe1(j)
two(j) = pe2(j)
four(j) = pe4(j)
sconx(j) = xcons(j)
pitz(j) = pitzer(j)
10 continue
flag = 0.0
call gpstop(2)
call filnam('tmaf')
100 continue
call lincol(0)
call pspace(0.15,0.85,0.15,0.85)
if(flag.eq.1.0) goto 103
call map(0.0,2.2,-1.0,7.0)
if(flag.ne.1.0) goto 104
103 continue
call map(0.0,1.5,-1.0,7.0)
104 continue
call axorig(0.0,0.0)
call axes
call ptplot(ionic,sconx,1,ndata,232)
call curveo(ionic,sconx,1,ndata)
call ptplot(ionic,dh,1,ndata,243)
call curveo(ionic,dh,1,ndata)
call lincol(2)
call ptplot(ionic,one,1,ndata,244)

```

```
call curveo(ionic,one,1,ndata)
call lincol(3)
call ptplot(ionic,two,1,ndata,245)
call curveo(ionic,two,1,ndata)
call lincol(4)
call ptplot(ionic,four,1,ndata,251)
call curveo(ionic,four,1,ndata)
call ptplot(ionic,pitz,1,ndata,235)
call curveo(ionic,pitz,1,ndata)
call frame
flag = flag + 1.0
do 50 j=1,30
ionic(j)=ionic(j)**0.5
continue
if(flag.eq.1.0) goto 100
return
end
```



# Appendix

6

## Section 1

The following listing contains the main subroutines of the FORTRAN program H2OD2O which was used to calculate the internal pressure of water and deuterium oxide and to fit the data using the method of linear least squares to equation [10.20] of Chapter 10.

Subroutine DATA(JJ) contains the parameters for equations used by Fine and Millero<sup>8,9</sup> to calculate the volumes, expansibilities and compressibilities for both water and deuterium oxide. Subroutine VANALY sets up the arrays and necessary variables from which the volumes (subroutine VCALC), compressibilities (subroutine XCOMP), expansibilities (subroutine XPAN) and internal pressures (subroutine PANALY) are calculated. The same subroutine also sets up arrays for various plot routines e.g. subroutines PIMAP and PILOT.

Finally the internal pressure, temperature and pressure data are set up for equation [10.20] of Chapter 10 in subroutine XPIFIT. The data are fitted to this equation using the method of linear least squares using a separate subroutine (subroutine XLSQ) called from within XPIFIT.

At the start of the program the integer variable JJ is set equal to zero, this ensures the program analyses data for water. However on successful completion of subroutine XPIFIT the program loops back to the start and resets JJ = 1. The program then carries out the same analysis for deuterium oxide and on successful completion of XPIFIT for the second time the program is terminated.

```

program h2od2o
c *****
c *      internal pressures
c *      A.W.Hakin & M.J.Blandamer
c *      University of Leceister
c *****
implicit double precision(A-H,o-Z)
common/mike/p(11),tk(31),pi(31,11),tc(31),b(5),
$al(5),a2(5),dv(6),d0(2),vol(31,11),comp(31,11),yexp(31,11)
common/anne/rk(50),prk(50),nrk,delta(500),point(500)
common/will/btot,altot,dtot,a2tot,zv,dog
common/pete/dvz,db,da1,da2,tcpi,lind,zpos(31,11)
common/jess/xtc
common/dan/kcont,setpi,excomp,pnew
c *****
c *      internal pressure and kinetics
c *****
c *****
c *      anne is kinetics
c *****
itop=0
jtop=0
nout=6
c *****
c *      jj = 0      water
c *      jj = 1      d2o      lind is a counter for plots
c *****
jj=0
lind=1
dog=1
call paper(1)
200  continue
call head(jj)
call data(jj)
call vanaly
call xpifit
30  format(1h ,10x,'signals')
write(6,40) itop, jtop
40  format(1h ,10x,'itop=', i3,2x,'jtop=',i3)
if(jj.eq.1) goto 100

```

```
      jj=1
      goto 200
100   continue
      call grend
      write(6,20)
20    format(1h0,20x,'that is all, folks')
      end
```

```

subroutine data(jj)
implicit double precision(A-H,O-Z)
common/mike/p(11),tk(31),pi(31,11),tc(31),b(5),
$al(5),a2(5),dv(6),d0(2),vol(31,11),comp(31,11),yexp(31,11)
common/pete/dvz,db,da1,da2,tcpi,lind,zpos(31,11)
common/anne/rk(50),prk(50),nrk,delta(500),point(500)
common/will/btot,altot,dtot,a2tot,zv,dog
c *****
c * data from fine and millero
c * water J.Chem.Phys., 1973,59,5529.
c * d2o J.Chem.Phys., 1975,63,89.
c * b- parameters equation 6''
c *****
c if(jj.eq.1) goto 10
c *****
c * water data
c *****
c b(1)=19654.320
c b(2)=147.037
c b(3)=-2.21554
c b(4)=1.0478e-2
c b(5)=-2.2789e-5
c *****
c * d0 parameters numerator for v0
c * equation 6'
c *****
c d0(1)=1.00
c d0(2)=18.159725e-3
c *****
c * a1 parameters equation 6''
c *****
c a1(1)=3.2891
c a1(2)=-2.3910e-3
c a1(3)=2.8446e-4
c a1(4)=-2.8200e-6
c a1(5)=8.477e-9
c *****
c * a2 parameters equation 6''
c *****
c a2(1)=6.245e-5

```

a2(2)=-3.913e-6

a2(3)=-3.499e-8

a2(4)=7.942e-10

a2(5)=-3.299e-12

c \*\*\*\*\*

c \* dv( ) denominator in volume eqn.

c \*\*\*\*\*

dv(1)=0.9998396

dv(2)=18.224944e-3

dv(3)=-7.922210e-6

dv(4)=-55.44846e-9

dv(5)=149.7562e-12

dv(6)=-393.2952e-15

goto 20

c \*\*\*\*\*

c \* d2o data

c \*\*\*\*\*

10 continue

b(1)=1.860737e4

b(2)=170.26

b(3)=-2.40556

b(4)=1.02703e-2

b(5)=-1.5680e-5

d0(1)=1.00

d0(2)=17.96190e-3

a1(1)=3.129069

a1(2)=-4.53919e-3

a1(3)=4.3252e-4

a1(4)=-4.7659e-6

a1(5)=1.6244e-8

a2(1)=1.07903e-4

a2(2)=-5.5471e-7

a2(3)=-1.6758e-7

a2(4)=2.384e-9

a2(5)=-9.301e-12

dv(1)=1.104690

dv(2)=20.09315e-3

dv(3)=-9.24227e-6

dv(4)=-55.9509e-9

dv(5)=79.9512e-12

```

        dv(6)=0.0
20      continue
        write(6,100)
100     format(1h ,20x,'input parameters')
        do 110 i=1,5
            write(6,120) i,b(i)
120     format(1h ,2x,'b',2x,i3,2x,'=',2x,1pe15.6)
110     continue
        do 130 i=1,2
            write(6,140) i,d0(i)
140     format(1h ,2x,'d',2x,i3,2x,'=',2x,1pe15.6)
130     continue
        do 150 i=1,5
            write(6,160) i,a1(i),a2(i)
160     format(1h ,2x,i3,2x,'a1 = ',1pe15.6,3x,'a2 = ',1pe15.6)
150     continue
        do 180 i=1,6
            write(6,190) i,dv(i)
190     format(1h ,2x,i3,2x,'dv = ', 1pe15.6)
180     continue
        return
        end

```

```

subroutine vanaly
implicit double precision(a-h,o-z)
c *****
c * calc of volumetric parameters for water
c *****
common/mike/p(11),tk(31),pi(31,11),tc(31),b(5),
$al(5),a2(5),dv(6),d0(2),vol(31,11),comp(31,11),yexp(31,11)
common/anne/rk(50),prk(50),nrk,delta(500),point(500)
common/pete/dvz,db,da1,da2,tcpi,lind,zpos(31,11)
common/will/btot,altot,dtot,a2tot,zv,dog
dimension z(40),hts(20,50),x(40)
c *****
c * z is a plot dummy
c * hts is for 3-d plot
c *****
itop=0
jtop=0
write(6,10)
10 format(1h ,20x,'volumetric parameters')
icount = 0
write(6,20)
20 format(1h ,25x,'fine and millero')
c *****
c * set up for temp array (11,31) *
c *****
xts=0.5
do 30 i=1,40
icount=icount+1
itop=itop+1
jtop=0
tc(i)=(i-1)*xts
if(i.gt.12) xts=5.0
if(i.gt.12) tc(i)=(i-11)*xts
tk(i)=tc(i)+273.15
c *****
c * Alternative setup for pi surface plot (i.e (11,21))*
c *****
c xts=5.0
c do 30 i=1,21
c icount=icount+1

```

```

c      itop=itop+1
c      jtop=0
c      tc(i)=(i-1)*xts
c      tk(i)=tc(i)+273.15
c      *****
c      *          End of the alternative Setup          *
c      *****
do 40 j=1,11
jtop=jtop+1
p(j)=(j-1)*1.0e2
c      *****
c      *    0   to 110 celsius
c      *    0   to 1000 bar applied pressure
c      * p( )  is held in bar
c      * pn   is held in n m^-2
c      *****
pn=(p(j)*1.0e5)+101325.0
xtc=tc(i)
pug=p(j)
c      *****
c      * vcalc called with
c      *   xtc      temp/celsius
c      *   pug      xs pressure/bar
c      * returns  dum in cm^3 g^-1
c      *****
call vcalc(xtc,pug,dum)
c      *****
c      * vol(i,j) in cm^3 g^-1
c      *****
vol(i,j)=dum
c      *****
c      * xcomp called with
c      *   xtc      = temp/celsius
c      *   pug      = xs pressure/bar
c      *   dum      = vol/cm^3 g^-1
c      *   return  ycomp/(N m^-2)^-1
c      *****
call xcomp(xtc,pug,dum,ycomp)
comp(i,j)=ycomp
c      *****

```

```

c      *   xpan called with
c      *       xtc = temp/celsius
c      *       pug/excess pressure/bar
c      *dum = vol/cm^3 g^-1
c      * return   dum2   expansibility/K^-1
c      *****
c      call xpan(xtc,pug,dum,dum2)
c      yexp(i,j)=dum2
c      *****
c      *   call panaly with
c      *       xtc = temp/celsius
c      *       pug = excess pressure/bar
c      *       dum2 = expansibility
c      *       ycomp = compressibility
c      * return with   xpi/N m^-2 = internal pressure
c      *****
c      xtc=tc(i)
c      pug=p(j)
c      call panaly(xtc,pug,dum2,ycomp,xpi)
c      pi(i,j)=xpi
40     continue
c      if(tc(i).ge.100.0) goto 177
30     continue
177    continue
c      write(6,178) icount
178    format(1h ,10x,'number of data points=',i4)
c      do 200 k=1,4
c      if(k.eq.1) write(6,50)
50     format(1h0,20x,'volumes/cm^3 g^-1')
c      if(k.eq.2) write(6,51)
51     format(1h0,20x,'expansibilities/K^-1')
c      if(k.eq.3)write(6,52)
52     format(1h0,20x,'compressibilities/Pa^-1')
c      if(k.eq.4) write(6,53)
53     format(1h ,20x,'internal pressures/bar')
c      do 90 m=1,15,5
c      itop=m+4
c      if(itop.gt.11) itop=11
c      write(6,60) (p(i),i=m,itop)
60     format(1h ,4x,'pg/bar',7x,5(x,1pe15.6))

```

```

write(6,61)
61  format(1h ,2x,'temperature/R')
do 70 j=1,60
im=itop
if(k.eq.1) write(6,80)j,tk(j),(vol(j,i),i=m,im)
if(k.eq.2) write(6,80)j,tk(j),(yexp(j,i),i=m,im)
if(k.eq.3)write(6,80)j,tk(j),(comp(j,i),i=m,im)
if(k.eq.4)write(6,80)j,tk(j),(pi(j,i),i=m,im)
80  format(1h ,i2,x,1pe15.6,5(x,1pe15.6))
if(tc(j).ge.100.0) goto 77
if(j.ge.icount) goto 77
70  continue
77  continue
if(p(i).gt.1.0e3) goto 777
90  continue
777 continue
200 continue
c *****
c *      int pressure plot
c *****
ymin=pi(1,1)
ymax=ymin
do 4810 ix=1,icount
do 4820 iy=1,11
if(pi(ix,iy).lt.ymin) ymin=pi(ix,iy)
if(pi(ix,iy).gt.ymax) ymax=pi(ix,iy)
4820 continue
4810 continue
ymin=ymin-dabs(ymin/10.0)
ymax=ymax+dabs(ymax/10.0)
do4310 i=1,11
do4320 j=1,icount
zpos(j,i)=pi(j,i)
4320 continue
4310 continue
c *****
c *      attempt to plot internal press surface
c *****
call pimap
c call piplot

```

```

c      *****
c      * 3-d plot
c      *****
write(6,1010)
1010  format(1h ,2x,'iso plot')
write(6,1020)
1020  format(1h, 3x,'volumes')
      do 1030 i=1,50
      do 1040 j=1,20
      xtc=(i-1)*2
      pug=(j-1)*100
      call vcalc(xtc,pug,dum)
      hts(j,i)=dum
1040  continue
1030  continue
      ifail=0
1099  continue
      return
      end

```

```

subroutine vcalc(tcx,px,calcv)
implicit double precision(A-H,O-z)
common/mike/p(11),tk(31),pi(31,11),tc(31),b(5),
$al(5),a2(5),dv(6),d0(2),vol(31,11),comp(31,11),yexp(31,11)
common/pete/dvz,db,da1,da2,tcpi,lind,zpos(31,11)
common/anne/rk(50),prk(50),nrk,delta(500),point(500)
common/will/btot,altot,dtot,a2tot,zv,dog
c *****
c * input tcx = temp/celsius
c * px = pressure/bar (excess)
c * output = calcv/cm^3 g^-1
c *****
btot=b(1)
altot=a1(1)
a2tot=a2(1)
c *****
c * calc b a1 and a2 in eqn 6.
c *****
do 10 i=2,5
btot=btot+(b(i)*tcx**(i-1))
altot=altot+(a1(i)*tcx**(i-1))
a2tot=a2tot+(a2(i)*tcx**(i-1))
30 continue
10 continue
dtot=dv(1)
do 20 i=2,6
dtot=dtot+(dv(i)*tcx**(i-1))
40 continue
20 continue
xk1=altot*px
xk2=a2tot*px**2
xk=btot+xk1+xk2
c *****
c * xk = pres.zv/(zv -calv)
c *****
zv=(d0(1) +d0(2)*tcx)/dtot
calcv = zv -(px*zv/xk)
return
end

```

```

subroutine xcomp(temp,pres,calv,ycomp)
implicit double precision(a-h,o-z)
c *****
c * calc of compressibility
c *   temp = t/celsius
c *   pres = excess pressure/bar
c *   calv = volume/cm^3 g^-1
c *   return ycomp in (N m^-2)^-1 and not bar^-1
c *****
common/mike/p(11),tk(31),pi(31,11),tc(31),b(5),
$al(5),a2(5),dv(6),d0(2),vol(31,11),comp(31,11),yexp(31,11)
common/anne/rk(50),prk(50),nrk,delta(500),point(500)
common/pete/dvz,db,da1,da2,tcpi,lind,zpos(31,11)
common/will/btot,altot,dtot,a2tot,zv,dog
dum1 =btot-(a2tot*pres**2)
dum2 =btot+(altot*pres)+(a2tot*pres**2)
ycomp=zv*dum1/(calv*dum2**2)
ycomp=ycomp*1.0e-5
return
end
subroutine panaly(xtc,pug,xpan,ycomp,xpi)
implicit double precision(a-h,o-z)
c *****
c * calculation of internal pressure;
c * return calc in xpi
c * at pressure pug/bar and xtc/celsius
c *****
common/mike/p(11),tk(31),pi(31,11),tc(31),b(5),
$al(5),a2(5),dv(6),d0(2),vol(31,11),comp(31,11),yexp(31,11)
common/pete/dvz,db,da1,da2,tcpi,lind,zpos(31,11)
common/anne/rk(50),prk(50),nrk,delta(500),point(500)
common/will/btot,altot,dtot,a2tot,zv,dog
pug=(pug+1.0)*1.01325e5
xpi=((xtc+273.15)*xpan/ycomp) - pug)*1.0e-5
return
end

```

```

subroutine xpan(temp,pres,calv,expan)
implicit double precision(a-h,o-z)
c *****
c * temp = t/celsius
c * pres = excess pressure/bar
c * calv = calc volume/cm^3 g^-1
c * return expan/K^-1
c *****
common/mike/p(11),tk(31),pi(31,11),tc(31),b(5),
$al(5),a2(5),dv(6),d0(2),vol(31,11),comp(31,11),yexp(31,11)
common/pete/dvz,db,da1,da2,tcpi,lind,zpos(31,11)
common/anne/rk(20),prk(20)
common/will/btot,altot,dtot,a2tot,zv,dog
c *****
c * calc of expan.
c *****
db=b(2)
da1=a1(2)
da2=a2(2)
ddv=dv(2)
do 20 i=3,5
xtc=temp**(i-2)
c *****
c * calc db/dt
c * da1/dt
c * da2/dt
c *****
db=db+(i-1)*b(i)*xtc
da1=da1+((i-1)*a1(i)*xtc)
da2=da2+((i-1)*a2(i)*xtc)
20 continue
c *****
c * calc dv0/dt
c *****
do 30 i=3,6
xtc=temp**(i-2)
ddv=ddv+((i-1)*dv(i)*xtc)
30 continue
dum1 = d0(2)/dtot
dum2=d0(1)+d0(2)*temp

```

```

dum3= - dum2*ddv/(dtot**2)
dvz = dum1+dum3
c *****
c * first term in eqn 10 is dum4
c *****
dum4=dvz/calv
c *****
c * second term is dum5
c *****
sum1=(btot+(altot*pres)+(a2tot*pres**2))
dum5= - pres*dvz/(calv*sum1)
c *****
c * third term is dum6
c *****
sum2 = db+(da1*pres)+(da2*pres**2)
dum6 = pres*zv*sum2/(calv*sum1**2)
  expan=dum4+dum5+dum6
return
end

```

```

subroutine xpifit
c *****
c * analysis of internal pressures
c *
c *          dependences on T and p
c * fit pi dependence
c * pi = a1 + a2.(t-tref) + a3.(p-pref) + a4.(T-tref^2)
c *          + a5.(t-tref).(p-pref) + a6.(p-pref)^2 ....
c *****
implicit double precision(a-h,o-z)
common/mike/p(11),tk(31),pi(31,11),tc(31),b(5),
$ a1(5),a2(5),dv(6),d0(2),vol(31,11),comp(31,11),yexp(31,11)
common/anne/rk(50),prk(50),nrk,delta(500),point(500)
common/pete/dvz,db,da1,da2,tcpi,lind,zpos(31,11)
common/will/btot,altot,dtot,a2tot,zv,dog
dimension a(20),y(500),x(500,10),xt(10,500),w(10,10)
dimension wi(10,10),ycalc(500),picalc(40,11)
dimension z(500),unit(10,10),wkspce(10),wp(10,500)
dimension zx(1),xdelta(1,500),cx(30,30)
write(6,10)
10 format(1h ,10x,'pi -- lsq')
c *****
c * fit about midpoints
c *****
tref=323.15
pref=500
write(6,20) tref
20 format(1h ,20x,'tref/k=',1pe15.6)
write(6,30) pref
30 format(1h ,10x,'pref/bar=',1pe15.6)
c *****
c * clear arrays
c *****
do 33 j=1,500
y(j)=0.0
do 35 i=1,10
x(j,i)=1.0
35 continue
33 continue
c *****
c * set up arrays

```

```

c      * jfit is counter
c      *****
jfit=0
do 100 i=1,31
do 110 j=1,11
jfit=jfit+1
y(jfit)=pi(i,j)
x(jfit,1)=1.0
x(jfit,2)=tk(i)-tref
x(jfit,3)=p(j)-pref
x(jfit,4)=x(jfit,2)**2
x(jfit,5)=x(jfit,2)*x(jfit,3)
x(jfit,8)=x(jfit,3)**2
x(jfit,9)=x(jfit,2)**3
x(jfit,6)=x(jfit,4)*x(jfit,3)
x(jfit,7)=x(jfit,2)*x(jfit,3)**2
x(jfit,10)=x(jfit,3)**3
110  continue
100  continue
write(6,130) jfit
130  format(1h ,10x,'number of points=',i10)
c      *****
c      * least squares analysis
c      * set number of parameters and explore fit
c      *****
      if(lind.eq.1) ipar=7
      if(lind.eq.2) ipar=9
call xlsq(x,y,jfit,ipar,a)
write(6,1020)
1020 format(1h ,10x,'end of analysis')
return
end

```

## Section 2

Modification of the latter FORTRAN program produces a program which calculates the temperature of maximum density for both water and deuterium oxide as a function of pressure. The modification is achieved by removing subroutine XPIFIT from the program and replacing it with subroutine TMD(JJ) which in turn calls an external subroutine F.

Subroutine TMD(JJ) contains NAG routine C05ADF which locates a zero of a continuous function in a given interval by combination of the methods of interpolation, extrapolation and bisection. External subroutine F, called by the NAG routine, defines the function whose zero is to be determined. In the context of this problem the continuous function is the volume and hence for a given temperature the NAG routine searches for a pressure at which the volume is a minimum i.e. the pressure at which the expansibility should be zero. Enclosing the NAG routine within a 'do loop' ensures several different temperatures are examined.

The resulting temperature and pressure data are then fitted using the method of linear least squares (subroutine XLSQ called from within TMD(JJ)) to equation [10.21] of Chapter 10 to produce an equation for the temperature of maximum density as a function of pressure for both water and deuterium oxide.

```

subroutine tmd(jj)
  implicit double precision(a-h,o-z)
  common/mike/p(11),tk(31),pi(31,11),tc(31),b(5),
  $a1(5),a2(5),dv(6),d0(2),vol(31,11),comp(31,11),yexp(31,11)
  common/anne/rk(50),prk(50),nrk,delta(500),point(500)
  common/jess/xtc
  common/dan/kcont,setpi,excomp,pnew
  common/pete/dvz,db,da1,da2,tcpi,lind,zpos(31,11)
  common/will/btot,altot,dtot,a2tot,zy,dog
  dimension vmin(50),tmin(50),pmin(50)
  dimension a(20,1),y(500),x(500,10)
  external f
c *****
c * calc of TMD
c *****
  write(6,10)
10  format(1h ,20x,'TMD calculation')
  kcont=0
c *****
c * determine pressure at which E is zero at given Temp.
c *****
  do 20 i=1,8
  if(jj.eq.1) goto 13
  xtc = 4.0-(i-1)*1.0
  if(i.eq.1) xtc=3.984
c *****
c * 3.984 from Kell and 11.44
c * Gauss-Newton calc.
c *****
  goto 15
13  continue
  xtc = 10.0-(i-1)*1.0
  if(i.eq.1) xtc=11.44
15  continue
  tmin(i)=xtc+273.15
  pug=0.0
  if(i.eq.1) goto 60
  ilast=i-1
  pug=pmin(ilast)
  write(6,62) xtc

```

```

62  format(1h ,2x,'t/c=',2x,1pe15.6)
    write(6,64) pug
64  format(1h ,2x,'input p/bar =',2x,1pe15.6)
    ifail=0
    xtcc=xtc
c   *****
c   * calls to vcalc and xpan are dummy to obtain
c   *   contributing param.
c   *****
    call vcalc(xtcc,pug,calcv)
    call xpan(xtcc,pug,calcv,dum)
    eta=0.0
    eps=1.0e-8
    xa=-100
    xb=1.0e2
    call c05adf(xa,xb,eps,eta,f,pug,ifail)
60  continue
    write(6,70) pug
70  format(1h ,10x,'est p/bar=',2x,1pe15.6)
    write(6,80) ifail
80  format(1h ,10x,'ifail=',2x,i3)
    if(ifail.ne.0)stop
    pmin(i)=pug
    call vcalc(xtcc,pug,calcv)
    call xpan(xtcc,pug,calcv,dep)
    vmin(i)=calcv
    write(6,100) i,xtc,tmin(i),pmin(i),vmin(i),dep
100 format(1h ,2x,i3,2x,'t/c=',2x,1pe15.6,2x,'t/k=',2x,
$1pe15.6,2x,'p/bar=',2x,1pe15.6,2x,
$'v/cm^3 g^-1 =',2x,1pe15.6,2x,'ex= ',1pe15.6)
20  continue
c   *****
c   * add further analysis here
c   *****
    write(6,701)
701 format(1h ,10x,'lsq analysis')
    do 400 i=1,500
    do 410 j=1,10
    x(i,j)=1.0
410  continue

```

```

400  continue
c    *****
c    *   fit   T as a function of p
c    *****
write(6,505)
505  format(1h ,3x,'temp/c',5x,'p/bar')
do 500 i=1,8
x(i,1)=1.0
x(i,2)=pmin(i)
x(i,3)=pmin(i)**2
x(i,4)=pmin(i)**3
y(i)=tmin(i)-273.15
write(6,702) i,y(i),x(i,2)
702  format(1h ,4x,i3,2(3x,1pe15.6))
500  continue
jfit=8
do 503 ipar=2,4
call xlsq(x,y,jfit,ipar,a)
503  continue
return
end

```

```

real function f(pug)
implicit double precision(a-h,o-z)
common/mike/p(11),tk(31),pi(31,11),tc(31),b(5),
$al(5),a2(5),dv(6),d0(2),vol(31,11),comp(31,11),yexp(31,11)
common/anne/rk(50),prk(50),nrk,delta(500),point(500)
common/jess/xtc
common/dan/kcont,setpi,excomp,pnew
common/pete/dvz,db,da1,da2,tcpi,lind,zpos(31,11)
common/will/btot,altot,dtot,a2tot,zy,dog
if(kcont.eq.1) goto 500
if(kcont.eq.2) goto 700
xtcc=xtc
xpug=pug
call vcalc(xtcc,xpug,calcv)
call xpan(xtcc,xpug,calcv,dumx)
c *****
c *      btot      dtot      zv
c *      altot      a2tot      dvz      all known
c *      zv = v0      dvz = dv0/dt = s
c *      db1      da1      da2
c *****
dum=btot + (altot*pug) + (a2tot*pug**2)
dum1 = - pug*dvz/dum
zdum=db+(da1*pug)+(da2*pug**2)
dum2=pug*zv*zdum/dum**2
f=dvz+dum1+dum2-setpi
write(6,110) pug
110 format(1h ,2x,'in f( ), pug= ',1pe15.6)
write(6,20) f
20 format(1h ,'f =',2x,1pe15.6)
write(6,30) calcv,dumx
30 format(1h ,2x,'v=',2x,1pe15.6,2x,'expan=',
$2x,1pe15.6)
c *****
c *      expan should be zero
c *****
goto 510
500 continue
write(6,207) pug
207 format(1h ,2x,'in f, pug =', 1pe15.6)

```

```

call vcalc(tcpi,pug,calcv)
call xcomp(tcpi,pug,calcv,ycomp)
call xpan(tcpi,pug,calcv,expan)
f=((tcpi+273.15)*expan/ycomp)-(pug+1)-setpi
write(6,10) f
10  format(1h ,10x,'resid pi =',2x,1pe15.6)
    goto 510
700  continue
    ytc=pug
    write(6,707) ytc
707  format(1h ,2x,' in f, ytc= ', 1pe15.6)
    call vcalc(ytc,pnew,calcv)
    call xcomp(ytc,pnew,calcv,ycomp)
    call xpan(ytc,pnew,calcv,expan)
    denom=btot+(altot*pnew) + (a2tot*pnew**2)
    xnum=btot-(a2tot*pnew**2)
    dum1=db-(da2*pnew**2)
    dum2 = -2.0*(db+(da1*pnew) + (da2*pnew**2))*xnum/denom
    dum3=-xnum*expan
    f=dum1+dum2+dum3
    write(6,303) f
303  format(1h ,10x,'resid compress = ',1pe15.6)
510  continue
    return
end

```

Appendix  
7

This program, written in HP BASIC, reports how the excess pressures discussed in Chapter 11 can be calculated. In the example shown the program is set up to calculate the excess pressures of aqueous urea solutions. The following variables have been used within the program;

V2 = the apparent molar volume at infinite dilution,  
 $\phi(v_j)^\infty$ .

K2 = the limiting compression of the solute,  $K_j^\infty$ .

O1 = the occupied volume of the solute,  $O_j$ .

M1 = the molar mass of water.

M(i) = the molality of urea in solution.

V(i) = the apparent molar volume of the solute,  $\phi(v_j)$ .

Obtained from a polynomial expression in molality.

D1 & D2 = the parameters  $d_1$  and  $d_2$  of equations [11.10] and [11.11] of Chapter 11.

V1(i) = the differential of  $\phi(v_j)$  with respect to molality, multiplied by the molality of the urea.

The excess pressures are calculated in lines 160 to 340 of the program. On successful completion array P1 contains the excess pressure  $p^E(L)$ , P2 contains  $p^E(\phi-v_j)$ , P3 contains  $p_E(\phi-v_1)$  and P4 contains  $p_E(G2)$ . These calculations are based on equations [11.51], [11.61], [11.65] and [11.32] of Chapter 11 respectively.

Lines 350 to 720 of the program collect together the calculated data and produces plots of  $p^E(L)$ ,  $p^E(\phi-v_j)$ ,  $p^E(\phi-v_1)$  and  $p^E(G2)$  against molality on an HP 7475A plotter.

```

10 I GIBSON PAPER
20 I MULTI PLOT
30 I UREA
40 I ANDY HAKIN UNIV LEICESTER
50 OPTION BASE 10 CLEAR
60 DIM M(25),M1(25),M(25)
70 DIM P1(25),P2(25),P3(25),P4(
25)
80 V2=44.2 @ K2=-.00009 @ O1=.0
000494901
90 O1=.00000246636 @ O2=2993.39
4
100 M1=.018015 @ P=1
110 FOR I=1 TO 25
120 M(I)=I/2+.5
130 V(I)=44.2+.126*M(I)-.004*M(I)
)^2
140 M1(I)=(.126-.008*M(I))*M(I)
150 A1=(V2-V(I)-K2*(O2+P))*M(I)
01
160 A1=A1*M1*M(I)
170 A2=EXP(A1/O1)
180 A2=A2*(O2+P)
190 P1(I)=A2-(O2+P)
200 B1=M1(I)*.000001
210 B1=B1*M1*M(I)
220 B2=EXP(B1/O1)
230 B2=B2*(O2+P)
240 P2(I)=B2-(O2+P)
250 C1=(V2-V(I))*M(I)
260 C1=C1*M1*M(I)
270 C2=EXP(C1/O1)
280 C2=C2*(O2+P)
290 P3(I)=C2-(O2+P)
300 E1=M(I)*.000001
310 E1=O1-E1
320 E2=EXP(M(I)*M1*E1/O1)
330 P4(I)=(O2+P)*(E2-1)
340 NEXT I
350 PLOTTER IS 705
380 X1=0
390 X2=AMAX(M)
410 Z=(X2-X1)/4
420 SCALE X1-Z,X2+Z,-450,1650
430 XAXIS 0,Z,X1,X2
440 YAXIS X1,200,-400,1600
450 FOR I=1 TO 25
460 PLOT M(I),P1(I)
470 NEXT I
480 LABEL "LEYEN"
490 PEN 2
500 FOR I=1 TO 25
510 PLOT M(I),P2(I)
520 NEXT I
530 LABEL "BLAND/HAK"
540 PEN 3
550 FOR I=1 TO 25
560 PLOT M(I),P3(I)
570 NEXT I
580 LABEL "TINTAGEL"
590 PEN 4
600 FOR I=1 TO 25
610 PLOT M(I),P4(I)
620 NEXT I
630 LABEL "GIBSON"
640 PEN 1
650 FOR S=X1 TO X2 STEP Z
660 MOVE S,-75 @ LABEL VAL$(S)
670 NEXT S
680 FOR T=-400 TO 1600 STEP 200
690 MOVE X1-Z/2,T @ LABEL VAL$(I
NT(T#10)/10)
700 NEXT T
710 FRAME
720 END

```



# Appendix

8

## Section 1

Both of the programs reported below are written in HP BASIC for an HP 85 computer. The first program,  $\beta$  INFO, calculates the configurational partial molar heat capacity, defined by equation [12.40] of Chapter 12, as a function of  $\beta$ . Within this program the following variables are defined;

$$C1 = -\phi x_Y^{eq}(1-x_Y^{eq})\Delta_r C_{pz}^*$$

$$\text{and } C2 = -\phi x_Y^{eq}(1-x_Y^{eq})(1-2x_Y^{eq})\Delta_r H^2/RT^2$$

where  $\phi = [n_s \beta / m^{\circ} W]$ . The configurational partial molar heat capacity,  $C_{pz}^{\#}$  is thus obtained as the sum  $C1 + C2$ . Values of  $C_{pz}^{\#}$  are then stored on disk to be accessed when required.

The second program,  $\beta$  PLOT, reads  $C_{pz}^{\#}$  data from the disk into an array C and then produces a plot of  $C_{pz}^{\#}$  against  $\beta$  on an HP 7475A plotter.

```

10 ! @ INFO
20 OPTION BASE 1@ CLEAR
30 DIM C(21)
40 FOR B=-1 TO 1 STEP .1
50 J=B*10+11
60 M=.018@15 @ R=8.314
70 H=10000 @ D=8 @ K0=9
80 T=298.15
90 K=LOG(K0)+H/R*(1/298.15-1/T)
100 K=EXP(K)
110 X=K/(K+EXP(B))
120 Z=X
130 C1=-(B/M*Z*(1-Z)*D)
140 C2=-(B/M*Z*(1-Z)*(1-2*Z)*H^2
    / (R*T^2))
150 C(J)=C1+C2
160 PRINT B;Z
170 NEXT B
180 VOLUME ":0701" IS "DATA H"
190 ASSIGN# 1 TO "CP.DATA H"
200 PRINT# 1 ; C()
210 ASSIGN# 1 TO *
220 DISP "DATA ON DISC"
230 END

```

```

10 ! @ PLOT
20 OPTION BASE 1@ CLEAR
30 SHORT C(21)
40 MASS STORAGE IS ":0701"
50 CRT OFF
60 VOLUME ":0701" IS "DATA H"
70 ASSIGN# 1 TO "CP.DATA H"
80 READ# 1 ; C()
90 ASSIGN# 1 TO *
100 CRT ON
110 DISP "DATA RECEIVED"
120 PLOTTER IS 705
130 GCLEAR
140 Y2=AMAX(C)
150 Y1=AMIN(C)
160 U=(Y2-Y1)/20
170 SCALE -1.1,1.1,Y1-U,Y2+U
180 XAXIS Y1,.1,-1,1
190 YAXIS -1,U,Y1,Y2
200 MOVE -1,Y1
210 FOR B=-1 TO 1 STEP .1
220 J=B*10+11
230 PLOT B,C(J)
240 NEXT B
250 FOR B=-1 TO 1 STEP .1
260 MOVE B,Y1+30 @ LDIR 0 @ LABEL
    L VAL$(B)
270 NEXT B
280 FOR S=Y1 TO Y2 STEP 2*U
290 S=INT(S)
300 MOVE -.9,S @ LABEL VAL$(S)
310 NEXT S
320 MOVE -1,0 @ DRAW 1,0 @ PENUP
330 FRAME
340 END

```

## Section 2

This FORTRAN program, HEATCAP, is a modified version of the programs reported in Section 1. The insertion of a temperature loop within the program gives  $C_{pz}^{\#}$  as a function of  $\beta$  and temperature. Hence using a graphics GHOST package contained in subroutine SURFPLOT it was possible to produce the temperature/ $\beta$  surface of the configurational isobaric partial molar heat capacity.

```

program heatcap
implicit double precision (a-h,o-z)
common/andy/temp(11),beta(31),heat(11,31)
call paper(1)
*****
c   * program to calculate the temperature and beta dependence
c   * of the isobaric partial molar heat capacity.
c   * Calculates a partial molar isobaric heat capacity temperature
c   * beta surface
c   *****
sum=-2.0
do 10 i=1,31
beta(i)=sum+((i-1.0)/5.0)
10 continue
do 20 j=1,11
temp(j) = 263.15 + (j*10.0)
20 continue
xm = 0.018015
xr = 8.314
xh = 10000.0
xd = 8.0
xko = 9.0
do 30 i=1,11
do 40 j=1,31
xk = dlog(xko) + xh/xr*(1/298.15-1/temp(i))
xk = dexp(xk)
xx = xk/(xk+dexp(beta(j)))
zx = xx
c1 = -(beta(j)/xm*zx*(1.0-zx)*xd)
c2 = -(beta(j)/xm*zx*(1.0-zx)*(1.0-2*zx)*xh**2.0
$/ (xr*temp(i)**2.0))
heat(i,j) = c1+c2
40 continue
30 continue
call surfplot
call grend
end
subroutine surfplot
implicit double precision (a-h,o-z)
common/andy/temp(11),beta(31),heat(11,31)
real*4 cap(11,31),tem(11),bet(31)
integer ifail
do 10 i=1,11
do 20 j=1,31
cap(i,j)=heat(i,j)
20 continue
10 continue
call gpstop(2)
call filnam('capacity')
call pspace(0.15,0.85,0.15,0.85)
call suraxe(3,273.15,-2.0,10.0,0.2)
call surbas(1,1,0.0)
call surcol(0,2,3)
call surdir(0)
call surind(0)
call surplt(cap,1,11,11,1,31,31)
call ctrmag(18)
call poscen(0.5,-0.15,'Isobaric Heat Capacity
$ Surface')
call ctrmag(10)
call frame
return
end

```

### Section 3

This HP BASIC program, written for an HP 85 computer can be divided into two parts. The first part of the program deals with the calculations. On running the program the user is prompted for two values of  $\beta$ . The first value is used to represent a  $\beta$  value for the initial state, B(1), and the second a  $\beta$  value for the transition state B(2). Using B(1) and B(2) values of  $C_p^\#(z^\ddagger)$  (C(2,j)) and  $C_p^\#(z)$  (C(1,j)) are calculated at a series of temperatures using the method adopted in program HEATCAP of Section 2. The difference  $C_p^\#(z^\ddagger) - C_p^\#(z)$  is then calculated and stored in array C3(j).

The second part of the program uses all of the collected data to produce plots of  $C_p^\#(z^\ddagger)$ ,  $C_p^\#(z)$  and the difference  $C_p^\#(z^\ddagger) - C_p^\#(z)$  against temperature on an HP 7475A plotter.

```

10 ! & CP PLOT
20 OPTION BASE 1@ CLEAR
30 DIM X(50),C1(2,50),C2(2,50),
  C(2,50),M1(5),T(50),M0(5),B(
  2),C3(50)
40 FOR N=1 TO 2
50 DISP "B_PARAM";N;"=" @ INPUT
  B(N)
60 NEXT N
70 DISP "ISOBARIC CP OF SOLUTE
  Z IN WATER"
80 M=.018015 @ R=8.314
90 DISP "ANDY HAKIN"
100 H=10000 @ D=8 @ K0=9
110 DISP "DELTA H/J MOL^-1 =" ;H
120 DISP "DELTA CP/J K^-1 MOL^-1
  =" ;D
130 FOR J=1 TO 50
140 N=(J-1)*2
150 T(J)=298+(N-25)
160 DISP "T/K=" ;T(J)
170 K=LOG(K0)+H/R*(1/298-1/T(J))
180 K=EXP(K)
190 DISP "K=" ;K
200 FOR N=1 TO 2
210 X(J)=K/(K+EXP(B(N)))
220 Z=X(J)
230 C1(N,J)=-B(N)/M*Z*(1-Z)*D)
240 C2(N,J)=-B(N)/M*Z*(1-Z)*(1-
  2*Z)*H^2/(R*T(J)^2)
250 C(N,J)=C1(N,J)+C2(N,J)
260 DISP "X-EQ=" ;X(J)
270 DISP "1ST TERM=" ;C1(N,J) @ D
  ISP "2ND TERM=" ;C2(N,J)
280 DISP "TOTAL CP(Z)=" ;C(N,J)
290 NEXT N
300 C3(J)=C(2,J)-C(1,J)
310 DISP "DELTA CP=" ;C3(J)
320 NEXT J
330 DISP "END OF CALC"
340 GOSUB 370
350 GOSUB 540
360 DISP "THAT IS ALL FOLKS" @ E
  ND
370 DISP "PRINT DATA" @ INPUT Q
380 IF Q#1 THEN RETURN
390 PRINT "CP FOR SOLUTE "
400 PRINT "M.J.BLANDAMER"
410 PRINT "B-PARAMETER"
420 FOR J=1 TO 50
430 PRINT "POINT ";J @ PRINT "TE
  MP=" ;T(J)
440 FOR N=1 TO 2
450 PRINT "SUBST.=" ;N
460 PRINT "CP1=" ;C1(N,J)
470 PRINT "CP2=" ;C2(N,J)
480 PRINT "CP(Z)=" ;C(N,J)
490 NEXT N
500 PRINT "DELTA CP=" ;C3(J)
510 NEXT J

520 PRINT "END OF DATA"
530 RETURN
540 DISP "PLOTTING"
550 MAT M1=ZER@ MAT M0=ZER
560 M1(1)=AMAX(C1) @ M0(1)=AMIN(
  C1)
570 M1(2)=AMAX(C2) @ M0(2)=AMIN(
  C2)
580 M1(3)=AMAX(C) @ M0(3)=AMIN(
  )
590 M1(4)=AMAX(C3) @ M0(4)=AMIN(
  C3)
600 DISP "PLOTTER ?" @ INPUT Q0
610 IF Q0=1 THEN PLOTTER IS 705
  @ GOTO 630
620 GCLEAR
630 Y1=AMIN(M0) @ Y(2)=AMAX(M1)
640 Y2=AMAX(M1)
650 IF Y1>0 THEN Y1=-10
660 IF Y2<0 THEN Y2=10
670 Y3=Y2+ABS(Y2/10)
680 Y1=Y1-ABS(Y1/10)
690 X3=(T(50)-T(1))/5
700 X1=T(1) @ X2=T(50)
710 Y0=Y3-Y1 @ X0=X2-X1
720 S=Y1+ABS(Y0/10)
730 PEN 2
740 SCALE X1-7,X2+7,Y1-20,Y3+20
750 LAXES 20,Y0/5,273,Y1,373,Y2
760 DEG
770 FOR Q=273 TO 373 STEP 20
780 MOVE Q,S @ LDIR 90 @ LABEL V
  AL$(Q) @ NEXT Q
790 FOR Q=Y1 TO Y3 STEP 2*Y0/10
800 Z=INT(Q)
810 MOVE 280,Q @ LDIR 0 @ LABEL
  VAL$(Z)
820 NEXT Q
830 FOR N=1 TO 2
840 PEN 3
850 MOVE T(1),C(N,1)
860 LINETYPE 1 @ FOR I=1 TO 50 @
  PLOT T(I),C(N,I) @ NEXT I @
  PENUP
870 NEXT N
880 IF Q0=1 THEN PRINT "SP3"
890 PEN 4
900 MOVE T(1),C3(1)
910 LINETYPE 6 @ FOR I=1 TO 50 @
  PLOT T(I),C3(I) @ NEXT I @
  PENUP
920 PEN 2
930 MOVE 273,0 @ DRAW 373,0 @ PE
  NUP
940 LINETYPE 1
950 SCALE 0,100,0,100
960 PENUP @ PLOT 50,25,2
970 LABEL USING 980 ; "TEMP/K"
980 IMAGE 6A
990 PLOT. 80,50,2

1000 LABEL "DELTA CP"
1010 IMAGE 2A
1020 PLOT 25,50,2 @ LABEL "B1=" ;
  VAL$(B(1)); " B2=" ;VAL$(B(2)
  )
1030 FRAME
1040 IF Q0#1 THEN COPY
1050 IF Q0=1 THEN CRT IS 1
1060 RETURN

```

#### Section 4

The two programs reported below are written in HP BASIC for an HP 85 computer. The first program, VOL INFO, calculates the configurational partial molar volume at 298.15 K using equation [12.23] of Chapter 12. These data are stored immediately on disk.

The second program reads the volume data from the disk into an array V1() and then produces a plot of the configurational partial molar volume against  $\beta$  in the region  $-1 \leq \beta \leq 1$ .

```

10 ! VOL INFO
20 OPTION BASE 10 CLEAR
30 DIM V1(21)
40 FOR B=-1 TO 1 STEP .1
50 J=B*10+11
60 M=.018015 @ R=8.314
70 V=-6.4 @ D=8 @ K0=9
80 T=298.15 @ H=10000
90 K=LOG(K0)+H/R*(1/298.15-1/T)
100 K=EXP(K)
110 X=K/(K+EXP(B))
120 Z=X
130 V1(J)=-((1*V*(B/M)*Z*(1-Z))
140 PRINT B;Z;V1(J)
150 NEXT B
160 VOLUME ":D701" IS "DATA H"
170 ASSIGN# 1 TO "CP.DATA H"
180 PRINT# 1 ; V1()
190 ASSIGN# 1 TO *
200 DISP "DATA ON DISC"
210 END

```

```

10 ! VOL PLOT
20 OPTION BASE 10 CLEAR
30 SHORT V1(21)
40 MASS STORAGE IS ":D701"
50 CRT OFF
60 VOLUME ":D701" IS "DATA H"
70 ASSIGN# 1 TO "CP.DATA H"
80 READ# 1 ; V1()
90 ASSIGN# 1 TO *
100 CRT ON
110 DISP "DATA RECEIVED"
120 PLOTTER IS 705
130 GCLEAR
140 Y2=AMAX(V1)
150 Y1=AMIN(V1)
160 U=(Y2-Y1)/20
170 SCALE -1.1,1.1,Y1-U,Y2+U
180 XAXIS Y1,.1,-1.1
190 YAXIS -1,U,Y1,Y2
200 MOVE -1,Y1
210 FOR B=-1 TO 1 STEP .1
220 J=B*10+11
230 PLOT B,V1(J)
240 NEXT B
250 FOR B=-1 TO 1 STEP .2
260 MOVE B,Y1+1 @ LDIR 0 @ LABEL
    VAL$(B)
270 NEXT B
280 FOR S=Y1 TO Y2 STEP 2*U
290 MOVE -.9,S @ LABEL VAL$(S)
300 NEXT S
310 MOVE -1,0 @ DRAW 1,0 @ PENUP
320 FRAME
330 END

```

# KINETICS OF REACTIONS IN AQUEOUS SOLUTIONS

Andrew William Hakin

---

## Abstract

Rate constants for chemical reactions in various aqueous systems have been measured and analysed. A major part of this thesis discusses the effect of added salts on the reaction kinetics of organic substrates and the effect of added cosolvent on iron(II) complexes in solution. The thesis discusses the properties of aqueous solutions with reference to the prediction of trends in kinetic parameters.

Transfer chemical potentials for single ions in 'urea + water' mixtures have been estimated, using solubility data for salts in conjunction with the tetraphenylarsonium tetraphenylboronate assumption. Solvent effects on the initial and transition states for reactions between iron(II) 1,10-phenanthroline and iron(II) glyoxal bis-N methylamine with hydroxide ions are also reported.

Solvent effects on initial and transition states for reaction between three iron(II) complexes and hydroxide ions in 'methanol + water' mixtures are reported.

Effects of added salt on the neutral hydrolysis of phenyldichloroacetate and the para-methoxy derivative are discussed in terms of solvent cosphere interactions between ions.

With regard to computer-based studies osmotic coefficients for ammonium, alkylammonium and azoniaspiroalkane halides have been used with Pitzer's equations and the ideas of Wood et al to produce pairwise Gibbs function cosphere-cosphere interaction parameters.

The effects of added salt on rate constants for the alkaline hydrolysis of the sodium salt of bromophenol blue are reported and analysed using Pitzer's equation for the activity coefficients of single ions in aqueous salt solutions.

Internal pressures of water and deuterium oxide in the region  $273.15 \leq T/K \leq 373.15$  and  $0 \leq P/\text{bar} \leq 1000$  have been calculated and fitted to an equation based on a Taylor expansion about internal pressure  $\Pi_i(\pi, \theta)$  at temperature  $T = \theta$  and pressure  $p = \pi$ .

Calculations are reported which shed light on the controversy concerning the isobaric heat capacities for activation for the solvolysis of alkyl halides in water.